

INFORMATION TO USERS

This manuscript has been reproduced from the microfilm master. UMI films the text directly from the original or copy submitted. Thus, some thesis and dissertation copies are in typewriter face, while others may be from any type of computer printer.

The quality of this reproduction is dependent upon the quality of the copy submitted. Broken or indistinct print, colored or poor quality illustrations and photographs, print bleedthrough, substandard margins, and improper alignment can adversely affect reproduction.

In the unlikely event that the author did not send UMI a complete manuscript and there are missing pages, these will be noted. Also, if unauthorized copyright material had to be removed, a note will indicate the deletion.

Oversize materials (e.g., maps, drawings, charts) are reproduced by sectioning the original, beginning at the upper left-hand corner and continuing from left to right in equal sections with small overlaps.

Photographs included in the original manuscript have been reproduced xerographically in this copy. Higher quality 6" x 9" black and white photographic prints are available for any photographs or illustrations appearing in this copy for an additional charge. Contact UMI directly to order.

ProQuest Information and Learning
300 North Zeeb Road, Ann Arbor, MI 48106-1346 USA
800-521-0600

UMI[®]

NOTE TO USERS

Page(s) not included in the original manuscript and are unavailable from the author or university. The manuscript was microfilmed as received.

140

This reproduction is the best copy available.

UMI

**CHARACTERIZATION OF AMINOGLYCOSIDE PHOSPHOTRANSFERASE
APH(3')-IIIa AN ENTEROCOCCAL ENZYME CONFERRING RESISTANCE TO
AMINOGLYCOSIDE ANTIBIOTICS**

By

GEOFFREY A. M^cKAY, B.Sc.

A Thesis

Submitted to the School of Graduate Studies

In Partial fulfillment of the Requirements

For the Degree

Doctor of Philosophy

McMaster University

© Copyright by Geoffrey A. M^cKay, June, 1999

CHARACTERIZATION OF APH(3')-IIIa, KANAMYCIN KINASE

DOCTOR OF PHILOSOPHY (1999)
(Biochemistry)

McMaster University
Hamilton, Ontario

TITLE: **Characterization of Aminoglycoside Phosphotransferase APH(3')-IIIa an Enterococcal Enzyme Conferring Resistance to Aminoglycoside Antibiotics.**

AUTHOR: **Geoffrey A. McKay, B.Sc. (McGill University)**

SUPERVISOR: **Professor G.D. Wright**

NUMBER OF PAGES: **xxiii, 244**

ABSTRACT

Aminoglycosides antibiotics are a clinically relevant class of antibiotics that continue to find use despite the appearance of organisms resistant to these therapeutic agents. Resistance to aminoglycosides may be manifested through several mechanisms including alteration of the ribosomal target, active efflux of the compounds or chemical modification of the antibiotics. The latter mechanism of resistance can occur through *O*-adenylation, *N*-acetylation or *O*-phosphorylation. An aminoglycoside phosphotransferase, APH(3')-IIIa modifies a broad range of aminoglycoside antibiotics through ATP dependent phosphorylation of the 3' hydroxyl group rendering these antibiotics inoffensive to the bacterium. In an attempt to gain a more thorough understanding of the molecular mechanisms of this drug modification, studies were initiated to determine its substrate specificity and identify residues required for substrate recognition and enzyme activity. The results reported herein, identify residues which line the ATP binding pocket as well as identify substrate structures required for enzyme/substrate interactions. These mechanistic studies further identify a functional similarity between APH(3')-IIIa and eukaryotic protein kinases.

These data have mapped both enzyme and substrate structures required for aminoglycoside detoxification and form the basis for further rational drug design studies.

Dedication

I would like to dedicate this thesis in memory of my father, whose support and teachings taught me to do the best job I could regardless of the circumstances. I would also like to dedicate this thesis to my loving wife Lisa whose support, love and friendship made the writing of this thesis possible.

Acknowledgments

Firstly I would like to thank Gerry for all his supervision, suggestions, patience and commitment to my education. Beyond his professional attention I would also sincerely like to thank Gerry for his friendship over the years, something that always made work in his lab enjoyable. I would also like to thank the members of my committee, Dr. Andrews, Dr. Chan and Dr. Finan for their patience and suggestions over the years.

Numerous people have contributed to my studies in one way or another and as such are too numerous to mention but there are several people who made significant contributions in various aspects. Firstly, I would like to thank Paul Thompson whose collaboration on the project helped immensely and whose pep talk helped me through my defense. I also would like to thank Denis Daigle, Gary Marshall, Greg Broadhead and Byron DeLaBarre for their friendship and discussions. David Bareich, Suzanne Jacques, Sara Duffy, and all those I had the good fortune of working with who all helped to make my tenure enjoyable.

I would like to thank my brother Bruce for his suggestions, and friendship and numerous revisions of both my comprehensives and thesis.

Lastly I would like to thank my mother, my father and my wife for their support and help during the many years and without whose help none of this would have been possible.

TABLE OF CONTENTS

	PAGE
ABSTRACT	iii
DEDICATION	iv
ACKNOWLEDGMENTS	v
TABLE OF CONTENTS	vi
ABBREVIATIONS	xi
LIST OF FIGURES	xvi
LIST OF SCHEMES	xix
LIST OF TABLES	xx
LIST OF PDB FILES	xxii
PERSONAL PUBLICATIONS	xxiii
CHAPTER 1: GENERAL INTRODUCTION	1
1.1 Development of Antibiotics	2
1.2 General Antibiotic Resistance	6
1.3 Aminoglycoside Antibiotics	10
1.3.1 Aminoglycoside Aminocyclitol Structure	10
1.3.2 Mode of Action of Aminoglycosides	15
1.3.3 Aminoglycoside Entry	19
1.3.4 Unifying Hypothesis for Aminoglycoside Action	22
1.4 Aminoglycoside Resistance	24
1.4.1 Non-Enzymatic Resistance	24
1.4.2 Enzymatic Resistance	26
1.4.3 Nomenclature of Aminoglycoside Resistance Enzymes	28
1.4.4 Dissemination of aminoglycoside resistance genes in Nature	28
1.4.5 Aminoglycoside Nucleotidyltransferases (ANT)	29
1.4.6 Aminoglycoside Acetyltransferases (AAC)	32
1.4.7 Aminoglycoside Phosphotransferases (APH)	38
1.5 Synopsis	47
CHAPTER 2: OVEREXPRESSION, PURIFICATION AND CHARACTERIZATION OF APH(3')-IIIa	49
2.1 Introduction	50
2.2 Materials and Methods	51

2.2.1	General Materials	51
2.2.2	Preparation and Purification of Neamine	51
2.2.3	Preparation of Overproducing Constructs	52
2.2.4	Overexpression and Purification of APH(3')-IIIa	55
2.2.4a	APH(3')-IIIa from <i>E.coli</i> JM105 [pAT21-1]	55
2.2.4b	APH(3')-IIIa from <i>E.coli</i> BL21 (DE3) [pETAPHG6]	56
2.2.5	Physical Characteristics of APH(3')-IIIa	57
2.2.6	Enzyme Assay-Substrate Specificity Kinetic Analysis	57
2.2.7	Large Scale Preparation and Purification of Phosphorylated Aminoglycoside	60
2.3	Results	62
2.3.1	Purification of Neamine	62
2.3.2	Purification of APH(3')-IIIa	62
2.3.2a	APH(3')-IIIa from <i>E.coli</i> JM105 [pAT21-1]	62
2.3.2b	APH(3')-IIIa from <i>E.coli</i> BL21 (DE3) [pETAPHG6]	67
2.3.3	Kinetic Properties of APH(3')-IIIa	70
2.3.4	Use of De-Amino Aminoglycosides to Probe Enzyme-Structure Interactions	72
CHAPTER 3: KINETIC STUDIES OF APH(3')-IIIa AND RATE LIMITING STEP OF CATALYSIS IN SUPPORT OF A THEORELL-CHANCE MECHANISM		77
3.1	Introduction	78
3.2	Materials and Methods	83
3.2.1	General Materials	83
3.2.2	Initial Velocity Studies	83
3.2.3	Dead-End Inhibition Studies	84
3.2.4	Substrate Inhibition Studies	85
3.2.5	Product Inhibition Studies	86
3.2.6	Alternative Diagnostic Substrate Studies	86
3.2.7	Thio Effects on the Mechanism of APH(3')-IIIa Phosphorylation	87
3.2.8	Solvent Isotope Effects on the Mechanism of APH(3')-IIIa Phosphorylation	87
3.2.9	Calibration of Ostwald Viscometer and Calculation of Solvent Viscosity	88
3.2.10	Solvent Viscosity Assays	88
3.3	Results	89
3.3.1	Initial Velocity Patterns	89

3.3.2	Dead-End Inhibitor Studies	89
3.3.3	Substrate Inhibition Studies	93
3.3.4	Product Inhibition Studies	98
3.3.5	Alternative Substrate Diagnostic Studies	102
3.3.6	Solvent Isotope and Thio Effects on APH(3')-IIIa Kinetic Mechanism	102
3.3.7	Solvent Viscosity Effects on APH(3')-IIIa Kinetic Mechanism	105
CHAPTER 4:	ACTIVE SITE MAPPING AND MUTAGENESIS OF APH(3')-IIIa IDENTIFIES TWO RESIDUES WHICH LINE THE ATP BINDING POCKET	110
4.1	Introduction	111
4.2	Materials and Methods	112
4.2.1	General Materials	112
4.2.2	Inactivation of APH(3')-IIIa with FSBA	114
4.2.3	Substrate Specific Protection of APH(3')-IIIa from FSBA Inactivation	114
4.2.4	Determination of Stoichiometry of FSBA Labeling	115
4.2.5	Large Scale Affinity Labeling and Peptide Mapping	115
4.2.6	Characterization of Labeled Peptides by Narrowbore HPLC, Edman Degradation and Mass Spectroscopy	143
4.2.7	Generation of APH(3')-IIIa Site Directed Mutants	117
4.2.7a	Cloning of <i>aph(3')-IIIa</i> into M13mp18	117
4.2.7b	Generation of Single Stranded Template DNA	118
4.2.7c	Phosphorylation of Oligonucleotide	119
4.2.7d	Annealing of Phosphorylated Oligonucleotide to Single Stranded <i>aph(3')-IIIa</i> Template	119
4.2.7e	Synthesis of Second Strand	119
4.2.7f	Transformation of MV1190 with Synthesis Reaction	120
4.2.7g	Screening of Site Directed Mutants	120
4.3	Results	121
4.3.1	FSBA Labels APH(3')-IIIa at the ATP Binding Pocket	121
4.3.2	Kinetics of Inactivation of APH(3')-IIIa	121

	FSBA	
4.3.3	Stoichiometry of APH(3')-IIIa Inactivation by FSBA	126
4.3.4	Identification of FSBA-Labeled Peptides	126
4.3.5	Narrowbore HPLC Purification of FSBA-Labeled Peptides, Edman Degradation and Mass Spectroscopy of Identified Peptides	129
4.3.6	Analysis of APH(3')-IIIa K44A, K33A and K33AK44A Mutants	132
CHAPTER 5:	FUNCTIONAL COMPARISON BETWEEN APH(3')-IIIa AND EUKARYOTIC PROTEIN KINASES DEMONSTRATES SIMILAR ACTIVITIES	136
5.1	Introduction	136
5.2	Materials and Methods	141
5.2.1	General Materials	141
5.2.2	Purification of Casein Kinase I from E.coli BL21 (DE3) [pT7II-ckiΔ298]	144
5.2.3	Casein Kinase Activity Assays	146
5.2.4	Generation of APH(3')-IIIa Site Mutants	146
5.2.5	Survey of Protein Kinase Inhibitors and their Effects on APH(3')-IIIa	149
5.2.6	Growth of APH(3')-IIIa [Δ123.189]	149
5.2.7	Dead-End Inhibitor Analysis of Protein Kinase Inhibitors	150
5.2.8	Survey of APH(3')-IIIa Protein Kinase Activity	151
5.2.8a	Phosphorylation of p60^{c-src} Substrate II	151
5.2.8b	Phosphorylation of Histone H1, MBP and Poly (Glu:Tyr) (4:1)	152
5.2.8c	Phosphorylation of Peptide Substrates	152
5.2.9	Calculation of the Rate of Phosphorylation of MBP by APH(3')-IIIa	154
5.2.10	Calculation of the Rate of Phosphorylation of Peptides by APH(3')-IIIa	154
5.3	Results	155
5.3.1	Enzyme Kinetics of APH(3')-IIIa [G189R] and APH(3')-IIIa [Δ123-189]	155
5.3.2	Survey of Protein Kinase Inhibitors	157
5.3.3	APH(3')-IIIa Demonstrates Eukaryotic Protein Kinase-Like Activity	159

CHAPTER 6: DISCUSSION	163
6.1 Cloning of <i>aph(3')-IIIa</i>	164
6.2 Overexpression, Purification and Characterization of APH(3')-IIIa	165
6.3 Substrate Specificity of APH(3')-IIIa	168
6.4 Kinetic Mechanism Studies of APH(3')-IIIa	186
6.5 Active Site Mapping and Structure of APH(3')-IIIa	195
6.6 Protein Kinase Inhibitor Studies	205
6.7 Protein Kinase Substrate Studies	212
CONCLUSION:	214
REFERENCES:	216

ABBREVIATIONS

AAC	Aminoglycoside Acetyltransferase
ADP	Adenosine Diphosphate
AGRP	Aminoglycoside Resistance Profile
Amik	Amikacin
AMP	Adenosine Monophosphate
AMP-PNP	Adenylyl-imidophosphate
ANT	Aminoglycoside Nucleotidyltransferase
APH	Aminoglycoside Phosphotransferase
APH(3')-IIIa	Aminoglycoside Phosphotransferase Type IIIa
Apr	Apramycin
Arbek	Arbekacin
ATP	Adenosine Triphosphate
ATP-γ-S	Adenosine 5'-O-(3-thiotriphosphate)
But	Butirosin
cAMP DPK	Cyclic Adenosine Monophosphate Dependent Protein Kinase
CKI-7	N-(2-aminoethyl)-5-chloroisoquinoline-8 sulfonamide

CKI-8	1-(5-chloroisoquinoline-8-sulfonyl)piperazine
DMSO	Dimethyl Sulfoxide
DTT	Dithiothreitol
EDTA	<i>N,N,N',N'</i>Ethylenediaminetetraacetic Acid
EGTA	Ethylene Glycol <i>bis</i>(β-aminoethylether) <i>N,N'</i>-tetraacetic Acid
EPKs	Eukaryotic Protein Kinases
ESI-MS	Electrospray Ionization Mass Spectrometry
Fort	Fortimicin
FPLC	Fast Protein Liquid Chromatography
FSBA	5'-[ρ-(fluorosulfonyl)benzoyl]adenosine
Gent	Gentamicin
H-7	1-(5-isoquinolinesulfonyl)-2-methylpiperazine
H-9	<i>N</i>-(2-aminoethyl)-5-isoquinoline sulfonamide
HA-1004	<i>N</i>-(2-guanidinoethyl)-5-isoquinoline sulfonamide
HEPES	<i>N</i>-(2-hydroxyethyl)piperazine-<i>N'</i>-2-ethanesulfonic Acid
HPLC	High Pressure Liquid Chromatography
Hygr	Hygromycin
IPTG	Isopropyl β-D-thiogalactopyranoside
Isep	Isepamicin

Kan A	Kanamycin A
Kan B	Kanamycin B
k_{cat}/K_m	Specificity Constant
k_{cat}	Catalytic Constant
kDa	KiloDaltons
K_I	Substrate Inhibition Constant
K_i	Binding Constant for a Covalent Inactivator
K_{ii}	Intercept Inhibition Constant
K_{is}	Slope Inhibition Constant
K_m	Michaelis-Menten Constant
LDH	Lactate Dehydrogenase
LB	Luria Broth
Livid	Lividomycin
MALDI-Tof	Matrix-Assisted Laser Desorption Time of Flight
MAP	Mitogen Activated Protein Kinase
MARCKS K	Myristolated Alanine-Rich Protein Kinase-C
	Substrate Lysine Rich
MARCKS R	Myristolated Alanine-Rich Protein Kinase-C
	Substrate Arginine Rich
MBP	Myelin Basic Protein
MES	2-(<i>N</i>-morpholino)ethanesulfonic Acid

MIC	Minimal Inhibitory Concentration
MOPS	3-(<i>N</i>-morpholino)propanesulfonic Acid
NAD⁺	Nicotinamide Adenine Dinucleotide
NADH	Nicotinamide Adenine Dinucleotide Reduced Form
Neo	Neomycin
Net	Netilmicin
Paro	Paromomycin
PCR	Polymerase Chain Reaction
PEG	Polyethylene Glycol
PK	Pyruvate Kinase
PKC	Protein Kinase C
PMSF	Phenylmethylsulfonylfluoride
PY	Peptone Yeast Media
PTH	Phenylthiohydantoin
Ribos	Ribostamycin
SDS	Sodium Dodecyl Sulfate
SDS-PAGE	Sodium Dodecyl Sulfate Polyacrylamide Gel Electrophoresis
Siso	Sisomicin
Spec	Spectinomycin
Strep	Streptomycin

TCA	Trichloroacetic Acid
TFA	Trifluoroacetic Acid
TLC	Thin Layer Chromatography
Tob	Tobramycin
TPCK	<i>N</i>-p-tosyl-L-Phenylalanine Chloromethyl Ketone
Tris	Tris-(hydroxymethyl)aminomethane
V_m	Maximal Velocity

LIST OF FIGURES

Chapter 1		PAGE
1.1	Effect of antimicrobials on the number of deaths caused by all infective diseases.	3
1.2	Structure of early antibiotics: salvarsan, protosil, sulfanilamide and benzykpenicillin (penicillin G).	4
1.3	Structure and crosslinking of peptidoglycan of the cell wall of <i>Staphylococcus aureus</i> .	8
1.4	Hydrolysis of β -lactams (penicillin) by β -lactamase enzymes.	9
1.5	Structure of aminoglycoside antibiotics. (A) 4,6-disubstituted deoxystreptamine, (B) 4,5-disubstituted deoxystreptamine and (C) class 3 aminoglycosides.	11, 12, 13
1.6	NMR structure of paromomycin bound to synthetic oligonucleotide of the 16S rRNA (modified and redrawn from Fourmy <i>et al</i> , Science, 1996: PDB code 1PBR).	17
1.7	Typical aminoglycoside uptake curve for a streptomycin sensitive and streptomycin resistant strain (modified and redrawn from R.E.W. Hancock, J. Antimicrobial Chemotherapy 8: 249-276.	20
1.8	Covalent inactivation of aminoglycoside antibiotics by <i>O</i> -adenylation, <i>O</i> -phosphorylation and <i>N</i> -acetylation.	27
1.9	Structure of ANT(4')-Ia dimer. (A) side view and (B) top view. Modified and redrawn from Pedersen <i>et al</i> , 1995. PDB code 1KNY.	33
1.10	Primary sequence alignment of APH(3') family members (A) Motif I, (B) Motif II, (C) Motif III and (D) Alignment of APH(3')-IIIa and several eukaryotic protein kinases.	43
 Chapter 2		
2.1	Couple enzyme reaction. (A) forward reaction and (B) reverse reaction.	58
2.2	Purification of APH(3')-IIIa from <i>E. coli</i> JM105 [pAT21-1]. SDS-polyacrylamide gel (11%) was stained with Coomassie blue.	65
2.3	Purification of APH(3')-IIIa from <i>E. coli</i> BL21 (DE3) [pETAPHG6]. SDS-polyacrylamide gel (11%) was stained with Coomassie blue	68
2.4	Modified 4,5 and 4,6-disubstituted deoxystreptamine aminoglycosides. (A) Neamine aminoglycoside family members and (B) kanamycin A aminoglycoside family members.	73

Chapter 3		
3.1	Initial velocity patterns of APH(3')-IIIa.	90
3.2	Competitive inhibition of APH(3')-IIIa through the use of the dead-end inhibitor tobramycin.	94
3.3	Uncompetitive inhibition of APH(3')-IIIa through the use of the dead-end inhibitor tobramycin.	95
3.4	Competitive inhibition of APH(3')-IIIa through the use of the dead-end inhibitor AMP.	96
3.5	Noncompetitive inhibition of APH(3')-IIIa through the use of the dead-end inhibitor AMP.	97
3.6	Substrate inhibition of APH(3')-IIIa through the non-productive binding of paromomycin.	99
3.7	Substrate inhibition of APH(3')-IIIa through the non-productive binding of kanamycin A.	100
3.8	Inhibition of APH(3')-IIIa through the use of product kanamycin phosphate	101
3.9	PEG ₈₀₀₀ viscosity effects on the rates of APH(3')-IIIa catalyzed reactions.	106
3.10	Glycerol viscosity effects on the rate of APH(3')-IIIa catalyzed reactions.	107
3.11	Glycerol viscosity effects on the rates of APH(3')-IIIa catalyzed reactions.	108
Chapter 4		
4.1	Spacefill model of (A) p-fluorosulfonylbenzoyl adenosine (FSBA) and (B) adenosine triphosphate (ATP).	113
4.2	Time dependent inactivation of APH(3')-IIIa with FSBA.	123
4.3	Kinetics of inactivation of APH(3')-IIIa with FSBA.	126
4.4	Stoichiometry of APH(3')-IIIa labeling with FSBA.	127
4.5	Peptide mapping of [¹⁴ C]FSBA-labeled APH(3')-IIIa.	128
4.6	Peptide mapping of APH(3')-IIIa. (A) non-radiolabeled FSBA inactivated APH(3')-IIIa and (B) narrowbore reverse-phase HPLC.	130
Chapter 5		
5.1	Three-dimensional structural comparison of (A) APH(3')-IIIa and eukaryotic protein kinases (B) phosphorylase kinase, (C) casein kinase and (D) cyclic AMP dependent protein kinase.	139
5.2	Structure of isoquinoline derived protein kinase inhibitors. (A) H-series and (B) C-series.	140
5.3	Structure of protein kinase inhibitors. (A) isoflavone derived inhibitors and (B) staurosporine.	142
5.4	Structure of tyrosine protein kinase inhibitors tyrphostins. (A) tyrphostin A1, (B) tyrphostin B44 and (C) tyrphostin B50.	143

5.5	Protein kinase activity of APH(3')-IIIa. SDS-PAGE of myelin basic protein (redrawn and modified from Daigle <i>et al</i> , 1999, reference #44).	160
Chapter 6		
6.1	Proposed mechanisms of phosphoryl transfer. (A) meta phosphate transition state and (B) pentacoordinate transition state.	175
6.2	Three-dimensional structural comparison of APH(3')-IIIa. (A) APH(3')-IIIa with bound ADP (front view), (B) apo APH(3')-IIIa (front view), (C) APH(3')-IIIa with bound ADP (side view) and (D) apo APH(3')-IIIa (side view).	182
6.3	Primary sequence alignment of seven APH(3') family members.	189
6.4	Three-dimensional structural comparison of active sites residues for: (A) APH(3')-IIIa and eukaryotic protein kinases (B) phosphorylase kinase, (C) casein kinase-1 and (D) cyclic AMP dependent protein kinase.	193
6.5	Three-dimensional structural comparison of (A) staurosporine bound to cyclic AMP dependent protein kinase and (B) staurosporine bound to cyclin dependent kinase.	197
6.6	Three-dimensional structural comparison of (A) cyclic AMP dependent protein kinase with co-crystal APT and (B) cyclic AMP dependent protein kinase with co-crystal H-7 isoquinoline inhibitor.	202

LIST OF SCHEMES

SCHEME		PAGE
1	Competitive Inhibition	81
2	Non-Competitive Inhibition	81
3	Un-Competitive Inhibitor	81
4	Sequential Kinetic Mechanism (A) Ordered (B) Random	91
5	Ping Pong Kinetic Mechanism	91
6	APH(3')-III Theorell-Chance Kinetic Mechanism	171
7	Free Energy Reaction Coordinate	184

LIST OF TABLES

Chapter 1	PAGE
1.1 Aminoglycoside-aminocyclitol antibiotics	14
1.2 Aminoglycoside nucleotidyltransferases	30
1.3 Aminoglycoside acetyltransferases	35
1.4 Aminoglycoside phosphotransferases	39
 Chapter 2	
2.1 Purification of APH(3')-IIIa from <i>E.coli</i> JM105 [pAT21-1]	64
2.2 Kinetics of APH(3')-IIIa monomer and dimer	66
2.3 Purification of APH(3')-IIIa from <i>E.coli</i> BL21(DE3) [pETAPHG6]	69
2.4A Kinetic parameters of purified, overexpressed APH(3')-IIIa	71
2.4B Steady-state kinetic parameters for the synthetic aminoglycoside substrates	74
2.5 Structure-activity analysis of APH(3')-IIIa	76
 Chapter 3	
3.1 Summary of kinetic inhibition constants	92
3.2 Alternative substrate diagnostic with fixed concentration of aminoglycoside substrates using ATP as the variable substrate	103
3.3 Solvent isotope and thio effects for APH(3')-IIIa	104
3.4 Viscosity effects on APH(3')-IIIa	109

Chapter 4

4.1	Inactivation of APH(3')-IIIa by FSBA	122
4.2	Analysis of tryptic peptides from FSBA labeled APH(3')-IIIa	131
4.3	Steady-state kinetics of APH(3')-IIIa [K44A], APH(3')-IIIa [K33A] and APH(3')-IIIa [K33AK44A]	133

Chapter 5

5.1	Kinetics of APH(3')-IIIa [G189R] for aminoglycoside substrates	156
5.2	Effects of protein kinase inhibitors on APH(3')-IIIa	158
5.3	Survey of APH(3')-IIIa activity using protein kinase substrates	161

Chapter 6

6.1	Microscopic rate constants for APH(3')-IIIa with substrate ATP and kanamycin A	185
------------	---	------------

Protein Database Codes

PDB Code	PDB Description	Reference
1AQ1	Human cyclin dependent kinase 2 complexed with the inhibitor staurosporine.	183
1ATP	CAMP dependent protein kinase (Catalytic Subunit) complex with the peptide inhibitor Pki (5-24) and MnATP.	19
1CSN	Binary complex of casein kinase-1 with MgATP.	203
1KNY	Structural investigation of the antibiotic and ATP binding sites in kanamycin nucleotidyltransferase.	146
1PBR	Structure of the A site of <i>Escherichia coli</i> 16S ribosomal RNA complexed with an aminoglycoside antibiotic.	55
1PHK	Two structures of the catalytic domain of phosphorylase kinase: An active protein kinase complexed with nucleotide, substrate analogue and product.	142
1STC	CAMP dependent protein kinase, alpha catalytic subunit in complex with staurosporine.	183
1YDR	Structure of cAMP dependent protein kinase-alpha catalytic subunit in complex with H7 protein kinase inhibitor 1-5(-isoquinolinesulfonyl)-2-methylpiperazine.	51

PERSONAL PUBLICATIONS

1. **G.A. McKay, P.R. Thompson and G.D. Wright** (1994) Broad spectrum aminoglycoside phosphotransferase type III from enterococcus: Overexpression, purification and substrate specificity. *Biochemistry* 33: 6936-6944.
2. **G.A. McKay, R.A. Robinson, W.S. Lane and G.D. Wright** (1994) Active site labeling of an aminoglycoside 3'-phosphotransferase (APH(3')-IIIa). *Biochemistry* 33: 14115-14120.
3. **G.A. McKay and G.D. Wright** (1995) Kinetic mechanism of aminoglycoside phosphotransferase type IIIa: Evidence of a Theorell-Chance Mechanism. *J. Biol. Chem.* 270: 24686-24692.
4. **G.A. McKay and G.D. Wright** (1995) Catalytic mechanism of enterococcal kanamycin kinase (APH(3')-IIIa): Viscosity and solvent isotope effects support a Theorell-Chance mechanism. *Biochemistry* 35: 8686-8695.
5. **J.R. Cox, G.A. McKay, G.D. Wright and E.H. Serpersu** (1996) Arrangement of substrates at the active site of an aminoglycoside antibiotic 3'-phosphotransferase (APH(3')-IIIa) as determined by NMR. *J. Am. Chem. Soc.* 118: 1295-1301.
6. **G.A. McKay, J. Roestamadji, S. Mobashery and G.D. Wright** (1996) Recognition of aminoglycoside antibiotics by the enterococcal/staphylococcal aminoglycoside 3'-phosphotransferase type IIIa: Role of substrate amino groups. *Antimicrob. Agents Chemother.* 40: 2648-2650.
7. **W.-C. Hon, G.A. McKay, P.R. Thompson, R.M. Sweet, D.S.-c. Yang, G.D. Wright and A.M. Berghuis** (1997) Structure of an enzyme required for aminoglycoside antibiotic resistance reveals homology to eukaryotic protein kinases. *Cell* 89: 887-895.
8. **D.M. Daigle, G.A. McKay and G.D. Wright.** (1997) Inhibition of aminoglycoside antibiotic resistance enzyme by protein kinase inhibitors. *J. Biol. Chem.* 272: 24755-24758.
9. **D.M. Daigle, G.A. McKay, P.R. Thompson and G.D. Wright** (1997) Aminoglycoside phosphotransferases APH(3')-IIIa and AAC(6')-APH(2'') are serine protein kinases. *Chemistry and Biology* 6: 11-18.

CHAPTER 1

A General Introduction to Antibiotics and Mechanisms of Antibiotic Resistance.

Chapter 1

Introduction

1.1 *Development of Antibiotics*

There are few discoveries that have had a greater impact on both the length and quality of life of humans than the development of modern antibiotics (Figure 1.1). The earliest medical records describe the use of many different salves, ointments and solutions, including frankincense, arsenic and mercury in the treatment of a panolpy of infections. The development of these antimicrobial therapies was empirical in nature and it wasn't until the late nineteenth century that a more rational approach to drug design was undertaken by a variety of researchers.

Modern chemotherapy as a “magic bullet” is a term Paul Ehrlich first used to describe his belief that infectious disease could be treated with synthetic compounds (57). He is often referred to as the "father" of modern scientific chemotherapy and is responsible for the development of some of the earliest antimicrobial chemicals, some of which find use in modern clinical therapy. Ehrlich is probably best known for his work on arsenical compounds which led to the development of salvarsan (Figure 1.2), used in the treatment of both trypanosome and spirochete infections (reviewed in 114). His methodology involved identifying a compound with a desired clinical outcome and using this structure

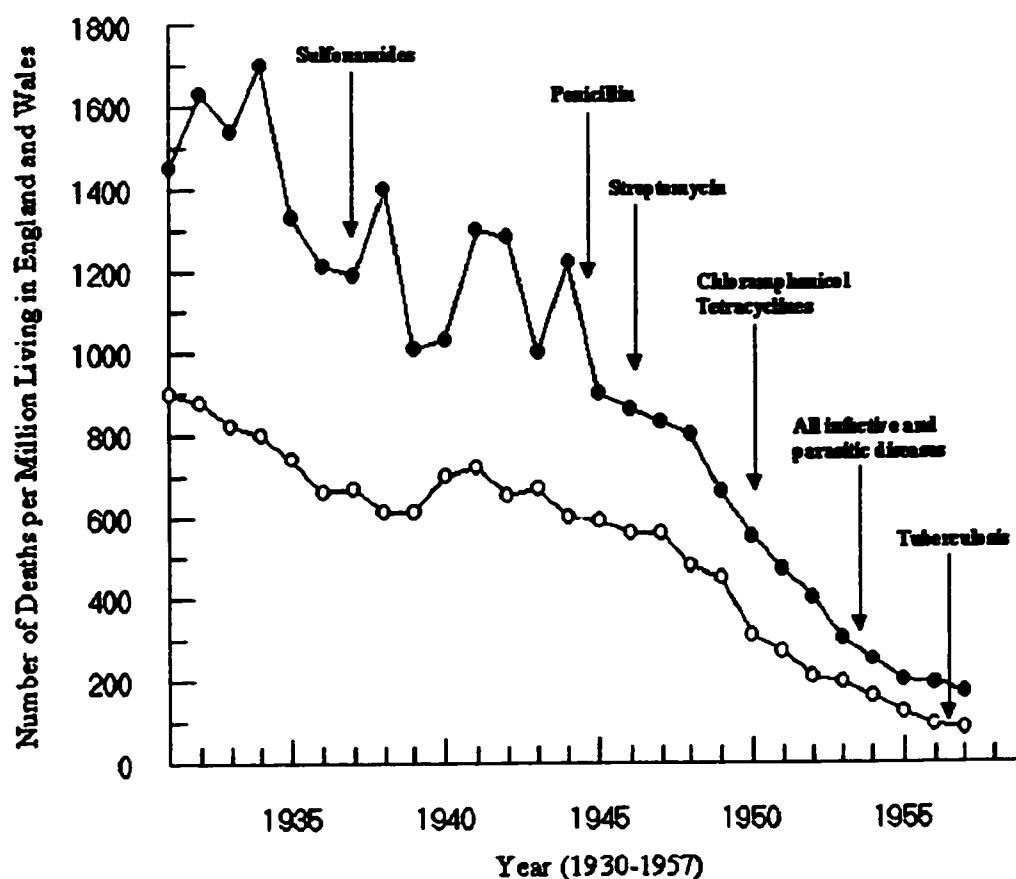
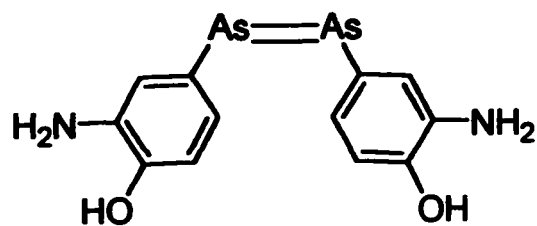
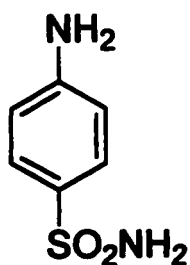


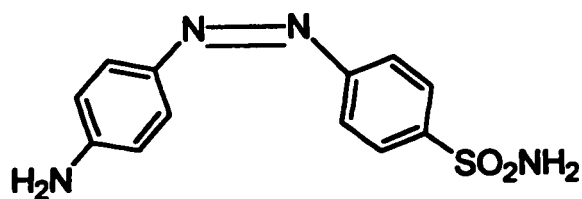
Figure 1.1. Effect of antimicrobials on the number of deaths caused by all infective diseases. Data sampled from England and Wales from 1930 to 1957. Closed circles (●) represent the number of deaths per million living in England and Wales caused by all infective diseases while open circles (○) represent the number of deaths caused by tuberculosis. Modified and redrawn from *The Use and Abuse of Antibiotics: Drug-Resistant Staphylococcal Infection*, Mary Barber, M.D.



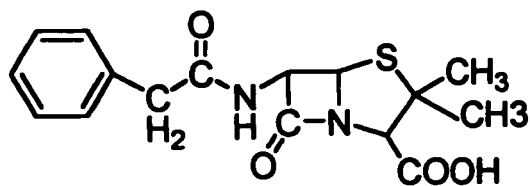
Salvarsan



Sulfanilamide



Protonsil



Benzylpenicillin (penicillin G)

Figure 1.2. Structure of early therapeutic agents: salvarsan, protonsil, sulfanilamide and benzylpenicillin (penicillin G).

as a starting point for further modification. After several rounds of this analysis/synthesis, the ideal therapeutic agent would be generated.

Various researchers began to follow Ehrlich's systematic approach to drug testing and this eventually led to the synthesis of the sulfonamide protonsil (Figure 1.2) by Klarer and Mietzsch (reviewed in 114). Several groups demonstrated the usefulness of protonsil in the treatment of streptococcal infections *in vivo* and it was subsequently demonstrated by Trefouel that the reduction of protonsil occurred *in vivo* yielded the active component sulfanilamide (Figure 1.2) (reviewed in 114). Since sulfanilamide's identification, many family members have been derived from the parent compound, generating more potent and less toxic therapeutics (reviewed in 114).

Often, the importance of the sulfanilamide drugs are under emphasized due to the discovery of penicillin (Figure 1.2) which occurred during roughly the same period as the development of protonsil. The fortuitous nature of penicillin's discovery by Fleming (54) led to one of the most important changes in antimicrobial research. Most of the early antimicrobials were discovered by empirically screening large numbers of synthetic compounds, many of which, although toxic to the micro-organisms, were also in part toxic to the patient being treated. It was this toxicity and relatively narrow spectrum of action which was the driving force for the discovery of new antimicrobials. The discovery and development of penicillin from the mold *Penicillium notatum* heralded the beginning of the era of natural product antibiotics and began to shift the focus of drug development away from chemical synthesis and on to natural product discovery.

The benefits of penicillin therapy include its relatively broad spectrum of activity (most Gram positive and some Gram negative bacteria) and apparent lack of toxicity (the exception being extremely high doses of intrathecally delivered penicillin (11)). Its discovery was the first of many natural products which demonstrated some antimicrobial activity. Using the identification of penicillin as a model, Waksman and colleagues began an exhaustive search for natural products from soil bacteria. Their group screened over ten thousand soil samples which eventually led to the discovery of bacteria which produced streptomycin (168) and neomycin (196). These two antibiotics were the first two cases where a systematic, high volume screening process was employed in an attempt to identify antimicrobial agents. Within several years, a large assortment of antibiotics had been isolated from various producing organisms, and these drugs targeted a wide range of micro-organisms and cellular processes.

It is evident that the development of antimicrobial agents had a profound effect upon mortality levels associated with infectious diseases (Figure 1.1). It has similarly become quite apparent even from the outset, that microbial resistance to developed antibiotics posed a serious threat to the continued usefulness of some, if not all antibiotics currently in use.

1.2 *General Antibiotic Resistance*

The first account of drug resistance to a chemotherapeutic agent was observed and detailed by Ehrlich in 1907 while testing arsenical compounds on trypanosomal parasites. It wasn't long after the initial introduction of sulphanilamides into clinical use that

resistance to this class of drugs appeared (reviewed in 114). Although these antibiotics are currently perhaps clinically less prevalent than many others, the problem of drug resistance to most classes of drugs is still a major health crisis (69, 129, 140).

The best studied of all antibiotics, and also associated resistance mechanisms, is that of the penicillins. Early studies indicated that a buildup of cell wall components, including N-acetyl muramic acid and N-acetyl glucosamine occurred when *Staphylococcus* was treated with penicillin (reviewed in 114, 118). This led to the belief that penicillin acted on cell wall biosynthesis and eventually transpeptidases (penicillin binding proteins (PBPs)) were identified as the specific target of penicillin. These PBPs are now known to cross-link a free amine (R-group side chain) of a dibasic amino acid (L-lys or meso-diaminopimelic acid) to the penultimate D-alanine of a neighboring chain (Figure 1.3). This link is either accomplished directly or through a multiglycine peptide linker (118). The absence of cross-linking reduces the structural support usually provided by the cell wall and the bacteria become more sensitive to environmental stress in the form of osmotic pressures.

Resistance to β -lactam antibiotics can be achieved through an enzymatic alteration of penicillins. These novel PBPs, or as they are more commonly referred to, β -lactamases, are capable of hydrolyzing the 4 membered ring of the β -lactams thus rendering them inoffensive to the cells (Figure 1.4). To date there have been isolated greater than 200 distinct PBPs which can detoxify penicillins, cephalosporins or both family of drugs, thus severely reducing the usefulness of β -lactam antibiotics (118).

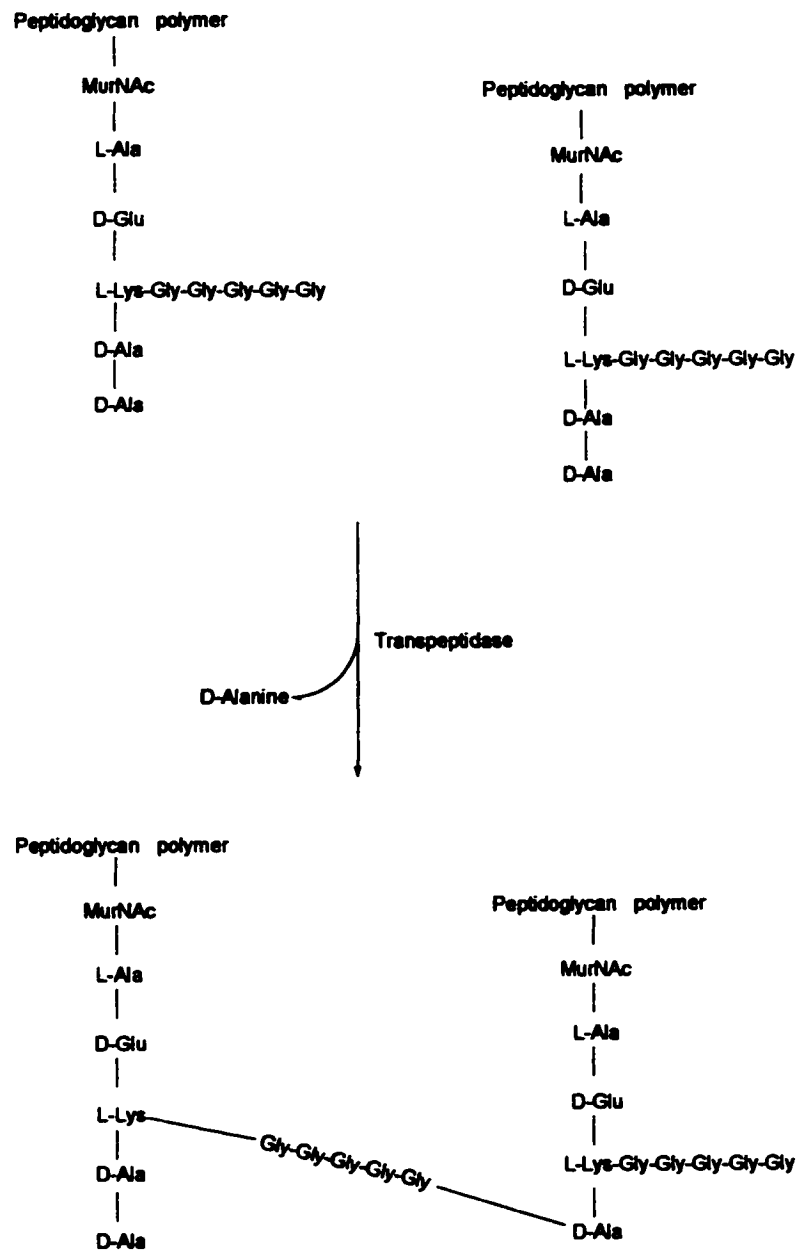


Figure 1.3. Structure and enzymatic crosslinking of peptidoglycan of the cell wall of *Staphylococcus aureus*.

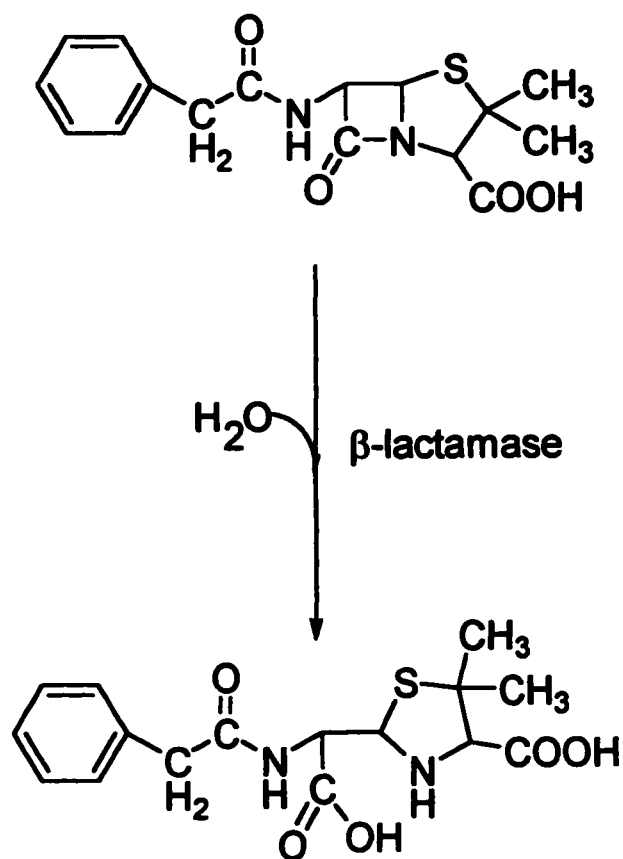
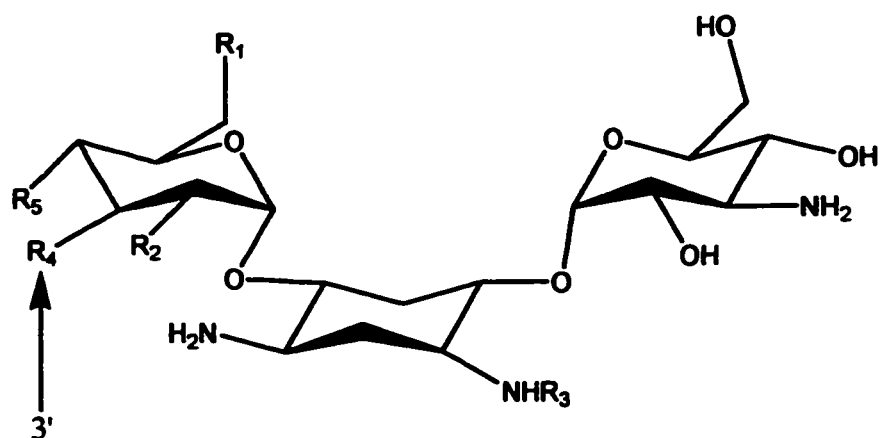


Figure 1.4. Hydrolysis of β -lactams (penicillin G) by β -lactamase enzymes.

1.3 *Aminoglycoside Antibiotics*

1.3.1 *Aminoglycoside Aminocyclitol Structure*

A second family of antibiotics whose mechanism of antimicrobial activity has been well studied are the aminoglycoside-aminocyclitols. The aminoglycosides are a large group of related antibiotics which share several characteristics including both structure and general mode of action. All family members are highly positively charged and are found to have a broad spectrum of antimicrobial activity, finding use in the treatment of both Gram positive and Gram negative pathogens. The wide range of susceptible organisms makes these antibiotics an extremely important therapeutic agent in the treatment of a variety of infections. An important second feature of aminoglycosides are their bactericidal, rather than bacteriostatic, properties (47). The aminoglycosides are grouped into three distinct classes based upon their chemical structure and all members share a common central aminocyclitol ring, at which various positions are derivatized to generate distinct drugs (Figure 1.5A-C, Table 1.1). The first group of compounds is substituted at the 4 and 6 position of the 2-deoxystreptamine aminocyclitol ring and includes such family members as kanamycin and amikacin (Figure 1.5A, Table 1.1); whereas the second closely related group is substituted at the 4 and 5 positions of the central 2-deoxystreptamine ring and includes such drugs as neomycin, ribostamycin, paromomycin and butirosin (Figure 1.5B, Table 1.1). The third group while also sharing the aminocyclitol ring is a rather loose association of aminoglycoside antibiotics which do not belong to either of the first two classes and includes such antibiotics as spectinomycin and streptomycin (Figure 1.5C, Table 1.1).



	R ₁	R ₂	R ₃	R ₄	R ₅
Kanamycin A	NH ₂	OH	H	OH	OH
Kanamycin B	NH ₂	NH ₂	H	OH	OH
Amikacin	NH ₂	OH	X	OH	OH
Tobramycin	NH ₂	NH ₂	H	H	OH
Dibekacin	NH ₂	NH ₂	H	H	H
Isepamicin	NH ₂	OH	Y	OH	OH
Netilmicin	NH ₂	NH ₂	CH ₂ CH ₃	H	NH ₂
Gentamicin A	OH	NH ₂	H	OH	OH

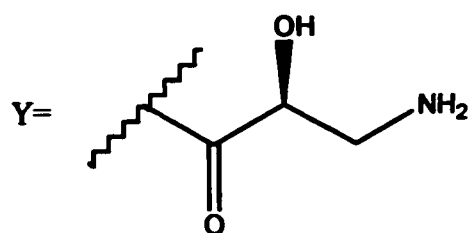
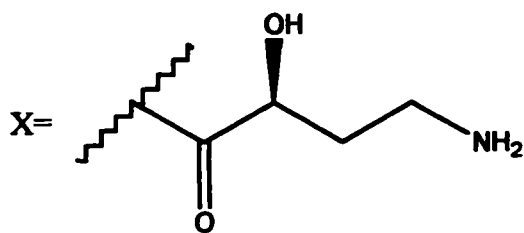
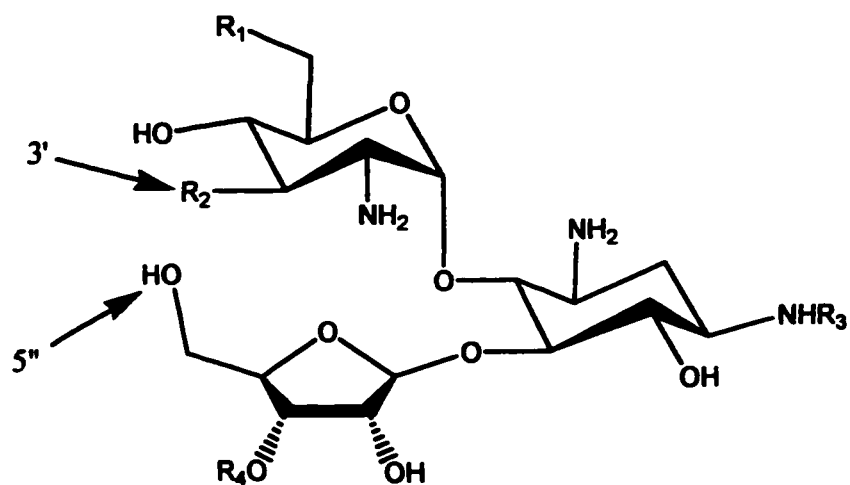


Figure 1.5A. Structure of aminoglycoside antibiotics: 4,6-disubstituted deoxystreptamine.



	R ₁	R ₂	R ₃	R ₄	R ₅
Neomycin B	NH ₂	OH	H	X	H
Paromomycin	OH	OH	H	X	H
Lividomycin A	OH	H	H	X	Mannose
Ribostamycin	NH ₂	OH	H	H	lacks this ring
Butirosin	NH ₂	OH	Y	H	lacks this ring
Neamine	NH ₂	OH	H	lacks this ring	lacks this ring

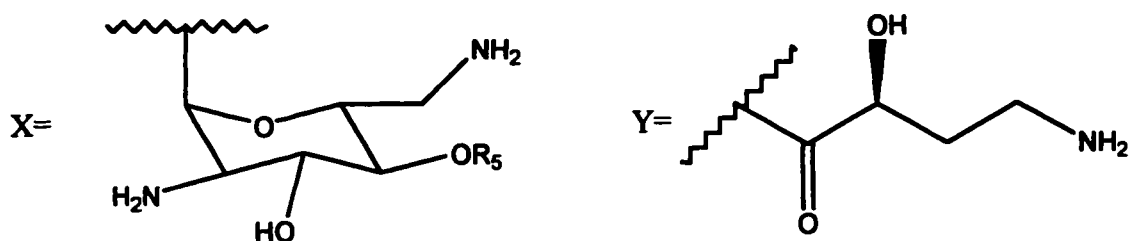


Figure 1.5B. Structure of aminoglycoside antibiotics: 4,5-disubstituted deoxystreptamine.

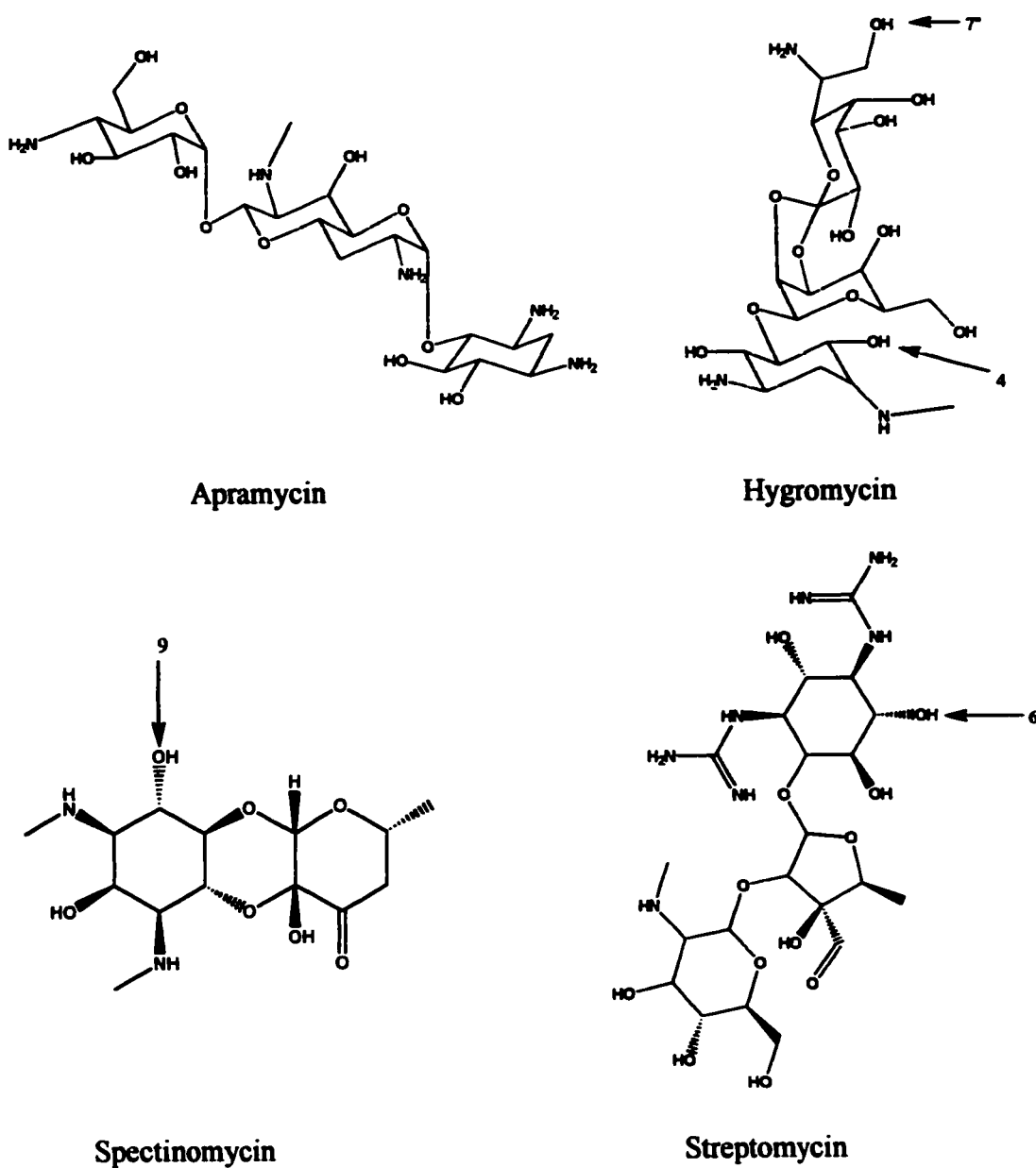


Figure 1.5C. Class 3 aminoglycosides, apramycin, hygromycin B, spectinomycin and streptomycin.

Table 1.1: Aminoglycoside-aminocyclitol antibiotics

2-deoxystreptamine aminoglycosides		
4,5-disubstituted	4,6-disubstituted	other aminoglycosides
neomycin	kanamycin A	streptomycin
ribostamycin	kanamycin B	spectinomycin
butirosin	amikacin	hygromycin
lividomycin	gentamicins	apramycin
paromomycin	isepamicin	fortimicin
	tobramycin	
	netilimicin	
	sisomicin	
	dibekacin	

Most of these antibiotics including kanamycin, gentamicin and streptomycin are natural products and are purified from such organisms as *Streptomyces*, *Micromonospora* and *Bacillus* others, however, such as amikacin, netilmicin and isepamicin are semi-synthetic derivatives of other aminoglycoside antibiotics (Figure 1.5A, B, Table 1.1).

1.3.2 Mode of Action of aminoglycosides

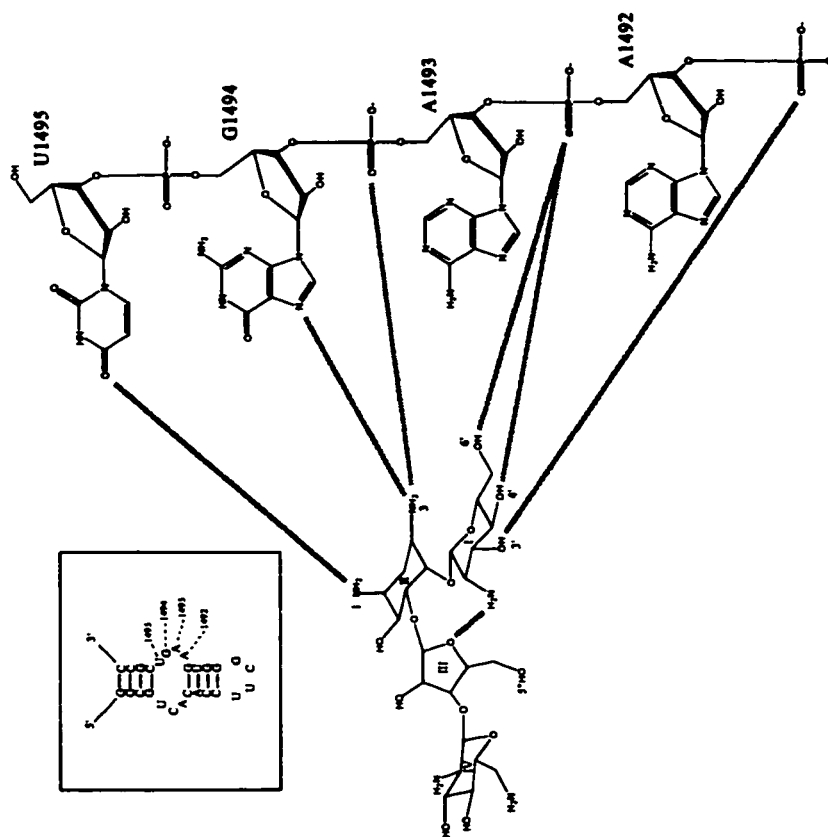
A tremendous wealth of literature exists specific for the antimicrobial activity of aminoglycoside antibiotics. Following treatment of bacterial cells with aminoglycosides, a marked inhibition of protein synthesis is observed (180, 181, 197). This is specific to 70S ribosomes and thereby specific to bacterial cells. Assays on bacterial cellular extracts demonstrate substantial inhibition of both protein initiation and elongation suggesting that aminoglycosides exert their bactericidal effects by perturbing the A-site of the 70S ribosome. Further experiments using reconstituted ribosomes from both sensitive and resistant strains have identified the 30S subunit as the specific target for streptomycin (reviewed in 57). These reconstitution experiments have also been confirmed by binding assays which show radioactively labeled aminoglycosides binding to the 30s subunit (5). These experiments although suggestive of A-site binding do not decidedly implicate this target as the site of aminoglycoside interaction. More specific targets of streptomycin interaction have emerged implicating ribosomal protein S12 and the 16s rRNA of *E.coli*. Mutations in S12 (16, 144) and a C to U transition at position 912 of the 16s rRNA (133) have both been separately implicated in conferring resistance to streptomycin. Similar studies have implicated other ribosomal proteins and RNA

residues in spectinomycin resistance, where mutations at either S5 or a C to U transition at position 1192 of the 16s rRNA are sufficient to render this antibiotic ineffective as a therapeutic agent (94, 174).

Chemical footprinting of the 16s rRNA has been effectively used by several groups in an attempt to confirm aminoglycoside interactions. The closely related aminoglycosides kanamycin, gentamicin, paromomycin and neomycin protect A1408 and G1494 from chemical modification by dimethyl sulfate (DMS) (131). Woodcock and co-workers similarly demonstrated that neamine, which is a fragment of neomycin protects residues A1408, G1491 and G1494 (202). This suggests that the pentose ring (other rings are further substituted off the pentose ring) (Figure 1.5B) plays a limited role in the mode of action of neomycin C. Such protection is consistent with a pattern observed for tRNA A-site footprinting (131). Streptomycin has been found to footprint slightly differently and strongly protects A913, A914 and A915 (132).

Recently Fourmy and colleagues have synthesized a 27 nucleotide synthetic oligonucleotide which encompasses the A-site sequence of the 16s rRNA (55). Using NMR studies, the conformation of paromomycin bound to the synthetic oligonucleotide has been determined (Figure 1.6). Numerous hydrogen bonds are formed between paromomycin and several bases of the RNA. Of particular interest is G1494 (G22 synthetic oligo numbering) which forms a hydrogen bond with an amino substituent from the C3 position of the 2-deoxystreptamine aminocyclitol ring. This position on the aminoglycoside antibiotic is likely to play an important role in aminoglycoside ribosome interactions as it is completely conserved across both the 4,5-disubstituted 2-

A.



B.

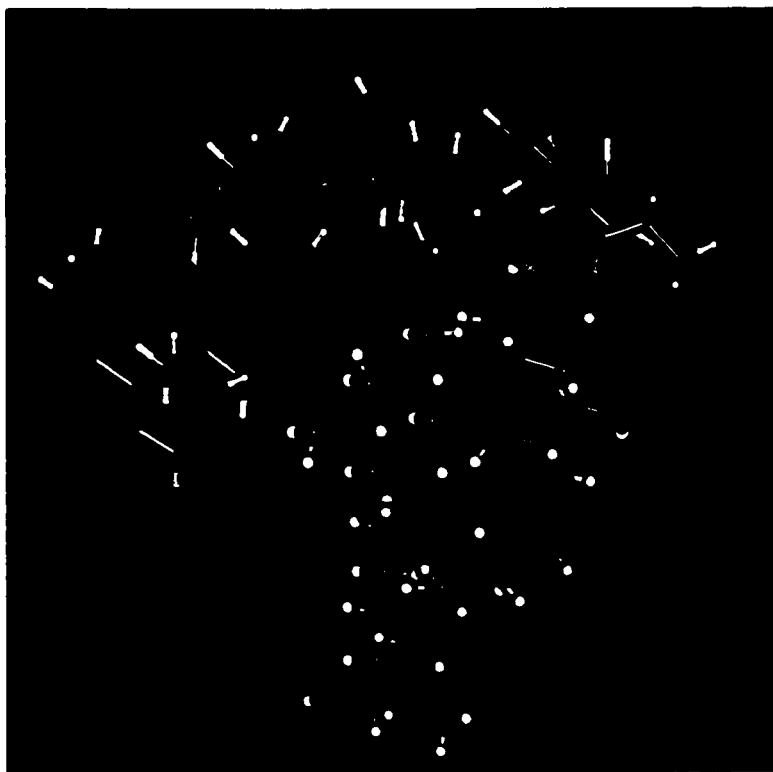


Figure 1.6. Paromomycin bound to a 16 S rRNA 27 base synthetic oligonucleotide. (A) Hydrogen bond interactions between paromomycin and oligonucleotide. Inset: secondary structure of oligonucleotide. (B) Hydrogen bond interactions between paromomycin and oligonucleotide.

deoxystreptamine and 4,6-disubstituted 2-deoxystreptamine aminoglycosides (Figure 1.5A, B). A number of hydroxyl groups and amino groups are involved in forming hydrogen bonds from rings I and II of paromomycin and residues U1495, G1494, A1493 and A1492 (Figure 1.6). No hydrogen bonds were detected between rings III or IV and the synthetic oligonucleotide (55). These results are consistent with MIC data for neamine (40 $\mu\text{g/mL}$), neomycin (5 $\mu\text{g/mL}$) and ribostamycin (10 $\mu\text{g/mL}$) which suggest that the interaction between aminoglycosides and the ribosome is minimally affected by removal of ring IV (paromomycin \rightarrow ribostamycin) or removal of rings III and IV (neomycin \rightarrow neamine) (56). Although there is only a 10 fold difference in dissociation constants upon removal of ring III removal of the pentose ring permits binding of neamine in two distinct conformations. The primary conformation is identical to that of neomycin while the alternate binding demonstrates different interactions between N1 of neamine and N7 of G1494 and N3 of neamine and O4 of U1495 which gives an inverted appearance.

Although this target is well characterized, the mechanism(s) by which these drugs exert their bactericidal effects is still widely debated and remain to be unequivocally determined. Part of the difficulty in delineating the toxic effects of aminoglycosides is due to their pleiotropic effects within the cell. At low concentrations there is a marked decrease in translation fidelity and synthesis, whereas at high concentrations of antibiotics protein synthesis is totally inhibited (70, 71). According to Tai and colleagues (181) at low concentrations, the antibiotic binds to actively translating ribosomes and thereby leads to errors in fidelity. At high concentrations, the drug binds to inactive

ribosomes preventing initiation from occurring. In the latter case as peptides are released from the ribosome, the antibiotic is at such high concentrations that it immediately fills the vacant spot left by the departing protein. From such a proposal one might speculate that the total inhibition in protein synthesis would eventually lead to cell death by inhibiting all cellular processes, and thus be the main bactericidal activity of aminoglycosides. This, however, might not prove to be the case.

1.3.3 *Aminoglycoside Entry*

Preliminary studies on aminoglycoside action identified that these highly cationic compounds bound to the cell surface of Gram negative bacteria. This interaction was determined to occur at the cell surface and could easily be reversed by washing of cells in various buffers (134). For streptomycin it appears to be an ionic interaction (134) that is essentially complete after a few seconds and is linearly dependent on the concentration of this aminoglycoside (93). Following this very rapid initial interaction of the drug and cell surface there are several other distinct phases. Bryan and Van den Elzen have identified a slow energy dependent phase (EDPI) where, following the initial adsorption of drug to cell surface, a small amount of aminoglycoside gains entry to sensitive cells (Figure 1.7) (25). It is important to note at this point that this energy dependent phase (and prior adsorption obviously) occurs in resistant cells. Hancock demonstrated that the uptake and thus bactericidal effect of streptomycin required the electron transport system and was readily inhibited by anaerobic growth, carbon monoxide and many other electron transport inhibitors (78). This energy requirement was observed for both streptomycin

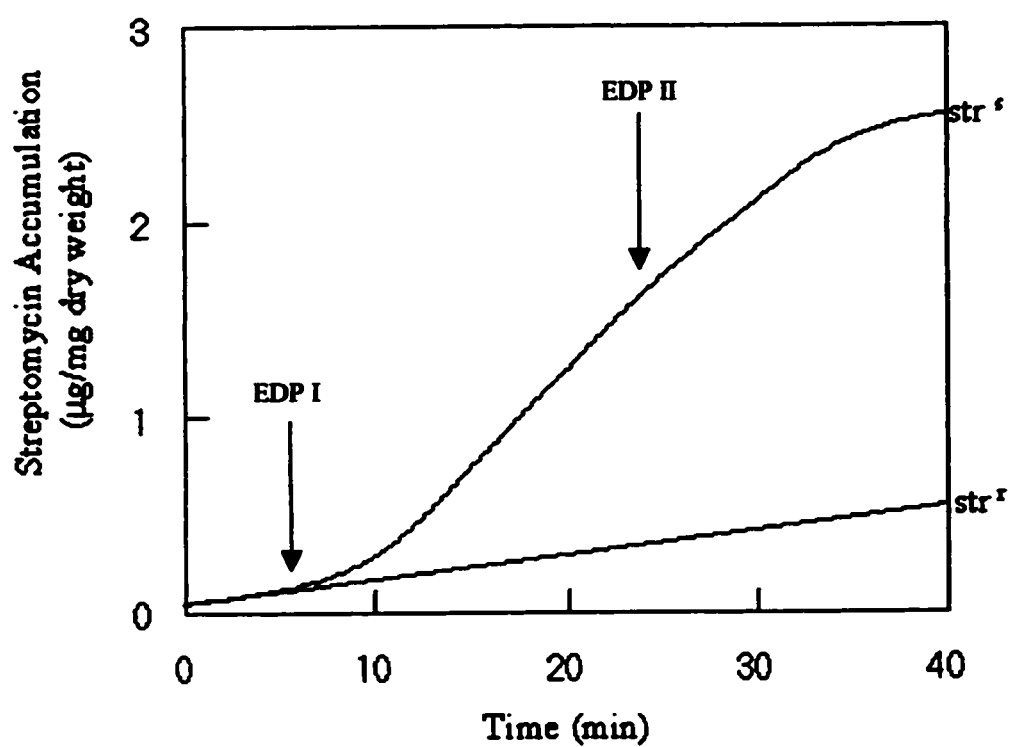


Figure 1.7. Typical aminoglycoside uptake curve for a streptomycin sensitive and streptomycin resistant strain (modified and redrawn from R.E.W. Hancock, J. Antimicrobial Chemotherapy 8: 249-276).

and gentamicin and is accepted as consistent for all bactericidal aminoglycosides. It is also important to note that this energy requirement for EDPI is not limited to *E. coli* but is also a feature of drug action in such species as *Pseudomonas aeruginosa* (26, 27) and *Staphylococcus aureus* (130). This requirement of EDPI for the electron transport system should not be taken as a requirement for O₂ as it has been demonstrated that under anaerobic conditions the alternate electron transport chain terminal acceptor nitrate (NO₃⁻) can be used as an alternate electron acceptor (24). These results are confirmed in the obligate anaerobes *Clostridium perfringens* and *Bacteroides fragilis* where aminoglycoside uptake requires anaerobic electron transport (79). The effect of anaerobic growth or electron transport inhibitors is readily reversible upon their removal.

Studies with mutants and inhibitors of the proton motive force (PMF) have demonstrated its requirement for aminoglycoside uptake. The ΔpH component of the PMF appears to have little contribution to drug entry whereas the $\Delta\Psi$ component appears to be required for aminoglycoside entry during EDPI (23, 25).

The next phase of drug entry is generally referred to as energy dependent phase II (EDPII) and is unique to aminoglycoside sensitive strains (Figure 1.7). Resistant *E. coli* strains do not exhibit an EDPII stage but continue to show low levels of drug uptake similar to EDPI levels (Figure 1.7). Interestingly, drug entry during both EDPI and EDPII is irreversible even upon extensive washing of antibiotic treated cultures (135). It is during this phase, EDPII, that inhibition of protein synthesis occurs and loss of cell viability is observed (25). Once aminoglycoside entry during EDPII occurs there is an irreversible change leading eventually to cell death.

Early in aminoglycoside research it was observed that sensitive cells exhibited significant loss of cell membrane integrity (7, 8, 77) allowing non-specific permeability to such species as K^+ , nucleotides, and amino acids as well a variety of other compounds. Conversely resistant cells did not demonstrate appreciable membrane damage upon exposure to aminoglycoside antibiotics. These results seem to implicate some membrane component as the resistance determinant for aminoglycoside antibiotics (7, 8). Within a year, Spotts and Stanier (179) demonstrated that resistance to aminoglycoside was manifested in ribosomes, and not the membrane, leading many researchers to conclude that the cumulative membrane damage was simply a secondary effect of aminoglycoside action within sensitive cells. For this reason membrane damage as a primary cause of cell death was virtually ignored until the early eighties when Davis proposed linking the observed membrane damage with the known target of aminoglycosides (30s subunit) and the observed mistranslation of proteins. Although the mechanism is not entirely understood Davis has proposed a unifying hypothesis which nonetheless remains controversial (47).

1.3.4 *Unifying Hypothesis for Aminoglycoside Action*

The mode of aminoglycoside action involves several steps, each of which is necessary but not sufficient for cell death. Consistent with studies discussed previously there is a rapid binding of aminoglycosides with the cell surface, presumably through an ionic interaction. This is then followed by EDPI where small amounts of drug enter the cell leading to mistranslation of proteins. These proteins, some of which normally are

targeted to the cytoplasmic membrane (CM) and periplasm, incorrectly incorporate into the CM (48) creating channels allowing greater influx of aminoglycosides initiating a cataclysmic cascade ending ultimately with cell death. This is found to coincide with the second energy dependent phase (EDPII) and loss of cell viability. The final step in aminoglycoside action involves entry of sufficient amounts of drug leading to total protein synthesis shutdown. This dual effect of membrane damage and total protein synthesis shutdown are both needed to cause cell death.

This hypothesis is supported by most of the data obtained to date. Davis has shown (48) that general periplasmic pools of ^{35}S labeled proteins significantly decrease upon exposure of sensitive cells to aminoglycosides. More specifically alkaline phosphatase (AP), a secretory protein, is found to partition primarily in the residual fraction (which includes the membrane fraction) and is no longer properly exported (48).

Co-treatment of cells with low levels of puromycin, a bacteriostatic antibiotic which causes premature termination of translation, has been shown to potentiate aminoglycoside killing. Puromycin is now known to lead to membrane damage (47, 48) and thereby facilitates aminoglycoside entry and cell death (92) by allowing EDP II to proceed immediately following aminoglycoside binding, thus bypassing EDP I. At high concentrations of puromycin the release of nascent peptides occurs more rapidly and these small peptides are unable to enter the membrane and cause structural damage and are thereby antagonistic to the effects of aminoglycosides. Similar results are observed with chloramphenicol, also a bacteriostatic antibiotic, which is known to exert its effect at the ribosome causing premature termination of proteins. Co-administration of

chloramphenicol and aminoglycosides has been demonstrated to lead to a resistant phenotype (in aminoglycoside sensitive cells) (26, 27, 47, 93, 152). As with puromycin it is now believed that premature release of nascent peptides prevents the synthesis of mistranslated products and their subsequent incorporation into the membrane, thus producing the resistant phenotype (7).

While it is clear that aminoglycoside action is multi faceted, requiring both membrane damage and inhibition of protein synthesis, there is much research, which needs to be completed to clarify both the initial mode of entry during EDPI and also the exact mechanism of drug toxicity.

1.4 *Aminoglycoside Resistance*

Within a year of the discovery and development of streptomycin, resistance to this aminoglycoside also became manifest (reviewed in 114). Resistance to aminoglycoside antibiotics can be grouped into two distinct mechanisms. The first group involves non-enzymatic resistance mechanisms. This method which occurs much less frequently is nonetheless clinically relevant in *Mycobacterium tuberculosis* and *Mycobacterium leprae* (137). The second group involves enzymatic resistance whereby either the antibiotic is modified in some way or the aminoglycoside target is altered enzymatically.

1.4.1 *Non-Enzymatic Resistance*

Mycobacterium tuberculosis, for which streptomycin was shown to be initially useful as a therapeutic agent, frequently shows resistance to this aminoglycoside through

non-enzymatic means. Resistance to streptomycin is conferred by a mutation in *rps L* which encodes the ribosomal protein S12 (16, 144). Two amino acids have been identified at positions 42 and 87 either of which will provide streptomycin resistance resulting in a 10 000 fold reduction in binding affinity (33). Ribosomal mutations in S12 have yet to be identified for gentamicin resistant strains. Mutations of ribosomal proteins conferring resistance to aminoglycosides is not limited to either S12 or the 30S subunit. A mutation in *rplF*, which codes for L6 of the 50S subunit is able to confer resistance to not only streptomycin but other bactericidal aminoglycosides such as gentamicin, kanamycin and neomycin (28, 46, 111). Non-enzymatic resistance to aminoglycosides can also be mediated through several other changes in *Mycobacteria* including alterations of *rrs* (codes for 16s rRNA), *hemA* (no electron transport chain) and *ubiD* (reduced levels of electron transport chain) which have been shown to confer resistance to both streptomycin and gentamicin by blocking aminoglycoside uptake (79). Conversely, there are a variety of mutations identified in *E. coli*; *rps D* (altered S4) and *rps E* (altered S5) which enhance streptomycin sensitivity (strep only) by promoting aminoglycoside binding to ribosomes (17). It is believed that these latter mutations are able to suppress mutations in *rps L* (S12) by facilitating ribosomal binding and enhancing a rapid initiation of EDPII.

It is clear from this brief review on non-enzymatic aminoglycoside resistance that many targets can be modified or altered which confer upon the bacteria the ability to thrive when challenged with these antibiotics. A broad review of these mutations is

beyond the scope of this chapter and is carefully and thoroughly reviewed elsewhere (79, 137).

1.4.2 Enzymatic Resistance

Most bacteria that exhibit resistance to aminoglycosides do so through enzymatically mediated means. It is obvious that any modification which interferes with the interaction between the drug and its target will also affect its ability to function as an antibacterial agent. Whether this modification is at the ribosome or the aminoglycoside should have little bearing on the outcome. Target modification is an effective means for a variety of organisms to evade such other antibiotics as macrolide, lincosamide and streptogramins. Strains of *Staphylococcus aureus* expressing *erm A*, *erm B* and *erm C* have been shown to confer macrolide, lincosamide and streptogramin (MLS) resistance through methylation of A2508 of the 23s rRNA (116). Many aminoglycoside producing organisms maintain self protection by methylating the N7 position of G1405 (14, 88). This resistance mechanism interestingly is limited to aminoglycoside producing strains and has yet to be isolated from a clinical setting.

The more common mechanism of resistance involves covalent modification of the aminoglycoside-aminocyclitol antibiotics. Presently, three distinct mechanisms have been clinically identified: *O*-adenylation (ANT), *O*-phosphorylation (APH), and *N*-acetylation (AAC) (Figure 1.8).

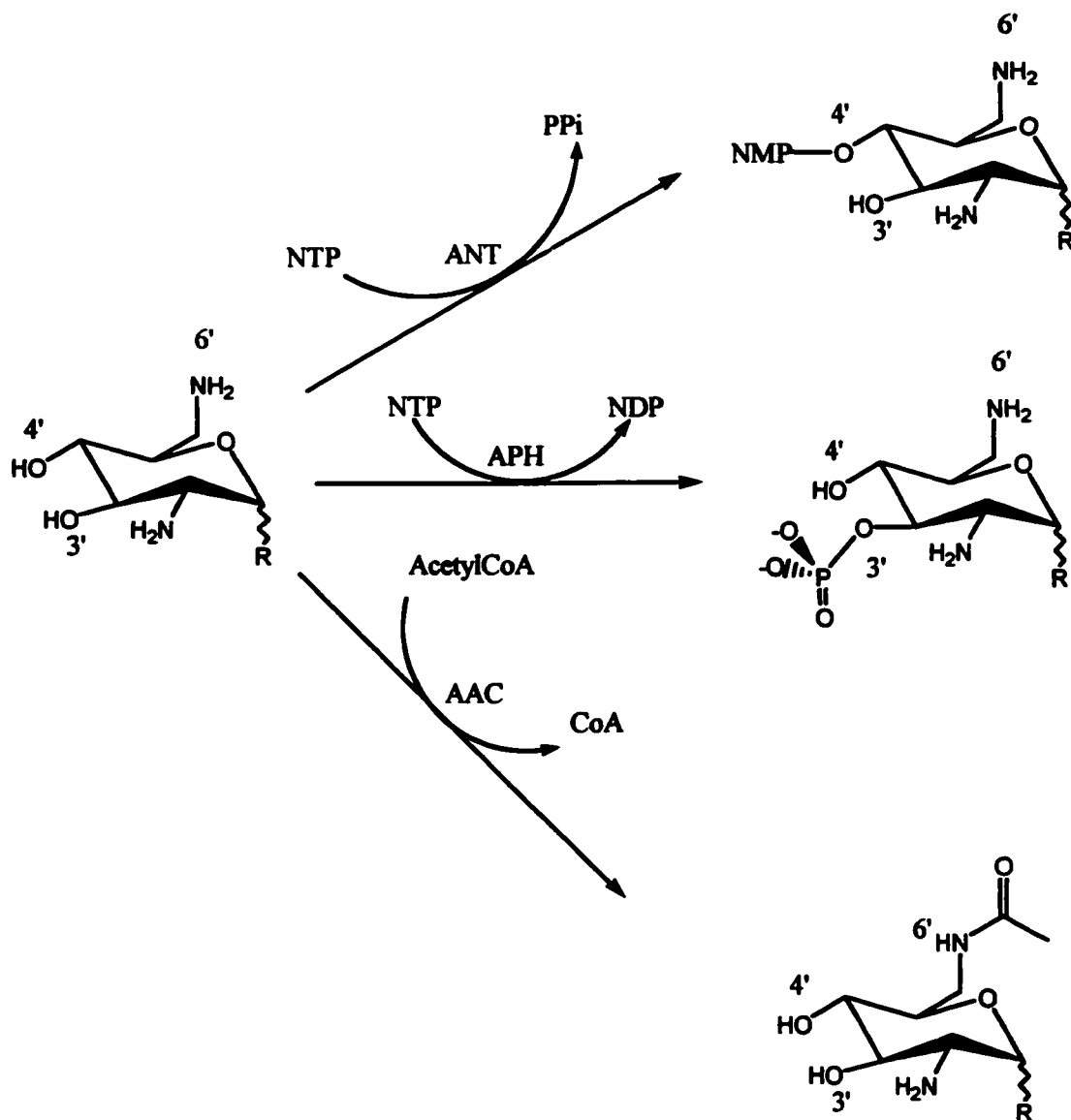


Figure 1.8. Covalent inactivation of aminoglycoside antibiotics by *O*-adenylation, *O*-phosphorylation and *N*-acetylation.).

1.4.3 Nomenclature of Aminoglycoside Resistance Enzymes:

Given the number of genes identified which confer resistance to various aminoglycosides, a systematic nomenclature was developed by Shaw and colleagues in an attempt to catalogue and group them (170). Three distinct mechanisms of aminoglycoside modification have been characterized; this includes aminoglycoside phosphotransferase (APH), aminoglycoside acetyltransferase (AAC) and aminoglycoside nucleotidyltransferase (ANT). The regiospecific site of modification is identified as a numbered position of the antibiotic. Unique aminoglycoside resistance profiles (AGRP) are identified by a Roman numeral while distinct genes conferring identical AGRP are represented by lower case letters. Thus this gene, *aph(3')-IIIa*, identifies an aminoglycoside phosphotransferase which modifies the 3' hydroxyl with a specific AGRP. The nucleotidyltransferases ANT(9)-Ia and ANT(9)-Ib share identical resistance profiles and sites of adenylation, yet differ in their gene sequence and are thus differentiated as forms a and b.

1.4.4 Dissemination of Aminoglycoside Resistance Enzymes in Nature

Protection from aminoglycoside antibiotics through the synthesis of modifying enzymes is frequently found in a wide range of aminoglycoside producing organisms allowing these bacteria to survive in high concentrations of these drugs. All three mechanisms have been detected in producing organisms and clinically obtained bacteria. Aminoglycoside producing organisms such as *Streptomyces* may harbour two distinct

modifying enzymes (e.g. APH and AAC) where expression of each is required by the organism in order to obtain high level resistance (151, 185). When expressed individually in *Streptomyces*, either AAC or APH are only able to confer low level resistance. This implies that the dually modified aminoglycoside has substantially reduced affinity for the ribosome although through what exact means this high level resistance is manifest at present remains unclear. At present *in vivo* doubly inactivated product has yet to be identified.

Modification of aminoglycosides by any of these mechanisms impairs their ability to interact with the ribosome and thus renders them ineffective as antibiotics (117).

1.4.5 *Aminoglycoside Nucleotidyltransferase (ANT)*

Seven distinct nucleotidyltransferases are now classified based upon their distinct AGRP (Table 1.2) and the genes are widely distributed in nature (170). These enzymes catalyze the transfer of an adenosine monophosphate (AMP) moiety to specific aminoglycoside hydroxyl residues (Figure 1.8) thus reducing the modified aminoglycosides therapeutic usefulness. This group of enzymes has been found to modify aminoglycoside antibiotics from all 3 classes where hydroxyls at positions 4' of the 4,5-disubstituted and 4,6-disubstituted aminoglycosides and 2" of the 4,6-disubstituted deoxystreptamine aminoglycosides are frequent targets. Similarly positions 6 and 3" of streptomycin and position 9 of spectinomycin are also known targets for modification (Figure 1.5C, Table 1.2).

Table 1.2: Aminoglycoside nucleotidyltransferases

Enzyme	Profile	Source	AGRP ^a
ANT (2")	Ia	<i>Enterobacteriaceae</i>	kan, gent, tob ^b
ANT (3")	Ia	<i>Enterobacteriaceae</i>	strep, spec
ANT (4')	Ia	<i>Staphylococcus aureus</i>	kan, tob, amik, neo
ANT (6)	Ia	<i>Enterococcus faecalis</i>	strep
ANT (6)	Ib	<i>Bacillus subtilis</i>	strep
ANT (9)	Ia	<i>Staphylococcus aureus</i>	spec
ANT (9)	Ib	<i>Enterococcus faecalis</i>	spec

^a AGRP: aminoglycoside resistance phenotype.

^b Abbreviations: amik, amikacin; kan, kanamycin; gent, gentamicin; neo, neomycin; spec, spectinomycin; strep, streptomycin; tob, tobramycin.

As discussed earlier, single organisms can harbour and express multiple resistance enzymes as is the case for ANT(2'')-Ia and ANT(3'')-Ia which are both expressed in Gram negative *Enterobacteriaceae*. This enzyme, ANT(2'')-Ia along with ANT(4')-Ia are the two most thoroughly studied aminoglycoside nucleotidyltransferases.

ANT(2'')-Ia was first isolated from a gentamicin resistant strain of *Klebsiella pneumoniae* where it was found to be expressed from plasmid pJR66 along with an APH(3') (125, 138). This raises an important side point. Aminoglycoside resistance mechanisms are primarily classified by their AGRP from clinical isolates. These AGRP are determined by minimal inhibitor concentrations (MICs) which measure growing cultures' sensitivity to increasing concentrations of antibiotic. This can lead to incorrectly identified and classified resistance mechanisms due to expression of multiple resistance proteins within the same strain. Thus it is important to identify the individual resistance gene and unequivocally identify its substrate profile prior to its assignment to a specific AGRP and mechanism.

Northrop and colleagues have completed a detailed structure-function and kinetic analysis of ANT(2'')-Ia. Initial studies identified kanamycin, gentamicin and tobramycin as the AGRP specific for this enzyme but upon more thorough *in vitro* analysis it was discovered that ANT(2'')-Ia had a much broader aminoglycoside substrate range than initially identified (63). Most of the aminoglycoside substrates assayed were found to exhibit varying degrees of substrate inhibition. This phenomenon occurs when one substrate is able to bind non-productively to the enzyme thus affecting the overall enzyme reaction (169). This behavior is often exhibited by enzymes which follow a

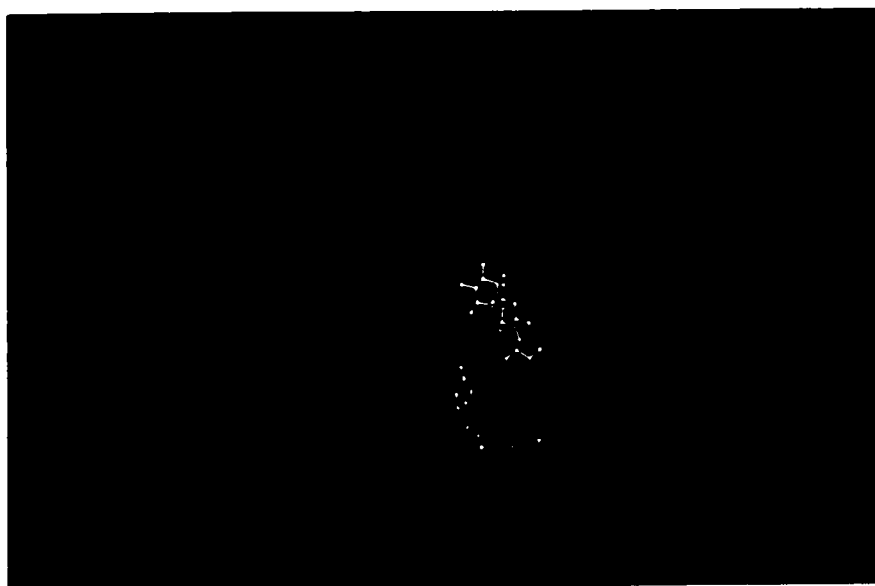
Theorell-Chance type kinetic mechanism as has been determined in the case of ANT(2'')-Ia (61, 62). A more thorough discussion of enzyme kinetics and inhibition will be presented in Chapter 3 of this thesis.

ANT(4')-Ia has also been thoroughly investigated by several groups. Similar to ANT(2'')-Ia this second enzyme is also plasmid encoded and was originally isolated from *Staphylococcus aureus*. Its resistance profile includes kanamycin, tobramycin, amikacin and neomycin (127). The three dimensional structure of this enzyme has been solved in both its native state (163) and the enzyme complexed with both β - γ -methylenadenosine 5'-triphosphate (AMPCPP: a non-hydrolyzable ATP analogue) and kanamycin (147). In both structures the enzyme forms a head to tail homodimer where the interface between the two monomers contains two enzyme active sites (Figure 1.9). Extensive interactions are required from both subunits in order to form both the ATP and aminoglycoside binding pocket and thus the monomeric form is inactive.

1.4.6 *Aminoglycoside Acetyltransferases (AAC)*

Aminoglycoside acetyltransferases are able to detoxify aminoglycosides through covalent modification of specific amino groups. Modifications have been observed at positions 1 and 3 of the 2-deoxystreptamine aminocyclitol ring as well as positions 2' and 6' of the 6-aminohexose ring (Figure 1.5A, B). These enzymes transfer an acetyl group from a donor, most often acetyl-CoA, to the aminoglycoside amino group releasing CoA and *N*-acetylated aminoglycoside (Figure 1.8).

A.



B.

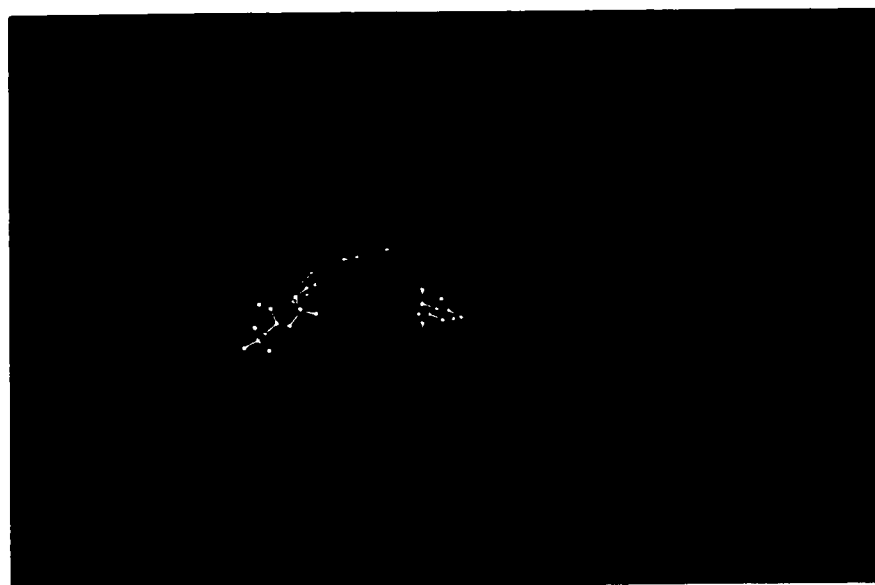


Figure 1.9. Structure of ANT(4')-Ia dimer (A) top view and (B) side view. Monomers are coloured red and blue, while ATP/aminoglycoside pairs are coloured purple or white (for each pair).

More than 30 distinct AACs have been isolated from a broad range of bacterial hosts including both Gram negative and Gram positive organisms. Many AAC have been isolated from aminoglycoside producing strains of *Streptomyces* where presumably they serve to protect the host from produced aminoglycosides. This family of enzymes is extremely diverse sharing little sequence homology although they are all generally within the 15-22 kDa range (Table 1.3). While the vast majority of the AAC genes are plasmid encoded, there have been identified several AAC (2') and AAC (6') which are chromosomally encoded (3, 42, 158, 168, 171). The AAC (1), of which there is only one identified isozyme (type I) and AAC (3) thus far have only been found to be plasmid encoded (171, 203).

The *aac(2')-I* genes, of which there are 5 identified, are of interest due to their chromosomal expression. These genes have been isolated from *Providencia stuarti* and *Mycobacteria* species and exhibit the AGRP of gentamicin, tobramycin and amikacin (3, 90, 158). The *aac(2')-Ia* which has been cloned from *P. stuarti* has recently been proposed to have a role in maintaining cell structure. *Providencia* species contain *O*-acetylated peptidoglycan as a normal component of its cell wall. Mutants of *aac(2')-Ia* have been demonstrated to have altered cell morphology due to changes in the levels of *O*-acetylation suggesting a possible role for AAC(2')-Ia in peptidoglycan synthesis (148). This hypothesis is supported by results that show that AAC(2')-Ia can acetylate gentamicin using *O*-acetylated peptidoglycan in place of acetyl CoA (149). While the origins of aminoglycoside resistance enzymes are widely debated these results suggest a

Table 1.3: Aminoglycoside acetyltransferases ^d

Enzyme	Profile	Source	AGRP ^a
AAC(2')	Ia ^c	<i>Providencia stuartii</i>	Gent, Tob, Amik ^b
AAC(2')	Ib-e ^c	<i>Mycobacteria</i>	Gent, Tob
AAC(2')	II	<i>Streptomyces kasugaaensis</i>	Gent, Arbek
AAC(6')	Ia	<i>Citrobacter diversus</i>	Kan, Tob, Amik, Neo
AAC(6')	Ib	<i>Enterobacteriaceae</i>	Kan, Tob, Amik, Neo
AAC(6')	Id	<i>Serratia marcescens</i>	Kan, Tob, Amik, Neo
AAC(6')	If	<i>Klebsiella sp.</i>	Kan, Tob, Amik, Neo
AAC(6')	Ig, h, j, k	<i>Acinetobacter sp</i>	Kan, Tob, Amik, Neo
AAC(6')	Ii ^c	<i>Enterococcus faecium</i>	Kan, Tob, Amik, Neo
AAC(6')	II	<i>Citrobacter freundii</i>	Kan, Tob, Amik, Neo
AAC(6')	Im	<i>Escherichia coli</i>	Kan, Tob, Amik, Neo
AAC(6')	In	<i>Citrobacter freundii</i>	Kan, Tob, Amik, Neo
AAC(6')	Ie	<i>Enterococci, Staphylococci</i>	Kan, Tob, Amik, Neo, Fort
AAC(6')	II	<i>Pseudomonas aeruginosa</i>	Kan, Tob, Amik, Neo
AAC(1)	I	<i>Escherichia coli</i>	Neo, Apra
AAC(3)	Ia	<i>Enterocacteriaceae</i>	Gent, Fort
AAC(3)	Ib	<i>Pseudomonas aeruginosa</i>	Gent, Fort
AAC(3)	IIa	<i>Enterobacteriaceae</i>	Gent, Tob, Dibek, Net, Siso
AAC(3)	IIb	<i>Serratia marcescens</i>	Gent, Tob, Dibek, Net, Siso
AAC(3)	IIc	<i>Escherichia coli</i>	
AAC(3)	IIIa	<i>Pseudomonas sp.</i>	Gent, Tob, Dibek
AAC(3)	IIIb	<i>Pseudomonas aeruginosa</i>	

AAC(3)	IIIc	<i>Pseudomonas aeruginosa</i>	
AAC(3)	IV	<i>Salmonella sp.</i>	Gent, Tob, Dibek, Net, Apra
AAC(3)	VI	<i>Enterobacter cloacae</i>	Gent, Tob, Siso, Net
AAC(3)	VII	<i>Streptomyces rimosus</i>	
AAC(3)	VIII	<i>Streptomyces fradiae</i>	Gent, Kan, Neo, Paro, Livid
AAC(3)	IX	<i>Micromonospora chalybeata</i>	Gent, Kan, Neo, Paro, Livid
AAC(3)	X	<i>Streptomyces griseus</i>	Gent, Kan, Neo, Paro, Livid

^a AGRP: aminoglycoside resistance phenotype.

^b Abbreviations: amik, amikacin; kan, kanamycin; gent, gentamicin; neo, neomycin; spec, spectinomycin; strep, streptomycin; tob, tobramycin; Fort, fortimicin; Net, netilmicin; Siso, sisomicin; Apr, apramycin; But, butirocin; Isep, isepamicin; Arbek, arbekacin; Ribos, ribostamycin; Paro, paromomycin; Livid, lividomycin.

^c Chromosomal gene.

^d Table modified from G.D. Wright, A.M. Berghuis and Shahriar Mobashery, *in press*.

possible “housekeeping” function for AAC enzymes and the aminoglycoside modifying activity of AAC(2')-Ia may simply be a fortuitous secondary activity.

The AAC(6') family of enzymes have been isolated from a wide range of organisms. These enzymes range in mass between 16 and 22 kDa. The *aac (6')-Ii* from *Enterococcus faecium*, which is chromosomally located, has recently been cloned, overexpressed, purified and characterized in some depth (204). This enzyme shows an AGRP of kanamycin, tobramycin, amikacin and neomycin (42). While this enzyme bears a similar substrate profile to other members of the AAC(6') family it shares only limited similarity to most family members. The AAC(6')-Ii does however share 42.2% identity with AAC (6')-Ia isolated from *Citrobacter diversus* and *Shigella sonnei* (42) suggesting that these two members are more closely related and form a subfamily within the AAC(6')-I enzymes.

One of the most extensively studied aminoglycoside acetyltransferases is AAC (6')-Ib. This enzyme which has a molecular mass of 24.5 kDa was identified from several sources (141, 189) and has an AGRP of kanamycin, tobramycin, amikacin and neomycin. Radika and Northrop have completed exhaustive substrate specificity studies and kinetic analysis of this enzyme and AAC(6')-Ib exhibits a much broader substrate profile than the AGRP would suggest. It is able to acetylate a number of other aminoglycosides such as gentamicin C1a, gentamicin B, sisomicin and nebramycin 4 (156). It is also capable of using *n*-propionyl-CoA, *n*-butyryl-CoA and 1,N⁶-ethaneacetyl-CoA as alternate acyl donors (154, 156). AAC(6')-Ib shares 76% sequence identity with AAC(6')-IIa yet they differ in their AGRP where the latter enzyme shows

resistance to gentamicin and sensitivity to amikacin, the reverse of which is seen for AAC(6')-Ib. Shaw and colleagues have demonstrated through domain swapping experiments and site directed mutagenesis that a leucine to serine mutation at position 119 (AAC(6')-Ib numbering) is sufficient to convert its AGRP to that of AAC(6')-IIa implicating this residue as critical for aminoglycoside recognition (157).

1.4.7 *Aminoglycoside Phosphotransferases (APH)*

Aminoglycoside phosphotransferases show the greatest diversity (in that there are different enzymes which can phosphorylate 7 distinct hydroxyl residues) of all aminoglycoside modifying enzymes (Table 1.4). These enzymes are widely distributed in nature being found in both Gram positive and Gram negative bacteria. Through an ATP dependent fashion, aminoglycoside phosphotransferases are able to covalently modify these antibiotics by transferring the γ -phosphate of the nucleotide to one of the aminoglycoside hydroxyl residues impairing its ability to interact at the ribosome and thereby reducing its clinical usefulness (Figure 1.8). The most thoroughly studied APHs are the APH (3') family of enzymes which phosphorylate many 2-deoxystreptamine aminoglycosides from both the 4,5 and 4,6-disubstituted aminoglycosides including both kanamycin and neomycin. For this reason this section dealing with aminoglycoside phosphotransferases will concentrate on this group of enzymes and particular attention will focus on APH(3')-IIIa which is the topic of this thesis. Within this family of APHs there have been identified twelve phosphotranferases sub-grouped into 7 distinct families (Table 1.4). These enzymes have been isolated from both Gram positive and Gram

Table 1.4: Aminoglycoside phosphotransferases ^a

Enzyme	Profile	Source	AGRP ^b
APH(3')	Ia	<i>Escherichia coli</i>	Kan, Neo, Ribos, Livid
APH(3')	Ib	<i>Escherichia coli</i>	
APH(3')	Ic	<i>Klebsiella pneumoniae</i>	
APH(3')	II	<i>Escherichia coli</i>	Kan, Amik, Neo, But, Ribos
APH(3')	III	<i>Enterococcus faecalis</i> , <i>Staphylococcus aureus</i>	Kan, Amik, Isep, Neo, But, Ribos, Livid
APH(3')	IV	<i>Bacillus circulans</i>	Kan, Neo, But, Ribos
APH(3')	Va ^c	<i>Streptomyces fradiae</i>	Neo, Ribos
APH(3')	Vb ^c	<i>Streptomyces ribosidificus</i>	
APH(3')	Vc ^c	<i>Micromonospora chalybeata</i>	
APH(3')	VI	<i>Acinetobacter baumannii</i>	Kan, Amik, Isep, Neo, But, Ribos
APH(3')	VII	<i>Campylobacter jejuni</i>	Kan, Amik, Isep, Neo, But, Ribos, Livid
APH(4)	Ia	<i>Escherichia coli</i>	Hygr
APH(7'')	Ia	<i>Streptomyces hygroscopicus</i>	Hygr
APH(2'')	Ia	<i>Enterococcus faecalis</i>	Gent, Net, Siso, Kan, Amik, Isep, Neo, But
APH(2'')	Ic	<i>Staphylococcus aureus</i> , <i>Enterococcus gallinarum</i>	Ribos, Livid
APH(3'')	Ia	<i>Streptomyces griseus</i>	Strep
APH(3'')	Ib	<i>Escherichia coli</i>	
APH(6)	Ia	<i>Streptomyces griseus</i>	Strep
APH(6)	Ib	<i>Streptomyces glaucescens</i>	
APH(6)	Ic	<i>Escherichia coli</i>	
APH(6)	Id	<i>Escherichia coli</i>	

APH(9)	Ia	<i>Legionella pneumophila</i>	Spec
APH(9)	Ib	<i>Streptomyces flavopersicus</i>	Spec

^a Modified from G.D. Wright, A.M. Berghuis and S. Mobashery, *in press*.

^b AGRP, aminoglycoside resistance profile.

^c Chromosomal gene.

Abbreviations: Kan, kanamycin; Amik, amikacin; Isep, isepamicin; Neo, neomycin; But, butirotin; Ribos, ribostamycin; Livid, lividomycin; Gent, gentamicin C; Net, netilmicin; Siso, sisomicin; Hygr, hygromycin; Strep streptomycin; Spec, spectinomycin.

negative organisms including such aminoglycoside producers as *Streptomyces griseus* (84) and *Bacillus circulans* (85) and from such clinical isolates as *Enterococcus faecalis* (190) and *Staphylococcus aureus* (74). All these enzymes have pIs around 4-5 and are roughly 30 kDa in size, with the only exceptions being APH(4')-Ia and APH(4')-Ib which are both 41 kDa (75, 212) and the bifunctional AAC(6')-APH(2'') which is 57 kDa (53, 162).

Many of the identified aminoglycoside phosphotransferases have been isolated from clinical strains and are therefore of medical importance. AAC(6')-APH(2'') is a 57 kDa bifunctional enzyme isolated from both *Enterococcus faecalis* (53) and *Staphylococcus aureus* (162), organisms that are a frequent cause of nosocomial infections. This bifunctional enzyme is the most frequent cause of high level gentamicin resistance in Gram positive cocci such as *Streptococcus* and *Staphylococcus* (50). The acetyltransferase domain, AAC(6')-Ie, and the phosphotransferase domain, APH(2'')-Ia of the bifunctional enzyme combine to produce an AGRP of kanamycin, tobramycin, neomycin, lividomycin and gentamicin C. The two domains have long been predicted to function independently with the AAC(6') activity in the N-terminal region and the APH(2'') in the C-terminal region. This has been confirmed by expressing the domains separately in both *E. coli* (53) and *Bacillus subtilis* (45). The sites of drug modification have unequivocally been assigned for both kanamycin (9) and arbekacin (109). More importantly these studies have also characterized an aminoglycoside which was both *N*-acetylated and *O*-phosphorylated. The ability of this enzyme to dually modify aminoglycosides provides bacteria harboring the *aac(6')-aph(2'')* gene with the ability to

detoxify virtually all clinically useful aminoglycosides. Martel and colleagues demonstrated that both activities bind substrate in a rapid equilibrium random fashion, although whether the singly modified substrates follow a similar mechanism at present remains unclear (124). The origin of the bifunctional enzyme has long been the source of much debate but recent studies should help to clarify the argument. APH(2'')-Ic and APH(2'')-Id have been cloned from *Enterococcus gallinarum* (35) and *Enterococcus casseliflavus* (191) and show ~25% and ~31% identity respectively with the phosphotransferase domain of the bifunctional enzyme. These results support the hypothesis proposed by Ferretti and colleagues that the bifunctional enzyme arose as the result of a gene fusion event (53). Initially this resistance mechanism was believed to be restricted to Gram positive organisms but recently it has been detected in Gram negative bacteria (100) raising an alarming possibility that this resistance gene might disseminate to more virulent bacteria rendering these organisms virtually untreatable with aminoglycoside therapy.

Alignment of the APH(3') identified regions of homology in the carboxy terminal third of the primary sequence (126, 166, 190). These regions have been divided into three discrete motifs (I-III) sharing the highest degree of homology and are proposed to also share functional roles (126).

Motif I (Figure 1.10A), which includes the consensus sequence V₁₈₅xxHGDxxxxN (where x is any amino acid) was initially proposed to have a role in phosphate transfer from ATP to the aminoglycoside acceptor (126). Martin and colleagues went as far as to propose a role for H188 as a phosphate accepting residue in a

A.		B.	
IIIa	: ELVFSHGDLGDSNIF	IIIa	: VSGFIDLGRSGRAD
Ia	: DSVVTHGDFSLDNLI	Ia	: LIGCIDVGRVGIAD
IIa	: DLVVTHGDACLPNIM	IIa	: FSGFIDCGRLGVAD
IVa	: DLVFAHGDYCAPNLI	IVa	: LSGFIDLGRAGVAD
Va	: DLVVCHGDLCPNNVL	Va	: VTGVIDVGRRLGVAD
VIa	: RLVFSHGDITDSNIF	VIa	: EIYFLDLGRAGLAD
VIIa	: ELCLSHGDM-ANFF	VIIa	: I-YFYDLARCGVAD
C.		D.	
IIIa	: DWEKIKYYILLDE	IIIa	: HGD LGDSNIFVK-----DGKVSGFIDLG
Ia	: DMNKLQFTLMLDE	c-SRC	: HRDLRAANILVG-----ENLVCKVADEFG
IIa	: DSQRIAFYRLLDE	PKA	: YRDLKPENILLD-----KNGHIKITDFG
IVa	: DEDKVRYYIRLDE	PKC-α	: YRDLKLDNVMLD-----SEGHIKIADEFG
Va	: DKEKLAFYQLLDE	PhK	: HRDLKPENILLD-----DDMNIKLTDFG
VIa	: D--KRNYFLKLDE	CDK2	: HRDLKPQNLLIN-----TEGAIKLADEFG
VIIa	: DYKKINYYILLDE	CK-I	: YRDIKPDNFIIGRPSSRNANMVYMVDRG

Figure 1.10. Primary sequence alignment of APH(3') family members (A) Motif I, (B) Motif II, (C) Motif III. Red residues are absolutely conserved residues while green represents conservation across most APH(3') family members. (D) Alignment of APH(3')-IIIa and several eukaryotic protein kinases. Enzymes are: Ia, APH(3')-Ia; IIa, APH(3')-IIa; IIIa, APH(3')-IIIa; IVa, APH(3')-IVa; Va, APH(3')-Va; VIa, APH(3')-VIa; VIIa, APH(3')-VIIa. PKA, protein kinase A; PKC, protein kinase C; PhK, phosphorylase kinase; CDK2, cyclin dependent kinase 2; CK-I, casein kinase type I.

phospho-enzyme intermediate mechanism (126) (All numbering of residues is that of APH(3')-IIIa unless otherwise indicated). This proposal, however, was based solely upon sequence alignment of APHs and other phospho transfer proteins including bacterial phosphoenolpyruvate-dependent sugar phosphotransferases which similarly were postulated to use a histidine as the phosphate acceptor for an enzyme intermediate (20, 126). The putative role for this invariant histidine residue in APH(3') was somewhat supported by mutagenesis experiments wherein this conserved histidine was mutated to such residues as tyrosine, serine and leucine. These mutations resulted in a non-functional protein (18). Results obtained by Kocabiyik and Perlin on APH (3')-IIa, however, raise doubt as to H188's putative involvement as a phosphate accepting residue. Their results demonstrate that although a H188Q mutation has reduced activity as measured through MICs and whole cell extract *in vitro* assays, the enzyme is capable of detoxifying various aminoglycoside antibiotics (107). In particular APH(3')-IIa [H188Q] demonstrates an MIC of greater than 512 µg/ml for gentamicin A which is identical to the value for wild type APH(3')-IIa. These values would tend to suggest a role incompatible for H188 functioning as a phosphate accepting residue.

Random hydroxylamine mutagenesis was employed by Blazquez and colleagues to generate five individual mutations in APH(3')-IIa (18). Of these five mutations, four mapped to Motifs I-III and only one mapped outside this region. Of the four identified mutations, within Motifs I-III, two were identified as unique H188Y mutations suggesting an important role for this residue in conferring aminoglycoside resistance. It is important to note, however, that these mutations were screened and analyzed through

in vivo methods only (18) and thereby protein expression levels could be a factor on aminoglycoside resistance. A third mutation identified within Motif I in these studies is G189R. Similar to results obtained for H188Y, the G189R mutant shows a significantly decreased resistance to aminoglycoside antibiotics as observed through replicate plating on several different aminoglycosides. The neighboring residue D190 was the target of mutagenesis studies where when altered to a glycine the enzyme APH(3')-IIa showed a significantly reduced ability to detoxify aminoglycosides as evidenced by reduced MICs and *in vitro* phosphotransferase assays (107).

These studies indicate the importance of Motif I for APH(3') activity although the exact nature of these requirements remains ill defined. The mutations discussed above (H188Y, H188Q, D190G and G189D) were analyzed by either *in vivo* drug resistance assays (MICs or replicate plating) or *in vitro* phosphotransferase assays with whole cell extracts. These studies, although laying the ground work for APH(3') mutagenesis studies, do not distinguish between binding mutants, chemical mechanism mutants or simply structural mutants. The latter possibility was to some extent addressed by Kocabiyik and co-workers (105, 107) but a more thorough investigation of Motif I needs to be completed.

The second conserved Motif (Figure 1.10B) includes the consensus sequence G₂₀₅xxDxGRxG (105, 107, 126). This sequence is also found in other ATP requiring enzymes including adenylate kinase (83) and cAMP dependent protein kinase (82) where it is proposed to function as a glycine rich flexible loop (P-loop) (59, 105, 107, 126). This proposal has lead to an intensive study of this region by several research groups.

Two of the three glycines (G205, G210) were individually mutated in APH(3')-IIa in order to assess their involvement in enzyme function. These two mutants, G205E and G210A show virtually identical MICs to each other although they are substantially reduced comparative to wild type APH(3')-IIa (105). *In vitro* assays on whole cell extracts show that both G205E and G210A have reduced affinity for ATP ($\sim 2.4\Delta K_m$) while similar studies on adenylate kinase show a more substantial effect in both ATP binding ($\sim 7.5\Delta K_m$) and AMP ($\sim 19\Delta K_m$) (159, 193). A common feature of P-loops from various sources is an invariant lysine immediately to the carboxyl side of the last glycine residue. This lysine residue is proposed to function in phosphate binding (60). Studies on K21 of ras p21 (173) and *E. coli* adenylate kinase K13 (159) show that mutations at these sites dramatically lower catalytic activity. These two lysine mutants show significant effects with K21 showing a 20 fold increase in K_m . While APH(3') appear to lack, based on primary sequence alignments, this invariant lysine it has been proposed by Kocabivik and Perlin that R211 may fulfill an analogous function for the aminoglycoside phosphotransferases (105). Mutations R211K, R211H, R211Q and R211P all show similarly reduced yet measurable MICs when compared to wild type APH (3')-IIa (105, 107). Surprisingly R211K and R211H show significantly reduced *in vitro* activity as compared to wild type (107). R211K and R211P show only slightly elevated K_m values for ATP yet substantially reduced k_{cat} values compared to wild type suggesting that although the lysine or proline can substitute for substrate binding, the active site geometry is sufficiently perturbed as to impair phosphate transfer (107).

Most APH(3') research has focused on Motifs I and II while the third identified Motif (III) remains the least clearly defined. The consensus sequence, D₂₅₀xxR/KxxF/YxxxLDE (Figure 1.10C), is present in both aminoglycoside phosphotransferases and nucleotidyltransferases but not in aminoglycoside acetyltransferases (18, 126). It is therefore proposed by Martin and colleagues that this motif may be involved in the hydrolysis of the phosphodiester bond of ATP (126). This conserved sequence has also been located within such other proteins as herpes virus DNA polymerase (68) and HIV polyprotein polymerase (195) suggesting possibly a similar role in phosphodiester hydrolysis. Other proteins identified which share this consensus sequence include human vitronectin and murine laminin and is proposed to be involved in a possible enzyme conformational change in response to its aminoglycoside substrate (126).

1.5 Synopsis

It is quite evident from the preceding sections that although much work has been targeted towards understanding aminoglycoside action and resistance mechanisms, at present a clear understanding of these areas remains lacking. It is apparent that aminoglycoside entry has a requirement for the electron transport system, in what context remains uncertain. Drug targeting to the ribosome is now quite firmly established, but what contribution to toxicity this may have is also widely debated. Resistance mechanisms to aminoglycoside antibiotics have been the focus of much research yet the molecular mechanism of most of these enzymes is quite poorly understood.

Aminoglycoside phosphotransferases, in particular the APH(3')s have been the focus of many mutagenesis studies but much of the data remains ambiguous and vague. These studies for the most part have been limited to *in vivo* resistance assays (MICs) or *in vitro* whole cell extract assays and though they are informative they are not sufficient to gain a detailed molecular understanding of aminoglycoside resistance mechanisms. To obtain such important knowledge it is vital that subsequent studies utilize highly purified resistance enzyme samples in order to better delineate enzyme substrate interactions and the mechanism of drug detoxification.

The focus of this thesis is to gain a clearer understanding of how APH(3')-IIIa is able to bind and detoxify such a broad range of aminoglycoside antibiotics.

CHAPTER 2

Overexpression, Purification and Initial Characterization of APH(3')-IIIa: Substrate Specificity Including Contribution of Amino Groups Towards Substrate Recognition.

Adapted from

McKay, G.A., Thompson, P.R., and Wright, G.D.
Biochemistry, 1994, vol. 33, pp. 6936-6944

Chapter 2

2.1 Introduction

The APH(3')-IIIa exhibits an AGRP characterized by resistance to Kan A, Kan B, Amik, Ribos, But, Neo, Paro and Livid (190). Aminoglycosides which are not substrates include tobramycin and dibekacin. These latter two aminoglycosides both lack a 3' hydroxyl (Figure 1.5A, Table 1.1). Lividomycin A, which also lacks a 3' hydroxyl, is surprisingly a substrate for the APH(3')-IIIa and this resistance has been interpreted as evidence for a 5" phosphotransferase activity.

The *aph(3')-IIIa* gene has been isolated from *Enterococcus faecalis* (formerly *Streptococcus faecalis*) (190) and *Staphylococcus aureus* (74), where the two expressed enzymes are essentially identical, with the latter form having a deletion of Val35. This would tend to suggest that the transfer between these organisms occurred relatively recently and illustrates the concern of cross species resistance gene transfer. An identical APH(3')-IIIa has also been characterized from *Streptococcus pneumoniae* BM4200 where it appears to be chromosomally expressed (40). Of equal concern is the appearance of APH(3')-IIIa in *Camphylobacter coli* (184). This is noteworthy due to the fact that only an APH(3')-IIIa isozyme has presently been identified in both Gram positive and Gram negative organisms.

aph(3')-IIIa has been isolated, cloned and sequenced from a 72.6 kb R plasmid pJH1 (190). This plasmid was originally isolated from a clinical strain of *Enterococcus*

faecalis (95). The 792 bp gene codes for a 264 amino acid protein with a predicted molecular mass of 29200 Da, agreeing with the value of 32 500 Da determined by SDS-polyacrylamide gel electrophoresis (40). Trieu-Cuot and colleagues subcloned a 1489 bp *Cla I* fragment into pBR322 to generate plasmid pAT21-1 (190). This plasmid was expressed in *E. coli* generating the aminoglycoside resistant transformant BM2182.

In order to gain a better understanding of APH(3')-IIIa's ability to phosphorylate and detoxify such a broad range of structurally diverse aminoglycosides, a thorough analysis of the enzyme substrate profile was completed. Initial substrate-function analysis necessitated large quantities of homogeneously pure enzyme and thus the construct pAT21-1 was insufficient. Towards this end an improved expression system was developed in order to generate the quantities of enzyme necessary for these studies.

2.2 Materials & Methods

2.2.1 General materials

Amik, But, Dibek, Gent C complex (mixture of C1, C1a and C2), Isep, Kan A, Kan B, Livid, Neo, Paro, Ribos and Tob were from Sigma Chemical Co. (St. Louis, MO). De-aminoaminoglycosides were prepared by Roestamadjji and coworkers (161). Pyruvate kinase/lactate dehydrogenase (PK/LDH), nicotinamide adenine dinucleotide reduced (NADH), phosphoenolpyruvate (PEP) and adenosine 5'-triphosphate (ATP) were from Sigma Chemical Co. (St. Louis, MO). Tris (hydroxymethyl) aminomethane (Tris),

anhydrous magnesium chloride and potassium chloride were from British Drug House (BDH) (Toronto, Ont).

2.2.2 Preparation and Purification of Neamine

Neamine was prepared and purified by modification of a previously reported protocol (192). Absolute methanol was prepared by incubating pre-baked (110 °C for 4 hrs) 4 Å molecular sieves with 800 mL of methanol in a round bottom flask overnight. The flask was evacuated of air by blowing N₂ gas over the methanol and then sealed with vacuum grease and parafilm.

Methanolic hydrochloride was prepared by bubbling a side reaction of NH₄Cl solid in H₂SO₄ into a flask containing 100 mL of anhydrous methanol under N₂ gas. One milliliter fractions were removed and titrated using 0.1 N NaOH until an end point of 1.8 M methanolic hydrochloride was obtained.

A reflux apparatus was set up with 280 mL of anhydrous methanol to which was then added 2.81 g of neomycin B (free base) and 60 mL of 1.8 M methanolic hydrochloride. This solution was refluxed for 2.5 hr under N₂. A 1 mL sample was removed at 75 minutes and the refluxing was then terminated at 150 minutes. The progress of the reaction was monitored by silica thin layer chromatography (TLC) in a 5:2 methanol:NH₄OH mobile phase. The R_f value of neomycin B is 0.1. Samples from the reaction taken at t=75 min and t=150 min had R_f values of 0.1, 0.24 and 0.55 which corresponds to unreacted neomycin, neamine and methanolysis product #2.

Following reflux, the methanol solution was allowed to cool on ice for 1 hr and then filtered through a sintered glass funnel. The filtrate was collected to which was added 200 mL of ice cold diethyl-ether. The sample was then allowed to precipitate overnight on ice. The following day this solution was vacuum filtered through a sintered glass funnel. The solid collected during this filtration step (F2) was resuspended in 20 mL absolute methanol to which was added ~10 g of silica gel (63-200 mesh).

A silica flash column (63-200 mesh) was prepared (2.5 cm x 50 cm) and was presaturated with 5:2 methanol:NH₄OH. The resuspended F2 fraction was added to the top of the column and subsequently eluted with ~1500 mL of 5:2 methanol:NH₄OH. Fifteen milliliter fractions were collected and analyzed by silica plate TLC using a 5:2 methanol:NH₄OH mobile phase and visualized by ninhydrin staining (0.1% w/v in 95% ethanol). Purified fractions were also assayed as substrates for APH(3')-IIIa using the coupled enzyme assay. Fractions which were substrates for APH(3')-IIIa were lyophilized until dry and subsequently analyzed by electrospray mass spectroscopy.

2.2.3 Preparation of Overproducing Constructs

A plasmid designed to overproduce APH(3')-IIIa was constructed using the polymerase chain reaction (PCR) to amplify the gene. PCR primers were designed to create a unique *Nde* I (5'-- GC TCT AGA CAT ATG GCT AAA ATG AGA --3') site 5' to the initiation codon and a unique *Hind* III (5'-- CG AAG CTT GGA CTA AAA CAA TTC ATC CAG --3') site 3' of the termination codon. These primers were used to amplify the aminoglycoside phosphotransferase gene (*aph(3')-IIIa*) from plasmid pAT21-

1 (gift of Dr. P. Courvalin, Institute Pasteur, Paris, France) by standard PCR methods.

Reaction #1 consisted of 20 mM Tris-HCl pH 8.8 @ 25 °C, 10 mM KCl, 10 mM $(\text{NH}_4)_2\text{SO}_4$, 2 mM MgSO_4 , 0.1% Triton X-100, 0.4 mM each dNTP, 1 μM *Nde I* primer, 1 μM *Hind III* primer and 10 ng of pAT21-1 template. Reaction #2 was identical with the exception that it was supplemented with 2 mM MgSO_4 . Both reaction #1 and reaction #2 were preincubated at 94 °C for 2 minutes, following which the tubes were spun briefly to collect the condensate. One unit of thermophilic Vent DNA polymerase was added to each reaction following which they were overlayed with sterile mineral oil. The reaction cycles consisted of 1 minute for denaturation at 94 °C, 1 minute at 50 °C for annealing and lastly 2 minutes at 72 °C for extension. Twenty cycles were completed followed by a 4 °C overnight incubation.

The mineral oil was extracted twice with 100 μL CHCl_3 and then the DNA was precipitated by addition of 1/10 volume 3 M sodium acetate pH 5.2 and 2 volume of ice cold 95% ethanol. The tubes were incubated at -20 °C for 15 minutes followed by a 30-minute centrifugation at 4 °C whereupon the ethanol was removed and the pellet air dried. Once dry the pellet was resuspended in 20 μL sterile deionized distilled water.

The isolated fragment was digested with *Nde I* and *Hind III* and ligated into pET-22b (+) (Novagen, Madison, WI) cut with the same restriction endonucleases. The gene was then sequenced in order to ensure that no mutations occurred during the PCR procedure. This construct places the *aph(3')-IIIa* gene under control of a bacteriophage T7 promoter and the lac operator. The new plasmid, pETAPHG6, was transformed into CaCl_2 -competent *Escherichia coli* BL21 (DE3).

2.2.4 Overexpression and Purification of APH(3')-IIIa

All purification steps were carried out at 4 °C. All Tris buffers are Tris-HCl pH 8.0 at room temperature. To insure that the overexpression of APH(3')-IIIa produced fully functional protein the original clone pAT21-1 was also used to purify enzyme as a comparative measure.

2.2.4a APH(3')-IIIa from *E. coli* JM105 [pAT21-1]

A 2-L solution of Luria broth (LB) (10 g tryptone, 10 g NaCl, 10 g yeast extract per liter) containing 100 µg/mL ampicillin was inoculated with 20 mL of an overnight culture of *E. coli* JM105 [pAT21-1] which carries the *aph(3')-IIIa* gene from *Enterococcus faecalis* inserted in the unique *Cla* I of pBR322 (190). Cells were grown at 37 °C and 250 RPM to late log phase (6 hr), harvested by centrifugation at 3000g for 10 min, and washed with 20 mL ice cold 0.85% NaCl. Cells were resuspended in 20 mL of lysis buffer (50 mM Tris-HCl pH 7.5, 5 mM EDTA (N,N,N',N'Ethylenediaminetetraacetic acid), 200 mM NaCl, 1 mM PMSF (phenylmethanesulfonylfluoride) (stock solution made in 95% ethanol) and 0.1 mM DTT (dithiothreitol)) and lysed by two passages through a French pressure cell at 20 000 psi followed by removal of cell debris by centrifugation at 10000g for 20 min. The supernatant was applied to a column containing MacroPrep Q (2x10 cm) equilibrated with buffer A (50 mM Tris pH 8.0, 1 mM EDTA). APH(3')-IIIa was eluted by a 0-50% linear gradient at 3 mL/min in buffer B (50 mM Tris-HCl pH 8.0, 1 mM EDTA and 1 M NaCl) over 70 mL. Fractions containing APH(3')-IIIa were identified by enzyme assay,

pooled and applied to a Mono Q (HR 5/5, Pharmacia) equilibrated with buffer A. Enzyme was recovered by a linear gradient to 50% buffer B over 30 mL. APH(3')-IIIa activity eluted in two distinct peaks at ~34% B and ~39% B. Each of these was concentrated over Centricon 10 (Amicon) filters and applied separately at 0.4 mL/min to a Superdex 200 column (HR 10/30, Pharmacia) equilibrated with 50 mM Tris-HCl pH 8.0, 1 mM EDTA and 200 mM NaCl. Fractions containing APH(3')-IIIa were identified by enzyme activity, pooled, and stored at 4 °C.

2.2.4b APH(3')-IIIa from *E.coli* BL21 (DE3) [pETAPHG6]

Cells were grown from overnight inocula at 37 °C (250 RPM) in Luria broth containing 100 µg/mL ampicillin to a 0.5 Abs₆₀₀ nm. Isopropyl β-D-thiogalactopyranoside (IPTG) was then added to a final concentration of 1 mM, and the cells were grown for an additional 2 hr. Cells were harvested as described above. The lysate was loaded onto a MacroPrep Q column (2x10 cm) equilibrated with buffer A, and APH(3')-IIIa was eluted by a 0-50% linear gradient in buffer B at 3 mL/min over 70 mL (fast gradient). Fractions containing APH activity were pooled and dialyzed overnight at 4 °C against 2 L of buffer A. The following day the sample was reapplied to the MacroPrep Q column, and eluted with a gradient to 50% in buffer B over 150 mL (slow gradient). The enzyme is stable at 0, 4 and -20 °C (in the presence of 5% glycerol) for several months.

2.2.5 Physical Characteristics of APH(3')-IIIa

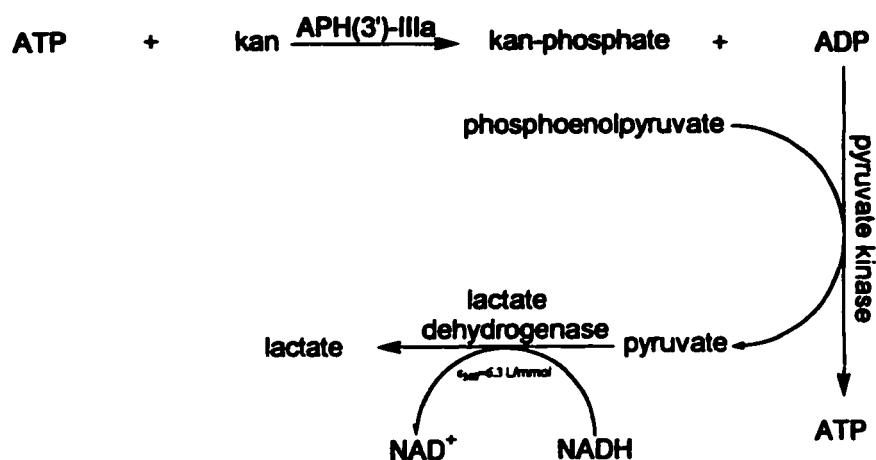
Magnesium is generally required by enzymes binding ATP and APH(3')-IIIa was assessed for its ability to phosphorylate aminoglycosides in the presence of alternate divalent cations; 10 mM Zn^{2+} , 10 mM Cu^{2+} , 10 mM Mn^{2+} , 10 mM Co^{2+} and 10 mM Sn^{2+} .

Purified samples of APH(3')-IIIa were analyzed by gel filtration using a Superdex 200 (HR 10/3) at a flow rate of 0.4 mL/min in 50 mM Tris-HCl pH 8.0, 1 mM EDTA and 200 mM NaCl. Samples of β -amylase (200 kDa), alcohol dehydrogenase (150 kDa), bovine albumin (66 kDa), carbonic anhydrase (29 kDa), cytochrome c (12.4 kDa) and blue dextran (~2000 kDa) were used as standards to obtain a calibration curve from which an estimate of the molecular weight of APH(3')-IIIa could be obtained. Purified enzyme samples were sent to Dr. Richard Smith of the McMaster Chemistry Department for electrospray mass spectroscopy.

2.2.6 Enzyme Assay- Substrate Specificity Kinetic Analysis

Phosphorylation of aminoglycoside antibiotics was monitored by coupling the release of ADP to a pyruvate kinase/lactate dehydrogenase (PK/LDH) reaction (Figure 2.1A). The oxidation of NADH was followed by continuously monitoring the absorbance at 340 nm using a Cary 3E UV-vis spectrophotometer. In a typical experiment 975 μL of assay buffer (50 mM Tris-HCl pH 7.5, 40 mM KCl, 10 mM MgCl_2 , 0.7 mM NADH, 2.5 mM phosphoenolpyruvate, 1 mM ATP) was mixed with 10 μL aminoglycoside solution and 5 μL PK/LDH (3.5 units PK & 5 units LDH) enzyme

A.



B.

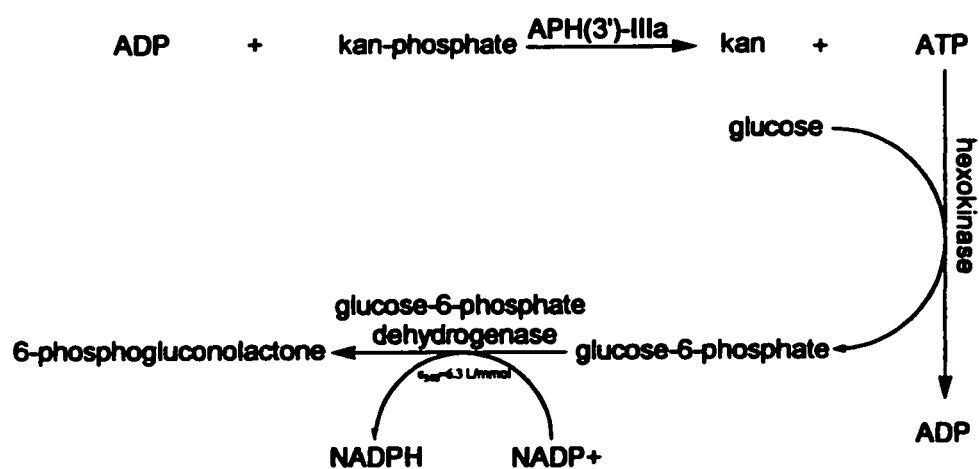


Figure 2.1. Coupled enzyme reaction. (A) Coupled enzyme reaction for forward direction kinetics. (B) Coupled enzyme reaction for reverse direction kinetics.

solution. The mixture was preincubated for 10 min at 37 °C and the assay initiated by rapid addition of 10 µL of purified APH(3')-IIIa (0.5 nmol per 10 µL).

The reverse reaction which converts;



was monitored using a second distinct coupled enzyme assay. This system couples the release of a ATP to the eventual reduction of NADP⁺ (Figure 2.1B). A typical reaction consisted of 980 µL of assay buffer (100 mM HEPES-HCl, pH 7.5, 7.5 mM MgCl₂, 100 mM KCl, 0.2 mM NADP⁺, 2 mM glucose, 9.4 units hexokinase, 1.9 units glucose-6-phosphate dehydrogenase). The variable substrate was either kanamycin 3'-phosphate or ADP while the second substrate was held saturating at concentrations of 5 mM and 1 mM respectively. All reactions were performed at 37 °C and the assay was initiated by addition of 0.12 nmol purified APH(3')-IIIa unless otherwise indicated.

Assays on partially purified enzyme, e.g., during enzyme purification, were carried out with 0.1 mM kanamycin A. The values indicated have been normalized for background ATPase activity, which was monitored by assay in the absence of aminoglycoside substrate.

All antibiotic stock solutions (for kinetics) were titrated using this assay under the assumption that addition of a phosphate group to the antibiotic was a 1:1 stoichiometric event (*vide infra*) for 4,6-disubstituted deoxystreptamine aminoglycosides. In order to determine the kinetic parameters initial rates were obtained directly from progress curves and analyzed by nonlinear least squares fitting of eq 1 by Grafit 3.0 (115),

$$\text{Eq}^n 1: \quad v = V_{max} S / (K_m + S)$$

or eq 2 for substrate inhibited reactions,

$$\text{Eq}^n 2: \quad v = V_{max} S / (K_m + S + S^2/K_I)$$

2.2.7 Large-Scale Preparation and Purification of Phosphorylated Aminoglycosides

Large-scale production of phosphorylated kanamycin A was performed by modification of the method of Coombe and George (41). The protocol was modified by P. Thompson. Incubations consisted of 100 mg of kanamycin A in 50 mM HEPES-HCl pH 7.5, 40 mM KCl, 10 mM MgCl₂ and used 1 mg of purified APH(3')-IIIa (an additional 1 mg of purified APH(3')-IIIa was added after 20 hr to drive the reaction to completion). The reactions were carried out at 37 °C with 250 RPM shaking and in sufficient volume such that the final concentration of kanamycin A was an order of magnitude below its K_I . A 2-fold molar excess of ATP was added to ensure complete phosphorylation of the aminoglycoside.

The progress of the reaction was monitored by measuring the amount of active antibiotic by a *Bacillus subtilis* susceptibility disk assay. Reaction mixture (15 µL) was applied to filter paper disks (6.4 mm) at various time points, and these disks were overlaid onto a Muellen-Hinton agar plate (300 g beef infusion, 17.5 g acid hydrolysate of casein, 17 g agar, 1.5 g starch, pH to 7.4, bring to 1 L) freshly inoculated with 200 µL of an overnight liquid culture of *B. subtilis* grown in PY media (10 g peptone, 10 g yeast extract, 5 NaCl, bring to 1 L with deionized distilled water). Plates were incubated at 37 °C overnight, and the amount of remaining antibiotic was estimated by measuring the

radius of the clear zone surrounding the disk. Once the *B. subtilis* showed no further sensitivity to the samples, the reaction was deemed complete (the MIC of kanamycin A for *B. subtilis* is $<1 \mu\text{g/mL}$).

The reaction mixture was then applied to an AG50W-X8 (Bio-Rad) (NH_4^+ form) column (10x3 cm). The column was washed with 200 mL of H_2O , and bound phosphorylated aminoglycoside was eluted by the addition of 200 mL 0.1% NH_4OH . Fractions (4 mL) were collected and analyzed by TLC on silica plates (Merck) using either methanol/ammonium hydroxide (5:2) or *n*-butyl alcohol/ethanol/chloroform/ammonium hydroxide (4:5:2:8) as mobile phases. Aminoglycosides were visualized by ninhydrin spray. Fractions containing phosphorylated aminoglycoside were pooled and lyophilized, and the residue was dissolved in 2 mL of H_2O .

The product was then applied to a BioRex 70 (Bio-Rad) (NH_4^+ form) column (11x3 cm) pre-equilibrated with 200 mL of H_2O . The column was washed with a further 200 mL of H_2O , and the product was eluted using a linear gradient of 0–1 M NH_4OH . The presence of phosphorylated drug was determined by TLC analysis of the fractions and the pooled lyophilized matter dissolved in 500 μL of H_2O .

The sample was applied to a Sephadex G-25 column (82x2 cm) equilibrated in H_2O , and the phosphorylated drug was desalted at a flow rate of 1.5 mL/min. Fractions were monitored by TLC as described above and those containing phosphorylated aminoglycoside were pooled and lyophilized.

2.3 Results

2.3.1 Purification of Neamine

Two peaks were identified eluting from the silica flash column, P1 and P2, which had individual R_f values of 0.55 and 0.24 when analyzed by silica TLC (methanol/ammonium hydroxide (5:2) mobile phase). The sample, P1, was not a substrate for APH(3')-IIIa while P2 was a substrate. P2 was found to have a mass to charge ratio of 323.4 Da/e a difference of 1.6 Da from the predicted value of neamine, 325.0 Da. The yield of P2 was calculated to be 1.4 g (~50%) and was determined by titrating the purified sample using the coupled enzyme assay. The value was calculated from the average of four separate assays.

2.3.2 Purification of APH(3')-IIIa

Samples of APH(3')-IIIa were purified from two sources to insure that overexpression of the enzyme did not affect its kinetic parameters and ability to detoxify its aminoglycoside substrate.

2.3.2a Purification of APH(3')-IIIa from *E. coli* JM105 [pAT21-1]

This initial construct was a kind gift of Dr. P. Courvalin of the Pasteur Institute. This expression system placed the *aph(3')-IIIa* gene under the control of its *E. faecalis* promoter in the plasmid pBR322. This low level constitutive expression provided a

means to purify small amounts of APH(3')-IIIa to generate a baseline activity profile for this enzyme.

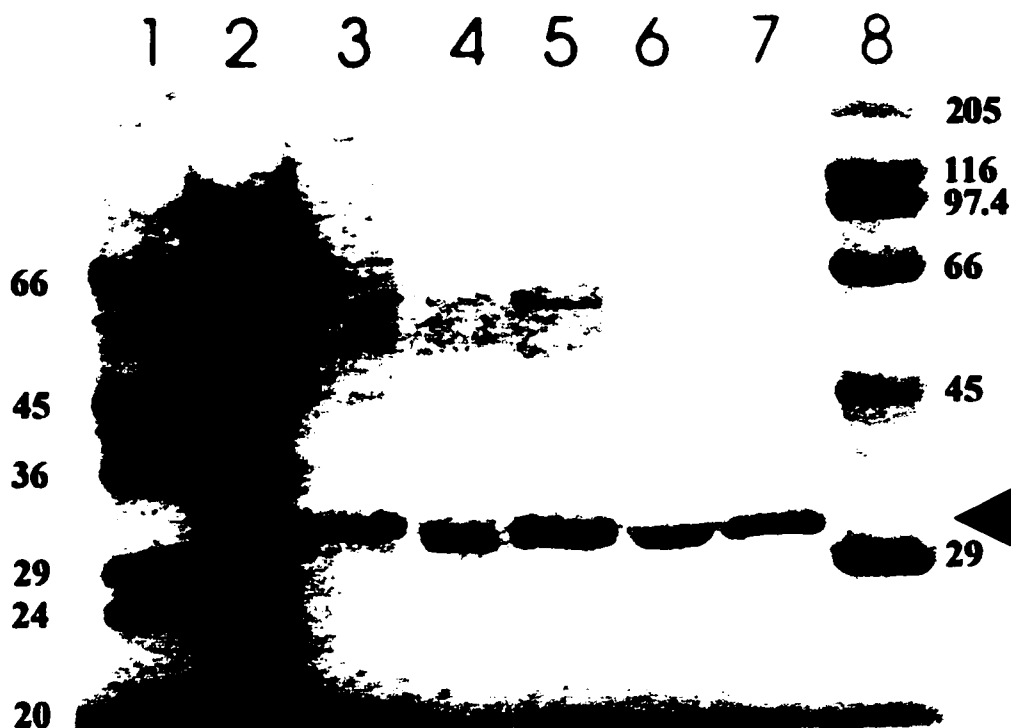
Purification of APH(3')-IIIa from *E. coli* JM105 [pAT21-1] was followed using a coupled assay to monitor kanamycin dependent ADP release. Purification of APH(3')-IIIa resulted in two different protein peaks with phosphotransferase activity from the Mono Q column (Table 2.1). These fractions were applied separately to a size exclusion column, Superdex 200, where phosphotransferase activity eluted at two different times, 41 min for Mono Q peak 1 and 37 min for Mono Q peak 2. The Superdex 200 column was standardized with proteins of known molecular weight from which a standard curve was generated. The apparent molecular mass of Mono Q peak 1 was thus calculated to be ~30 kDa while Mono Q peak 2 was determined to be ~60 kDa. These numbers are indicative of a monomer/dimer mixture, while the SDS-polyacrylamide gel electrophoresis indicated a homogeneous band of ~30 kDa (Figure 2.2).

Steady state kinetic analysis of the both the monomer form and dimer form, using the pyruvate kinase/lactate dehydrogenase coupled enzyme assay, display identical results within experimental error, demonstrating that the two forms are catalytically identical and have two active sites per dimer (Table 2.2). Dissociation of the dimer was not influenced by either salt, concentration or temperature but was sensitive to addition of 2-mercaptoethanol which converted the dimer to the monomeric form. The yield of APH(3')-IIIa from a 2 L saturated culture of *E. coli* JM105 [pAT21-1] expression system was 1.0 mg and 0.7 mg for the monomer and dimer respectively. This is a total yield of 1.37 mg of pure APH(3')-IIIa, as both the monomer and dimer are functionally identical.

Table 2.1: Purification of APH (3')-IIIa from *E. coli* JM105/pAT21-1

fraction	protein (mg)	act. (units)	sp. act. (units/mg)	purif n (-fold)	recov (%)
cell extract	299	-^a	-	-	-
Macroprep Q	13.5	15.6	1.2	-	100
Mono Q					
fraction 1	2.6	5.9	2.3	1.9	54
fraction 2	1.3	2.5	1.9	1.6	
Superdex 200					
fraction 1	1	2.5	2.5	2.1	
fraction 2	0.37	1.6	4.3	3.6	26

^a High background ATPase activity in whole cell lysates prevented accurate measurement of APH (3')-IIIa activity.



Lane	
1	Low molecular weight standards (20, 24, 29, 36, 45 and 66 kDa)
2	Whole cell extract of <i>E. coli</i> JM105 [pAT21-1]
3	Pooled Macroprep Q eluent
4	Pooled Mono Q peak 1 eluent
5	Pooled Mono Q peak 2 eluent
6	Superdex 200 peak 1 eluent
7	Superdex 200 peak 2 eluent
8	High molecular weight standards (29, 45, 66, 97.4, 116 and 205 kDa)

Figure 2.2. Purification of APH(3')-IIIa from *E. coli* JM105 [pAT21-1]. SDS-polyacrylamide gel (11%) was stained with Coomassie blue. Lane 1, low molecular weight standards (14.5, 20, 24, 29, 36, 45 and 66 kDa); lane 2, whole cell extract of *E. coli* JM105 [pAT21-1]; lane 3, pooled Macroprep Q eluent; lane 4, pooled mono Q peak 1 eluent; lane 5, pooled mono Q peak 2; lane 6, high molecular weight standards (29, 45, 66, 97.4, 116 and 205 kDa). Bullet indicates APH(3')-IIIa (▲).

Table 2.2: Kinetics^a of APH(3')-IIIa monomer and dimer

Enzyme Form	$K_{m(ATP)}$ (μ M)	k_{cat} (s^{-1})
monomer	18 ± 5.3	1.6 ± 0.15
dimer	16 ± 3.8	1.6 ± 0.11

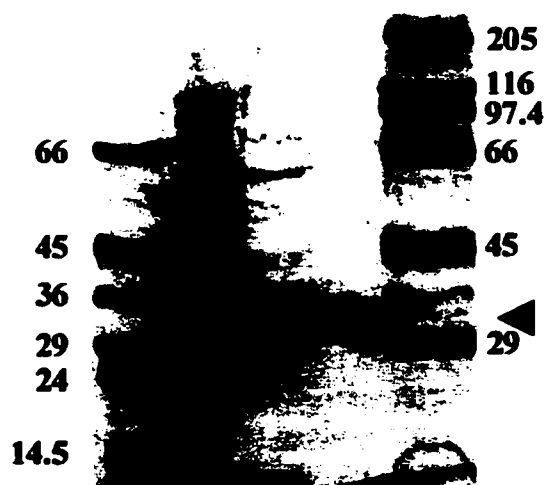
^a Kinetics were performed using identical conditions.

Although the monomer and dimer were kinetically indistinguishable, samples of enzyme were stored at 4 °C in the presence of 0.1 mM DTT and 5% glycerol, in which the monomeric form would predominate.

2.3.2b Purification of APH(3')-IIIa from *E. coli* BL21 (DE3) [pETAPHG6]

While purification of APH(3')-IIIa from pAT21-1 provided sufficient quantities of enzyme for initial comparative studies, large quantities of enzyme were necessary for subsequent studies and thus an overexpression system was designed and a construct prepared, pETAPHG6, which gave excellent overproduction of APH(3')-IIIa (Figure 2.3, Table 2.3). A two step purification yielded 30–40 mg of pure enzyme per liter of culture.

This overexpressed form of the enzyme was found to purify similarly to APH(3')-IIIa from pAT21-1, exhibiting a mixture of both monomer and dimer as determined by size exclusion chromatography. Matrix-assisted laser desorption time of flight (MALDI-TOF) mass spectrometry had significant peaks at $m/z=31030$ and 61834 indicative of a mixture of monomer and dimer consistent with the predicted masses of 30978 and 61956 respectively. Electro-spray mass spectrometry indicated proteins of $m/z=30842.0$ and 61685.5 . The values measured by electro-spray indicates a mass discrepancy of roughly 136 Da for the monomer and 271 Da for the dimer indicative of N-terminal methionine cleavage (mass of methionine 131 Da). These two forms were also found to be catalytically indistinguishable from each other. Regardless of which form was assayed, APH(3')-IIIa required Mg^{2+} as a cofactor for activity. Other metals including Mn^{2+} , Zn^{2+} , Cu^{2+} , Co^{2+} , Ca^{2+} , Sn^{2+} and Fe^{2+} could not substitute as a divalent metal cation. All metals



Lane	
1	Low molecular weight standards (14.5, 20, 24, 29, 36, 45 and 66 kDa)
2	Whole cell extract of <i>E. coli</i> BL21 (DE3) [pETAPHG6]
3	Pooled Macroprep Q fast gradient eluent
4	Pooled Macroprep Q slow gradient eluent
5	High molecular weight standards (29, 45, 66, 97.4, 116 and 205 kDa)

Figure 2.3. Purification of APH(3')-IIIa from *E. coli* BL21 (DE3) [pETAPHG6]. SDS-polyacrylamide gel (11%) was stained with Coomassie blue. Lane 1, low molecular weight standards (14.5, 20, 24, 29, 36, 45 and 66 kDa); lane 2, whole cell extract of *E. coli* BL21 (DE3) [pETAPHG6]; lane 3, pooled Macroprep Q fast gradient eluent; lane 4, pooled Macroprep Q slow gradient eluent; lane 5, high molecular weight standards (29, 45, 66, 97.4, 116 and 205 kDa). Bullet indicates purified APH(3')-IIIa (▲).

Table 2.3: Purification of APH (3')-IIIa from *E. coli* BL21 (DE3)/pETAPHG6

fraction	protein (mg)	act. (units)	sp. act. (units/mg)	purif n (- fold)	recov (%)
cell extract	600	280	0.47		100
MacroPrep Q					
fast gradient	155	248	1.6	3.4	88
slow gradient	76	167	2.2	4.7	60

were added to a final concentration of 10 mM. The coupled enzyme assay was found to be unaffected by all tested metals and thus the loss of activity was specific to APH(3')-IIIa.

2.3.3 Kinetic Properties of APH(3')-IIIa

Purified overexpressed APH(3')-IIIa from *E. coli* BL21 (DE3) [pETAPHG6] was used to determine the kinetic parameters of a series of 4,5 and 4,6-disubstituted aminoglycosides by pyruvate kinase/lactate dehydrogenase coupled assay (Table 2.4A). Most of the aminoglycoside substrates demonstrated substrate inhibition, a property which has previously been reported for an aminoglycoside acetyltransferase and an aminoglycoside nucleotidyltransferase (63, 156). Substrate inhibition was weak for most aminoglycosides, particularly the 4,6-disubstituted aminoglycosides, with both amikacin and kanamycin B showing no inhibition at all. Paromomycin, a 4,5-disubstituted aminoglycoside, demonstrated the most profound substrate inhibition with a K_i roughly 27 fold greater than its K_m .

As the 3' or 5" hydroxyl were predicted to be the regiospecific site of phosphorylation 6-amino - α -methyl glucoside, α -methyl glucoside and ribose (the former two compounds were prepared by G. Wright) were assayed as potential substrates. These three compounds were found to be neither substrates nor inhibitors of APH(3')-IIIa when added to levels of 10 mM. The minimum requirement for substrate is neamine which contains the first two rings of neomycin C (Figure 1.5B, Table 1.1, Table 2.4B).

Table 2.4A: Kinetic parameters of purified overexpressed APH(3')-IIIa

substrate	K_m (μM)	k_{cat} (s^{-1})	K_i (mM)	k_{cat}/K_m ($\text{M}^{-1}\text{s}^{-1}$)
kanamycin A	12.6 \pm 2.6	1.79 \pm 0.09	6.38 \pm 1.67	1.43 $\times 10^5$
kanamycin B	19.4 \pm 2.2	3.51 \pm 0.19	nd ^b	1.81 $\times 10^5$
amikacin	245 \pm 27	2.46 \pm 0.11	nd ^b	1.00 $\times 10^4$
neomycin B	7.72 \pm 0.9	2.08 \pm 0.07	2.65 \pm 0.59	2.69 $\times 10^5$
paromomycin	19.5 \pm 3.5	3.62 \pm 0.25	0.53 \pm 0.11	1.86 $\times 10^5$
lividomycin A	31.6 \pm 5.1	3.97 \pm 0.25	1.53 \pm 0.42	1.26 $\times 10^5$
ribostamycin	9.30 \pm 1.8	1.89 \pm 0.10	1.73 \pm 0.66	2.03 $\times 10^5$
butirosin	34.3 \pm 3.1	2.02 \pm 0.07	2.17 \pm 0.41	5.87 $\times 10^4$
isepamicin	198 \pm 28	1.41 \pm 0.21	nd ^b	7.12 $\times 10^3$
ATP ^d	27.7 \pm 3.7	1.76 \pm 0.08	nd ^b	6.37 $\times 10^4$
dATP ^d	46.3 \pm 3.9	1.0 \pm 0.02	nd ^b	2.17 $\times 10^4$
kanamycin phosphate ^c	400 \pm 85	0.11 \pm 0.01	nd ^b	2.84 $\times 10^2$
ADP ^{c,e}	21.6 \pm 3.3	0.11 \pm 0.01	nd ^b	5.09 $\times 10^3$

^a Kinetic parameters were determined using purified overexpressed APH (3') -IIIa at 37 °C as described in Materials and Methods using 1 mM ATP. The data for ATP were collected using 100 μM kanamycin A.

^b Substrate inhibition was not detected at the highest concentration of substrate tested (2-2.5 mM).

^c Kinetic parameters for reverse reaction.

^d Kan A held fixed at 120 μM .

^e Kan phosphate held at 1.3 mM.

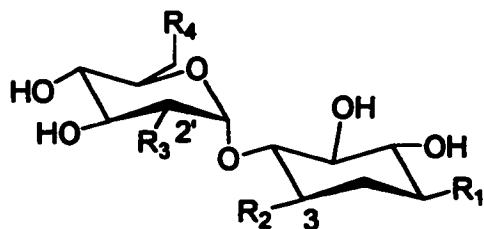
2.3.4 Use of De-amino Aminoglycosides to Probe Enzyme-Structure

Interactions

Removal of the amino groups from the C-1 position (Compound 1, Figure 2.4A) results in a poorer substrate as evidenced by a fivefold lowering of k_{cat}/K_m . These results are consistent with the data for Amik and Isep, which when substituted at the C-1 position with an amino-2-hydroxybutyramide group and an amino-2-hydroxypropionylamide group respectively are relatively poor substrates for APH(3')-IIIa with a $\Delta k_{cat}/K_m$ of 0.07 and 0.05 respectively. The effect is predominantly observed in the substrate binding with a K_m change of 19 and 16 for Amik and Isep respectively. Conversely, modification of the amino group linked to the C-3 position (Figure 1.5A, B, Compound 2 Figure 2.4A) has virtually no effect on substrate binding (Table 2.5).

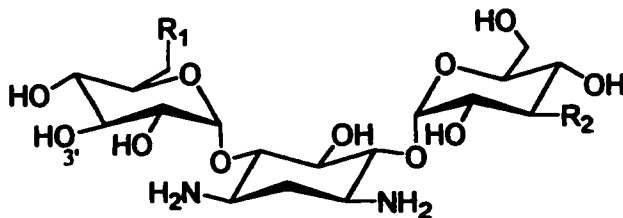
Loss of specific amino groups in the 6-aminohexose ring also proved highly significant. This ring contains the 3' hydroxyl, which is the site of aminoglycoside phosphorylation. Removal of the amino group from the C-2' position of the aminohexose (Compound 3 Figure 2.4A) ring resulted in a 10 fold loss of specificity (Table 2.4B, Table 2.5) while removal of the 6' amino group (Compound 4, Figure 2.4A) had a more profound effect upon substrate specificity with a 30 fold decrease in k_{cat}/K_m . The relative importance of this 6'-amino group is demonstrated by its removal in a kanamycin analogue (Compound 5, Figure 2.4B) which leads to a 150 fold drop in specificity. These changes in specificity in both cases are predominantly a K_m effect indicating the importance of these amino groups in aminoglycoside substrate binding.

A.



	R ₁	R ₂	R ₃	R ₄
neamine	NH ₃ ⁺	NH ₃ ⁺	NH ₃ ⁺	NH ₃ ⁺
compound 1	H	NH ₃ ⁺	NH ₃ ⁺	NH ₃ ⁺
compound 2	NH ₃ ⁺	H	NH ₃ ⁺	NH ₃ ⁺
compound 3	NH ₃ ⁺	NH ₃ ⁺	H	NH ₃ ⁺
compound 4	NH ₃ ⁺	NH ₃ ⁺	NH ₃ ⁺	H

B.



	R ₁	R ₂
kanamycin A	NH ₃ ⁺	NH ₃ ⁺
compound 5	H	NH ₃ ⁺
compound 6	NH ₃ ⁺	H

Figure 2.4. Modified 4,5 and 4,6-disubstituted deoxystreptamine aminoglycosides. (A) Neamine aminoglycoside family members and (B) kanamycin A aminoglycoside family members.

Table 2.4B: Steady-state kinetic parameters for the synthetic aminoglycoside substrates

Substrate	K_m (μM)	k_{cat} (s^{-1})	K_i^a (mM)	k_{cat}/K_m ($\text{M}^{-1} \text{s}^{-1}$) $\times 10^5$
neamine	20.0 \pm 2.8	2.00 \pm 0.15	2.00 \pm 0.4	1.0
compound 1	51.8 \pm 6.0	1.03 \pm 0.05	ND ^b	0.2
compound 2	7.1 \pm 2.5	1.16 \pm 0.11	ND	1.6
compound 3	35.9 \pm 5.7	0.39 \pm 0.01	ND	0.11
compound 4	81.8 \pm 20.7	0.28 \pm 0.04	ND	0.034
kanamycin A	12.6 \pm 2.6	1.76 \pm 0.06	6.3 \pm 1.6	1.4
compound 5	1000 \pm 580	0.93 \pm 0.41	ND	0.0093
compound 6	21.3 \pm 3.0	1.52 \pm 0.11	0.56 \pm 0.16	0.71

^a K_i is due to substrate inhibition resulting from binding of unphosphorylated aminoglycoside to the ADP•APH (3')-IIIa complex.

^b ND, no substrate inhibition detected.

Removal of the C-3" amino group from the kanamycin aminoglycoside (Compound 6 Figure 2.4B) had a modest effect on specificity where a 2 fold decrease was observed. This is consistent with the observation that specificity for neamine was virtually identical to the specificity for neomycin B (Table 2.4A, Table 2.4B).

A variety of aminoglycosides have naturally substituted hydroxyl groups in place of amino groups. Kanamycin B, which differs from kanamycin A by replacement of the 2' amino group with a hydroxyl, is an equally efficient substrate. Similarly paromomycin and lividomycin A which replace the 6' amino group with a hydroxyl, are excellent substrates for APH(3')-IIIa (Table 2.4A, Table 2.5).

Table 2.5: Structure-activity analysis of APH(3')-IIIa

Parent Compound	Structural Change	ΔK_m (%)	Δk_{cat} (%)	$\Delta k_{cat}/K_m$ (%)
Kanamycin A	2' OH→NH ₂	+50	+96	+27
Kanamycin A	1 NH ₂ →NH-AHB ^a	+1800	+37	-90
	1 NH ₂ →NH-AHP ^b	+1470	-20	-20000
Neomycin B	1 NH ₂ →OH	+150	+70	-45
Ribostamycin	1 NH ₂ →NH-AHB	+270	+6	-246

^a AHB=(S)-4-amino-2-hydroxybutyryl^b AHP=(S)-4-amino-2-hydroxypropionyl

CHAPTER 3

Kinetic Studies of APH(3')-IIIa and Rate-Limiting Step of Catalysis in Support of a Theorell-Chance Mechanism.

Adapted from

McKay, G.A., and Wright, G.D.
Journal of Biological Chemistry, 1995, vol. 270, pp. 24686-246922

McKay, G.A., and Wright, G.D.
Biochemistry, 1996, vol. 35, pp. 8680-8685

Chapter 3

3.1 *Introduction*

To date, few aminoglycoside modifying enzymes have been subject to extensive kinetic or mechanistic studies. The aminoglycoside acetyltransferase AAC(3)-I was found to follow a random kinetic mechanism (199) as was the bifunctional enzyme AAC(6')-APH(2'') (124). A third acetyltransferase AAC(6')-Ib has been established to follow a rapid equilibrium random sequential kinetic mechanism in which catalysis is the rate-limiting segment (154). The aminoglycoside nucleotidyltransferase ANT(2'')-I was demonstrated to detoxify antibiotics through a Theorell-Chance kinetic mechanism (61) where product release of the nucleotidylated aminoglycoside was found to be the rate limiting step in the reaction (62).

To date, the aminoglycoside phosphotransferases have been virtually ignored and have not been the target of any rigorous kinetic analysis. For this reason this makes APH(3')-IIIa particularly attractive to such mechanistic studies, also in part due to the availability of large quantities of pure enzyme.

Towards a greater understanding of how APH(3')-IIIa detoxifies such a broad range of aminoglycoside substrates, a thorough knowledge of the kinetic mechanism of this enzyme is essential. This type of mechanistic information is necessary to serve as the ground work towards developing either additional aminoglycosides or inhibitors of APH(3')-IIIa thus restoring the usefulness of current aminoglycoside therapies.

Criteria that often serve to characterize and compare the ability of enzymes to utilize various substrates include the kinetic constants k_{cat} , K_m , and k_{cat}/K_m the 'specificity constant'. These constants are steady state constants and are unique for a given enzyme substrate reaction. The Michaelis-Menten constant, K_m , is an apparent dissociation constant for a given enzyme/substrate complex and is reported as a unit of concentration. The true definition of K_m , however, is the substrate concentration at $\frac{1}{2}V_m$ (maximal velocity) and can therefore be a more complex expression than a true dissociation constant. The second kinetic constant often used when comparing enzyme substrate reactions is k_{cat} , the catalytic constant which represents the maximal rate of substrate to product conversion when substrate is present in saturating concentrations. This constant is reported in units of s^{-1} ($time^{-1}$) and indicates the number of substrate molecules converted to product per unit time and per enzyme active site. The final criterion that is frequently used to evaluate enzymes is the specificity constant, k_{cat}/K_m , which is reported in units of $M^{-1} s^{-1}$. This constant is biologically more relevant as a comparative tool as it is a measure of the rate of reaction at subsaturating substrate levels which is frequently the case for most enzyme-substrate interactions within an organism.

Enzyme inhibitors, which bind and affect enzyme reactions, are often used as diagnostic tools helping to delineate enzyme kinetic mechanisms. Reversible enzyme inhibitors can be grouped into three distinct classes based upon the enzyme form with which they interact. The three classes of reversible enzyme inhibitors are competitive, non-competitive and uncompetitive. The simplest, conceptually, type of inhibition is the competitive form which in effect 'competes' with the substrate for the binding site on the

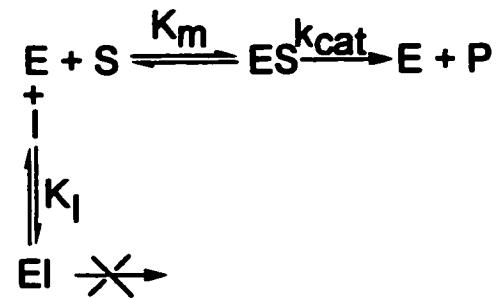
enzyme (Scheme 1). With formation of the EI complex, binding of substrate is excluded and a dead-end complex is formed. Owing to the reversible nature of this reaction the EI complex can dissociate and the enzyme is now free to form a productive ES complex (or reform the EI complex). At sufficiently high concentrations of substrate the ES complex formation becomes favoured thus a competitive inhibitor affects only the binding of substrate (K_m) and not the rate of reaction (k_{cat}).

The second form of reversible enzyme inhibition is referred to as non-competitive inhibition (Scheme 2). This form of inhibition affects only the rate of reaction (k_{cat}) and not substrate binding (K_m). This occurs because the inhibitor and substrate bind independent sites and inhibitor binding does not influence substrate binding.

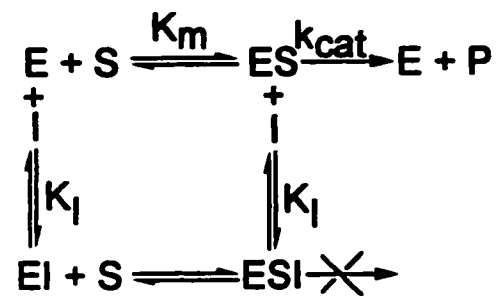
The third general form of reversible enzyme inhibition is referred to as uncompetitive inhibition (Scheme 3). This manifests itself by affecting both substrate binding and the rate of reaction. In this case inhibitor binding is dependent upon substrate binding. By forming the dead end complex ESI, this affects the $E + S$ to ES equilibrium and thus influences the substrate binding (K_m). Similarly formation of the ESI complex affects the rate of reaction (k_{cat}) by decreasing the pool of productive ES complex.

Due to the necessary requirements for each form of inhibition these species can serve as useful diagnostic probes for determining enzyme mechanism (36, 58, 163). Inhibitors can be used in a variety of studies to effectively delineate both the order of substrate addition and the order of product release. Product inhibition as a tool to differentiate bi-substrate sequential mechanisms was first proposed by Alberty (6) where

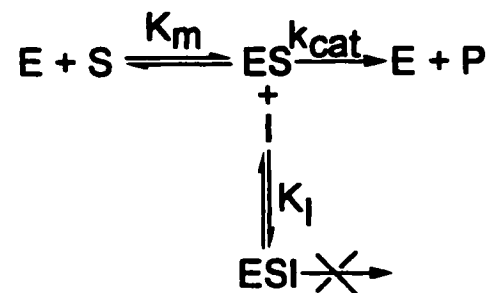
Scheme 1: Competitive Inhibition



Scheme 2: Non-competitive Inhibition



Scheme 3: Un-competitive Inhibition



he demonstrated that the order of substrate addition could be determined. Fromm and Zewe suggested that competitive inhibitors could also effectively be used to differentiate between random and ordered mechanisms and in the latter case identify the order of substrate binding (58).

The final form of inhibition that will be presented is that of substrate inhibition. While to most enzyme researchers this is often considered a nuisance, it provides an excellent means for obtaining mechanistic information.

These inhibition studies used in conjunction with each other provide an effective means to determine both the order of substrate addition and order of product release. Such mechanistic information can be valuable when considering the design of APH(3')-IIIa inhibitors.

Although informative these kinetic mechanism studies are not sufficient to delineate which step is rate-limiting. This however is frequently determined through the use of rapid quench stop flow apparatus which allows a researcher to dissect each individual rate constant. Failing the opportunity to complete such studies, alternative methodology often employed to determine various rate constants is solvent viscosity studies. This has successfully been used in the determination of rates which are controlled by diffusion (1, 10, 13, 22, 29, 39, 175). It has been demonstrated that a bimolecular collision is inversely proportional to the viscosity of the medium (110) and this provides a means to determine the viscosity effects on both k_{cat} and k_{cat}/K_m .

3.2 Materials & Methods

3.2.1 General Materials

AMP, adenylyl-imidophosphate (AMP-PNP), Tob, Dibek and ATP- γ -S were from Sigma (St. Louis, MO). D₂O (99.9%) was from Isotec. Phosphorylated kanamycin was prepared as described in section 2.2.7.

All assays were performed at 37 °C and monitored by coupling the production of ADP to the oxidation of NADH. This permits real time monitoring at 340 nm of the reactions using a Cary 3E UV-vis spectrophotometer. Unless otherwise indicated kanamycin A was held at 100 μ M as the second substrate, and ATP was held at 1 mM as the fixed second substrate. All reactions were initiated by the addition of 0.5 nmol enzyme, unless otherwise specified.

3.2.2 Initial Velocity Studies

A family of five kinetic Michaelis-Menten curves were generated under identical conditions. The variable substrate, kanamycin A, ranged in concentrations from 10 μ M to 100 μ M (K_m to $\sim 10K_m$). It is important to note that the highest concentration of kanamycin A was substantially lower than its determined K_i thus substrate inhibition in this case was not observed and did not contribute to the observed rates. The fixed substrate, ATP, was held constant at five distinct concentrations: 5 μ M, 10 μ M, 50 μ M, 200 μ M and 1000 μ M, which covers the range of $\sim 0.2K_m$ to $\sim 35K_m$. Each concentration of ATP was used to generate a separate Michaelis-Menten curve. Initial velocities were

fit to equation 3 by non-linear least squares where $K_{ia}=k_{-1}/k_1$ and represents the true dissociation constant of the first substrate in an ordered BiBi system. The rates constant k_1 is a bimolecular rate constant describing the interaction of enzyme and substrate while k_{-1} is a unimolecular rate constant describing the breakdown of the ES complex back to S and free enzyme.

$$\text{Eq}^n 3: \quad v=V_m[A][B]/(K_{ia}/K_m(B) + K_m(A)[B] + K_m(B)[A] + [A][B])$$

3.2.3 *Dead End Inhibitor Studies*

Dead end competitive inhibitors were available for both the aminoglycoside and ATP substrates. The aminoglycoside tobramycin, which lacks the 3'OH, and AMP were used as dead inhibitors of their respective substrates. Tobramycin was used as a competitive inhibitor of both kanamycin A and amikacin. ATP was held saturating at 1 mM as the fixed substrate while kanamycin A (or amikacin) was varied from $0.5K_m$ to $80K_m$ as the variable substrate. Tobramycin was held at various fixed concentrations: 0, 0.5, 1, 1.5 and 3.0 μM generating a family of plots where each line corresponds to an individual concentration of tobramycin.

AMP as a competitive inhibitor was assayed in a similar manner. Kanamycin A was held constant at 100 μM while the concentration of ATP was varied from 10 μM to 1 mM, a range of $\sim 0.3K_m$ to $\sim 35K_m$. A family of plots is generated where each line corresponds to an individual concentration of AMP. The concentration of AMP was held at 0 mM, 2.5 mM, 5.0 mM and 10 mM.

Tobramycin was then assayed as a dead end inhibitor of ATP. A family of plots was generated where amikacin was held fixed at 250 μM , roughly equal to its K_m . ATP was varied at concentrations of 10, 20, 50, 100, 200, 500 and 1000 μM which covers a range of $\sim 0.3K_m$ to $\sim 35K_m$. Tobramycin was held at fixed concentrations of 0, 0.5, 1.0, 1.5, 2.0 and 2.5 μM generating a family of curves.

AMP was similarly assayed as a dead end inhibitor of the aminoglycoside substrate kanamycin A. ATP was held fixed at a concentration of 25 μM where $K_m=27.7$ μM while kanamycin A was varied from 10 μM to 1000 μM a range of $\sim K_m$ to $\sim 80K_m$. AMP was held fixed at concentrations of 0 mM, 2.5 mM, 5.0 mM and 7.5 mM generating a family of curves.

3.2.4 *Substrate Inhibition Studies*

Both paromomycin and kanamycin A were investigated as high concentration substrate inhibitors. These two aminoglycoside substrates were assayed in a similar manner that involved varying the concentration of ATP from 10 μM to 1000 μM as in standard kinetic assays. The fixed substrate paromomycin was held constant at several different concentrations 30, 100, 300, 500, 750 and 1500 μM ; a range of $\sim K_m$ to $\sim 50K_m$ (for paromomycin) generating a family of curves. Kanamycin A was similarly assayed with its fixed concentrations ranging from 100 to 1200 μM (~ 10 to $\sim 100K_m$).

3.2.5 *Product Inhibition Studies*

The assay being used to monitor APH(3')-IIIa activity couples the release of ADP from the reaction to the eventual oxidation of NADH. The use of ADP by these coupling enzymes obviates its use as a product inhibitor in these studies and thus limits the use of phosphorylated aminoglycoside to this task.

The effect of kanamycin A phosphate was investigated under 2 conditions; where kanamycin A was held fixed at 12.6 μM (K_m) and where kanamycin A was held fixed at 126 μM ($10K_m$). All assays were similarly completed under the above two conditions. Concentrations of ATP were varied from 10 μM to 1000 μM at several fixed concentrations of kanamycin phosphate: 0, 100, 400 and 1000 μM . A family of curves was generated for both cases and data were fit by non-linear least squares to equations 4, 5, and 6 using Grafit (115).

$$\text{Eq}^n 4: \quad v = V_m[S] / (K_m(1 + I/K_{is}) + [S])$$

$$\text{Eq}^n 5: \quad v = V_m[S] / (K_m + [S](1 + I/K_{ii}))$$

$$\text{Eq}^n 6: \quad v = V_m[S] / (K_m(1 + I/K_{is}) + [S](1 + I/K_{ii}))$$

3.2.6 *Alternative Substrate Diagnostic Studies*

For these assays ATP was varied from concentrations of 10 μM to 1000 μM while the second fixed substrate aminoglycoside was held constant at a value of $10K_m$. The fixed substrate was one of the following, 100 μM kanamycin A ($\sim 10K_m$), 200 μM kanamycin B ($\sim 10K_m$), 200 μM paromomycin ($\sim 10K_m$) or 300 μM lividomycin A ($\sim 10K_m$). A Michaelis-Menten curve was generated using each fixed substrate where the

data was analyzed by non-linear least squares fitting to equation 1 (Section 2.2.6) using Grafit (115).

3.2.7 Thio Effect on the Mechanism of APH(3')-IIIa Phosphorylation

Kinetics were completed in an identical fashion as reported in Chapter 2. Aminoglycoside substrate, kanamycin A, was held at a fixed concentration of 100 μM while ATP- γ -S was varied over a range of 10 to 1000 μM . Rates were collected and analyzed by non-linear least squares fitting of data to equation 1 (Section 2.2.6) using the computer program Grafit (115).

3.2.8 Solvent Isotope Effects on the Mechanism of APH(3')-IIIa Phosphorylation

Reaction mixtures were prepared in D_2O including all substrates. All substrates were initially dissolved in 1 mL D_2O , lyophilized and then redissolved in D_2O thus exchanging all available protons. Stock enzyme solution were added in H_2O to a maximum final concentration of 5% (v/v). pD values were determined by measuring pH and adding 0.4 units ($\text{pD}=\text{pH}+0.4$). Assays were completed as previously described using ATP as the variable substrate while kanamycin A was held fixed at 100 μM , or using kanamycin A as the variable substrate while ATP was held fixed at 1000 μM . All data were analyzed by equation 1 (Section 2.2.6) for standard Michaelis-Menten kinetics and equation 2 (Section 2.2.6) for substrate inhibited reactions by non-linear least squares using the computer program Grafit (115).

3.2.9 Calibration of Ostwald Viscometer and Calculation of Solution Viscosity

The viscosity of a solution is calculated in an Ostwald viscometer by the equation $\eta = \rho B t$ where ρ is the density of water (or a particular solvent). The density of water is 0.997 g/mL at 25 °C (Merck Manual). B is a constant specific for the individual viscometers and must be empirically determined. Four separate assays were performed measuring the time (t) for water to pass through the viscometer. The viscosity of water (η) is a constant at 25 °C which allows the determination of B . Solution viscosities were determined at 25 °C in quadruplicate relative to a 50 mM HEPES-HCl, pH 7.5, 40 mM KCl, 10 mM MgCl₂ using the viscometer and the constant (B).

3.2.10 Solvent Viscosity Assays

Assays were performed with glycerol (0-30%), sucrose (0-30%) and PEG₈₀₀₀ (0-6.7%). The viscosity (of all solutions) was measured as described in the previous section. Kinetic assays were completed by standard methodologies. Glycerol was used as a viscogen where relative viscosities used were 1, 1.25, 1.81 and 2.58. The effects of glycerol as a viscogen were assayed versus variable substrate kanamycin A while ATP was held constant at 1 mM. Glycerol was also used as a viscogen towards the variable substrate ATP while kanamycin A was held constant at 100 μ M. Identical experiments were performed using either sucrose (η_{rel} =1.0, 1.24, 1.75 and 2.29) or PEG₈₀₀₀ (η_{rel} =1.0, 1.43, 1.92 and 3.30) as the viscogen.

3.3 Results

3.3.1 Initial Velocity Patterns

As a first step in the determination of the kinetic mechanism of APH(3')-IIIa, the velocity reaction with kanamycin A, a 4,6-disubstituted deoxystreptamine aminoglycoside, was determined at several fixed concentrations of ATP. Double reciprocal plots of $1/v$ versus $1/[\text{kan A}]$ are an efficient graphical means to assess and examine data (Figure 3.1) whereas they are an ineffective means for determining kinetic parameters. For this reason data is presented graphically in such plots while kinetic parameters are determined by non-linear least fit squares of appropriate equations.

The observed initial velocity patterns of intersecting lines in these plots is indicative of a sequential (Scheme 4A and 4B) rather than a ping pong (Scheme 5) mechanism. Paromomycin, a 4,5-disubstituted deoxystreptamine aminoglycoside also exhibits an intersecting pattern of initial velocity plots (data not shown) indicating that APH(3')-IIIa follows a sequential kinetic mechanism regardless of the class of aminoglycoside substrate analyzed. A K_{ia} value (for ATP) of $26.0 \pm 8.4 \mu\text{M}$ is indistinguishable from the K_m of $27.7 \pm 3.7 \mu\text{M}$ previously determined, consistent with rapid equilibrium binding of ATP (169).

3.3.2 Dead End Inhibitor Studies

Substrate analogue inhibitors of aminoglycoside (tobramycin) and nucleotide (AMP) were assayed as inhibitors of both substrates in order to elucidate substrate binding order. These results are summarized in Table 3.1. Tobramycin, which lacks the

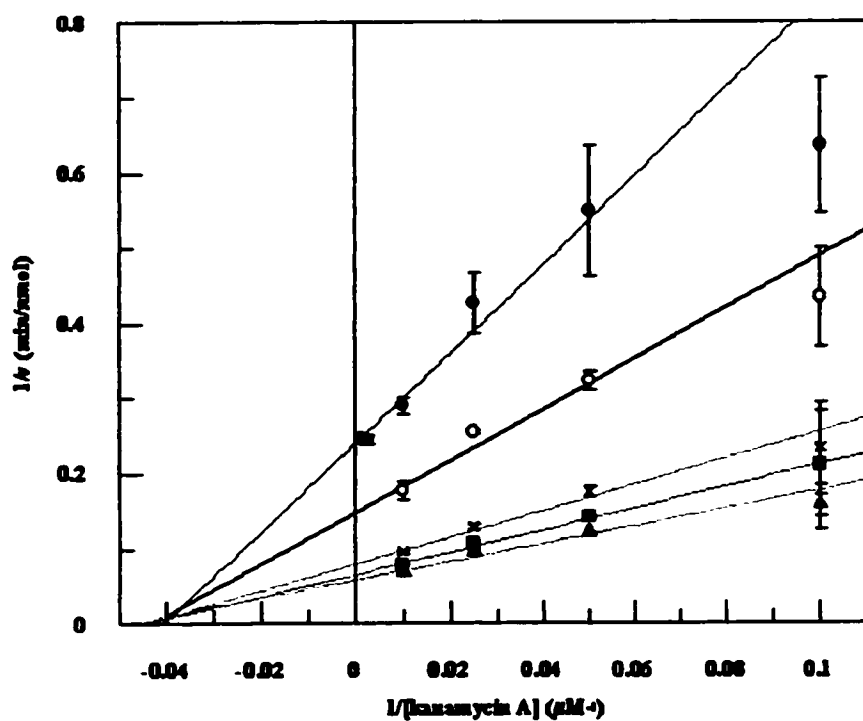
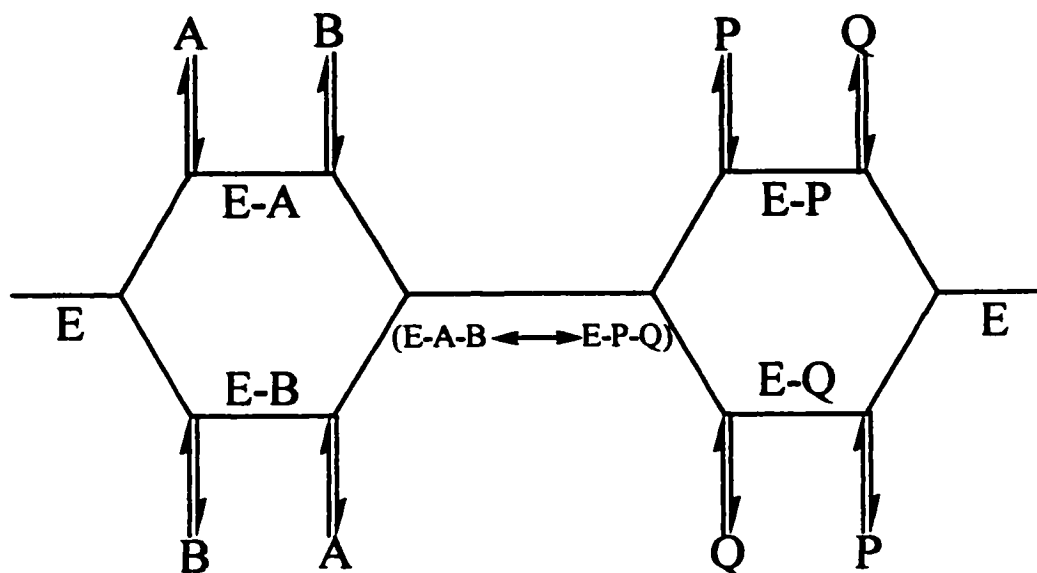


Figure 3.1. Initial velocity patterns for APH(3')-IIIa. Lineweaver Burke plots at five fixed concentrations of ATP. ATP was held at 5 μM (●), 10 μM (○), 50 μM (×), 200 μM (■) and 1000 μM (▲).

Scheme 4A: Ordered Sequential Bi-Bi Kinetic Mechanism



Scheme 4B: Random Sequential Bi-Bi Kinetic Mechanism



Scheme 5: Ping-Pong Kinetic Mechanism

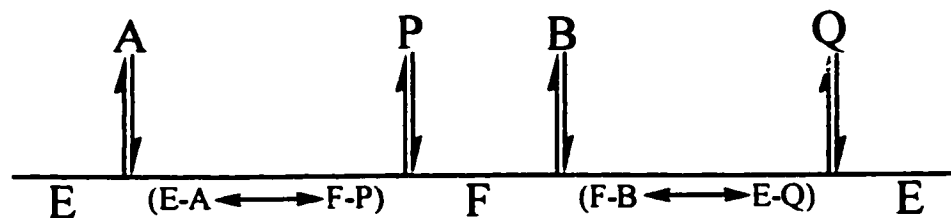


Table 3.1: Summary of Kinetic Inhibition Constants

Inhibitor	Substrate	Pattern ^a	K_{is} (μM)	K_{ii} (μM)	Equation ^b
dibekacin	amikacin	C	2.64 ± 0.77		4
tobramycin	amikacin	C	0.35 ± 0.02		4
tobramycin	kanamycin	C	0.58 ± 0.40		4
tobramycin	ATP ^c	UC		0.64 ± 0.02	5
AMP	ATP	C	4900 ± 590		4
AMP	kanamycin	NC	10000 ± 2400	7800 ± 510	6
AMP-PNP	ATP ^d	C	350 ± 50		4
AMP-PNP	amikacin ^e	NC	1800 ± 740	990 ± 80	7
kanamycin phosphate	ATP ^f	NC	10000 ± 7100	3700 ± 470	7
kanamycin phosphate	ATP ^d	- ^g			
kanamycin	ATP	UC ^h		3240 ± 225	5
paromomycin	ATP	UC ⁱ		3450 ± 320	5

^a C, competitive; NC, noncompetitive; UC, uncompetitive.

^b Data fit to equation number.

^c [amikacin] as the second substrate was held at 250 μM where $K_{m(\text{amik})} = 245 \mu\text{M}$.

^d [kanamycin A] was held at 126 μM ($=10 \times K_{m(\text{kanA})}$)

^e [ATP] was held at 25 μM ($=K_{m(\text{ATP})}$)

^f [kanamycin A] was held at 12.6 μM ($=K_{m(\text{kanA})}$)

^g No inhibition observed at 5000 μM kanamycin phosphate.

^h Substrate inhibition by kanamycin A, a 4,6-disubstituted deoxystreptamine aminoglycoside.

ⁱ Substrate inhibition by paromomycin, a 4,5-disubstituted deoxystreptamine aminoglycoside.

3'-OH, was found to be a potent competitive inhibitor of kanamycin A with a K_{is} of $0.58 \pm 0.40 \mu\text{M}$ as well as a competitive inhibitor of amikacin with a K_{is} of $0.35 \pm 0.02 \mu\text{M}$ (Figure 3.2, Table 3.1). It was also found to be an uncompetitive inhibitor of ATP with a K_{ii} of $0.64 \pm 0.02 \mu\text{M}$ (Figure 3.3, Table 3.1).

AMP was found to be a weak competitive inhibitor of ATP (Figure 3.4, Table 3.1) with a K_{is} of $4.9 \pm 0.59 \text{ mM}$. It was also found to be a noncompetitive inhibitor of kanamycin A with a K_{is} of $10 \pm 2.4 \text{ mM}$ and K_{ii} of $7.8 \pm 0.51 \text{ mM}$ (Figure 3.5, Table 3.1). This is consistent with an ordered BiBi substrate addition where ATP is the obligate first substrate followed by aminoglycoside addition.

A second nucleotide analogue, AMP-PNP (a nonhydrolyzable ATP isostere) was found to be a competitive inhibitor of ATP with a K_{is} of $350 \pm 50 \mu\text{M}$ (Table 3.1). It was also found to be a noncompetitive inhibitor of amikacin with a K_{ii} of $990 \pm 80 \mu\text{M}$ and a K_{is} of $1.8 \pm 0.74 \text{ mM}$ (data not shown). These results are consistent with inhibition results obtained using AMP and indicate an order of obligate ATP addition first followed by aminoglycoside addition.

3.3.3 Substrate Inhibition Studies

At high concentrations of aminoglycoside, a decrease in the rate of reaction is observed. This is indicative of nonproductive binding of the drug to a catalytically incompetent form of the enzyme. I initially examined substrate inhibition by paromomycin as it exhibited strong inhibition. Over a wide range of paromomycin concentrations ($\sim K_m$ to $\sim 50K_m$), the family of reciprocal plots shows a decrease in the

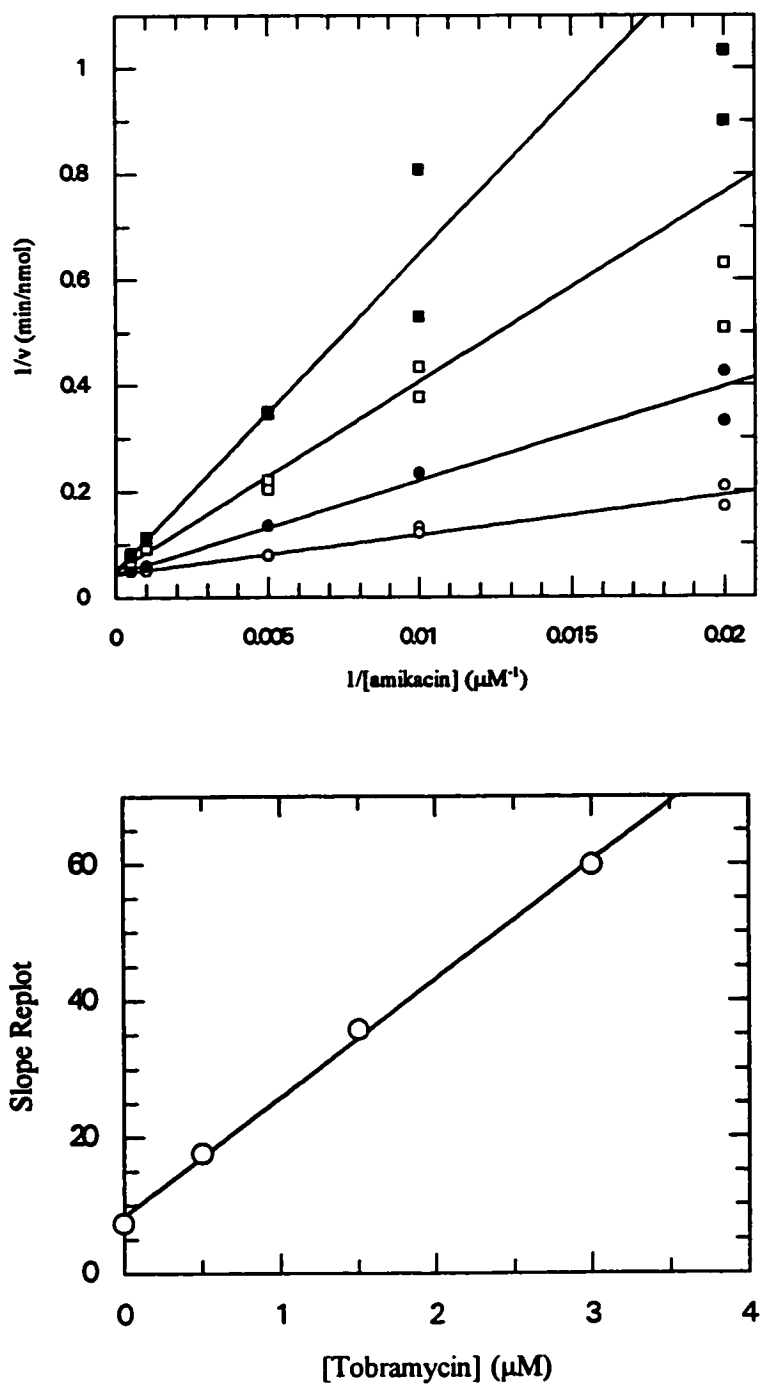


Figure 3.2. Competitive inhibition of APH(3')-IIIa through the use of the dead-end inhibitor tobramycin. Slope replot of amikacin versus the inhibitor tobramycin.

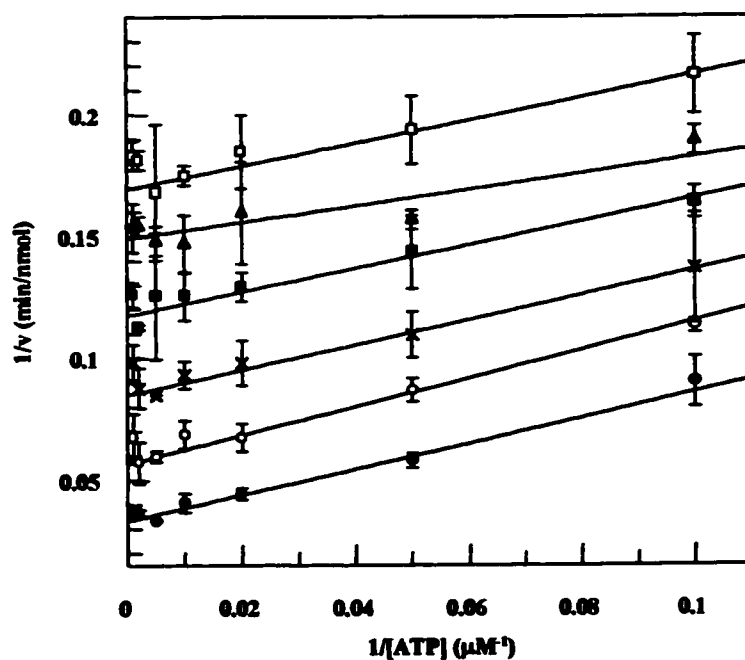
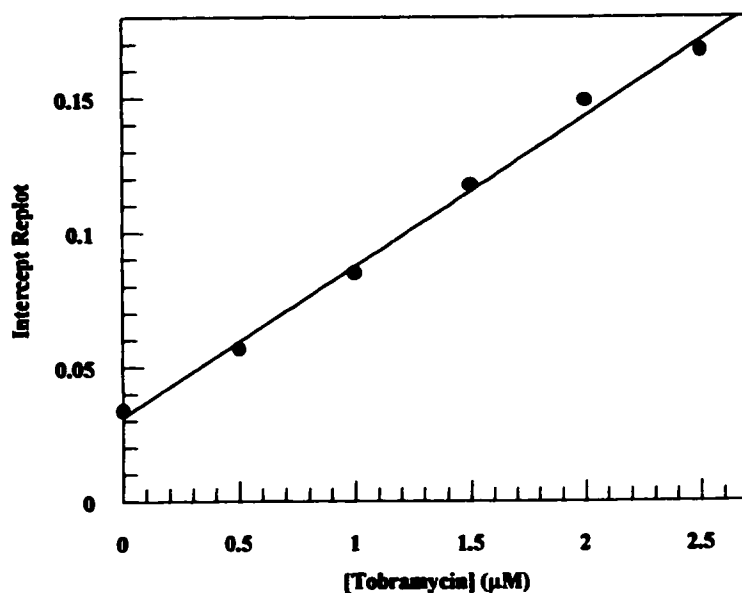
A.**B.**

Figure 3.3. Uncompetitive inhibition of APH(3')-IIIa through the use of the dead-end inhibitor tobramycin. (A) Lineweaver Burke plots at 6 fixed concentrations of tobramycin. Tobramycin was held fixed at 0 μM (●), 0.5 μM (○), 1.0 μM (×), 1.5 μM (■), 2.0 μM (▲) and 2.5 μM (□). (B) Intercept replot for ATP versus $[\text{Tobramycin}]$.

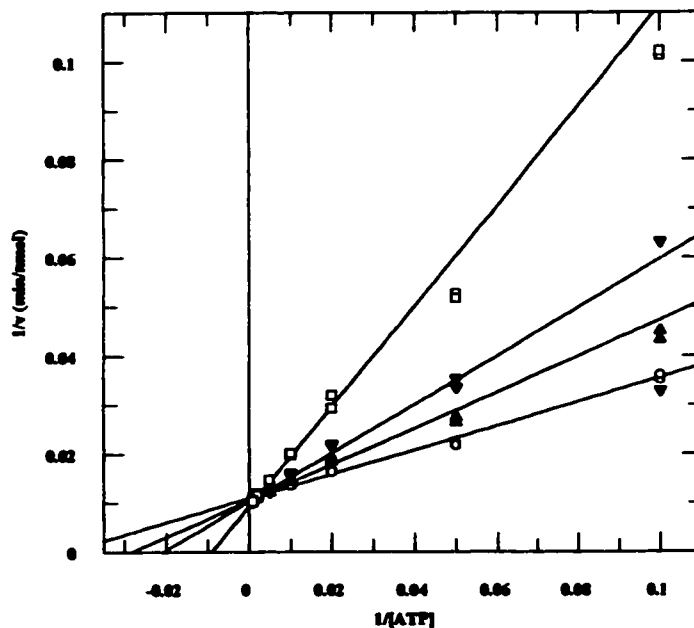
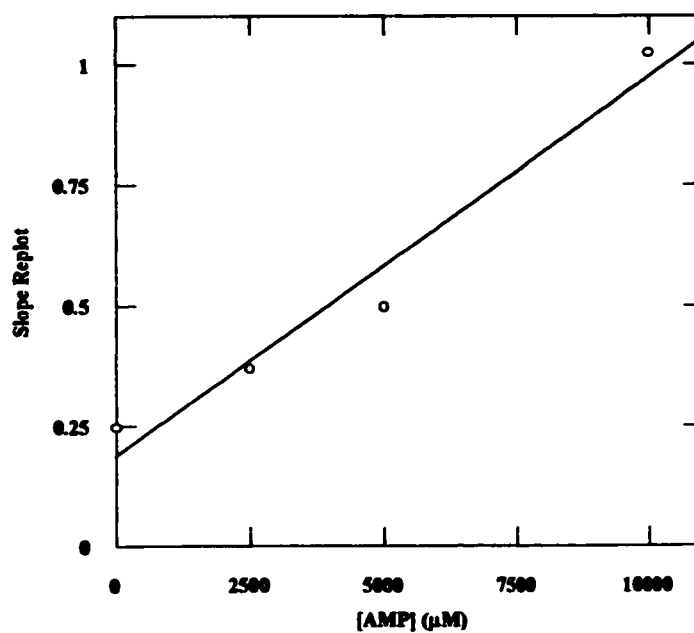
A.**B.**

Figure 3.4. Competitive inhibition of APh(3')-IIIa through the use of the dead-end inhibitor AMP. (A) Lineweaver Burke plot at 4 fixed concentrations of AMP. Concentrations of AMP were 0 mM (O), 2.5 mM (▲), 5.0 mM (▼) and 10 mM (□). (B) Slope replot for ATP versus $[AMP]$.

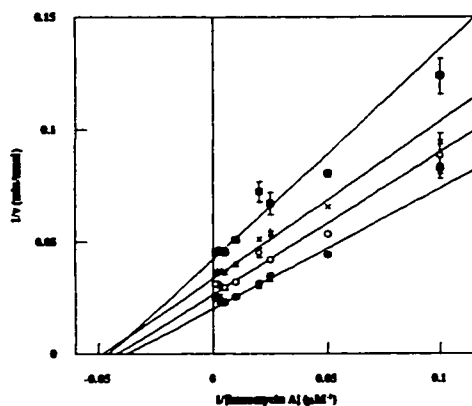
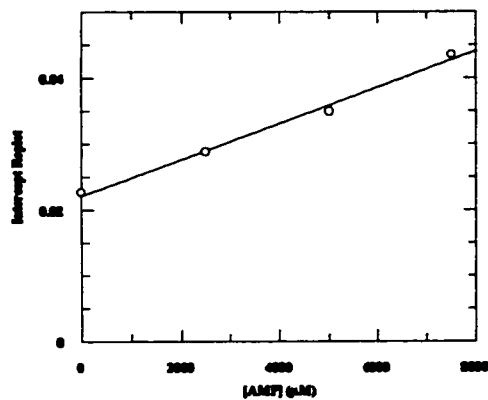
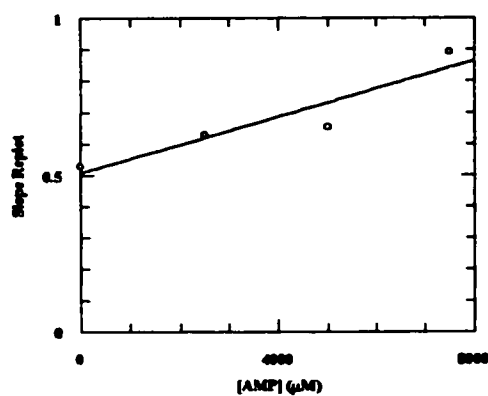
A.**B.****C.**

Figure 3.5. Non-competitive inhibition of APH(3')-IIIa for kanamycin A through the use of the dead-end inhibitor AMP. (A) Lineweaver Burke plot at 4 fixed concentrations of AMP. Concentrations of AMP were 0 mM (O), 2.5 mM (\blacktriangle), 5.0 mM (\blacktriangledown) and 7.5 mM (\square). (B) Intercept replot for kanamycin A versus $[\text{AMP}]$. (C) Slope replot for kanamycin A versus $[\text{AMP}]$.

slopes ($K_{m(ATPapp)}/V_m$) approaching the normal limit of $K_{m(ATP)}/V_m$ (Figure 3.6). As the concentration of aminoglycoside continues to increase, the family of plots generated forms a series of parallel lines indicative of uncompetitive inhibition. The slope replot therefore decreases over low concentrations of aminoglycoside reaching a minimum above $10K_m$ (Figure 3.6, Table 3.1). To more closely examine the nature of the substrate inhibition, a second aminoglycoside substrate, kanamycin A, was chosen as the fixed substrate at several saturating levels in order to avoid confusing the replot data with initial velocity effects and to limit the results to substrate inhibition effects. The inhibition is again uncompetitive with a linear intercept replot (Figure 3.7, Table 3.1), and a standard slope replot (not shown) was associated with linear uncompetitive inhibition. This indicates nonproductive binding of kanamycin to the (E•ADP) complex suggesting at least partial rate-limiting ADP product release. This linear uncompetitive inhibition is observed for both classes of aminoglycoside substrates.

3.3.4 *Product Inhibition Studies*

Due to the limitations of the coupled assay, which consumes product ADP, only kanamycin phosphate was available for use as a product inhibitor. Kanamycin phosphate was found to be a noncompetitive inhibitor with respect to ATP when the concentration of kanamycin was held at $12.6 \mu\text{M}$ ($K_m=12.6\pm2.6 \mu\text{M}$) with a K_{is} of $10\pm7.1 \text{ mM}$ and K_{ii} of $3.7\pm0.47 \text{ mM}$ (Table 3.1). Increasing the concentration of kanamycin A to $126 \mu\text{M}$ ($10K_m$) eliminated inhibition by kanamycin phosphate (Figure 3.8, Table 3.1). The results are consistent with a rapid release of the first product, kanamycin phosphate

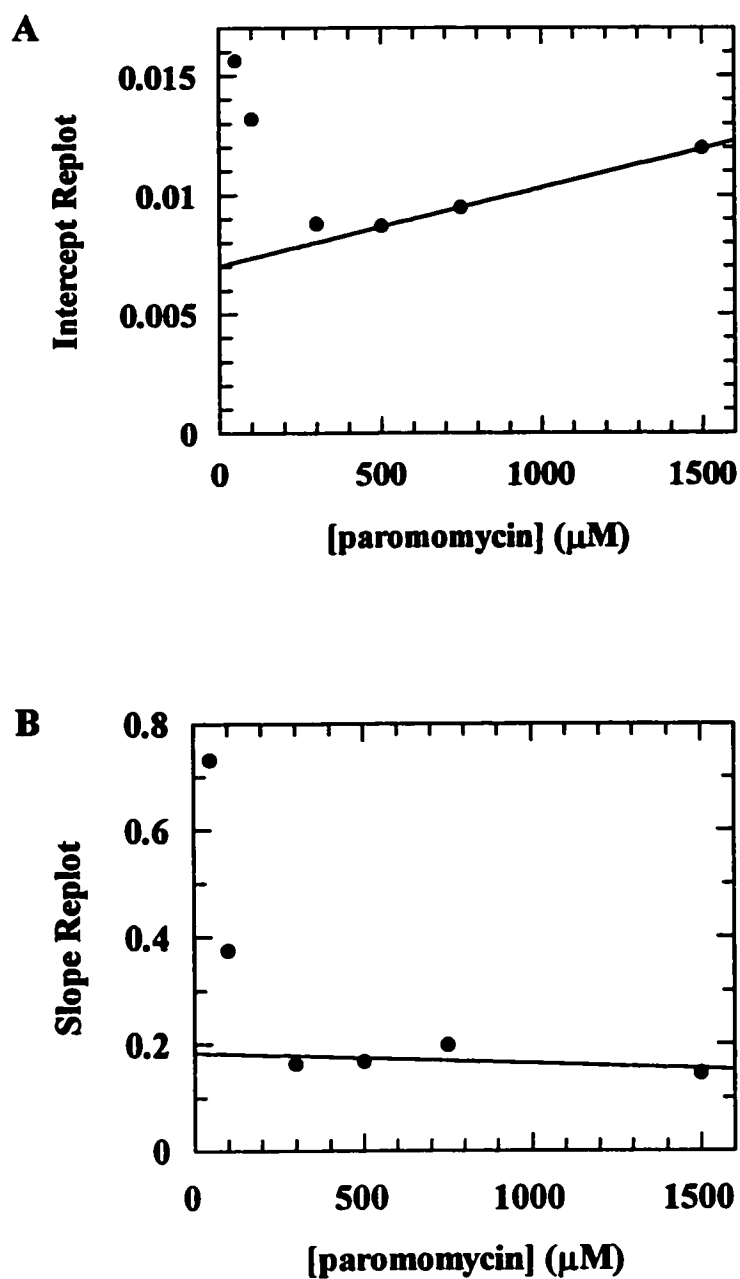


Figure 3.6. Substrate inhibition of APH(3')-IIIa through the nonproductive binding of aminoglycosides. A, intercept replot versus [paromomycin]. B, slope replot versus [paromomycin]

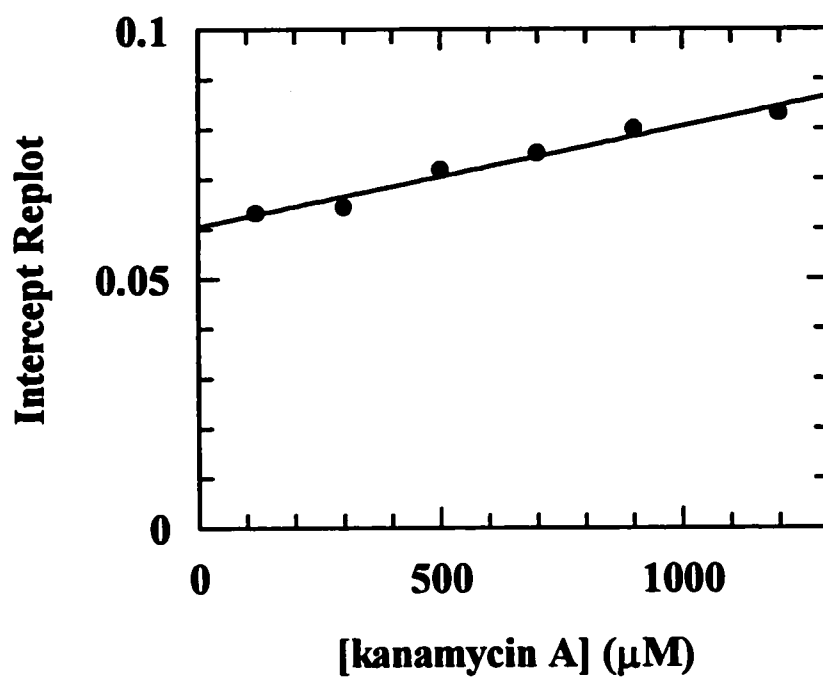
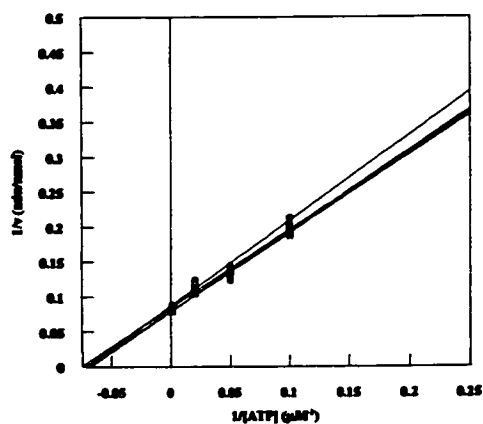
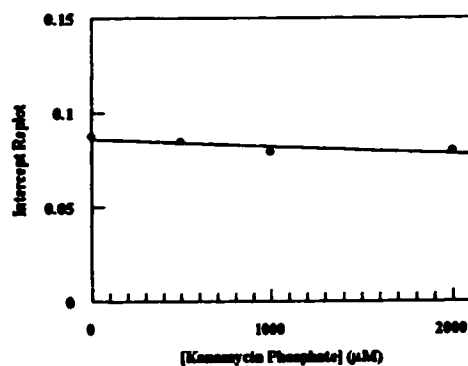


Figure 3.7. Substrate inhibition of APH(3')-IIIa through nonproductive binding of kanamycin A. Slope replot versus [kanamycin A]

A.



B.



C.

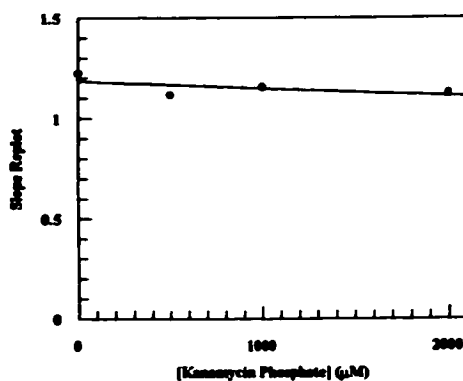


Figure 3.8. Inhibition of APH(3')-IIIa through the use of product kanamycin phosphate. Substrate ATP was varied while [kanamycin] was held at 126 μM. (A) Lineweaver Burke plots at 4 fixed concentrations of kanamycin phosphate 0 μM (●), 500 μM (○), 1000 μM (×) and 3000 μM (■). (B) Intercept replot of ATP versus [kanamycin phosphate]. (C) Slope replot of ATP versus [kanamycin phosphate].

followed by a relatively slow release of ADP as the second product. This is indicative of a Theorell-Chance mechanism, a specialized case of the ordered Bi Bi mechanism.

3.3.5 *Alternative Substrates Diagnostic*

APH(3')-IIIa has a broad aminoglycoside substrate range, which makes it amenable to analysis by the alternative substrate method of Radika and Northrop (155). For a series of both 4,5- and 4,6-disubstituted deoxystreptamine antibiotics, we see k_{cat} vary only 1.1 fold and k_{cat}/K_m vary 1.4 fold (Table 3.2). This results in a series of essentially coincident lines in reciprocal plots (not shown) indicative of an ordered sequential mechanism, specifically an Theorell-Chance mechanism where ATP binds first followed by the aminoglycoside (155).

3.3.6 *Solvent Isotope and Thio Effects*

Since aminoglycoside phosphorylation implies at least one deprotonation event (3'-OH), we sought to evaluate the effect of substituting this OH for OD by performing the reaction in D₂O. Solvent effects were minor at two pDs (6.5 and 7.5) for both kanamycin A and ATP with k_{cat}^H/k_{cat}^D of 1.5-1.6 (Table 3.3).

Similarly, substitution of ATP- γ -S for ATP resulted in only a small V_{max} change ($k_{cat}^{ATP}/k_{cat}^{ATP\gamma S} \approx 2$) (Table 3.3).

Table 3.2: Alternative substrate diagnostic with fixed concentration of aminoglycoside substrate using ATP as variable substrate

Antibiotic	Concentration (μM)	k_{cat} (s^{-1})	$k_{\text{cat}}/K_{\text{m}}$ ($\mu\text{M}^{-1} \text{s}^{-1}$)
kanamycin A	100	1.71 ± 0.050	0.16 ± 0.03
kanamycin B	200	1.96 ± 0.020	0.19 ± 0.01
paromomycin	200	1.83 ± 0.012	0.13 ± 0.01
lividomycin A	300	1.88 ± 0.012	0.16 ± 0.01

Table 3.3: Solvent isotope and thio effects for APH(3')-IIIa

varied substrate	K_m (μM)	k_{cat} (s^{-1})	K_i (mM)	$k_{cat}^{\text{H}}/k_{cat}^{\text{D}}$	$k_{cat}^{\text{ATP}}/k_{cat}^{\text{ATP}\gamma\text{S}}$
ATP					
pH 7.5	27.7 \pm 3.7	1.76 \pm 0.08			
pD 7.5	11.6 \pm 1.7	1.08 \pm 0.04		1.63	
kanamycin A					
pH 6.5	4.4 \pm 0.9	1.7 \pm 0.05	2.4 \pm 0.5		
pD 6.5	16.2 \pm 0.7	1.2 \pm 0.05	1.3 \pm 0.3	1.47	
pH 7.5	12.6 \pm 2.6	1.8 \pm 0.1	6.4 \pm 1.7		
pD 7.5	3.8 \pm 0.8	1.2 \pm 0.04	2.0 \pm 0.4	1.5	
ATP γ S, pH 7.5	49.5 \pm 6.9	0.8 \pm 0.2			2.09 \pm 0.1

3.3.7 Solvent Viscosity Effects

In an effort to elucidate which catalytic step was rate limiting, we determined steady-state parameters for APH(3')-IIIa in solvents of varying viscosity. We sought to distinguish between effects due to global viscosity changes versus effects on diffusion-controlled equilibria by monitoring effects due to the macroviscogen PEG₈₀₀₀ and the microviscogens glycerol and sucrose (10). The polymer PEG₈₀₀₀ had no effect on the relative k_{cat} or k_{cat}/K_m when either kanamycin A or ATP was varied (Figure 3.9, Table 3.4). This is an important result which demonstrates that the macroviscosity of the solutions has no effect on the enzymatic rates as predicted for polymeric species which do not affect the rate of diffusion of small molecules (10). Glycerol and sucrose, on the other hand, had a dramatic effect on k_{cat} when either substrate was varied (Figure 3.10, Table 3.4). Additionally, k_{cat}/K_m was affected for ATP but not for the aminoglycoside substrate kanamycin A (Figure 3.11). Similar results were obtained with another aminoglycoside, amikacin, which has a 20 fold higher K_m (245 μ M) than kanamycin but an unchanged k_{cat} .

Kanamycin A and other aminoglycosides, except amikacin, show substrate inhibition. We see no significant effect due to glycerol or sucrose induced viscosity changes in K_I (Table 3.4).

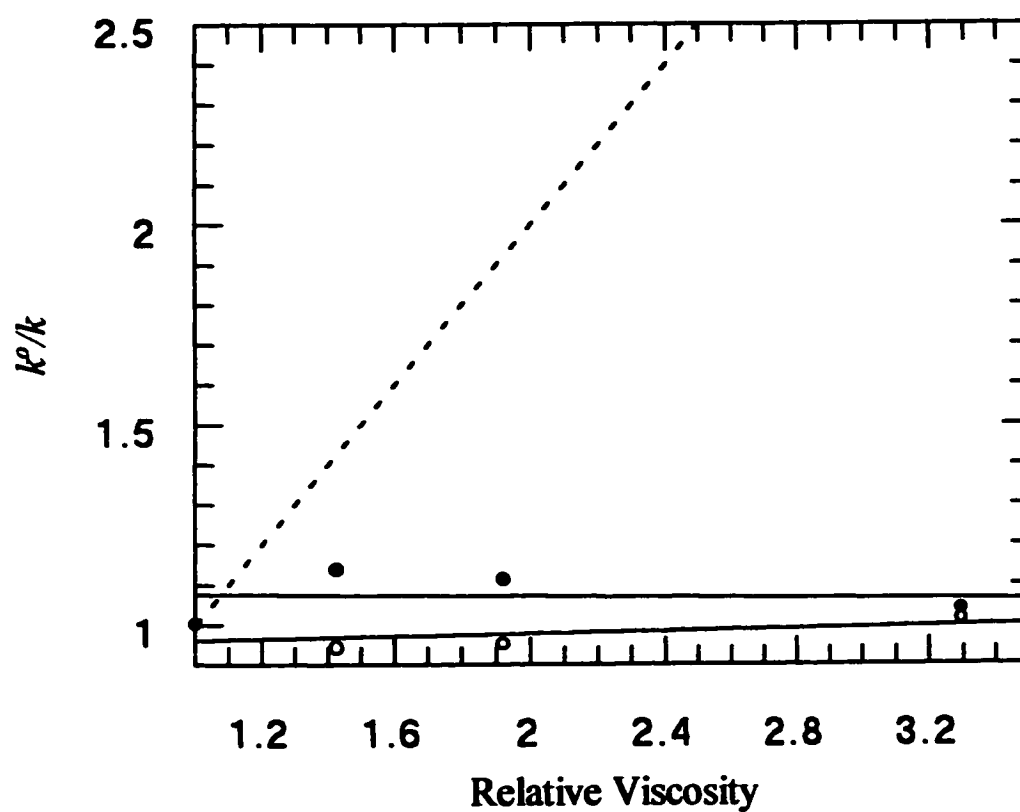


Figure 3.9. PEG8000 viscosity effects on the rates of APH(3')-IIIa catalyzed reactions. The dotted line has a slope of 1. Variable kanamycin A with constant ATP (1 mM). (o) k_{cat}^0/k_{cat} and (●) $(k_{cat}/K_m)_0/(k_{cat}/K_m)$.

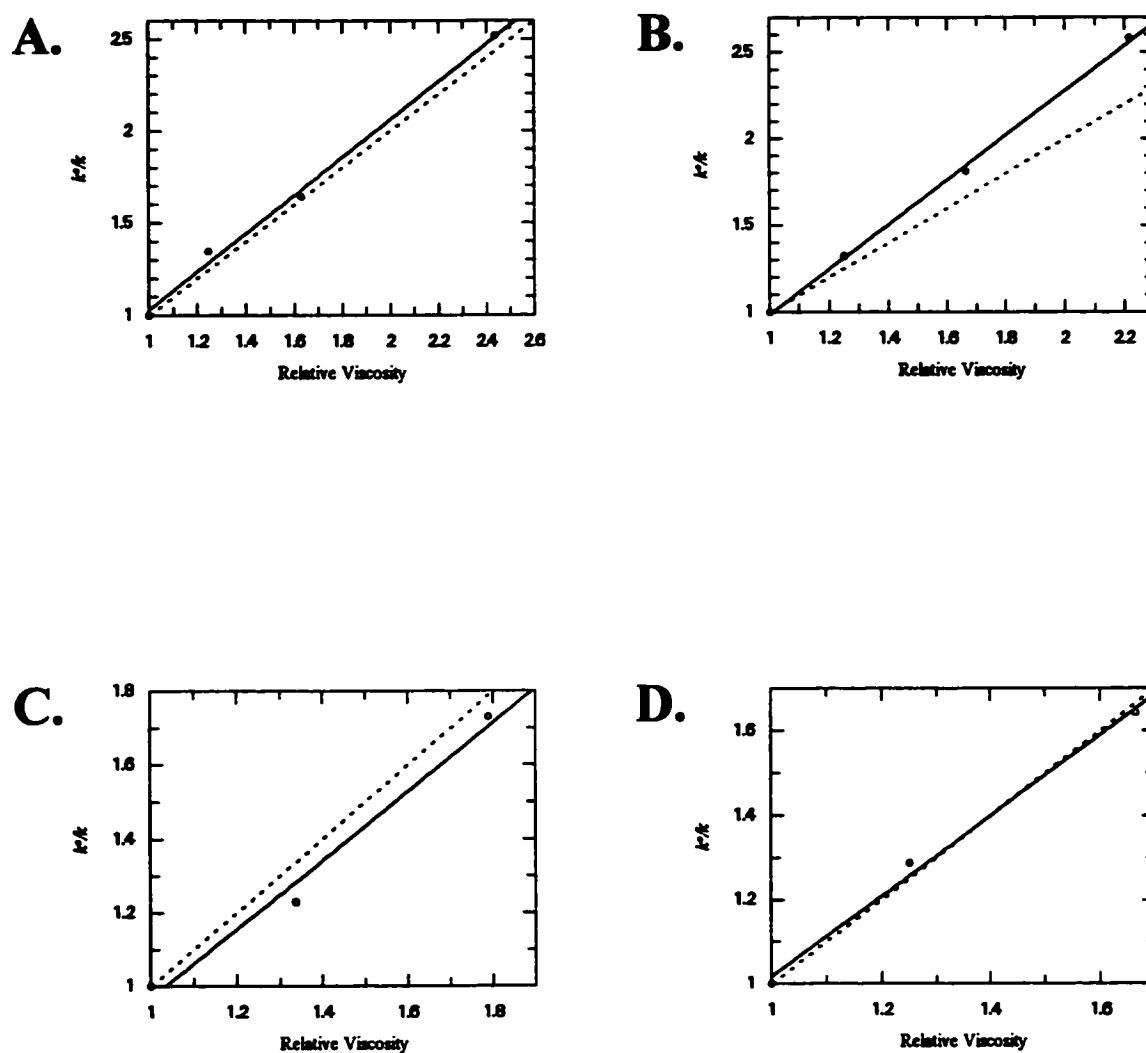


Figure 3.10. Glycerol viscosity effects of the rates of APH(3')-IIIa catalyzed reactions. (A) Variable ATP at constant kanamycin A (125 μ M). (B) Variable kanamycin A at constant ATP (1 mM). (C) Variable ATP at constant amikacin (2.5 mM). (D) Variable amikacin at constant ATP (1 mM). Dashed line has a slope of 1. (\circ) k_{cat}^0/k_{cat} .

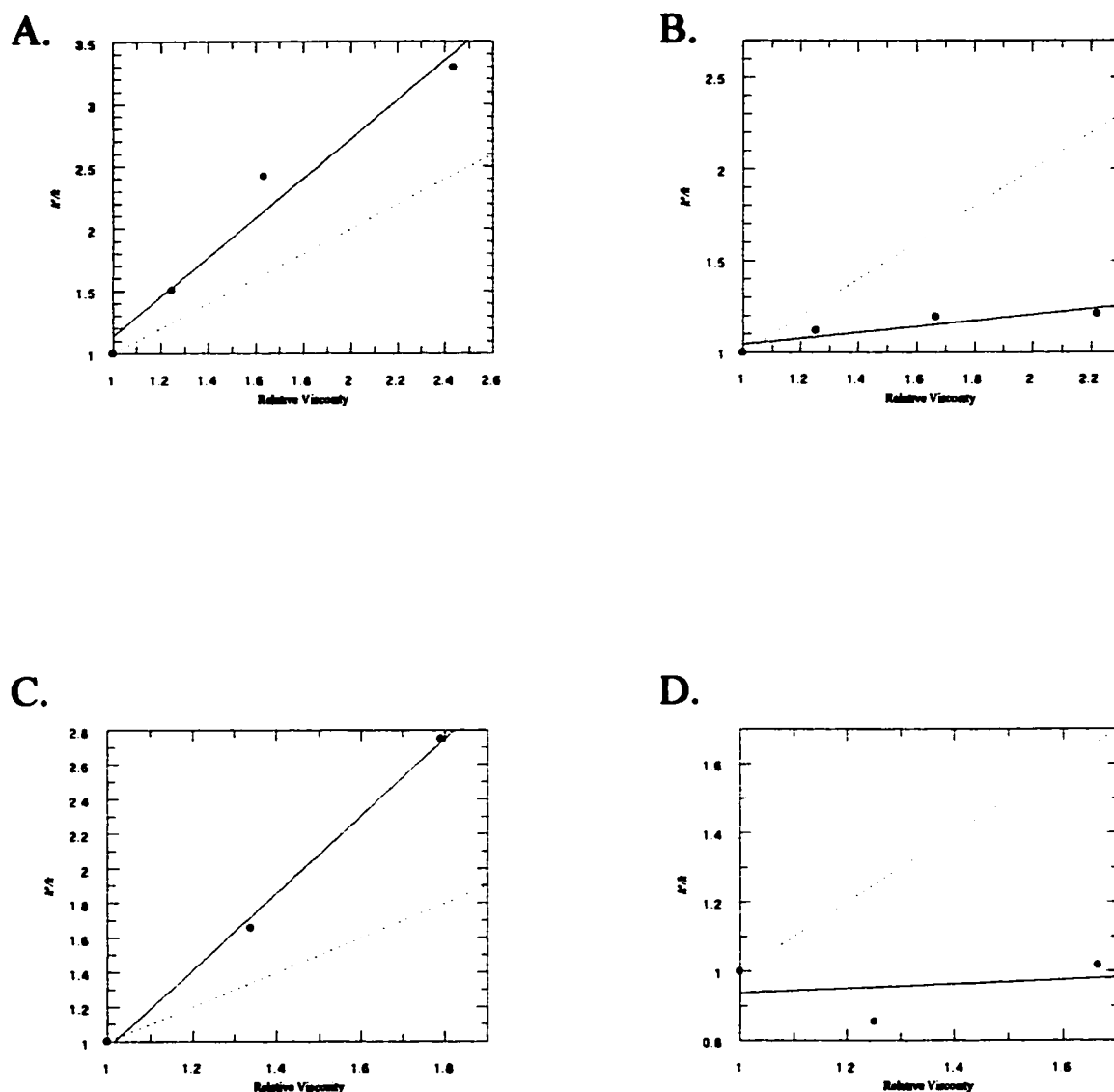


Figure 3.11. Glycerol viscosity effects on the rates of APH(3')-IIIa catalyzed reactions. The dotted line has a slope of 1. (A) Variable ATP at constant kanamycin A (125 μM). (B) Variable kanamycin A at constant ATP (1 mM). (C) Variable ATP at constant amikacin (2.5 mM). (D) Variable amikacin at constant ATP (1 mM). (●) $(k_{cat}/K_m)^0 / k_{cat}/K_m$.

Table 3.4: Viscosity effects on APH(3')-IIIa

viscogen	varied substrate	fixed substrate	$(k_{cat}^0/k_{cat})^{\eta^a}$	$((k_{cat}/K_m)^0/k_{cat}/K_m)^{\eta^a}$
glycerol	ATP	kanamycin A (0.125 mM)	1.03±0.05	1.58±0.22
glycerol	ATP	kanamycin A (1 mM)	1.37±0.14	2.10±0.19
glycerol	kan A	ATP (1 mM)	1.29±0.03	0.15±0.06
glycerol	ATP	amikacin (2.5 mM)	0.93±0.12	2.23±0.13
glycerol	ATP	amikacin (0.1 mM)	0.56±0.03	0.56±0.07
glycerol	amikacin	ATP (1 mM)	1.00±0.08	0.06±0.26
sucrose	ATP	amikacin (2.5 mM)	0.76±0.10	0.83±0.11
sucrose	kan A	ATP (1 mM)	1.05±0.05	-0.12±0.13
sucrose	amikacin	ATP (1 mM)	0.76±0.08	-0.02±0.06
PEG ₈₀₀₀	kan A	ATP (1 mM)	0.02±0.02	0.00±0.04
PEG ₈₀₀₀	ATP	kan A (1 mM)	0.02±0.00	-0.05±0.02

^a k_{cat}^0 and $(k_{cat}/K_m)^0$ are the rates with no added viscogen. Values are the slopes of plots for either k_{cat}^0/k_{cat} or $(k_{cat}/K_m)^0/k_{cat}/K_m$ versus relative viscosity of the solution.

CHAPTER 4

Active Site Mapping and Mutagenesis of APH(3')-IIIa Identify Two Residues Which Line the ATP Binding Pocket.

Adapted from

McKay, G.A., Robinson, R.A., Lane, W.S., and Wright, G.D.
Biochemistry, 1994, vol. 33, pp. 14115-14120

Hon, W-C., McKay, G.A., Thompson, P.R., Sweet, R.M., Yang, D.S.C., Wright, G.D.,
and Berghuis, A.M.
Cell, 1997, vol. 89, pp. 887-895

Chapter 4

4.1 *Introduction*

Information gained from kinetic mechanism studies, while insightful, is in itself not sufficient to provide a solid basis for drug design. It is important for the understanding of how a particular enzyme functions to identify residues involved in both the chemistry of a reaction and also the binding of the enzyme's substrates. The most direct and informative means to identify residues involved in both substrate binding and enzyme chemistry is through a determined X-ray 3-dimensional crystal structure. In the absence of such a structure there are many tools available which can provide mechanistic and structural information, if albeit through a slightly more indirect means.

The vast majority of structural and functional knowledge which exists for the APH(3') family of enzymes has been the result of one of two approaches. First, work to date has relied upon primary sequence alignment of APH(3') family members, whereby highly conserved regions were identified and targeted for mutagenesis studies (105-107). Second, studies have used a more random approach targeting the aminoglycoside phosphotransferase genes with hydroxylamine hydrochloride (18). These approaches, while often informative, suffer from distinct problems. Studies based upon homology alignments require a researcher to make an assessment as to the potential importance of a residue, or region, for enzyme function and thus frequently important residues or regions are overlooked. Random hydroxylamine mutagenesis removes this bias of selection but

poses another problem in that often mutations generated are eventually deemed uninformative.

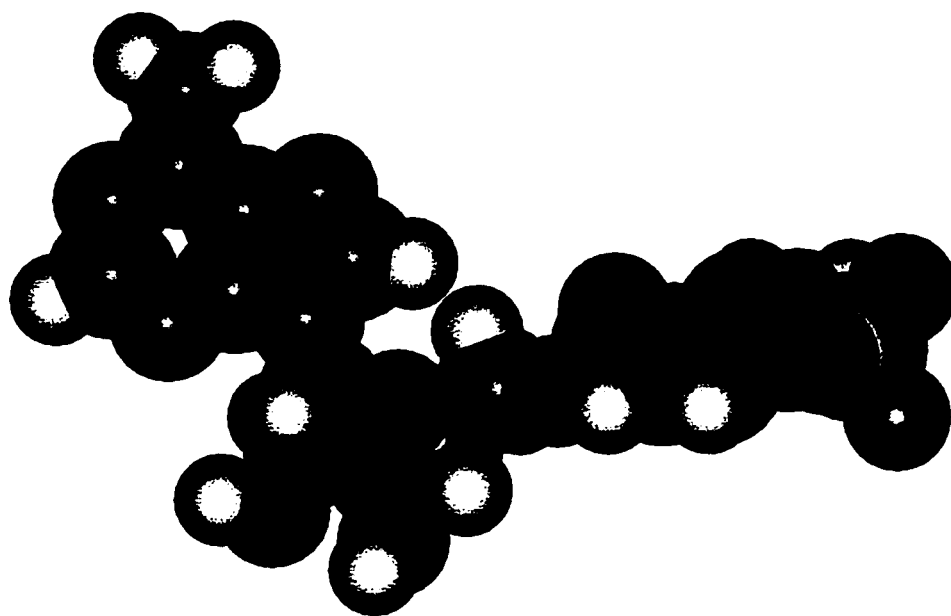
Here I approached the problem through the use of an electrophilic ATP analogue, 5'[p-(fluorosulfonyl)-benzoyl]adenosine (FSBA) (Figure 4.1). This compound was first synthesized and described by Roberta Colman and colleagues who successfully used it to probe the diphospho pyridine site of bovine liver glutamate dehydrogenase (145). FSBA has since been successfully used to probe the ATP binding pocket of many enzymes (102, 108, 207, 215). Active site residues; lysine, tyrosine, cysteine, histidine and serine have been shown to form covalent adducts by nucleophilic attack at the sulfonyl halide bond of FSBA. This reactive group is positioned similarly to the gamma phosphate of ATP thus permitting the identification of residues surrounding the terminal phosphate.

4.2 *Materials & Methods*

4.2.1 *General Materials*

FSBA and N-p-tosyl-L-phenylalanine chloromethyl ketone (TPCK) treated trypsin were from Sigma (St. Louis MO). Sephadex G-25 was from Pharmacia (Montreal, PQ). [^{14}C]FSBA (radioactive label is incorporated in the purine ring) was from Dupont NEN (Mississauga, Ont).

A.



B.

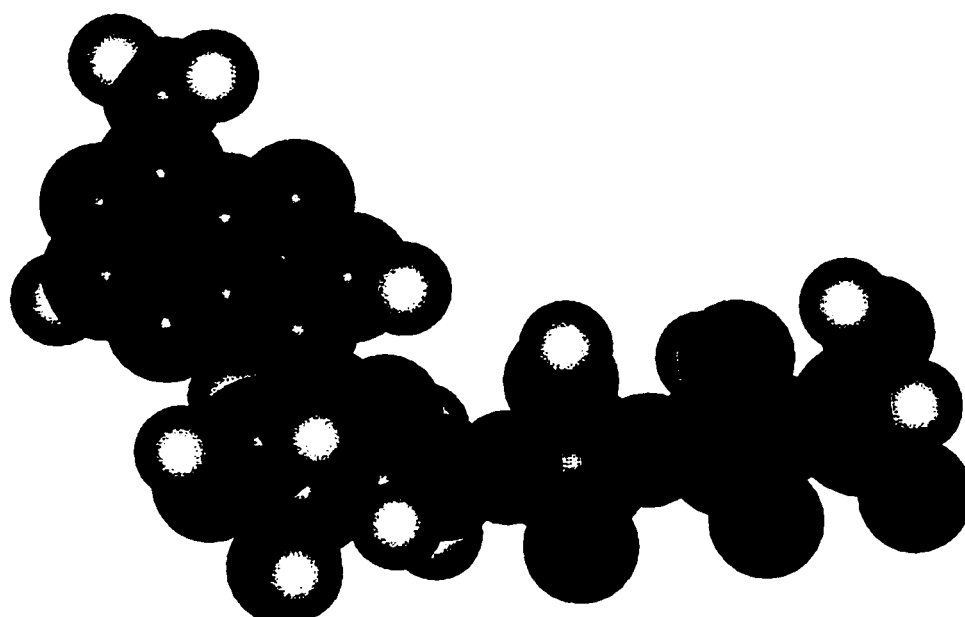


Figure 4.1. Spacefill model of (A) p-fluorosulfonylbenzoyl adenosine (FSBA) and (B) adenosine triphosphate (ATP). Fluoride atom is coloured pink in panel A.

4.2.2 *Inactivation of APH(3')-IIIa with FSBA*

Typically, FSBA inactivation experiments were conducted in 50 mM Tris-HCl, pH 7.5, 10 mM MgCl₂ with various amounts of FSBA dissolved in dimethyl sulfoxide (10% v/v final for all FSBA concentrations including controls) in a total volume of 225 µL at 37 °C. Reactions were initiated by the addition of purified APH(3'')-IIIa (4.8 nmol) and aliquots (10 µL) removed and assayed for phosphotransferase activity. Enzyme activity was measured as previously presented, in section 2.2.6, where substrates ATP and kanamycin A were held at 1 mM and 100 µM, respectively, unless otherwise indicated.

4.2.3 *Substrate Specific Protection of APH(3')-IIIa from FSBA Inactivation*

In order to assess the nature of FSBA inactivation, several assays were performed to determine whether either ATP or tobramycin could protect APH(3')-IIIa from FSBA inactivation and labeling. Five separate reactions were completed investigating the ability of ATP to afford protection from FSBA inactivation. Each reaction contained 70 µg APH(3')-IIIa, 50 mM Tris-HCl, pH 7.5, 10 mM MgCl₂ and 0.5 mM FSBA (5 mM stock FSBA solution dissolved in 100% DMSO). Concentrations of ATP used were 0, 0.05, 0.1 and 0.5 and 1.0 mM. To insure that inactivation was specific to FSBA and not a by-product from the addition of DMSO a control reaction was performed where 10% DMSO (dimethylsulfoxide) was substituted for FSBA. The ability of tobramycin to afford similar protection was also investigated. The first reaction consisted of 70 µg APH(3')-IIIa, 50 mM Tris-HCl pH 7.5, 10 mM MgCl₂, 0.5 mM FSBA and 0.21 mM

tobramycin ($K_{is}=0.35\ \mu\text{M}$). The second reaction was designed to assess if ATP and tobramycin afforded synergistic protection. This reaction consisted of 70 μg APH(3')-IIIa, 50 mM Tris-HCl pH 7.5, 10 mM MgCl_2 , 0.5 mM FSBA and 0.21 mM tobramycin and was additionally supplemented with 1 mM ATP. All eight reactions, including the control, were incubated for 60 min at 37 °C following which the tubes centrifuged for 10 sec. The activity was measured in duplicate using the coupled enzyme assay as described in section 2.2.6. Activity was normalized to a $t=0$ minute sample in the absence of any additions except DMSO.

4.2.4 Determination of Stoichiometry of FSBA Labeling

APH(3')-IIIa (60 nmol) was added to a solution of 0.45 mM [^{14}C]FSBA (2.2 $\mu\text{Ci}/\mu\text{mol}$) in 50 mM Tris-HCl, pH 7.5, 10 mM MgCl_2 to give a final volume of 1.5 mL and incubated at 37 °C. Aliquots (100 μL) were removed at various time points (0, 6.5, 10, 20, 35, 42, 60, 90, 130, 187, 275 min) and reactions quenched by the addition of 2-mercaptoethanol to a final concentration of 1.35 mM. Unbound label was removed by application to two successive Sephadex G-25 spin columns (400 μL) (150). The sample was then assayed for APH(3')-IIIa activity in duplicate and scintillation counted to determine label incorporation.

4.2.5 Large Scale Affinity Labeling and Peptide Mapping

Large scale inactivations of APH(3')-IIIa for peptide mapping consisted of enzyme (100 nmol), 50 mM Tris-HCl, pH 7.5, 10 mM MgCl_2 , and 0.75 mM FSBA in a

final volume of 0.5 mL. A control incubation was carried out without FSBA, and a reaction with 0.75 mM [^{14}C]FSBA (1.2 $\mu\text{Ci}/\mu\text{mol}$) was also performed. Reactions were incubated at 37 °C for 3 hr, the volumes were then increased to 1.5 mL by addition of deionized distilled water, and the solutions were dialyzed against 2.25 L of 25 mM NH_4HCO_3 , pH 8.3, at 4 °C overnight. The following day the dialyzed sample was lyophilized to dryness following which the samples were taken up in 100 μL of 8 M urea, 100 mM NH_4HCO_3 , pH 8.3, and incubated at room temperature for 15 minutes followed by the addition of 45.5 μL of 100 mM NH_4HCO_3 , pH 8.3. Trypsin (220 μg activated in 1.2 M HCl) was added to each sample, and the digestion was allowed to proceed for 24 hr in the dark at ambient temperature. Samples were frozen at -80 °C until further use.

Tryptic digests were analyzed by reverse-phase HPLC using a Spherisorb-ODS2 C18 column (4 mm x 20 cm) at ambient temperature at a flow rate of 0.8 mL/min. Samples were applied in a solution of 0.1% trifluoroacetic acid (TFA), and peptides were eluted by a gradient of 0.07% TFA in CH_3CN (B). The gradient consisted of 0-35% B over 55 minutes, 35-75% B over 30 minutes, and 75-90% B over 15 minutes. Samples were monitored simultaneously at 214 and 260 nm, and radiolabeled APH(3')-IIIa digest was additionally analyzed by scintillation counting of 800 μL fractions.

4.2.6 Characterization of Labeled Peptides by Narrowbore HPLC, Edman Degradation and Mass Spectroscopy

Samples labeled with non-radioactively labeled FSBA and unlabeled APH(3')-IIIa were sent to Dr. William Lane, Harvard Microchemistry, for further analysis by narrowbore HPLC, Edman degradation, and mass spectroscopy.

4.2.7 Generation of APH(3')-IIIa Site Mutations

The following mutants S27A (5'-TA TAC CTT AGC AGG AGC CAT TCC TTC CGT ATC-3'), K33A (5'-TTC TCC CAC CAG CGC ATA TAC CTT AGC AGG-3'), K44A (5'-GCT GTC CGT CAT TGC TAA ATA TAG GTT TTC ATT-3') and K33AK44A were all generated using an oligonucleotide directed mutagenesis protocol. Mutagenesis of K44A was completed by Paul Thompson following which I subcloned the fragment.

4.2.7a Cloning of *aph(3')-IIIa* into M13mp18

The *aph(3')-IIIa* gene was cloned into M13mp18 using the generated restriction endonuclease sites *Nde I* and *Hind III* and then was transformed into *E. coli* MV1190 as follows. The ligation reaction mix (10 μ L, ~50 ng DNA) was added to 250 μ L CaCl_2 competent MV1190 cells (1.5×10^5 cells/ μ g DNA). Cells were incubated on ice following which they were heat shocked at 37 °C for 5 minutes. To this tube was added 250 μ L saturated overnight culture of MV1190 and 2.5 mL of 50 °C top agar. This mix was

pipetted onto a LB agar plate and allowed to solidify. Plates were incubated overnight at 37 °C and plaques were selected the following day.

4.2.7b *Generation of Single Stranded Template DNA*

Plaques were selected using sterile toothpicks and used to inoculate 1.5 ml sterile LB broth to which was then added 15 µL of overnight culture of CJ236 (*duf*, *ung*⁻) This tube was incubated at 37 °C for 5 min without agitation following which the cells were permitted to grow for 8 hr at 250 RPM agitation. Cells were harvested by microcentrifugation and the supernatant was removed to a fresh eppendorf tube containing 15 µL of CHCl₃ as an antiseptic. The cell pellet was frozen at -20 °C from which could be purified the replicative form of M13mp18::*aph(3')-IIIa*. The supernatant containing the phage was further purified to obtain the single stranded DNA needed for the template in the mutagenesis reactions.

One milliliter of phage supernatant was precipitated using 200 µL of 20% PEG/2.5 M NaCl by incubating the mix at room temperature for 15 min following which the tube was spun for 5 min. All supernatant was removed and the inside of the tube was carefully dried using a Kimwipe. The phage pellet was resuspended in 200 µL TE (10 mM Tris-HCl pH 8.0, 1 mM EDTA) and then incubated on ice for 45 min. The phage solution was extracted once with phenol, once with phenol:CHCl₃ and twice with CHCl₃. Extraction involved mixing of the phage with the organic phase followed by a 5 min incubation at room temperature and then the tubes were spun for 2 min and the aqueous phase removed. The final extracted aqueous phase was brought to 250 µL with deionized

distilled water to which was added 28 μL 7.8 M ammonium acetate and 2 volumes absolute ethanol. The sample was thoroughly mixed and then incubated at $-70\text{ }^{\circ}\text{C}$ for 120 min. The tube was spun at 12000 RPM in a microcentrifuge for 20 min and the pellet subsequently washed with 700 μL of 70% ethanol. The pellet was air dried for 1 hr at room temperature.

4.2.7c *Phosphorylation of Oligonucleotide*

A reaction mix containing 200 pmol oligonucleotide, 100 mM Tris-HCl pH 8.0, 10 mM MgCl_2 , 5 mM DTT, 0.4 mM ATP in a total volume of 30 μL . T4 polynucleotide kinase was added to the reaction (4.5 units) and incubated at $37\text{ }^{\circ}\text{C}$ for 45 min.

4.2.7d *Annealing of Phosphorylated Oligonucleotide to ssDNA aph(3')-IIIa Template*

An annealing reaction was mixed which included 250 ng of single stranded template DNA, 3 pmol phosphorylated oligonucleotide, 100 mM Tris-HCl pH 7.6 in a total volume of 10 μL . A control reaction was also mixed which omitted the phosphorylated oligonucleotide.

4.2.7e *Synthesis of Second Strand*

A synthesis reaction was added in the following order to the annealing reaction: 1 μL of 10X synthesis buffer, 4 units of T4 ligase and 1 unit of T4 polymerase. This mix

was incubated on ice for 5 min, followed by a 5 min incubation at room temperature and a final 90 min incubation at 37 °C. The reaction was quenched by addition of 90 µL of 5 mM EDTA. The synthesis reaction was then frozen at -20 °C.

4.2.7f *Transformation of MV1190 with Synthesis Reaction*

To 300 µL of MV1190 cells was added 5 µL of synthesis reaction followed by incubation in ice for 40 min. The cells were heat shocked at 37 °C for 5 min. Transformed cells (100 µL) were added to 300 µL overnight MV1190 and 2.5 mL 50 °C top agar. The mix was then plated on an LB agar plate. The control reaction was similarly plated and the following day plaques were selected as previously described.

4.2.7g *Screening of Mutants*

Several plaques were picked using the described techniques and the single stranded DNA isolated (Section 4.2.6b). Mutant K44A was sequenced by Paul Thompson. The remaining mutants were sent for DNA sequencing at the central MOBIX facility to insure incorporation of the oligonucleotide and also to insure that no separate mutations were introduced during the synthesis process.

4.3 Results

4.3.1 FSBA Labels APH(3')-IIIa at the ATP Binding Site

Incubation of purified APH(3')-IIIa with FSBA resulted in inactivation of the enzyme (Table 4.1). The rate of inactivation is dependent on the concentration of FSBA (Figure 4.2). APH(3')-IIIa activity could not be restored even upon extensive dialysis of inactivated samples. Passage of inactivated enzyme through a G-10 Sephadex gel filtration matrix was also insufficient to restore enzyme activity indicating that the interaction of FSBA with APH(3')-IIIa was irreversible in nature. FSBA inactivation of APH(3')-IIIa was successfully inhibited by increasing amounts of ATP (Table 4.1) while the aminoglycoside, tobramycin, was unable to prevent enzyme inactivation. These results are consistent with the hypothesis that inactivation of APH(3')-IIIa by FSBA was occurring at the ATP binding site. Phenylmethylsulfonyl fluoride a compound with the same reactive group as FSBA did not inactivate APH(3')-IIIa even when present at levels of 1 mM, once again supporting the theory that FSBA inactivation of the enzyme was specific and targeted to the ATP binding pocket.

4.3.2 Kinetics of Inactivation of APH(3')-IIIa with FSBA

Inactivation was found to be both time dependent and concentration dependent (Figure 4.2) and was found to be consistent with the following reaction:



Table 4.1: Inactivation of APH (3')-IIIa by FSBA

FSBA (0.5 mM)	ATP (mM)	tobramycin (0.21 mM)	phosphotransferase activity (%) ^a
-	0	-	97±0.4
+	0	-	18±2.6
+	0.05	-	53±1.6
+	0.10	-	72±2.7
+	0.5	-	106±3
+	1.0	-	105±5
+	0	+	17.8±0.3
+	1.0	+	106±7

^a Activity was measured following a 60 minute incubation at 37 °C; values are the average of two assays. Values are normalized to t=0 minutes in the absence of any addition except DMSO. Activity was monitored through the use of PK/LDH coupled enzyme assay.

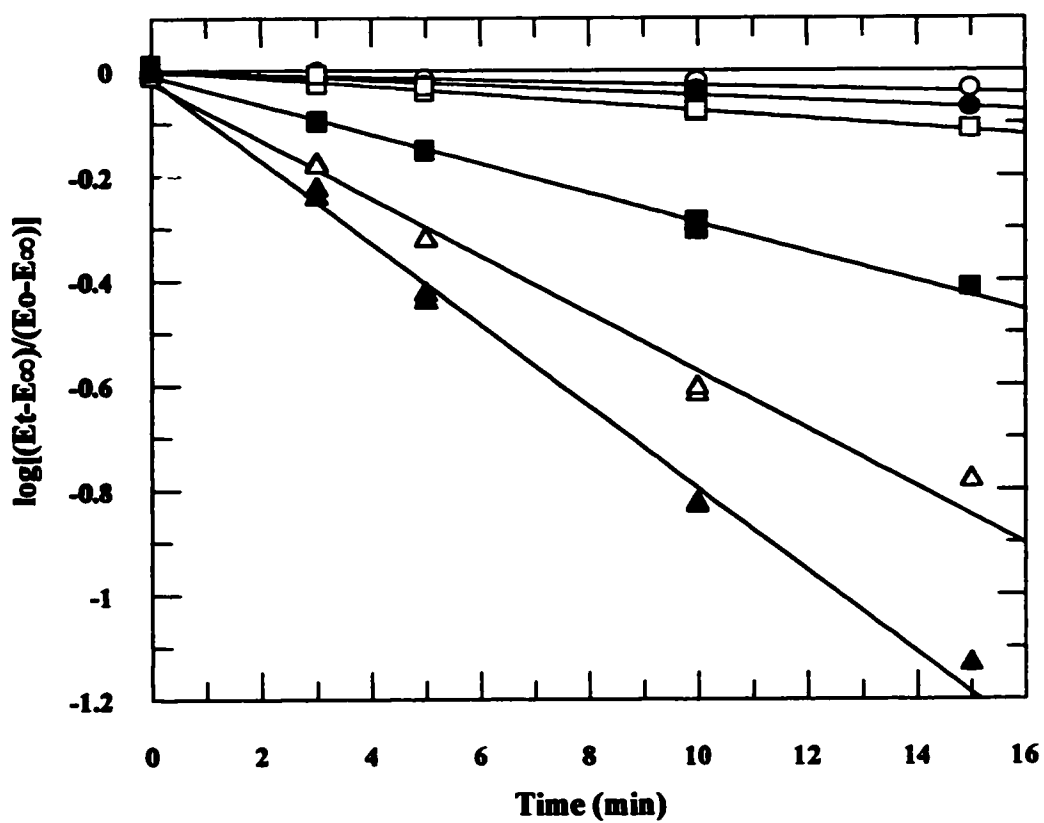


Figure 4.2. Inactivation of APH(3')-IIIa with FSBA. APH(3')-IIIa inactivated with FSBA at a final concentration of 12.5 (o), 20 (●), 50 (□), 200 (■), 500 (Δ) and 2000 (▲) μM . E_{∞} represents 2.5% residual activity following extended incubations with FSBA and E_t is the enzyme activity measured at various time points.

where K_i is the apparent binding constant, k_{max} is the rate of inactivation at saturating inactivator (I), and EI^* is the inactive enzyme. Inactivation of the enzyme was first order with respect to FSBA concentration for the first 10-15 minutes but then appeared to reach a limiting value (not shown). Similar behavior had previously been observed for other similar inactivators (12). It is proposed that the limiting value was reached due to the loss of FSBA by hydrolysis or interaction with buffer components. Addition of fresh FSBA to reactions led to further inactivation of APH(3')-IIIa to an absolute limit of 2.5% remaining activity. This value was therefore incorporated for the value of remaining enzyme activity (E_{∞}) into the calculations of k_{obs} .

It is evident that the preceding equation can be treated similarly to the Michaelis-Menten equation. For this situation a hyperbolic curve is generated (Figure 4.3) where a limit is reached corresponding to k_{max} . The inhibitor concentration at $1/2k_{max}$ corresponds to K_i which is analogous to the Michaelis constant K_m . Values for k_{max} and K_i were therefore calculated using non-linear least squares fitting of the following equation:

$$k_{obs} = (k_{max} [I]) / (K_i + I)$$

The data is also presented in a reciprocal format as the results are graphically informative (inset Figure 4.3). Using non-linear least fit squares, values of $406 \pm 28 \mu M$ and $0.086 \pm 0.077 s^{-1}$ were obtained for K_i and k_{max} respectively. The dissociation constant of FSBA is approximately 13.5 fold higher than the K_m for ATP ($27.7 \mu M$) suggesting the phosphates of ATP significantly contribute to the binding energy of ATP.

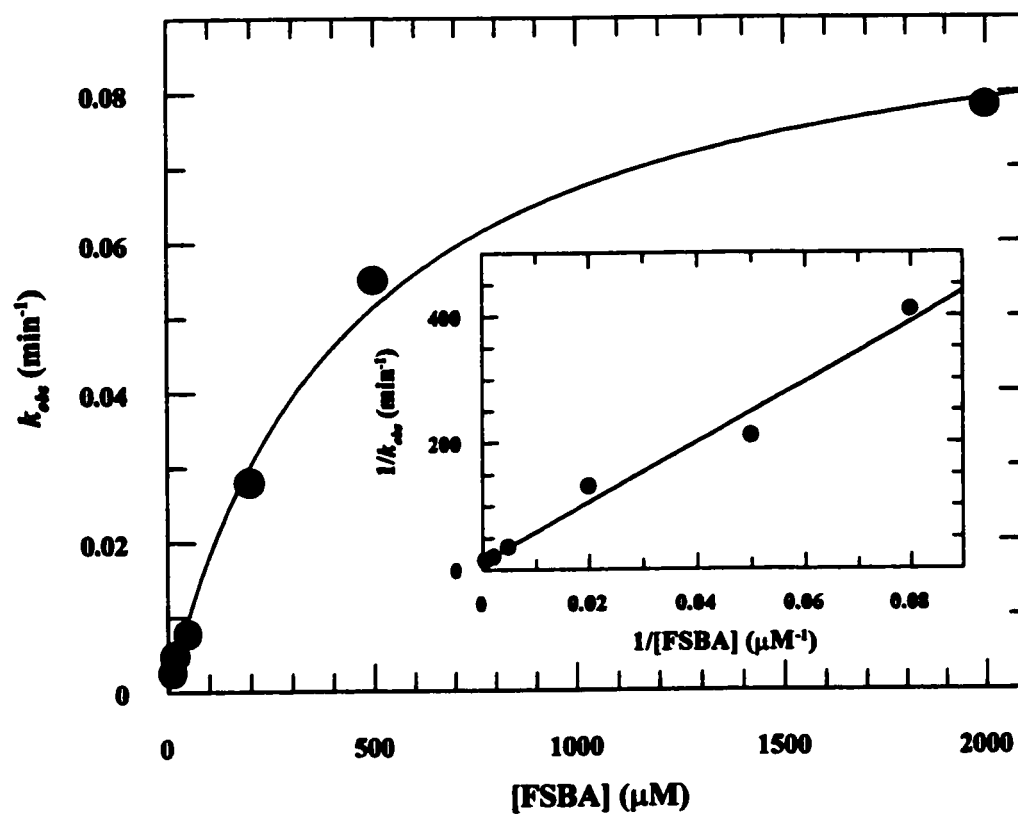


Figure 4.3. Inactivation of APH(3')-IIIa with FSBA. Plot of first-order rates of inactivation (k_{obs}) versus inactivator concentration. Inset: replot to determine K_i and k_{max} . The correlation coefficient (r) is 0.99.

4.3.3 Stoichiometry of APH(3')-IIIa Inactivation by FSBA

Inactivation studies were performed with ^{14}C -labeled FSBA in order to determine the stoichiometry of the inactivation event. By extrapolation of the curve, to 100% inactivation, this generates a ratio of enzyme to FSBA of 0.98 ± 0.03 (Figure 4.4) strongly supporting a unique inactivation event per monomer.

4.3.4 Identification of FSBA-Labeled Peptides

As a means to identify amino acid residues lining the ATP binding pocket of APH(3')-IIIa we performed a large scale inactivation of the enzyme with both ^{14}C -labeled and non-radioactive FSBA. The labeled proteins were then treated with activated trypsin and the peptides separated by reverse-phase HPLC.

Peptide maps of unlabeled APH(3')-IIIa and [^{14}C]FSBA labeled APH(3')-IIIa performed on 4.6 mm internal bore C18 column indicated a peak at ~77 min which absorbed at 260 nm which was present only in the labeled enzyme map (Figure 4.5). This peak was also found to contain greater than 58% of the total radioactivity. Those peaks denoted with an asterisks are species which are specific to [^{14}C]FSBA including peaks at 30.5 min and 82 min which have been identified as specific to adenosine (^{14}C label of FSBA is in the adenine ring).

The large scale inactivations which were preliminarily investigated using C18 reverse-phase HPLC were further analyzed by Dr. William Lane of the Harvard Microchemistry Department.

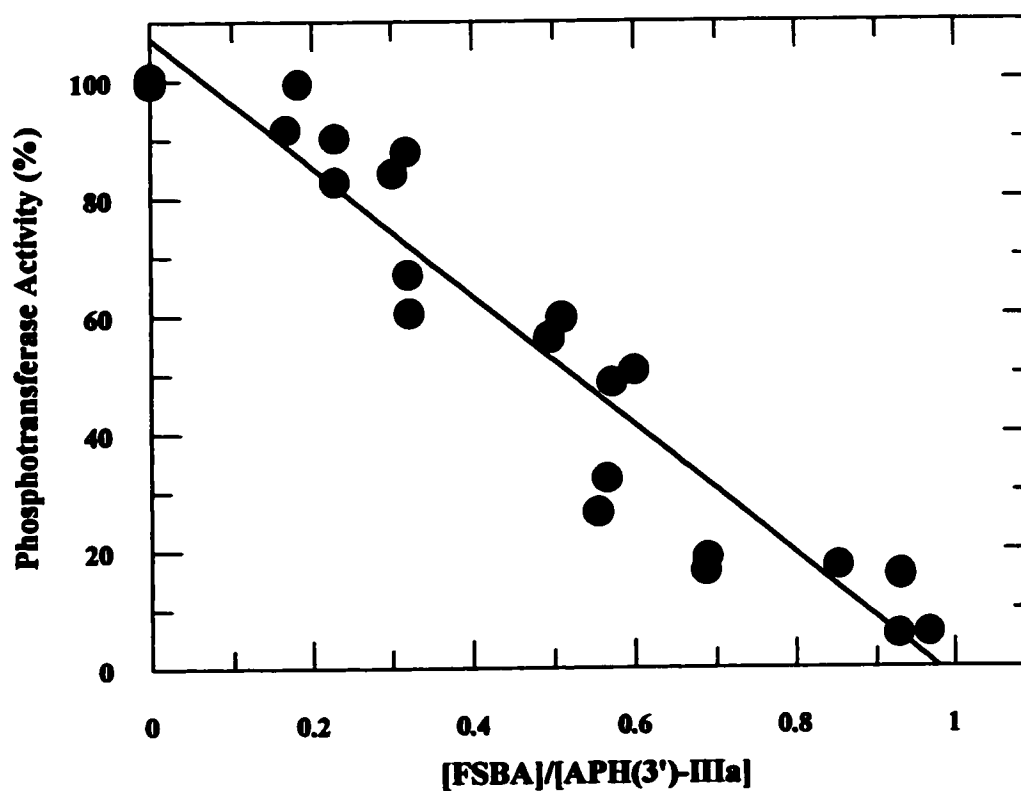


Figure 4.4. Stoichiometry of APH(3')-IIIa labeling by FSBA. APH(3')-IIIa was incubated with [^{14}C]FSBA and aliquots were removed at various time points and assayed for activity and label incorporation as measured by scintillation counting. The correlation coefficient (r) is 0.95.

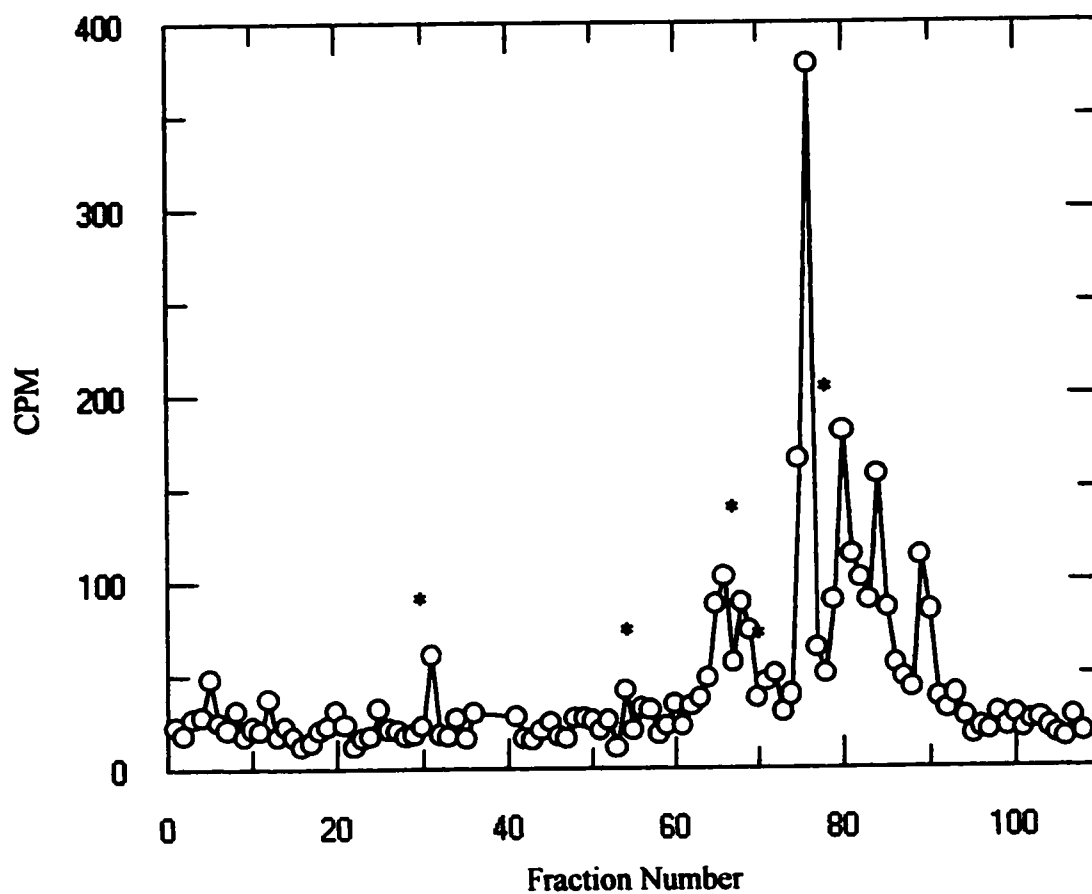


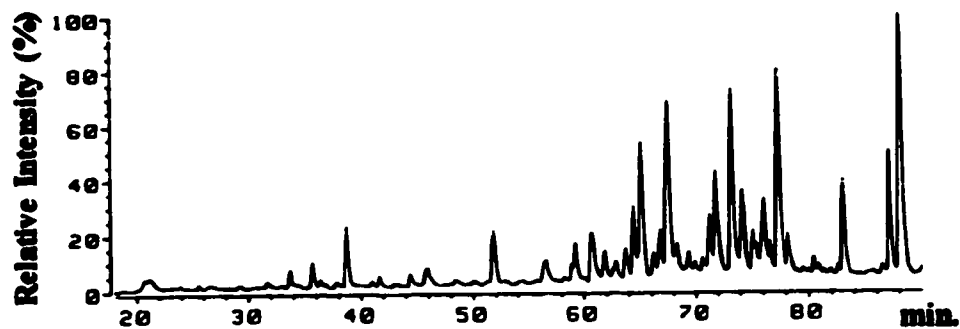
Figure 4.5. Peptide mapping of [^{14}C]FSBA labeled APH(3')-IIIa. The peptides were separated by Spherisorb-ODS2 C18 reverse phase HPLC. Fractions were monitored by A_{220} (not shown) and scintillation counting. Asterisks (*) denote peaks derived from [^{14}C]FSBA only.

4.3.5 Narrowbore HPLC Purification of FSBA Labeled Peptides, Edman Degradation and Mass Spectroscopy of Identified Peptides

Unlabeled APH(3')-IIIa and FSBA labeled enzyme were peptide mapped using narrowbore reverse phase HPLC. This technique provides a much better resolution than standard C-18 reverse phase HPLC as completed above in section 4.2.4. Through this technique, two peaks showing strong absorbance at 260 nm were identified as specific to the FSBA-labeled tryptic digest (Figure 4.6) with retention times of 61.7 min (peak 1) and 62.7 min (peak 2). Electrospray mass spectroscopy of peak 1 revealed two peptides with molecular weights of 2258.9 and 2114.8 (Table 4.2). These two peptides were N-terminal sequenced and the secondary peptide (as defined by relative amount) was found to have the sequence VY*LVGENENLYLK. The asterisk denotes a PTH-amino acid (phenylthiohydantoin amino acid derivative) which could not be identified. From the primary sequence of APH(3')-IIIa this amino acid is identified as K33. The mass of the peptide differs from the predicted mass of this peptide by 433.7 Da, consistent with labeling of this peptide with FSBA (mass of 433.4 Da with loss of F). The second peptide identified in this peak was found to correspond to Leu121-Arg139. This peptide was found to be unlabeled.

The peak identified at 62.7 min was also found to be comprised of two unique peptides. N-terminal sequencing and mass electrospray of the secondary peptide (again defined based on relative amount) identified a fragment with 2314.7 Da and the sequence LVGENENLYL*MTDSR, where as above the asterisk denotes a PTH-derivative which could not be identified. By the primary sequence this amino acid was identified as K44.

A.



B.

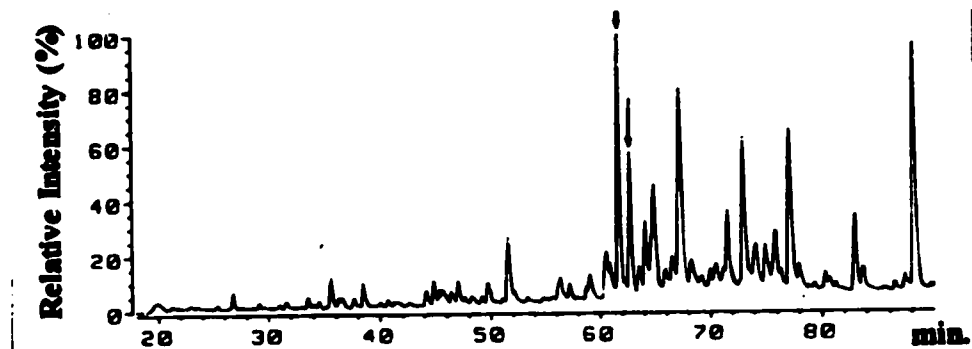


Figure 4.6. Peptide mapping of (A) APH(3')-IIIa and (B) non-radioactively labeled FSBA-inactivated APH(3')-IIIa by narrowbore reverse-phase HPLC. Traces are absorption at 260 nm and arrows in panel B represent peaks unique to FSBA-labeled peptide. (Modified and redrawn from McKay *et al*, Biochemistry, 1994).

Table 4.2: Analysis of tryptic peptides from FSBA-labeled APH(3')-IIIa

retention time ^a (min)	peptide sequence	mass (Da)		mass difference (Da)
		predicted	ESI-MS	
61.7	LFHSIDISDCPYTNSLDSR	2259.4 ^b	2258.9	0.5
	VY*LVGENENLYLK	1681.1	2114.8	433.7
62.7	IIELYAECIR	1297.8 ^b	1297.9	-0.1
	LVGENENLYL*MTDSR	1881.3	2314.7	433.4

^a Retention times were obtained following injection of the tryptic digest onto a narrowbore column and identified by their significant absorbance at 260 nm as compared to a control digest done without preincubation with FSBA. Peptides were analyzed by electrospray ionization mass spectrometry and sequenced by Edman degradation as indicated in Materials and Methods. Predicted masses were determined assuming a lys residue at positions marked with an asterisk as suggested by the primary sequence (185). An asterisk denotes an unidentified amino acid, approximately 10% of predicted Lys was observed.

^b Mass includes an additional disulfide with 2-mercaptoethanol.

The mass of this peptide was found to differ from its predicted mass by 433.4 Da, once again consistent with a single FSBA modification of the fragment (Table 4.2). The other peptide identified at 62.7 min was sequenced and identified as tryptic peptide Ile111-Arg120. This peptide's mass, 1297.8 Da, was identical to its predicted value indicating that it was not labeled by FSBA.

As a control, peaks at the same retention time were isolated from the unlabeled tryptic digest of APH(3')-IIIa. These peptides were analyzed by both Edman degradation and electrospray mass spectroscopy and they were found to be unlabeled as expected (not shown).

The combination of the enzymatic data, mass spectral data and N-terminal sequence data identify two sites of FSBA labeling of APH(3')-IIIa which are strongly indicated to lie proximally to the ATP binding pocket of the enzyme.

4.3.6 Analysis of APH(3')-IIIa K44A, K33A and K33AK44A Mutants

The steady-state kinetics of the three lysine mutants K33A, K44A and K33AK44A were completed and compared to wild type enzyme. Remarkably APH(3')-IIIa [K33A] demonstrated steady-state kinetic parameters very similar to wild type. The K_m values for both enzymes were virtually identical while the k_{cat} value decreased by less than 3 fold (Table 4.3) suggesting that this residue's contribution to enzyme function was limited and not likely involved in ATP binding. Similar results were obtained for steady state kinetics of kanamycin A where substrate binding was unaffected by this mutation. The steady-state kinetics for APH(3')-IIIa [K44A] shows interesting results. While

Table 4.3: Steady-state kinetic parameters of APH(3')-IIIa mutants

Mutant	ATP		Kanamycin A	
	K_m (μM)	k_{cat} (s^{-1})	K_m (μM)	k_{cat} (s^{-1})
Wild type	21.4 ± 1.2	1.83 ± 0.11	15.9 ± 1.7	2.04 ± 0.15
K33A	14.0 ± 1.5	0.62 ± 0.03	17.4 ± 3.4	0.68 ± 0.04
K44A	566 ± 49	1.58 ± 0.07	24.8 ± 3.2	1.28 ± 0.12
K33A, K44A	640 ± 89	0.62 ± 0.08	23.3 ± 7.5	0.56 ± 0.012

kinetics for kanamycin A remains virtually identical to those for wild type there is a substantial effect of ATP binding. While APH(3')-IIIa [K44A] demonstrates k_{cat} values virtually identical to that of wild type there is a 27 fold increase in K_m (Table 4.3) values for ATP binding indicating that this residue is likely involved in binding of ATP in some capacity.

CHAPTER 5

Functional Comparison Between APH(3')-IIIa and Eukaryotic Protein Kinases Demonstrates Similar Activities.

Adapted from

Daigle, D.M., McKay, G.A., and Wright, G.D.
Journal of Biological Chemistry, 1997, vol. 272, pp. 24755-24758

Daigle, D.M., McKay, G.A., Thompson, P.R., and Wright, G.D.
Chemistry and Biology, 1999, vol. 6, pp. 11-18

Chapter 5

5.1 Introduction

Much has been made of the recent discovery of apparent Ser/Thr and tyrosine kinases in prokaryotes (99). It was previously believed that bacteria favoured the use of histidine and carboxy amino acids as phosphoacceptors while eukaryotes preferred serine, threonine and tyrosine for signal transduction purposes (99).

As more serine/threonine and tyrosine protein kinases were identified and entered into the protein databases, features and primary sequence signatures were identified. Several of these sequences are named after Hanks, who was responsible in large part for defining these regions (80, 81). The first “eukaryotic” type protein kinase identified from bacteria was Pkn1 which was isolated from *Myxococcus xanthus* (136). Pkn1 is predicted to have between 27 and 31% identity over its putative catalytic domains when compared to Hanks type protein kinases such as cyclic AMP dependent protein kinase (cAMP DPK) and protein kinase C (PKC). Pkn1 autophosphorylates and mutagenesis studies have shown that the amino acids necessary for eukaryotic protein kinase function are also necessary for Pkn1 activity. While direct evidence of Pkn1 phosphorylation of protein substrates has not been readily forthcoming, both the autophosphorylation and mutagenesis studies are supportive of protein kinase function.

It is important to note that although other “protein kinases” have been identified prior to Pkn1, including Ser/Thr kinases for bacteriophage λ and ϕ 80 (37, 38) and a

protein phosphatase, taken as circumstantial evidence of the existence of a protein kinase activity, from *Yersinia pseudotuberculosis* (76) it is speculated that these genes were of foreign origin and not native to its present host (99). All three of these organisms are intracellular pathogens and thus making the origin of these genes ambiguous.

A number of groups have noted the similarity between protein kinases and APH(3') family members (21, 105, 126). In particular it was noted by Brenner that APH(3') proteins and identified protein kinases shared the consensus sequence HxDhxxxNhhhh where x represents any amino acid and h represents any large hydrophobic residue (21). He also noted the conservation of D208 (APH(3')-IIIa numbering) and suggested its possible involvement in coordinating Mg^{2+} and thus binding of ATP.

A second region of conserved residues was identified by Martin and colleagues (126) which was believed to have an analogous function to the P-loop initially identified by Hanks (81). For a more thorough discussion of this region see section 1.4.7. The possible involvement of this putative nucleotide binding loop in APH(3')-IIIa function was further investigated by Kocabivik and Perlin (105).

The recently solved crystal structure of APH(3')-IIIa has allowed a more detailed analysis of its similarities with eukaryotic protein kinases (EPKs) (89). Crystal structures now exist for such Ser/Thr protein kinases including casein kinase I from *Schizosaccharomyces pombe* (119, 209), and cAMP dependent protein kinase catalytic subunit isolated from porcine heart (19, 51, 214). Phosphorylase kinase has been structurally solved by X-ray crystallography (120, 143). What immediately becomes

apparent is that APH(3')-IIIa shows a reasonably strong similarity to the aforementioned eukaryotic protein kinases (Figure 5.1). A more thorough discussion of this similarity will be presented in the discussion. Briefly, however, several features are noticeably different between EPKs and APH(3')-IIIa. While the active sites are generally large and accessible for EPKs, presumably permitting entry of large protein substrates, the active site of APH(3')-IIIa is blocked by residues 135-180 (referred to hereafter as domain III) which form 2 antiparallel helices joined by a loose 19 amino acid coil (Figure 5.1). This loop region was removed by PCR mutagenesis in an attempt to open the active site to larger protein substrates. A second noticeable difference between EPKs and APH(3')-IIIa is the residue G189. Virtually all EPKs have an arginine residue at this position which has been demonstrated to be necessary for enzyme function (reference). This residue is known to interact with phosphothreonine residue 197 which is autophosphorylated in cAPK upon activation. This residue was therefore altered from a glycine to an arginine residue (APH(3')-IIIa) to assess its contribution if any to the enzyme's kinase activity.

Although there have been identified regions of conserved primary sequence between APH(3')-IIIa and EPKs and they also appear to share structural similarity as determined by X-ray crystallographic structures, it is quite conceivable that they might share no functional similarity other than the binding of ATP and the ability to transfer phosphate to their appropriate substrates. For this reason the similarity which exists between APH(3')-IIIa and EPKs was investigated thoroughly using both known inhibitors of EPKs including a variety of isoquinolinesulfonamide (Figure 5.2A and 5.2B), several

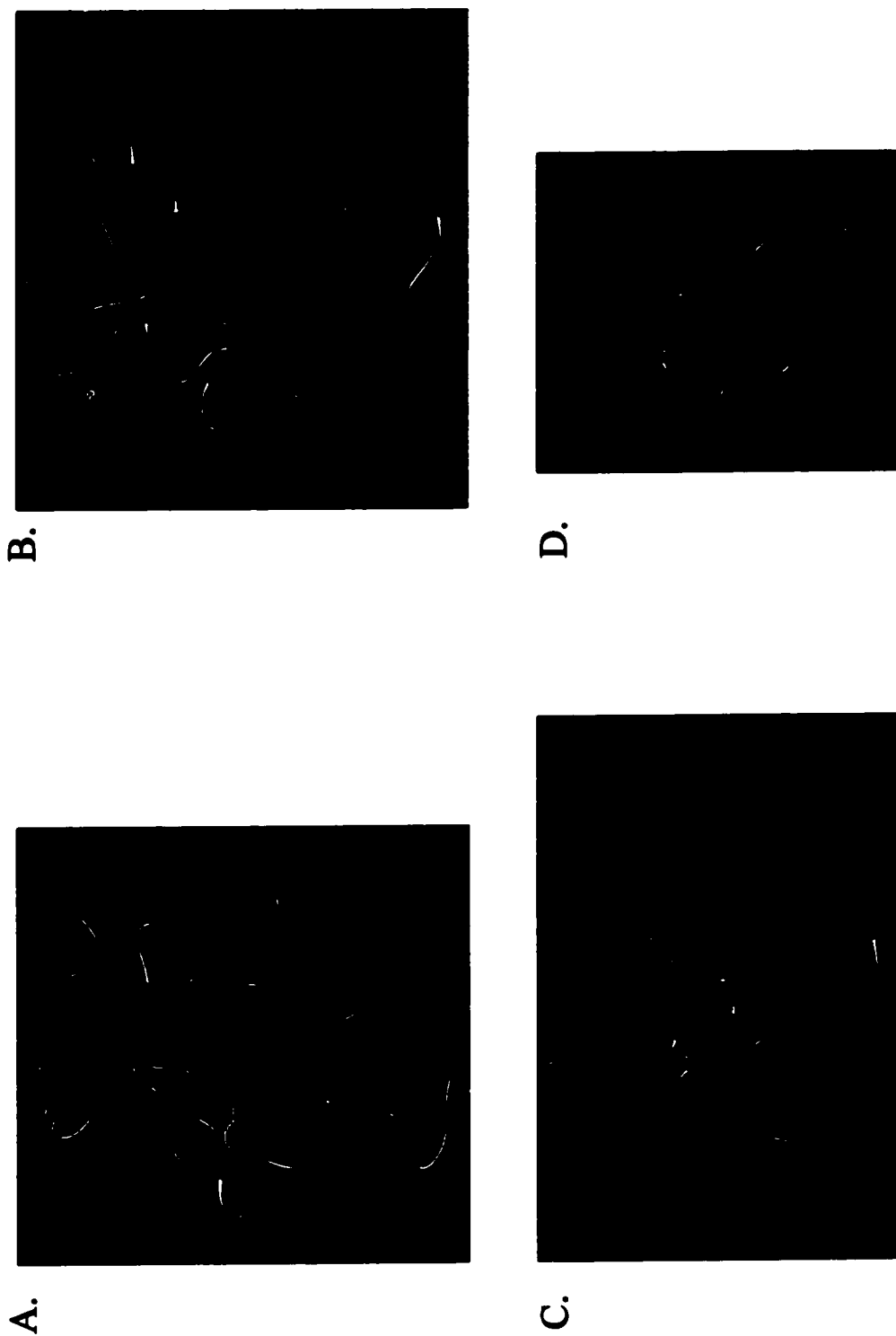


Figure 5.1. Three-dimensional structural comparison of (A) APH(3')-IIIa with bound $Mg^{2+}ADP$ and eukaryotic protein kinases (B) phosphorylase kinase with bound $Mg^{2+}ATP$, (C) casein kinase-1 with bound $Mg^{2+}ATP$ and (D) cAMP dependent protein kinase with bound $Mn^{2+}ATP$.

NOTE TO USERS

Page(s) not included in the original manuscript and are unavailable from the author or university. The manuscript was microfilmed as received.

This reproduction is the best copy available.

UMI

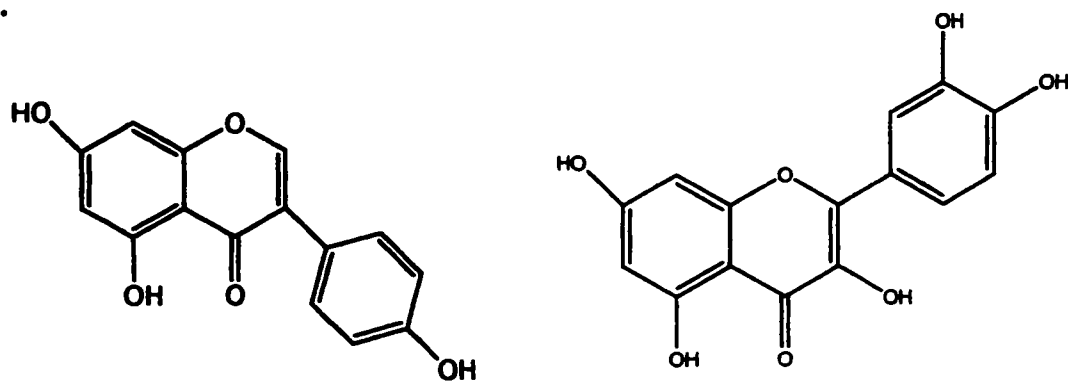
isoflavone (Figure 5.3A) derived inhibitors, staurosporine (Figure 5.3B) and numerous tyrphostin analogues (Figure 5.4). To further investigate and establish a possible functional similarity between APH(3')-IIIa and EPKs a series of protein kinase substrates were also surveyed. The protein kinase substrates assessed included, tyrosine kinase substrates poly (Glu,Tyr) (4:1) and p60^{c-src} substrate II a known substrate of c-src kinase (139). Numerous Ser/Thr protein kinase specific substrates were also investigated including myristolated alanine-rich C-kinase substrate protein (MARCKS) derived peptides MARCKS K and MARCKS R, protamine, casein, histone H1, Kemptide and the broad range substrate myelin basic protein (MBP).

5.2 *Materials and Methods*

5.2.1 *General Materials*

Genistein, quercetin, staurosporine, myelin-basic protein from bovine brain, Kemptide (LRRASLG), casein and poly (Glu,Tyr) (4:1) were from Sigma (St. Louis, MO). *N*-(2-aminoethyl)-5-chloroisoquinoline-8 sulfonamide (CKI-7) and 1-(5-chloroisoquinoline-8-sulfonyl)piperazine (CKI-8) were from Seikagaku America (Rockville, MD). 1-(5-isoquinolinesulfonyl)-2-methylpiperazine (H-7), *N*-(2-aminoethyl)-5-isoquinoline sulfonamide (H-9) and *N*-(2-guanidinoethyl)-5-isoquinoline sulfonamide (HA-1004) were from Research Biochemicals International (Nattick, MA). Histone H1 from calf thymus and p60^{c-src} Substrate II (Ac-IYGEF-NH₂) were from

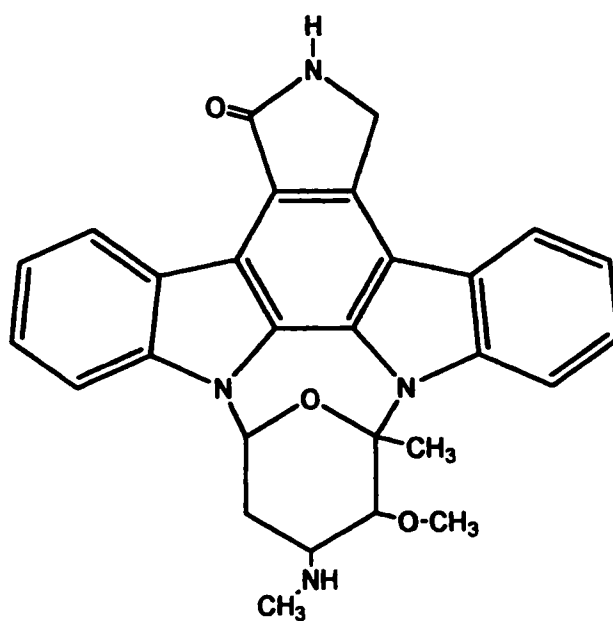
A.



genistein

quercetin

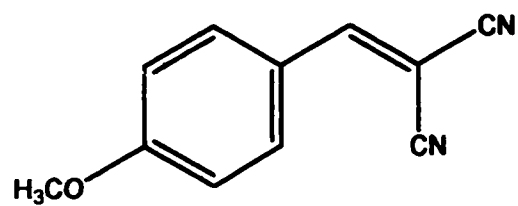
B.



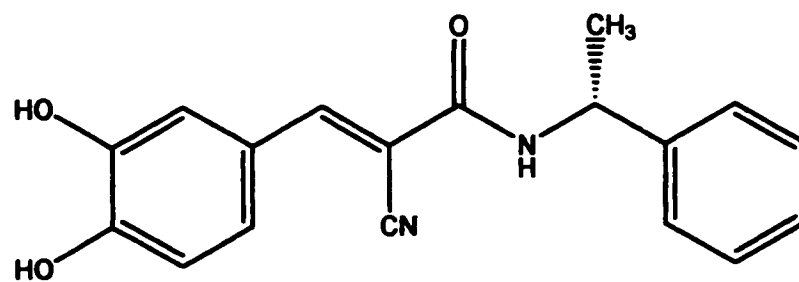
Staurosporine

Figure 5.3. Structure of protein kinase inhibitors. (A) Isoflavone derived protein kinase inhibitors. (B) Structure of protein kinase C inhibitor staurosporine.

A.



B.



C.

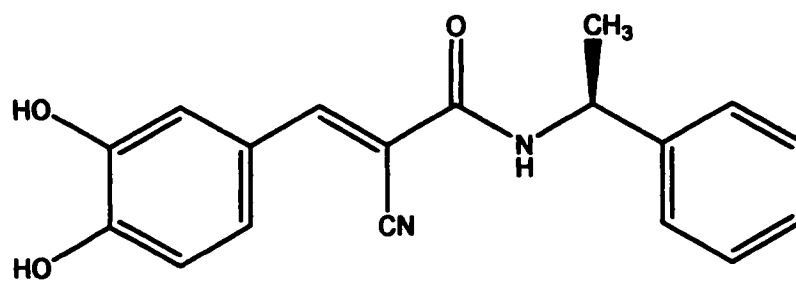


Figure 5.4. Structure of tyrosine protein kinase inhibitors (A) tyrphostin A1, (B) tyrphostin B44 and (C) tyrphostin B50.

Calbiochem. Protamine and MARCKS R peptide were the kind gift of Dr. Richard Epand, Department of Biochemistry, McMaster University. MARCKS K peptide was prepared by Dr. R.E. Williams, Institute for Biological Sciences, National Research Council, Ottawa, Ont. Rat brain PKC preparation (a mixture of α , β and γ isoforms) were a kind gift of Dr. R. Epand, Department of Biochemistry, McMaster University. Casein kinase-I clone pT7II-cki Δ 298 was a kind gift of Dr. Jeff Kuret, Department of Cell and Molecular Biology, Northwestern University Medical School, Chicago, IL and was purified as described in section 5.2.2.

5.2.2 Purification of Casein Kinase-I from *E. coli* BL21 (DE3)

[pT7II-cki Δ 298]

Casein kinase-I was purified by minor modification of the previously reported protocol (30). All steps were performed at 4 °C. *E. coli* harboring plasmid pT7II-cki Δ 298 was grown in Luria broth media containing 200 μ g/mL ampicillin at 37 °C to an A_{600} of 0.3 at which point IPTG was added to a final concentration of 1 mM. Cells were allowed to continue growing at 250 RPM for another 3 hr whereupon they were harvested by a 20-minute spin at 5000g. The cell pellet was then washed with 50 mL STE buffer (10 mM Tris-HCl, pH 8.0, 100 mM NaCl, 1 mM EDTA). The resultant cell pellet was then frozen overnight at -70 °C.

The following day, the cell paste was resuspended in 20 mL of lysis buffer (20 mM Tris-HCl, pH 7.5, 0.5 M NaCl, 5 mM imidazole, 10% glycerol, 1 mM PMSF) and disrupted by two passages through a French pressure cell at 20000 psi. The cell debris

was removed by two successive 20-minute centrifugation spins at 15000g. The detergent Brij35 was added to the crude extract to a final concentration of 0.1% (v/v) and then the sample was slowly brought to 75% saturation with addition of solid $(\text{NH}_4)_2\text{SO}_4$, stirred for 20 minutes and then centrifuged for 20 minutes at 20000g. The resultant pellet was resuspended in 5 mL buffer A (10 mM HEPES-HCl, pH 7.4, 150 mM NaCl, 0.1 mM EGTA) and then loaded onto a Sephadex G-100 (1.6 x 91 cm) column pre-equilibrated with buffer A. The column fractions were collected (0.5 min) at a flow rate of 30 mL/min and were monitored by both SDS-PAGE and casein kinase activity assays (Section 5.2.3).

Fractions containing CK-I were pooled and dialyzed against 1 L of buffer B (10 mM MOPS-HCl, pH 7.0, 50 mM NaCl, 0.1 mM EGTA, 0.02% Brij35 (v/v)). The following day the dialyzate was centrifuged (20 minutes at 20000g) and the supernatant applied onto a Sepharose-Q fast flow column (1.2 x 10 cm) equilibrated in buffer B. Protein that did not bind to the column was screened by SDS-PAGE and activity assays, following which positive fractions were combined.

The fractions of unbound protein were subsequently applied to a Mono S column (HR5/5) (Pharmacia) equilibrated in buffer C (10 mM MOPS-HCl, pH 7.0, 0.1 mM EGTA, 0.1% 2-mercaptoethanol, 50 mM NaCl). The column was washed with 20 ml buffer C and protein eluted with a 50 mM to 250 mM NaCl gradient in buffer C over 50 mL. Fractions were identified by SDS-PAGE and activity assays. Positive fractions were pooled and stored at 4 °C following the addition of 1 mM dithiothreitol. Samples were stable for up to 1 month.

5.2.3 *Casein Kinase Activity Assays*

Casein kinase I activity was assayed by modification of the procedure described for Ca²⁺/calmodulin-dependent casein kinase (112). Standard assay conditions consisted of a 100 µL reaction of 25 mM MES-HCl pH 6.5, 50 mM NaCl, 15 mM MgCl₂, 2 mg/ml casein, 2 mg EDTA and 100 µM [γ ³²P]ATP [250 000 CPM/nmol] and 10 µg of protein sample. Incubations proceeded at 30 °C for 15 minutes and were performed in duplicate. The reaction was terminated by addition of 10 µL of 300 mM EDTA and immediately spotted on Whatman GF/C glass fiber filters (24 mm diameter). Filters were washed in four changes of 10% trichloroacetic acid (w/v) and 100 mM sodium pyrophosphate followed by one rinse of 70% ethanol and one rinse of 100% ethanol (each wash 5 mL/filter). Filters were dried under a heat gun and samples analyzed in a scintillation counter.

5.2.4 *Generation of APH(3')-IIIa Site Mutants*

APH(3')-IIIa [G189R] was prepared by the QuikChange site-directed mutagenesis kit (Stratagene) using primers 5'-CCC AGG TCG CGG TGG GAA AAG AC-3' and 5'-GTC TTT TCC CAC CGC GAC CTG GG-3' while APH(3')-IIIa [Δ 123-189] was prepared using a modification of this procedure using primers 5'-A ACT GCA GCG ATA CAC CAA GGA GTT TTC GTG AAA GAG CCT GAT-3' and 5'-A ACT GCA GAC CTG GGA GAC AGC-3' which both incorporate *Pst* I sites at their 5'-end.

PCR reactions consisted of 150 ng pETAPHG6 plasmid, 0.5 µM primer 1 and 0.5 µM primer 2, 100 µM each dNTP, native PFU polymerase reaction buffer (10 mM KCl,

20 mM Tris-HCl, pH 8.8 at 25 °C, 10 mM (NH₄)₂SO₄, 2 mM MgSO₄, 0.1% Triton X-100 (v/v)). The reactions were heated to 94 °C to denature the sample following which was added 2.5 units of native *Pfu* polymerase. PCR cycles consisted of 1 minute at 94 °C, 1 minute at 52 °C and 6.5 minutes at 72 °C for elongation. Twenty-five cycles were completed and the reaction was stored at 4 °C overnight.

The pETAPHG6 [G189R] PCR reaction was precipitated by the addition of 1/10 volume 3 M sodium acetate pH 5.2 and 2 volumes of ice cold absolute ethanol. Following incubation for 20 minutes at -20 °C the mix was microcentrifuged at 4 °C for 10 min. The supernatant was removed and the pellet washed with 1 mL ice cold 70% ethanol. The pellet was allowed to dry and was then resuspended in 10 µL of deionized distilled water. A 15 µL digest reaction was prepared consisting of 10 µL of PCR reaction, 1.5 µL NEBuffer 4 and 5 units *Dpn I* and allowed to proceed for 1 hr at 37 °C. Three transformations of competent *E. coli* BL21 (DE3) were performed (CaCl₂ method) using 5, 10 and 50 ng of the *Dpn I* digested PCR reaction mix and transformants were plated on LB-agar plates containing 100 µg/ml ampicillin and permitted to grow at 37 °C overnight. The following day colonies were picked, DNA isolated by alkaline lysis minipreps, and sent the central MOBIX facility for DNA sequencing to insure correct incorporation of mutations.

The protocol for the deletion mutant pETAPHG6 [Δ 123-189] consisted of identical steps to and including PCR reaction DNA precipitation. Following precipitation of the PCR reaction, the DNA was digested with *Pst I* (1.5 µL 10x NEBuffer 3, 2.5 units *Pst I*, 10 µL PCR reaction) for 1 hr at 37 °C. The reaction was once again sodium

acetate/ethanol precipitated and the purified DNA ligated (10 μ L *Pst I* digested DNA, 1.5 μ L T4 ligase buffer NEB, 1 unit T4 DNA ligase (NEB)) overnight at 20 °C. The following day 2 transformations were performed using 50 and 200 ng of the ligated *Pst I* digested PCR reaction. Cells were plated on LB-agar plates containing 100 μ g/mL ampicillin and grown overnight at 37 °C.

Six clones were picked, plasmid was obtained by the alkaline lysis method and subsequently screened by restriction endonuclease digest mapping (using *Pst I* and *Nde I*, or *Pst I* and *Hind III*), Clones which were positive for insert were digested with *Pst I* (1 μ L 10x NEBuffer 3, 2.5 units *Pst I*, 200 ng plasmid) at 37 °C for 1 hr. Following digestion the 3' overhangs were removed by the Klenow fragment 3'-5' exonuclease activity. To the *Pst I* digest was added 1 μ L of 2.0 mM dNTP mix (0.5 mM each dNTP) and 5 units of the Klenow fragment of DNA polymerase. The reaction was incubated at 30 °C for 15 minutes following which it was extracted once with CHCl_3 :phenol and subsequently sodium acetate/ethanol precipitated. The pellet was redissolved in 8 μ L deionized distilled water to which was added 1 μ L 10x T4 ligation buffer (NEB) and 1 μ L T4 ligase (400 units/ μ L). The ligation was terminated after 2 hr at room temperature and used to transform competent *E. coli* BL21 (DE3). Six clones were prepared from positive transformants and sent to the MOBIX central facility for didexoy sequencing of the plasmid DNA.

5.2.5 Survey of Protein Kinase Inhibitors and their Effects on APH(3')-IIIa

Kinetic inhibition studies were assayed in a similar manner as presented in section 3.2.3. Inhibitors assayed include H-7, H-9, HA-1004, CKI-7, CKI-8 (Figure 5.2A, Figure 5.2B), genistein, quercetin (Figure 5.3A), staurosporine (Figure 5.3B) and a series of tyrphostins (A1, A25, B42, B44, B46, B48, B50 and B56) (Figure 5.4). In all cases the coupled enzyme assay remained unaffected by the level of inhibitor used.

For initial screening of inhibitors both APH(3')-IIIa substrates were held at subsaturating concentrations ($[ATP] = 25 \mu M$ and $[kan A] = 25 \mu M$). Staurosporine was assessed as an inhibitor of APH(3')-IIIa at only 500 nM due to the limited availability of this compound. Quercetin and genistein were assayed as inhibitors at concentrations of 0, 133, 267 and 533 μM and 0, 62.5, 125 and 250 μM respectively. HA-1004 and H-9 were assayed at concentrations of 0, 50, 100 and 200 μM and 0, 50, 100 and 150 μM respectively while H-7, CKI-7 and CKI-8 were all assayed at concentrations of 0, 53, 105, 210 and 427 μM in their respective trials. All tyrphostin species were assayed at concentrations of 0, 133, 200 and 333 μM .

All assays were completed at 37 °C in a reaction buffer consisting of 50 mM Tris-HCl, pH 7.5, 10 mM MgCl₂, 40 mM KCl.

5.2.6 Growth of APH(3')-IIIa [$\Delta 123-189$]

In an effort to increase the protein yield from APH(3')-IIIa [$\Delta 123-189$] cultures were heat shocked prior to the addition of IPTG using the following procedure.

Overnight cultures of APH(3')-IIIa [$\Delta 123-189$] were diluted 1:100 into 2 L fresh Luria

broth containing 100 $\mu\text{g/mL}$ ampicillin. Cells were grown with 250 RPM shaking at 30 $^{\circ}\text{C}$ until an OD_{600} of 0.4 was reached. The two liter culture was heat shocked by addition of 500 mL prewarmed Luria broth ($\sim 80^{\circ}\text{C}$). Following addition of the heated broth, IPTG was added to a final concentration of 0.1 mM and the flasks were returned to the 30 $^{\circ}\text{C}$ incubator and grown for 3 hr. Cells were then harvested and APH(3')-IIIa [$\Delta 123-189$] purified as described previously for wild type APH(3')-IIIa (Section 2.2.4b).

5.2.7 *Dead-End Inhibitor Analysis of Protein Kinase Inhibitors*

Only those compounds which demonstrated moderate to good levels of inhibition from the general survey were further screened as dead-end inhibitors of APH(3')-IIIa. Compounds which were studied further include H-7, H-9, HA-1004, CKI-7, CKI-8 and quercetin.

The five isoquinoline derived species were all analyzed as dead-end inhibitors of ATP. A family of plots was generated for each individual inhibitor where Kan A was held saturating at 120 μM while ATP was varied at concentration of 10, 25, 50, 100, 200 and 500 μM which covers a range of $\sim 0.3K_m$ to $\sim 18K_m$. HA-1004 was held at fixed concentrations of 0, 50, 100 and 200 μM , H-9 at fixed concentrations of 0, 50, 100 and 150 μM while the remaining isoquinoline derived inhibitors H-7, CKI-7 and CKI-8 were held at fixed concentrations of 0, 50, 105, 213 and 427 μM . Data were analyzed by equation 4 (see section 3.2.6).

The isoflavone derived compound quercetin was similarly analyzed. Kan A was held fixed at 120 μM while ATP was varied at concentrations of 10, 25, 50, 100, 200 and

500 μM spanning a range of $\sim 0.3K_m$ to $\sim 18K_m$. Quercetin was held fixed at concentrations of 0, 133, 267 and 533 μM generating a family of curves each corresponding to a unique concentration of inhibitor. Data were analyzed by fitting to equation 4 (see section 3.2.6).

To further characterize the nature of H-9 inhibition, this compound was assayed as a dead-end inhibitor of the second APH(3')-IIIa substrate Kan A. For these studies ATP was held fixed at 27 μM while Kan A concentrations were varied from 12, 25, 67, 100, 600 and 1000 μM covering a range of $\sim K_m$ to $\sim 80K_m$. H-9 was held at fixed concentration of 0, 53, 106 and 213 μM generating a family of curves where each curve corresponds to a unique concentration of H-9. Results were analyzed by fitting of data to equation 5 (see section 3.2.6).

5.2.8 Survey of APH(3')-IIIa Protein Kinase Activity

5.2.8a Phosphorylation of p60^{src} substrate II

Assay mixtures (20 μL) were comprised of peptide (500 $\mu\text{g/mL}$), 10 mM [$\gamma^{32}\text{P}$]-ATP (1.2×10^5 CPM/nmol), 100 mM Tris-HCl, pH 7.5, 10 mM MgCl_2 and 40 mM KCl. Reactions were initiated by the addition of 0.8 nmol purified APH(3')-IIIa and incubations were allowed to proceed for 4 hr at ambient temperature. Following completion of the reaction the mixture was diluted 5 fold to a final volume of 100 μL . Samples were analyzed by reverse phase HPLC using a Spherisorb-ODS2 C18 column (4 mm x 20 cm) at a flow rate of 0.5 mL/min) The entire sample was applied to the column

in a solution of 0.1% trifluoroacetic acid (v/v). Peptides were eluted by a gradient of 0.07% TFA in acetonitrile (CH₃CN) (B). The gradient consisted of 10 minutes 0% B, 0 to 40% B over 50 minutes, a 10 minute hold at 40% B followed by 40 to 90% B over 1 minute. Eluent was monitored by simultaneously monitoring wavelengths from 210 to 300 nm using a photodiode array detector. Fractions (0.5 mL) were collected and analyzed by scintillation counting.

5.2.8b *Phosphorylation of Histone H1, MBP and Poly (Glu:Tyr) (4:1)*

Incubations (10 μ L) consisted of 0.4 mg/ml histone H1, MBP or poly (Glu:Tyr) (4:1), 10 mM [γ ³²P]-ATP (1.2×10^5 CPM/nmol), 50 mM Tris-HCl pH 7.5, 10 mM MgCl₂ and 40 mM KCl. The assays were initiated by the addition of 0.8 nmol of purified APH(3')-IIIa and allowed to progress for 4 hr at ambient temperature. Mutants APH(3')-IIIa [G189R] (1-4 nmol) and APH(3')-IIIa [Δ 123-189] (1-2 nmol) were screened for the ability to phosphorylate MBP. The samples were quenched by the addition of EDTA to a final concentration of 35 mM followed by an equal volume of 2xSDS loading buffer (100 mM Tris-HCl, pH 8.8, 2 mM EDTA, 10% glycerol, 4% SDS) and separated on a 15% SDS-polyacrylamide gel. Phosphorylation of the substrates was monitored by autoradiography of the dried gel.

5.2.8c *Phosphorylation of Peptide Substrates*

A phosphocellulose binding assay was employed for substrates which are positively charged at neutral pH including MARCKS K (Ac-FKKSFKL-NH₂), MARCKS

R (Ac-FRRSFRL-NH₂), protamine and Kemptide (LRRASLG). The assay consisted of 100 μ M peptide substrate, 1 nmol purified APH(3')-IIIa, APH(3')-IIIa [G189R] 1 or 4 nmol, or APH(3')-IIIa [Δ 123-189] 1 or 2 nmol, 10 mM [γ ³²P]-ATP (1.2×10^5 CPM/nmol), 50 mM Tris-HCl, pH 8.0, 40 mM KCl, 10 mM MgCl₂, in a final volume of 10 μ L. The reactions proceeded at room temperature and were terminated after 4 hr by application onto Whatman P-81 phosphocellulose paper. The filter papers were washed once in boiling water for 5 minutes followed by 2 successive washes in cold water, and then dried with a heat gun. The filter papers were then placed in scintillation vials to which was added 5 mL of scintillation fluid and counted.

Casein, which is negatively charged at neutral pH, is not amenable to phosphocellulose trapping and thus was analyzed using glass fiber filters. Reactions consisted of 50 mM Tris-HCl, pH 7.5, 10 mM MgCl₂, 40 mM KCl, 2 mg/mL casein, 2 mg/mL EGTA, 100 μ M [γ ³²P]-ATP (2.5×10^5 CPM/nmol) and 1 nmol purified APH(3')-IIIa in a total volume of 100 μ L. Samples were incubated for 3 hr at 30 °C and were performed in duplicate following which they were quenched by the addition of 10 μ L of 300 mM EDTA and spotted on glass fiber filters. The filters were washed in four changes of 10% trifluoroacetic acid and 100 mM sodium pyrophosphate followed by one rinse of 70% ethanol and one rinse of 100% ethanol (each rinse 5 mL/filter). Filters were dried and then monitored in a scintillation counter.

Those substrates including both peptide and proteins which exhibited positive results in the APH(3')-IIIa protein kinase assays were further analyzed in order to determine the rates of reaction.

5.2.9 *Calculation of Rates of Phosphorylation of MBP by*

APH(3')-IIIa

A series of reactions were performed using a known concentration of MBP protein and varied concentrations of APH(3')-IIIa. Reactions (50 μ L) were performed in duplicate and consisted of 50 mM Tris-HCl, pH 7.5, 10 mM MgCl₂, 10 mM [γ ³²P]-ATP (1.2×10^5 CPM/nmol), 300 μ M MBP and were incubated at ambient temperature. Reactions were sampled by removal of 10 μ L aliquots at time points 15, 45, 90, 180, and 360 minutes and were quenched by addition of an equal volume of 2xSDS loading buffer. These 20 μ L samples were loaded on 15% SDS-polyacrylamide gels and separated at 200 V. Gels were stained for 15 minutes with Coomassie blue and destained for 15 minutes (30% methanol, 10% acetic acid in deionized distilled water), following which they were dried onto Whatman filter paper. Bands corresponding to MBP were excised from the gel and monitored by liquid scintillation counting. Negative controls were performed by excising similar size fragments of gel from unlabeled areas and monitoring their radioactive decay.

5.2.10 *Calculation of Rates of Phosphorylation of Peptides by APH(3')-IIIa*

Peptides MARCKS K, MARCKS R and protamine were analyzed in a similar manner to MBP. Reactions were performed in duplicate and consisted of 1 nmol purified APH(3')-IIIa, 10 mM [γ ³²P]-ATP (1.2×10^5 CPM/nmol), 50 mM Tris-HCl, pH 8.0, 40 mM KCl, 10 mM MgCl₂ in a final volume of 100 μ L. Peptide substrates were varied at concentrations of 50, 100, 250 and 400 μ M for MARCKS K, MARCKS R and

protamine. Aliquots (10 μ L) were removed at 5, 10, 40 and 60 minutes and immediately spotted on Whatman P-81 phosphocellulose paper. Filters were washed once in boiling water and twice in cold water, dried and then monitored by scintillation counting.

5.3 Results

5.3.1 Enzyme kinetics of APH(3')-IIIa [G189R] and APH(3')-IIIa [Δ 123-189]

Purified samples of APH(3')-IIIa [G189R] and APH(3')-IIIa [Δ 123-189] were used for kinetic studies (Table 5.1). No phosphorylation of either 4,5 or 4,6-disubstituted deoxystreptamine aminoglycosides was detectable when these antibiotics were incubated in the presence of APH(3')-IIIa [Δ 123-189]. Incubations were completed over a wide range of antibiotics (10 to 1500 μ M), a wide range of purified mutant enzyme (0.5 to 4 nmol), and a wide range of incubation times (1 to 30 min) and all results were negative.

Derivative G189R appeared to substantially affect enzyme activity by decreasing k_{cat} values and increasing K_m values for most aminoglycosides (Table 5.1). APH(3')-IIIa [G189R] was able to phosphorylate aminoglycosides kanamycin A, kanamycin B, neomycin C and ribostamycin while it was unable to detoxify amikacin, butirosin, isepamicin, lividomycin and paromomycin at concentrations of 10 to 1500 μ M.

Table 5.1. Kinetics of APH(3')-IIIa [G189R] for aminoglycoside substrates

Substrate ^a	k_{cat} (s ⁻¹)	K_m (μ M)	k_{cat}/K_m (M ⁻¹ s ⁻¹)
ATP	0.52±0.02	320±34	1.6x10 ³
Kanamycin A	0.10±0.01	1050±310	9.4x10 ¹
Kanamycin B	0.60±0.02	89.6±7.0	6.6x10 ³
Neomycin C	0.15±0.01	32.3±4.5	4.8x10 ³
Ribostamycin	0.09±0.005	91.3±14.3	9.9x10 ²

a Others substrates which were not phosphorylated include amikacin, butirosin, isepamicin, lividomycin and paromomycin.

5.3.2 *Survey of protein kinase inhibitors*

A series of known protein kinase inhibitors were screened to determine if they exhibited any effect on APH(3')-IIIa activity. Those species assayed included isoflavone derived inhibitors, isoquinoline derived inhibitors, the plant alkaloid staurosporine and a series of tyrphostins. The alkaloid staurosporine was found to have no inhibitory effect upon APH(3')-IIIa when present at levels of 0.7 μM while its inhibitory effect of PKC activity is generally in the range of 10 nM (86). Tyrphostins, A1, B42, B44, B46, B48, B50 and B56, showed no inhibition of APH(3')-IIIa when present at levels of 350 μM . Tyrphostin A25 (350 μM), showed extremely modest inhibition of APH(3')-IIIa and was therefore not further analyzed. The isoflavone derived inhibitors, genistein and quercetin have previously been demonstrated as effective tyrosine kinase inhibitors (4). Genistein was not an inhibitor of APH(3')-IIIa at levels of 250 μM while quercetin demonstrated moderate inhibition of APH(3')-IIIa. The inhibition was found to be competitive towards ATP with a K_{is} of 126 μM (Table 5.2).

The isoquinoline-derived inhibitors can be grouped into two families based upon their shared general structure. The first group, the H-series includes H-7, H-9 and HA-1004 (Figure 5.2A) while the second family, the C-series, includes CKI-7 and CKI-8 (Figure 5.2B). Although these two family members are structurally quite similar they show remarkable target specificity (34, 51, 87, 209).

All isoquinoline inhibitors assayed demonstrated competitive inhibition of APH(3')-IIIa with respect to ATP. The most potent inhibition of APH(3')-IIIa was demonstrated by HA-1004 (no equivalent C-series inhibitor) with a K_{is} of 48.9 μM . H-9

Table 5.2: Effects of protein kinase inhibitors on APH(3')-IIIa

Inhibitor	Variable substrate	Pattern ^a	K_{is} (μ M)	K_{ii} (μ M)	Equation ^b
CKI-7	ATP	C	66.1 \pm 7.5		1
CKI-8	ATP	C	290 \pm 89		1
H-7	ATP	C	730 \pm 130		1
H-9	ATP	C	138 \pm 40		1
H-9	kanamycin A	NC	155 \pm 26	260 \pm 19	3
HA-1004	ATP	C	48.9 \pm 12.3		1
Genistein	ATP	^c			
Quercetin	ATP	C	126 \pm 22		1
Staurosporine	ATP	^d			

^a C, competitive; NC, noncompetitive^b Data fit to equations in chapter 3^c No inhibition at 250 μ M^d No inhibition at 0.7 μ M

and its C-series equivalent, CKI-7, demonstrated moderate levels of inhibition with K_i values of 138 and 66 μM respectively. The least efficient inhibitors H-7 and its equivalent, CKI-8, demonstrated relatively poor inhibition of APH(3')-IIIa with K_i values of 730 and 290 μM respectively (Table 5.2).

The inhibitor H-9 was found to be noncompetitive with respect to its aminoglycoside substrate, consistent with the isoquinoline inhibitor interacting with the enzyme at the ATP binding pocket.

5.3.3 *APH(3')-IIIa Demonstrates Eukaryotic Protein Kinase Like Activity*

Initial surveys of various serine/threonine protein kinase and tyrosine kinase substrates demonstrated an apparent preference of APH(3')-IIIa for the former group. Tyrosine kinase substrates poly (Glu:Tyr) (4:1) and p60^{c-src} substrate II were not phosphorylated by APH(3')-IIIa. Serine threonine kinase substrates casein, histone H1 and Kemptide were similarly not substrates for APH(3')-IIIa. Substrates MARCKS K, MARCKS R, protamine and MBP (Figure 5.5A), however, were demonstrated to be substrates for APH(3')-IIIa phosphorylation during the initial survey and were therefore studied further to determine their rates of phosphorylation. MARCKS K, MARCKS R and protamine were all analyzed by phosphocellulose filter binding assay (Figure 5.5B). Kanamycin A, as a positive control, was analyzed using this assay and was found to have a rate of phosphorylation of 257 fmol/min. The two most efficiently phosphorylated substrates, efficiency being a measure of rate, MARCKS K and MARCKS R have phosphorylation rates of 58 and 53 fmol/min respectively (Table 5.3). The substrate

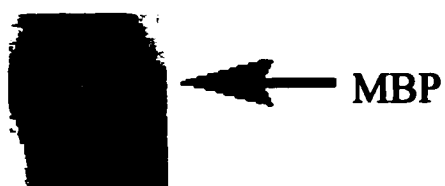


Figure 5.5. Protein kinase activity of APH(3')-IIIa, SDS-PAGE of myelin basic protein. Modified and redrawn from Daigle *et al*, 1999, reference #44.

Table 5.3. Phosphorylation of protein kinase substrates by APH(3')-IIIa

Substrate ^a	Rate of phosphorylation (fmol/min)
Kanamycin A	257±12
MARCKS K	58±8
MARCKS R	53±5
Protamine	43±4
Myelin basic protein	23±3

^a Substrates which were not phosphorylated include Kemptide, Histone H1, casein, Poly Glu-Tyr and p60^{c-src} substrate II.

protamine was demonstrated to have a phosphorylation rate of 43 fmol/min (Table 5.3). Owing to the quantities of peptide required to determine V_m and K_m we were unable to complete more thorough studies of a kinetic nature for MARCKS K, MARCKS R and protamine.

For MBP, however, we were able to determine a value of k_{cat}/K_m at sub- K_m values. At such substrate levels the Michaelis-Menten equation simplifies to:

$$\text{Eq}^n 7: \quad v = [S][E_{tot}](k_{cat}/K_m)$$

With defined levels of $[S]$ and $[E_{tot}]$ and measured (v) it is possible to calculate a value for k_{cat}/K_m although the two values, k_{cat} and K_m , are not separable. Using the above conditions, a value of $4.5 \times 10^2 \text{ M}^{-1} \text{ s}^{-1}$ was determined for the phosphorylation of MBP by APH(3')-IIIa. This specificity constant is 50 fold lower than the similarly obtained specificity constant for the phosphorylation of kanamycin A by APH(3')-IIIa demonstrating that although the enzyme is capable of phosphorylating certain protein substrates such activity is admittedly weak.

CHAPTER 6

Discussion.

Chapter 6

6.1 *Overexpression, purification and characterization of APH(3')-IIIa*

APH(3')-IIIa was found to purify as a mixture of monomer and dimer. The mass of 30842 Da, as determined by electrospray mass spectroscopy, is a very precise measurement (32, 123, 177) and differs from the predicted molecular mass of 30978 Da by 136 Da consistent with cleavage of the N-terminal methionine of the enzyme (Met 131 Da). A second substantial peak of 61685.5 Da was also detected by electrospray mass spectroscopy which is approximately double the mass of a single APH(3')-IIIa enzyme thus suggesting the formation of a stable dimer. The dimer was found to be sensitive to 2-mercaptoethanol indicating that presence of a disulphide bond stabilizing the dimer.

Samples of monomer and dimer were separately purified using size exclusion chromatography. Steady state kinetic parameters were determined for both forms yielding indistinguishable results when compared to one another. Although both forms were kinetically identical, purified samples of APH(3')-IIIa were isolated in the presence of the reducing agent dithiothreitol (DTT) in all further enzyme preparations. At present the exact nature of the proposed disulphide bond remains unclear as does its possible physiological role. The structure of APH(3')-IIIa has recently been solved using X-ray crystallographic methods and has determined that the enzyme forms a covalent dimer joined by two disulphide bonds (89). The dimer forms a "head to tail-tail to head" structure and the disulphide bonds are formed between C19 of one dimer and C156 on

the second dimer. The two active sites are separated by approximately 20 Å and are thus likely independent from one another as suggested by the steady state kinetic studies. It seems likely however that this disulphide bond would not exist in the cell cytoplasm as such an environment is reducing by nature and would tend to favour the monomeric form of the enzyme. This however is purely speculative and remains to be physically demonstrated.

6.2 *APH(3')-IIIa substrate specificity studies*

Large quantities of purified APH(3')-IIIa permitted a detailed substrate specificity analysis. Substrates assayed included representative members of both the 4,5 and 4,6-disubstituted deoxystreptamine aminoglycosides. Antibiotics assayed included kanamycin A, kanamycin B, amikacin, isepamicin, neomycin, paromomycin, lividomycin A, ribostamycin, butirosin and neamine. Nucleotide substrates assayed included ATP, dATP, GTP, CTP, UTP and thio-ATP. An initial examination of the data indicated for most aminoglycosides a small variation in substrate K_m values suggesting that binding affinities are fairly similar for both the 4,5 and 4,6-disubstituted deoxystreptamine aminoglycosides. Most aminoglycoside K_m values varied by only 3 fold for both classes of aminoglycosides. The noted exceptions include amikacin and isepamicin. These two substrates belong to the 4,6-disubstituted class of aminoglycosides and are substituted at the C-1 position of the aminocyclitol ring with an amino-2-hydroxybutyramide and an amino-2-hydroxypropionylamide group respectively. It is likely that these substituent groups sterically interfere with binding of these aminoglycosides to the enzyme active

site. Amikacin and isepamicin differ from kanamycin A solely at the C-1 position of the aminocyclitol ring and differ in their K_m s (relative to kanamycin A) by 19 and 15.7 fold respectively. The 4,5-disubstituted aminoglycoside butirosin is substituted at the equivalent C-1 position with an amino-2-hydroxybutyramide group. This aminoglycoside differs solely from ribostamycin by this substitution. Their K_m s are 9.3 μ M and 34.3 μ M differing by 3.6 fold. The contribution of this hydroxybutyramide group on butirosin binding is relatively limited suggesting binding of the 4,5 and 4,6-disubstituted aminoglycosides differ in their active site orientation at the C-1 position. While the K_m values are significantly affected by substitution at the C-1 position the k_{cat} values remain largely unaffected by the hydroxybutyramide and hydroxypropionylamide groups. Modification at either the 2' or the 6' position of the 6-aminohexose ring of both the 4,5 and 4,6-disubstituted deoxystreptamine aminoglycoside result in small changes in both the K_m and k_{cat} . Kanamycin A and kanamycin B differ at the 2' position by a hydroxyl and amino group respectively and show only a modest 1.5 fold difference in K_m values. Removal of the 6' amino group of kanamycin A to form 6'-deamino kanamycin A results in a 78 fold increase in K_m representing substantial loss of binding affinity. Conversely the k_{cat} values show only a modest effect. The effect of substitution of an amino group for a hydroxyl group at the 6' position of the aminohexose ring of the 4,5-disubstituted and 4,6-disubstituted aminoglycoside suggests that this position forms a hydrogen bond with the enzyme rather than an ionic interaction and is involved in helping to productively bind the substrate.

While it is apparent that the 6' position of aminoglycosides plays a role in substrate binding, removal of the 2' amino group from Kan A has only a 1.75 fold effect on substrate affinity and a 4.5 fold effect on k_{cat} suggesting a possible role for this group in positioning of the 3' hydroxyl for catalysis.

Removal of the amino group at the C-3 position of kanamycin A resulted in a modest 1.8 fold effect on K_m and a 1.2 fold effect on k_{cat} suggesting this group plays a limited role in enzyme substrate binding or the enzyme chemistry. This is supported by studies which demonstrate that neamine which encompasses only the 6' aminohexose and aminocyclitol ring of neomycin B is an excellent substrate for APH(3')-IIIa showing identical k_{cat} values and a moderate 2.5 fold increase in K_m values. The lack of a contribution by C-3 to substrate binding agrees well with Fourmy's observation that rings I and II of the aminoglycoside have the primary determinants necessary for binding to the 16S rRNA oligonucleotide (45, 46). APH(3')-IIIa appears to have evolved to modify a hydroxyl group located on the rings necessary for aminoglycoside binding. There is a general trend towards modification of rings I and II by all aminoglycoside modifying enzymes and this is best exemplified by the acetyltransferases which exclusively modify amino groups on these two rings. To further identify the minimum binding unit for aminoglycoside substrates, samples of 6-amino- α -methyl glucoside and ribose were assayed and found to be neither substrates nor inhibitors of APH(3')-IIIa at concentrations of 10 mM. This demonstrates that neamine is the minimal unit necessary for aminoglycoside binding.

6.3 *Kinetic mechanism studies of APH(3')-IIIa*

Presently, there are few cases when kinetic mechanisms have been determined for aminoglycoside modifying enzymes. The bulk of these studies have been completed by Northrop's group where they have identified the kinetic mechanisms for a kanamycin acetyltransferase (154), gentamicin acetyltransferase I (199) and the nucleotidyltransferase 2"-I (ANT(2")-I) (61). Martel and colleagues have demonstrated that the bifunctional enzyme AAC(6')-APH(2") follows a random kinetic mechanism for both enzyme activities (124).

A number of techniques were required in order to conclusively delineate the kinetic mechanism for APH(3')-IIIa. Initial velocity patterns demonstrate a family of intersecting lines indicative of a sequential mechanism thus excluding the possibility of a Ping Pong mechanism. Previously, studies by Kocabiyik had putatively identified H188 as a phosphate-accepting residue in a kinetic mechanism. Other studies refute this suggestion while the possibility of a phospho-enzyme intermediate was further discredited by the absence of a measurable positional isotope exchange (PIXs) (187). PIXs experiments demonstrated that phosphotransfer likely proceeded in a direct transfer mechanism (187). An intersecting pattern of initial velocity plots is observed for Kan A, Amik and Paro which indicates that aminoglycosides from both the 4,6- and 4,5-disubstituted deoxystreptamine aminoglycosides follow a sequential mechanism. It is also important to note that a sequential order is also maintained for both good (Kan A $k_{cat}/K_m = 1.43 \times 10^5 \text{ M}^{-1} \text{ s}^{-1}$) and poor (Amik $k_{cat}/K_m = 1.0 \times 10^4 \text{ M}^{-1} \text{ s}^{-1}$) substrates.

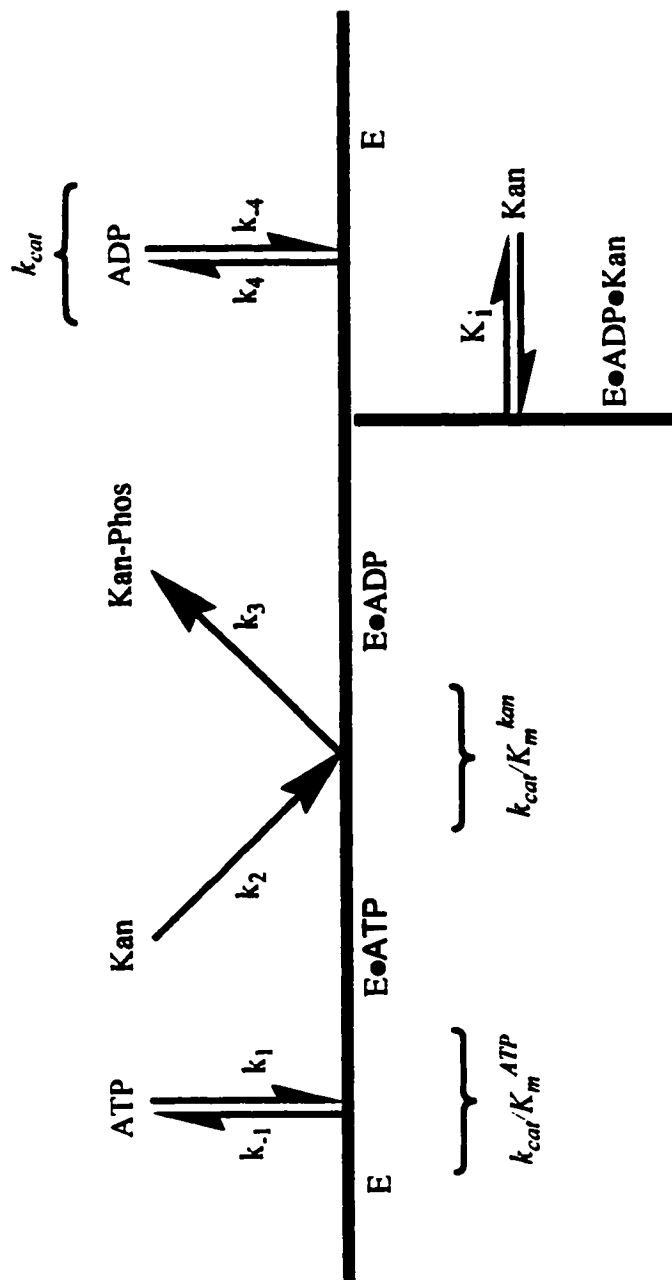
Inhibition studies are often used to help identify both the order of substrate binding and product release. Substrate analogue dead-end inhibitors of both the nucleotide and aminoglycoside substrates permitted us to probe the order of substrate addition. Tobramycin and dibekacin which both lack the 3' OH were found to be potent competitive inhibitors of aminoglycosides with K_{i_s} values of 0.35 μM and 2.64 μM respectively. Tobramycin was also demonstrated to be an uncompetitive inhibitor of ATP. For a species to demonstrate uncompetitive inhibition it requires that the substrate be bound initially, followed subsequently by inhibitor binding. This is therefore strongly suggestive of an ordered sequential substrate addition where ATP must bind prior to aminoglycoside binding (inhibitor binding). Two dead end inhibitors AMP-PNP and AMP were shown to bind competitively with respect to ATP and were also found to be non-competitive inhibitors of kanamycin A. These data support an ordered substrate addition where ATP must be bound prior to aminoglycoside entry into the active site. Due to the unique nature of the Ping Pong mechanism and the separation of the two substrate binding events (separated by product release) dead end inhibitors show uncompetitive inhibition of the second substrate while random mechanisms show non-competitive inhibition of the second substrate by the dead-end inhibitors. The latter phenomenon is due to the random order of addition for the substrates (58)

Product inhibition studies are a useful diagnostic tool to help in the identification of product release order. APH(3')-IIIa activity is measured by coupling the release of ADP from the reaction to a pyruvate kinase/lactate dehydrogenase reaction. This coupling reaction ultimately leads to the oxidation of NADH (regenerating ATP) and

monitoring this reaction at 340 nm. This obviates the use of ADP as a product inhibitor and limits product inhibition studies to the use of kanamycin phosphate (phosphorylated aminoglycoside). Large quantities of the phosphorylated aminoglycoside were purified and analyzed as a product inhibitor of ATP. Initially kanamycin A was held at saturating concentrations ($10K_{m \text{ Kan A}}$) as the fixed substrate while the concentration of ATP was varied. Even when present at concentrations of 2 mM, kanamycin phosphate was not found to inhibit the enzyme. When the concentration of the fixed substrate, kanamycin A, was lowered to subsaturating concentrations ($K_{m \text{ Kan A}}$) and ATP was varied it was observed that kanamycin phosphate was a weak non-competitive inhibitor with a K_{is} of 10 ± 7.1 mM and K_{ii} of 3.7 ± 0.47 mM. This observed pattern of product inhibition is consistent with the release of kanamycin phosphate prior to the release of ADP. The elimination of product inhibition by saturation with kanamycin A is consistent with two possible mechanisms including the Ping Pong and Theorell-Chance ordered Bi-Bi reaction. The possibility of the former mechanism had previously been eliminated on the basis of both initial velocity studies and dead-end inhibitor results. All the data collected is consistent however with the special case ordered Bi-Bi kinetic mechanism where ATP binds prior to kanamycin binding. This is followed by a chemical step and release of kanamycin phosphate and subsequent ADP release.

The Theorell-Chance mechanism is a special case of a bi substrate bi product reaction where the central kinetic complex ($E\text{-ATP-kan} \leftrightarrow E\text{-ADP-kanphos}$) becomes kinetically insignificant and does not contribute to the rate of reaction as presented in Scheme 6 (163). For APH(3')-IIIa following conversion of the two substrates to products

Scheme 6: Theorell-Chance Kinetic Mechanism of APH(3')-IIIa



there is a rapid release of kanamycin phosphate followed by a slower rate limiting release of the second product ADP. As discussed earlier, although the initial velocity patterns have established a sequential mechanism it is due to the transient nature of the ternary complex that the product inhibition patterns appear to be supportive of a Ping Pong mechanism.

Similar behaviour has previously been observed by Northrop for ANT(2'')-I (61). They observed an identical order of substrate addition followed by a quick chemical reaction and rapid release of ADP and ultimately a rate limiting release of nucleotidylated aminoglycoside. Both APH(3')-IIIa and ANT(2'')-I exhibit the phenomenon of substrate inhibition where when the aminoglycoside substrate reaches sufficiently high concentrations it begins to inhibit the enzyme rate of reaction. The non-productive binding of aminoglycoside leading to substrate inhibition is believed to occur in a similar fashion for both enzymes. As substrate is converted to product there is the rapid release of the first product (kanamycin phosphate for APH(3')-IIIa) followed by the relatively slow rate limiting release of the second product (ADP). We propose that following release of kanamycin phosphate a specific binding site is exposed allowing entry of a second aminoglycoside molecule. Binding of this second substrate aminoglycoside would then trap the enzyme in a non-productive complex (E-ADP-kan) leading to an overall decrease in V_m (measured rate) at high levels of aminoglycoside substrate. The inhibition observed is both full and uncompetitive in nature and therefore suggests that blockage of the E-ADP-kan complex is complete and must have no finite release of ADP. The observation of uncompetitive substrate inhibition implies that the aminoglycoside (I)

must bind to an enzyme form isolated by irreversible steps from the enzyme form that binds ATP.

A unique diagnostic technique capable of identifying each major class of kinetic mechanism was developed by Radika and Northrop (155) and has been successfully used to help delineate the kinetic mechanism of ANT(2'')-I (61), AAC(6')-4 (154) and APH(3')-Ia (176). The technique requires that several alternative substrates exist for both the nucleotide phosphoryl donor and the second substrate the aminoglycoside. Although numerous aminoglycoside substrates were readily available, APH(3')-IIIa, could only use ATP and dATP as the phosphoryl donor thus somewhat limiting the alternative substrate diagnostic. A substrate, such as ATP, is varied using several fixed alternative second fixed aminoglycoside substrates such as kanamycin A, kanamycin B, paromomycin and lividomycin. Similarly the second substrate kanamycin A, is varied using several alternative fixed phosphoryl donor substrates (ATP, dATP). As discussed previously this second series of plots was not generated due to the inability of APH(3')-IIIa to use sufficient alternative phosphoryl donor substrates. Unique families of plots are generated depending on the kinetic mechanism of the enzyme being assessed.

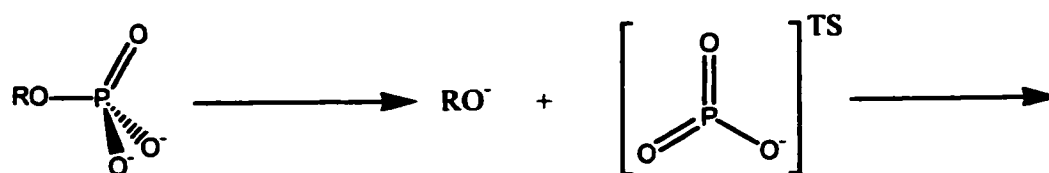
When ATP is varied using several distinct aminoglycoside substrates as the fixed second substrate a family of coincident lines are generated where k_{cat} values vary by only 1.15 fold and second order rate constants k_{cat}/K_m vary by only 1.38 fold. This pattern of coincident lines is consistent only with a Theorell-Chance kinetic mechanism (155) where ATP binding occurs first followed by aminoglycoside binding. One would expect the second substrate of a Theorell-Chance mechanism to have very little effect on the

overall rate of reaction, as is in fact observed, yet one would propose a more substantial effect on both k_{cat} and k_{cat}/K_m by the nucleotide substrate which unfortunately due to the limitation of the system can not be adequately addressed.

To further address and independently assess the conclusion of a Theorell-Chance type kinetic mechanism we have used solvent isotope, solvent viscosity and nucleotide thio effects to probe the contribution of each step to the overall rate of the reaction. Two possible mechanisms have been proposed theoretically to exist in which a phosphate group is transferred from a donor molecule (ATP) to a recipient molecule (kanamycin A or other aminoglycoside). These two mechanisms are associative reaction (Figure 6.1B) via a pentacoordinate transition state and a dissociative reaction (Figure 6.1A) via a monomeric metaphosphate (104). The former mechanisms involves the formation of a transition state where bond formation between the phosphate and donor is breaking as the bond between the recipient and phosphate is forming and thus the phosphate is never in a “free” state. The latter mechanism is proposed for the hydrolysis of phosphate monoesters with good leaving groups and in this mechanism a “free” metaphosphate anion (PO_3^-) is transiently formed prior to the second nucleophilic attack by the recipient compound.

In either case both mechanisms require a deprotonation event be it the secondary 3'OH or the primary 5'OH of the aminoglycosides to generate the attacking nucleophile. Enzyme kinetics for APH(3')-IIIa were performed in D_2O where all hydroxyls are deuterated. Assuming this, by Hook's law, one would expect to see a significant solvent isotope effect on the rate of reaction if a deprotonation event were contributing to the

A.



B.

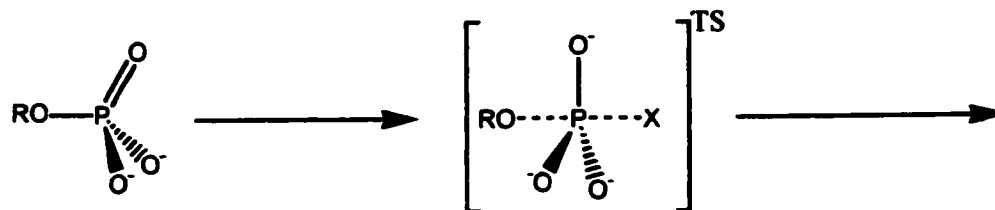


Figure 6.1. Proposed mechanisms of phosphoryl transfer. (A) Dissociative meta phosphate transition state and (B) associative pentacoordinate transition state.

overall rate of reaction. We demonstrated that there was roughly a 1.4-1.6 fold effect on k_{cat} for the enzyme at two distinct pH values thus insuring that results were not masked by a possible pKa effect. This small value is consistent with a minor contribution of deprotonation to the overall rate of aminoglycoside phosphorylation. A maximal isotope effect of 10 would be expected for a mechanism where proton transfer is solely rate limiting (113). Similar values have been observed for both C-terminal Src kinase and cAMP dependent protein kinase where solvent isotope effects of 1.2 and 1.6 were observed respectively (39, 210). Yoon and Cook also demonstrated and concluded that the relatively small observed deuterium solvent isotope effect was consistent with viscosity measurements and other kinetic studies which demonstrated that cAMP dependent protein kinase was controlled by ADP product release as the rate limiting step (210).

In an attempt to assess the contribution of nucleophilic attack at the phosphoryl center we have turned to using a sulfur substituted nucleotide (ATP- γ -S). This species is substituted at a non-bridging position on the γ -phosphate of ATP. This substitution (P—S) is substantially less electrophilic than the P—O group and this results in a lower rate of reaction if nucleophilic attack at the phosphoryl center contributes to the rate-limiting step of the reaction. The thio effect observed for APH(3')-IIIa which is a ratio of k_{cat} for ATP/ATP- γ -S was measured to be approximately 2 while the K_m values differed by only 1.8 fold indicating that nucleotide binding was minimally affected by the O to S substitution (an important consideration when trying to interpret thio effects). A thio effect of 10-20 has previously been reported for the phosphorylation of

poly(Glu:Tyr) by C-terminal Src kinase (39) while a thio effect of 18 has been measured for phosphorylation of lymphoid cell kinase (Lck- Δ NH₂-R) under identical conditions (178). This second substrate, Lck- Δ NH₂-R is a biologically relevant protein substrate for Csk (178). The presence of a thio effect for both the peptide substrate and biological protein substrate Lck suggests that it is probable that the chemical step for both substrates has a similar rate and both likely contribute to the rate-limiting segment of their respective kinetic mechanisms. It is important to note that the measured thio effects were observed using manganese as the divalent cation while substitution with magnesium leads to a thio effect of 136 fold on k_{cat} (71). Conversely cyclic AMP dependent protein kinase can phosphorylate phosphorylase kinase (its natural substrate) using ATP- γ -S at a rate virtually identical to that when ATP was used as the phosphoryl donor (72). These results indicate that while nucleophilic attack at the phosphorus center contributes to the rate limiting step of catalysis for C-terminal Src kinase whereas the rate-limiting step of the mechanism for cAMP dependent protein kinase does not appear have a significant contribution from a nucleophilic attack at the phosphorus center of ATP. This is in agreement with Yoon's studies showing ADP release as the rate limiting step of catalysis (210)

Both the solvent isotope and thio effects imply that APH(3')-IIIa has a rate limiting step which is independent of either deprotonation of the nucleophilic hydroxyl or nucleophilic attack at the phosphorus center. This observation independently confirms our previous kinetic studies which identified a Theorell-Chance mechanism where ADP release was the rate-limiting step of the kinetic mechanism.

Although the data was fairly conclusive that APH(3')-IIIa followed a Theorell-Chance kinetic mechanism and its rate of reaction was primarily governed by a rate-limiting release of the product ADP we sought to investigate the question of how solvent viscosity would affect the kinetic parameters for the enzyme reaction. Simplistically, the alterations of a solution viscosity should affect only diffusional steps of a reaction, such as binding and release of substrates and/or products. Thus in a two molecule system the rate of collision is inversely proportional to the viscosity of the solution (110). For such a statement to be true it must hold that viscogens have no non-specific effects on the enzymatic reactions. As such they must not generate their effects by altering/affecting the structure of the enzyme, substrate or product and they must have no secondary effect upon the reaction media. Often viscosity studies are controlled for such effects by completing identical studies using either a "poor" substrate or "poor" enzyme (10, 22). In both instances there should be no diffusion effects upon either a "poor" substrate or "poor" enzyme if their rates are limited by a chemical step. Neither of these species was available however at the time of these studies and therefore we used the substrate inhibition as a similar control. Neither of the two microviscogens sucrose nor glycerol had an effect upon the substrate inhibition constant indicating that these species did not interfere with the aminoglycoside interaction on the enzyme. Data for viscosity studies were all plotted in a similar fashion where the x-axis is relative viscosity calculated as described in Materials and Methods while the y-axis was either k_{cat}°/k_{cat} or $(k_{cat}/K_m)^{\circ}/(k_{cat}/K_m)$ where $^{\circ}$ represents values obtained in the absence of viscogen. These plots are generated at four distinct solution viscosities and the slope of the line calculated. The

maximal theoretical value for either of these ratios is predicted to be 1 (22). A value of 1 implies a diffusion controlled limit while a value of 0 denotes a step which is insensitive to viscosity changes.

When either sucrose or glycerol was used as the viscogen and ATP was held saturating as the fixed substrate our results demonstrated there was no viscosity effect on k_{cat}/K_m consistent with the Theorell-Chance kinetic mechanism. The second substrate in a Theorell-Chance mechanism should not contribute to the rate-limiting step and thus should be independent of the solution viscosity. The viscosity effect on k_{cat} under the same conditions is roughly 1 regardless of whether sucrose or glycerol is used as the viscogen demonstrating a sensitivity to solution viscosity consistent with a diffusion limited step. Both kanamycin A and amikacin show identical results when ATP is fixed at saturating levels. Thus although amikacin is a relatively poor substrate compared to kanamycin A both aminoglycosides appear to share viscosity sensitive and insensitive steps confirming our belief that the kinetic mechanism is identical for all aminoglycosides.

While most of the data demonstrate results consistent with a Theorell-Chance mechanism a discrepancy is observed for slope effects on V_{max}/K_m for ATP when the second fixed aminoglycoside was held at saturating amounts. It was found for both fixed substrates amikacin and kanamycin A that the slope exceeded the theoretical maximal value of 1. Simopoulos and Jencks have previously suggested that a value in excess of the theoretical limit could indicate that V_{max}/K_m for ATP is governed by two diffusion controlled equilibrium and thus are subject to solution viscosity effects (175).

Any such second diffusion controlled equilibria would have to affect V_{\max}/K_m for ATP such as a possible conformational change upon binding of ATP to the enzyme. We believe that such a conformational change might be present in the APH(3')-IIIa mechanism. A conformation change of this nature might be used to bring the γ -phosphate of ATP into the proximity of the catalytic base and the attacking hydroxyl. Without such a conformational change, one might expect to see some non-specific ATPase activity associated with APH(3')-IIIa upon transfer of the phosphate to a water molecule. Under no conditions was non-specific ATP hydrolysis observed. As presented in section 2.3.4 phosphate transfer required a minimum substrate of neamine and compounds such as 6-amino- α -methylglucoside were not phosphorylated by APH(3')-IIIa. Although the active site of APH(3')-IIIa can accommodate a wide variety of aminoglycoside substrates it is unable to "accommodate" such smaller substrates suggestive of a possible conformational change necessary to bring the two substrates into proximity. It has been demonstrated elsewhere that triosephosphate isomerase shows a solvent viscosity sensitive structural change similar to our proposal (167) while hexokinase requires a conformational change to bring glucose and ATP together prior to catalysis. As with APH(3')-IIIa, hexokinase does not show appreciable ATPase activity in the absence of its second substrate glucose (15).

Direct evidence of a conformational change was investigated using several techniques including circular dichroism (CD), tryptophan fluorescence and UV spectral changes following substrate binding. Changes in enzyme conformation were assessed using substrates ATP, ADP and competitive inhibitors AMP-PNP and tobramycin.

Under these conditions and using these methods co-incubation of APH(3')-IIIa with any of the compounds or combination of compounds did not lead to an observable change in the spectra being monitored. While the techniques of CD and tryptophan fluorescence are sensitive to small changes in protein structure it is possible that subtle changes might be invisible. CD measurements generate spectra based upon secondary structure and thereby identification of a conformational change using this technique would require a shift in secondary structure content in order to be detected. Tryptophan fluorescence detects perturbations in the environment surrounding tryptophan residues. In order to detect any effect it is necessary that one such residue be affected by a shift in enzyme structure. APH(3')-IIIa has 5 tryptophan residues and it is therefore conceivable that any slight effect upon the enzyme structure might in fact be obscured by the remaining tryptophan residues. In collaboration with Wai Ching Hon, Dr. Albert Berghuis and Dr. Daniel Yang the crystal structure of APH(3')-IIIa has been solved (89). Two forms have been determined including the apo enzyme and a second form with bound ADP. These two enzyme forms show two major important differences in structure. Firstly the apo enzyme demonstrates that a loop (green loop) comprised of residues 21-29 (Figure 6.2B and 6.2D) occupies the nucleotide binding cleft in the absence of the nucleotide substrate. Upon binding of ADP (nucleotide substrate) this loop adopts a more elongated conformation and swings up and out of the nucleotide binding cleft (Figure 6.2A and 6.2C). A second noticeable change is apparent between the apo and ADP bound forms of APH(3')-IIIa. The "Thumb region" formed by residues 135-180 (hereafter referred to as domain III) adopts a different conformation upon binding of ADP. Without a structure

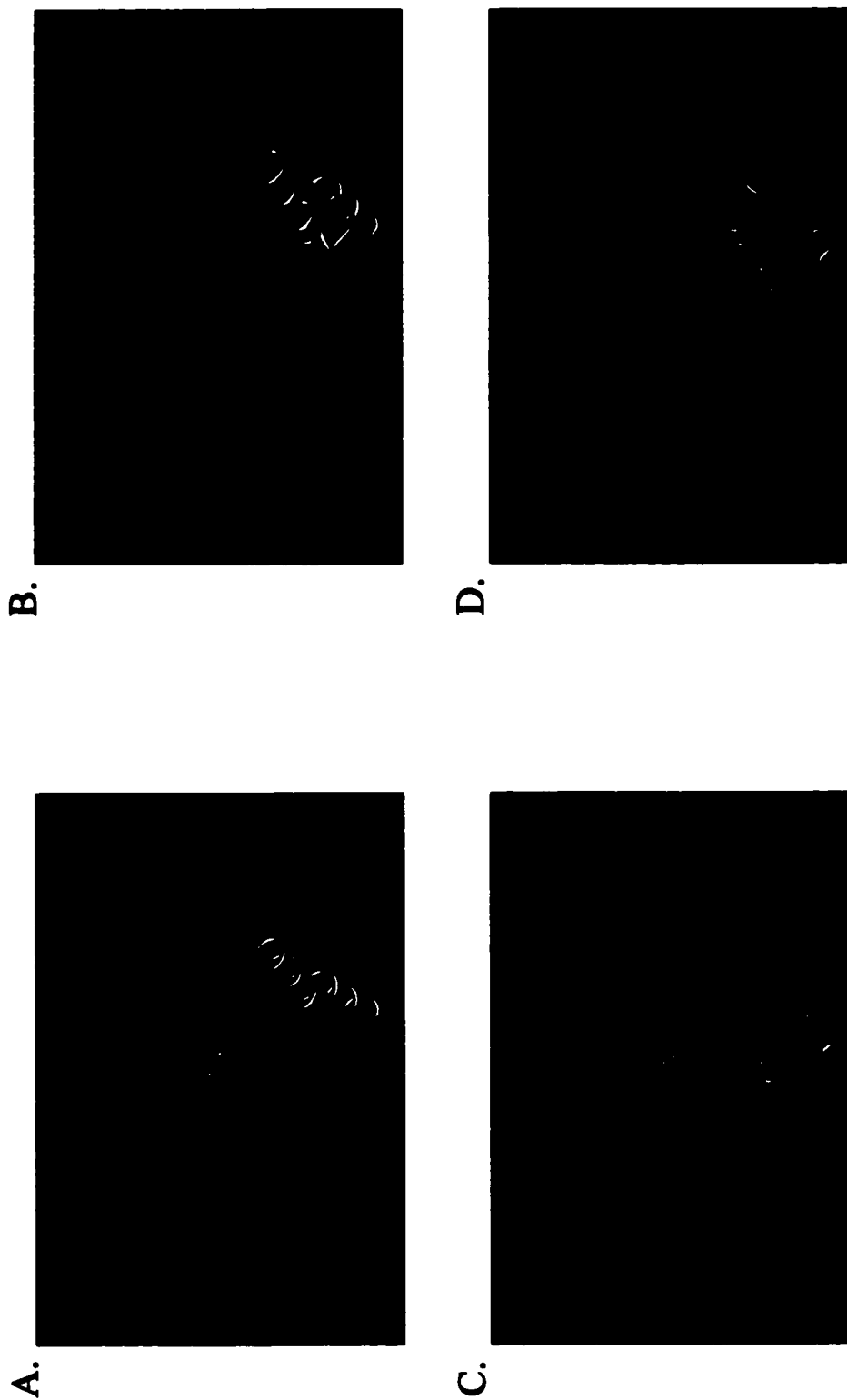


Figure 6.2. Three-dimensional structural comparison of (A) APH(3')-IIIa with bound ADP (front view), (B) apo APH(3')-IIIa (front view), (C) APH(3')-IIIa with bound ADP (side view) and (D) apo APH(3')-IIIa (side view). Amino acid loop of residues 21-29 is coloured green in all four structures. Amino acid domain III of residues 135-180 is coloured yellow in all four structures.

with bound aminoglycoside one can only speculate as to which residues are required on domain III (if any) for substrate binding. It is reasonable to assume however, that given the high degree of positive charge on aminoglycosides the binding pocket will likely have an overall net negative charge. Domain III is proposed to be involved in aminoglycoside substrate due to its position and high negative charge and likely adopts this conformation in order to make available the site and residues necessary for aminoglycoside binding. These structural changes are supportive of the proposed viscosity sensitive conformational change. As suggested both of these changes involve little (if any) secondary structure changes and thus would likely remain undetectable by CD spectra. While no tryptophan residue is found within loop 21-29 there is one found in domain III (135-180) suggesting that although the residue changes position as part of the conformational change, its environment remains essentially the same and therefore remains undetectable by tryptophan fluorescence.

The elucidation of a Theorell-Chance mechanism has permitted a detailed evaluation of several microscopic rate constants and is represented graphically in Scheme 7. The energetic profile indicated is constructed using standard state 1 M reactants and it is important to note that there are several limitations due to the techniques employed. Firstly the free energy of the ternary complex cannot be actually determined using steady state kinetics and is therefore represented by a bracket. Secondly it is possible that one or more steps in fact incorporate multiple equilibria, as is our proposal upon binding of ATP. The values calculated are presented in Table 6.1 and were found to be consistent with each other and the proposed mechanism with one noticeable exception. A Theorell-

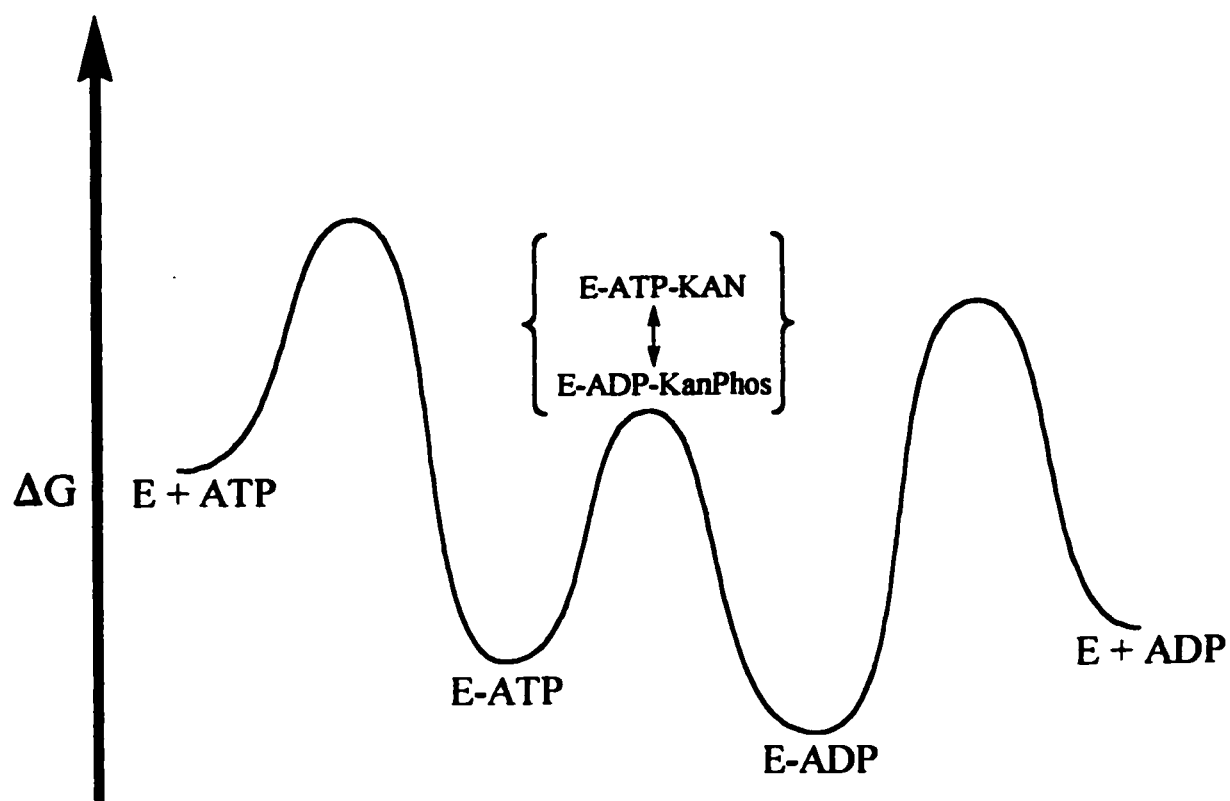
Scheme 7: APH(3')-IIIa Free Energy Reaction Diagram

Table 6.1. Microscopic rate constants for APH(3')-IIIa with substrates ATP and kanamycin A

Constant ^a	values	ΔG (kcal/mol)
k_1^b	$6.35 \times 10^4 \text{ s}^{-1} \text{ M}^{-1}$	11.3
k_{-1}^c	0.11 s ⁻¹	19.5
k_2^d	$1.40 \times 10^5 \text{ s}^{-1} \text{ M}^{-1}$	10.8
k_3^e	$86.4 \text{ s}^{-1} \text{ M}^{-1}$	15.4
k_4^f	1.76 s ⁻¹	17.8
k_{-4}^g	$4.68 \times 10^3 \text{ s}^{-1} \text{ M}^{-1}$	12.9

^a Constants are described in Scheme 6. ^b $k_1 = k_4/K_m^{\text{ATP}}$, ^c $k_{-1} = k_{\text{cat}(\text{reverse})}$, ^d $k_2 = k_4/K_m^{\text{kan}}$,
^e $k_3 = k_{\text{cat}(\text{reverse})}/K_m^{\text{kan-phosphate}}$, ^f $k_4 = k_{\text{cat}(\text{forward})}$, ^g $k_{-4} = k_{\text{cat}(\text{reverse})}/K_m^{\text{ADP}}$.

Chance mechanism is unique in that $k_{-1}=k_{cat}$ (reverse) by definition and thus should also equal K_{ia}/k_1 (169). It was found however that there was over a 10 fold discrepancy between the calculated value of 0.11 s^{-1} in the reverse direction and the expected value of 1.65 s^{-1} calculated from k_1 and K_{ia} (1.65 s^{-1}). Such a discrepancy is consistent with or proposal of a conformation change in APH(3')-IIIa following binding of ATP and agrees well with the observed conformational change following binding of the nucleotide substrate (Figure 6.2).

6.4 *Active site mapping and structure of APH(3')-IIIa*

As presented in section 1.4.7 considerable work has been directed towards identifying active site residues involved in the function of several aminoglycoside phosphotransferases (105-107). Primary sequence alignments have identified conserved regions of amino acid homology. The C-terminal third of the protein demonstrates the highest degree of homology and three motifs have been identified which have residues which are conserved across all APH(3') family members. These studies however had relied solely upon primary sequence alignments of the phosphotransferase family members to identify residues essential to the activity of these enzymes. This approach, although useful, can potentially ignore residues that are not identified by these sequence alignments. In a more direct means we attempted to identify residues in the ATP binding site by probing the enzyme with the electrophilic ATP analogue p-fluorosulfonylbenzoyl adenosine (FSBA).

Preliminary experiments with FSBA and purified APH(3')-IIIa demonstrated a substantial decrease in enzyme activity following an hour incubation. Co-incubation of ATP with the inactivation reactions resulted in a significant protection from FSBA labeling. Co-incubation of APH(3')-IIIa with its second substrate, an aminoglycoside, did not afford similar protection to that observed for ATP while co-incubation of both the aminoglycoside substrate and ATP afforded an identical level of protection to that observed with ATP alone suggesting that the two active site pockets were independent of one another.

Inactivation of APH(3')-IIIa by FSBA was demonstrated to be both concentration and time dependent. These rates of inactivation at increasing FSBA concentrations were used to generate a family of plots where the slope of each individual line corresponds to the observed first order rate (k_{obs}) of inactivation for a given FSBA concentration. A replot of k_{obs} values versus the inactivator concentration (FSBA) generates a rectangular hyperbola similar to that of a typical Michaelis-Menten curve. The curve approaches a limit of $0.086 \pm 0.077 \text{ min}^{-1}$ which indicates the maximal rate of inactivation of APH(3')-IIIa in the presence of saturating amounts of FSBA (k_{max}). The FSBA concentration at $\frac{1}{2}k_{max}$ represents the apparent dissociation constant (K_i) for the inactivator and enzyme complex. The estimation of the value of $406 \pm 28 \text{ } \mu\text{M}$ is substantially higher than the $27 \text{ } \mu\text{M}$ obtained for the K_m of ATP demonstrating that there is significant contribution to the binding energy of ATP from the phosphate groups which are lacking on FSBA. Other factors including geometry and steric constraints are likely to play a role in the increased apparent dissociation constant.

Large scale inactivation of APH(3')-IIIa was performed using either ^{14}C -labeled FSBA or non-radioactive FSBA. The labeled peptide was digested with TPCK-treated trypsin and the peptide mix separated by reverse phase HPLC followed by mass spectral analysis and N-terminal analysis of labeled peptides. Labeled peptides were identified by both an increase at 280 nm absorbance and the ^{14}C -labeled signal. The two residues, K33 and K44, were identified as the targets of FSBA inactivation. Labeling of these residues appeared to be mutually exclusive as no peptide was identified which had been labeled at both residues. This is in agreement with the stoichiometry of inactivation that had previously indicated a unique labeling event. The two residues are located outside the conserved C-terminal motifs and therefore this region had heretofore remained virtually totally ignored. Motif II which includes the sequence GXXXXGR/K had previously been proposed to be the nucleotide binding fold (18) identified in other ATP requiring enzymes by Fry and colleagues (60). For this reason most site-directed mutagenesis had focused on the terminal third of the phosphotransferase enzymes. Blazquez and colleagues identified a valine to methionine mutation at residue 36 of APH(3')-IIa which resulted in a 20 fold decrease in antibiotic resistance (18). This decrease in resistance was exclusively detected by MIC and therefore in the absence of analysis using purified enzyme it is not possible to elucidate the specific effect the V36M mutation has on APH(3')-IIa function.

Multiple sequence alignments of APH(3') family members using Clustal W (186) (Figure 6.3) demonstrates that K44 is conserved across all family members while K33 is less conserved within the aminoglycoside phosphotransferase family. The absolute

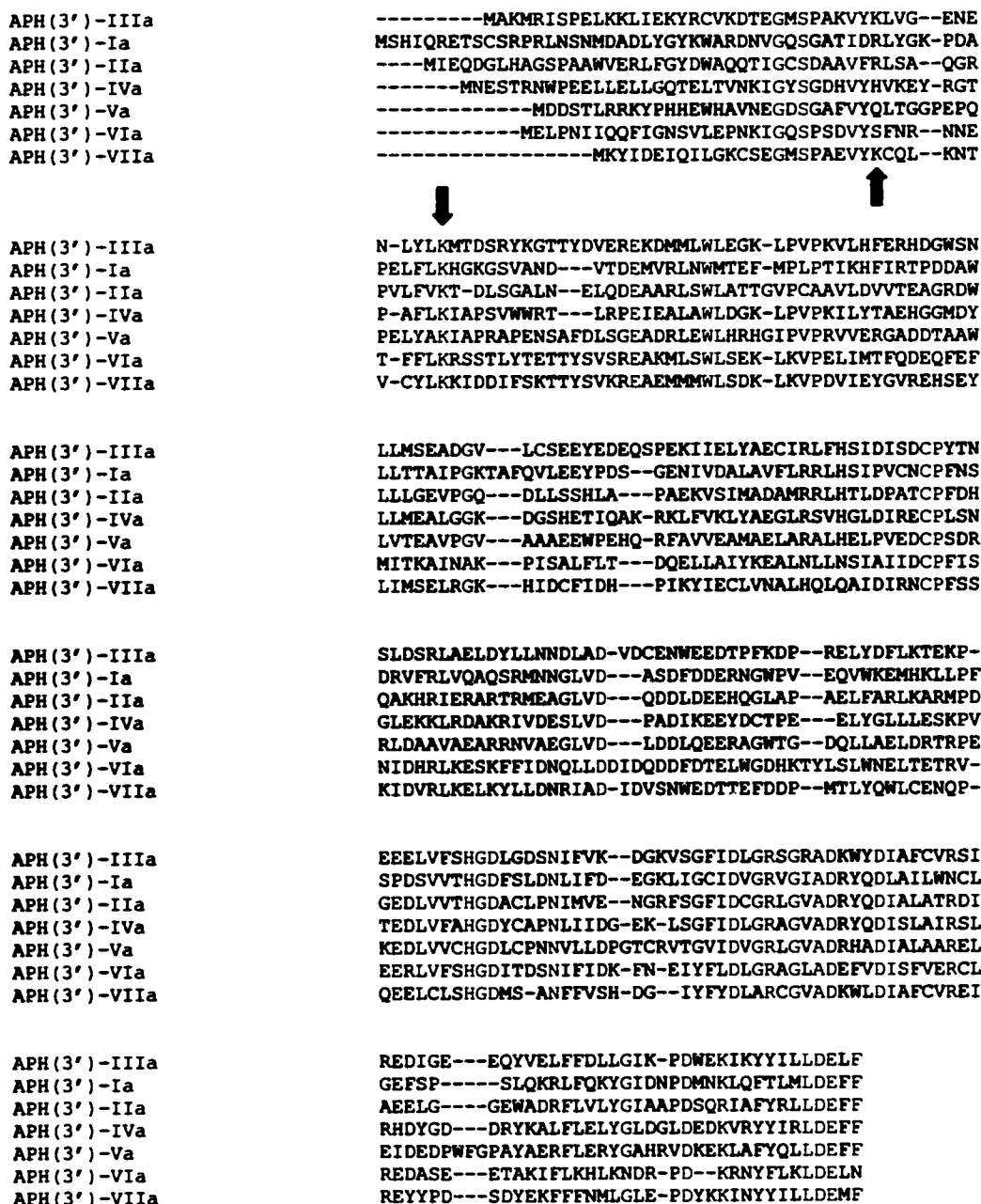


Figure 6.3. Primary sequence alignment of seven APH(3')-IIIa family members. Alignment was performed using Clustal W and the graphical interface Clustal X. Red amino acids indicate complete conservation across all family members, while green amino acids indicate conservation across most family members. Lysine 33 and lysine 44 are identified with purple bullets. Accession numbers are as follows: APH(3')-Ia, 547782; APH(3')-IIa, 125463; APH(3')-IIIa, 125464; APH(3')-IVa, 125465; APH(3')-Va, 125466; APH(3')-VIa, 125467 and APH(3')-VIIa, 125468.

conservation of K44 strongly suggests that this residue is adjacent to the terminal phosphate. Several other residues which include G25 and S27 are also universally conserved across all APH(3') family members while it is interesting to note that V31 (corresponds to V36 of APH(3')-IIa) is not universally conserved but is replaced with an isoleucine residue in both APH(3')-Ia and APH(3')-Ic while the other isozymes including APH(3')-IIIa have a conserved valine residue.

FSBA has frequently been used successfully to identify residues in the active site of a variety of enzymes. In smooth-muscle myosin light-chain kinase (108), type II calmodulin-dependent protein kinase (102), phosphoinositide 3-kinase (207), cAMP dependent protein kinase (215) v-SRC (96) and EGFR (164) a lysine residue has been identified by its covalent modification with p-FSBA. Selective mutagenesis of these lysine residues in the case of v-SRC (96), EGFR (164), cAMP dependent protein kinase (215) and phosphoinositide 3-kinase (207) have demonstrated that this residue is required for enzyme function. In all cases it was determined that the nucleotide substrate was competitively able to prevent FSBA inactivation of these lysine residues.

In all cases this lysine residue is located 10-25 amino acids on the C-terminal side of the GxGxxG motif identified in eukaryotic protein kinases (81). While this is true for EPKs this is obviously not as clearly defined for APH(3')-IIIa. While there is a putative GxxxxGR/K motif located in the C-terminal region of the enzyme, the lysine residues identified are located in the N-terminus. It is interesting to note that this glycine rich motif is distally located from the nucleotide substrate and thus likely plays no direct role in either substrate binding or the enzyme active site chemistry. While APH(3')-IIIa and

the identified EPKs show a similar protection from FSBA inactivation by co-incubation with their nucleotide substrate, it is quite clear that substantial differences do exist between the two enzymes.

Mutagenesis of K44 of APH(3')-IIIa to an alanine, while retaining substantial phosphotransferase activity was found to have a K_m ATP of 566 ± 59 μ M which is a 27 fold increase over wild type. Conversely, however, the k_{cat} was found to remain essentially identical to that of wild type where only a 1.1 fold difference was observed. While a substantial change was observed for the ATP kinetics virtually no change was observed for the second substrate aminoglycoside kanamycin A where binding (K_m) was unaffected by the K44A mutation. These results differ substantially from those observed for several EPKs where this similarly identified lysine residue demonstrates a much more substantial effect upon k_{cat} and not K_m values for both cAMP dependent protein kinase (67) and mitogen activated kinase ERK2 (160).

Mutagenesis studies on K33 yielded an enzyme with essentially wild type kinetics for both substrates ATP and kanamycin A. There was a slight decrease in k_{cat} values (2.7 fold) while the K_m remained unchanged. These mutagenesis studies would suggest that while both K33 and K44 are protected from FSBA inactivation only the latter residue likely plays a role in substrate binding and enzyme function. It is likely, given that the inactivation events are mutually exclusive, that when inactivation of K33 occurs, it prevents entry of further FSBA molecules and subsequent inactivation of K44. Similarly, inactivation of K44 prevents subsequent inactivation of K33. While K33 seems to play

little or no role in either substrate binding or catalysis, it is likely to lie close to the ATP binding pocket for reasons discussed above.

Recently the X-ray crystal structure of APH(3')-IIIa with bound ADP has been determined to a resolution of 2.2 Å (89). Currently other aminoglycoside modifying enzymes which has been solved using X-ray crystallography, ANT(4') (147, 165), AAC(3') (201) and AAC(6')-Ii (205) have also been demonstrated to exist as a homodimers. For ANT(4') however there are substantially more interactions between the monomers and in fact the two subunits combine to form the functional active site at the dimer interface. For this reason, ANT(4') functions only when present as a dimer, and thus this form is the physiologically relevant species. While the AAC(3') monomers show a significant interaction at their interface and are likely to form a dimer in the cell the active sites appear to be functional independent of one another (201).

This structural arrangement of APH(3')-IIIa shows strong similarity to eukaryotic protein kinases. Specifically the N-terminal β -sheets are highly similar between APH(3')-IIIa and the available eukaryotic protein kinase structures for cAMP dependent protein kinase (51, 121, 214), casein kinase I (119, 208) and phosphorylase kinase (120, 143). In addition the sections of the C-terminal core which form the ATP binding cleft in eukaryotic protein kinases are found to be virtually identical in APH(3')-IIIa (Figure 6.4).

Despite sharing little primary sequence identity, APH(3')-IIIa and several Ser/Thr and tyrosine kinases show distinct similarities using a structure-based alignment. Lysine 44 that was covalently labeled by FSBA shows absolute conservation across all eukaryotic protein kinases. This residue was initially proposed to be involved directly in

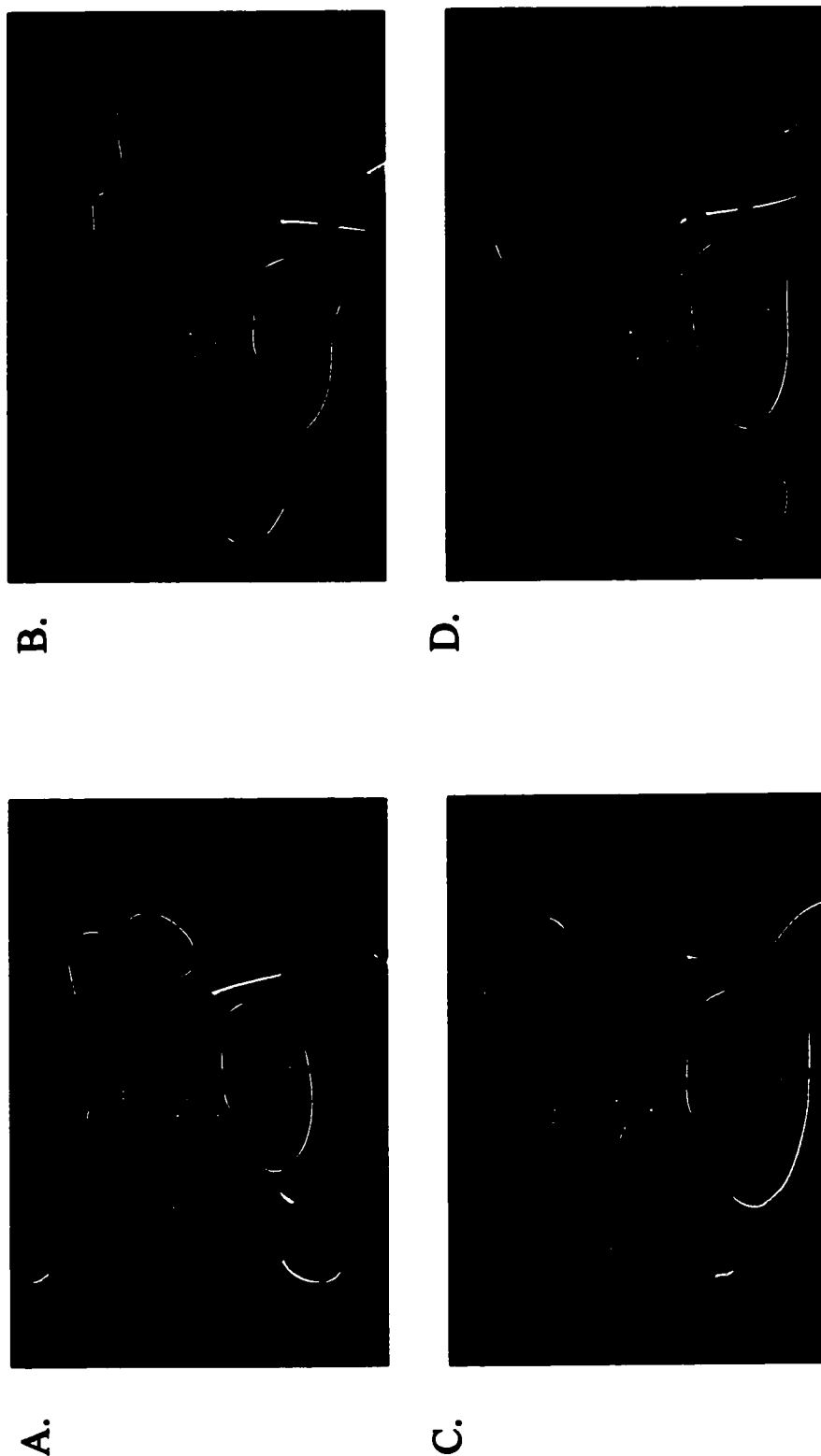


Figure 6.4. Three-dimensional structural comparison of active site residues. (A) APH(3')-IIIa; K33, lysine 33; K44, lysine 44; E60, glutamate 60; D190, aspartate 190; N195, asparagine 195; D208, aspartate 208. Metal cofactor is coloured pink. (B) phosphorylase kinase; K48, lysine 48; E73, glutamate 73; D149, aspartate 149; N154, asparagine 154; D167, aspartate 167. Metal cofactor is coloured purple. (C) casein kinase-1; K41, lysine 41; E55, glutamate 55; D131, aspartate 131; N136, asparagine 136; D154, aspartate 154. Metal cofactor is coloured pink. (D) cAMP dependent protein kinase; K72, lysine 72; E91, glutamate 91; D166, aspartate 166; N171, asparagine 171, D184, aspartate 184. Metal cofactor is coloured purple.

the phosphotransfer reaction by protonating the MgATP or stabilization of the negative charge generated during phospho transfer (96). With the increased number of eukaryotic protein kinase crystal structures it is clear that this invariant lysine functions not in direct phosphoryl transfer but rather plays a role in hydrogen bonding to the oxygen atoms of both the α and β phosphates of the nucleotide substrate (19). A similar interaction is observed for APH(3')-IIIa where K44 is found to interact with both the α and β phosphates of the co-crystal ADP molecule. In the APH(3')-IIIa and cyclic AMP dependent protein kinase, casein kinase I and phosphorylase kinase structures a conserved glutamate residue (E60 APH(3')-IIIa numbering) forms a salt bridge with the invariant lysine residue stabilizing its interaction with MgATP and thus making it implausible that K44 is involved directly in phosphoryl transfer. Direct physical evidence using the K44A mutant supports its proposed role in a hydrogen bond network. The ratio of k_{cat}/K_m wild type to K44A mutant is approximately 30 fold consistent with an ion-pair interaction of 2.1 kcal/mol (198). Surprisingly, a K72A mutation in cAMP dependent protein kinase demonstrates only a 5 fold decrease in K_m values while showing approximately a 1000 fold decrease in k_{cat} values (67). The mechanism of cAMP DPK has been shown to follow an ordered sequential Bi-Bi mechanism and thus k_{cat} reflects a relatively complex expression of several elementary rate constants. The kinetic mechanism of APH(3')-IIIa is a more uncommon case where the first order rate constant, k_{cat} , reflects the first order rate of dissociation of ADP and thus one might expect a less dramatic effect upon the phosphorylation reaction.

6.5 Protein kinase inhibitor studies

It is clear from the X-ray crystallographic studies that APH(3')-IIIa and several eukaryotic protein kinases share substantial homology over specific discreet regions. Conserved structures include the N-terminal β -sheet lobe and perhaps more importantly they show a remarkable conservation over the nucleotide binding fold. This homology over the ATP binding pocket is particularly striking when one considers the overall lack of primary sequence homology between APH(3')-IIIa and eukaryotic protein kinases. Residues which are conserved include K44 (numbering is based on APH(3')-IIIa), E60, D190, N195 and D208. While APH(3')-IIIa and eukaryotic protein kinases show these similarities it is quite possible that the similarity does not extend beyond their ability to bind and utilize the nucleotide substrate ATP. For this reason we chose to investigate a possible functional similarity between the two species. To investigate this we used two approaches. The first studies investigated a series of well characterized protein kinase specific inhibitors to determine if any were suitable inhibitors of APH(3')-IIIa function while the second approach screened a variety of eukaryotic protein kinase substrates specific for either Ser/Thr or tyrosine kinases. Substrates assayed were either full protein substrates or peptide substrates routinely used in EPK assays.

Staurosporine is an alkaloid compound initially isolated from *Streptomyces* sp. (142, 182) which has long been known to possess antifungal properties (182). Its inhibitory activity has also been shown to act on phospholipid/ Ca^{2+} dependent protein kinase (PKC) with a K_i value of between 1-2 nM (86, 182). Initially staurosporine was believed to be a PKC specific inhibitor but it was subsequently demonstrated that while

the compound was a very potent inhibitor of protein kinases it showed very little selectivity (86, 128). Kinases including PKC, phosphorylase kinase, PKA and EGFR kinase are inhibited by staurosporine at levels ranging from 2 nM to 15 nM while other kinases such as casein kinase I, casein kinase II and CSK are relatively refractory with K_i levels between 1000 nM and 13000 nM.. Crystal structures of both cAMP dependent protein kinase (Figure 6.5A) and CDK2 (Figure 6.5B) co-crystallized with staurosporine have shed light on the interactions necessary for binding. Residues E81, L83 and Q131 of CDK2 form hydrogen bonds with staurosporine while residues E121, V123, E127 and E170 form similar interactions between cAMP dependent protein kinase and the inhibitor (153, 188). These data strongly support the hypothesis that the staurosporine inhibitor binds competitively to ATP in the enzyme active site. Crystal structures of cAMP DPK and CDK2 demonstrated that the same residues are required for ATP binding in the enzyme active sites (19, 49). The residues which have been identified demonstrate that position E127 and E170 which are present in both cAMP dependent protein kinase and phosphorylase kinase yet absent in casein kinase-1 and CSK are indicators of susceptibility to staurosporine. Positions E121 and V123 appear to be more flexible where the residue seems to have poor correlation to staurosporine sensitivity with the only general trend being the presence of an acidic residue at position 121, although this is found in both sensitive and resistant enzymes. APH(3')-IIIa is found to code for a leucine and a serine at positions 127 and 170 respectively which would disrupt the hydrogen bonds necessary for staurosporine binding and thus likely explains its apparent refractory behaviour.

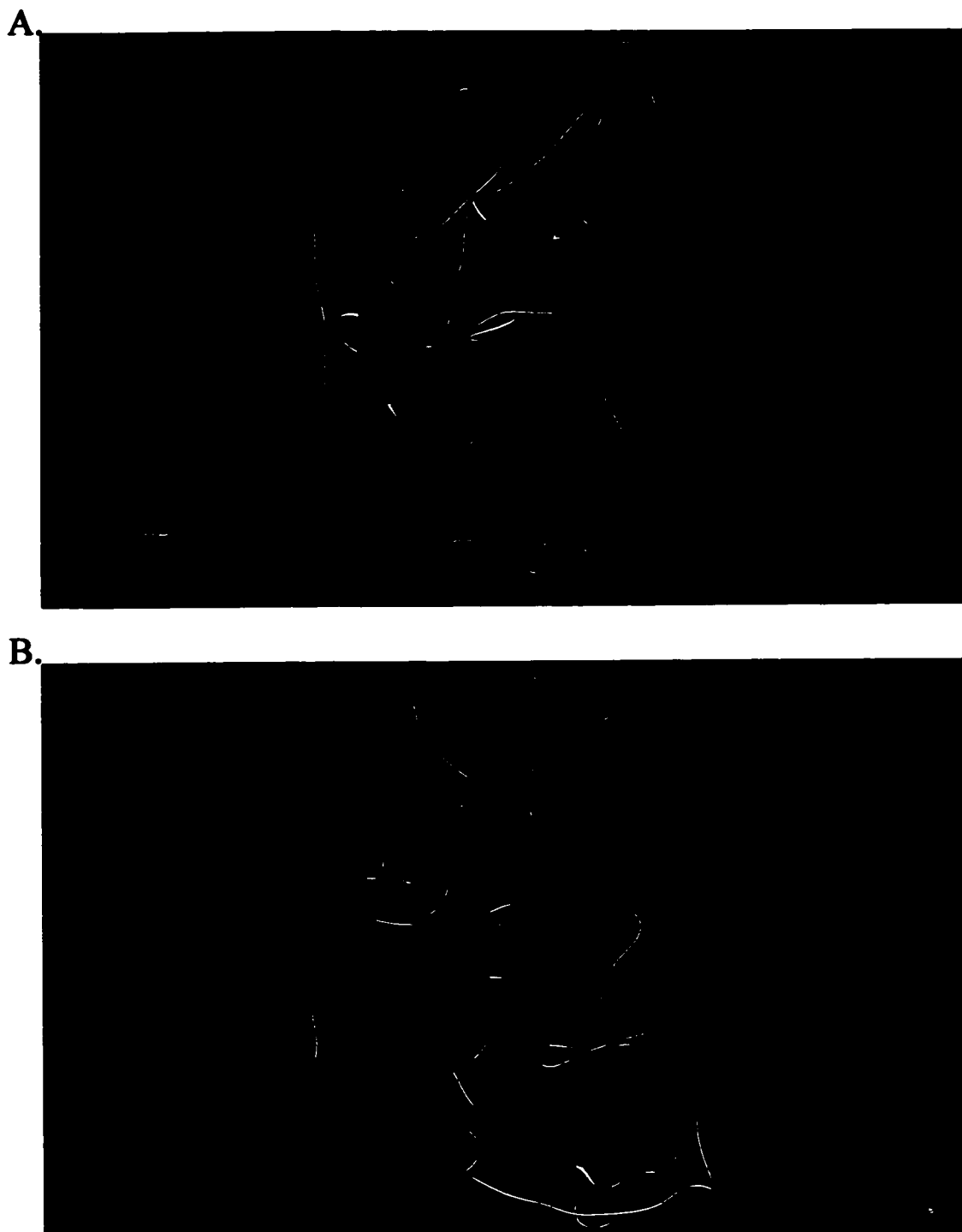


Figure 6.5. Three-dimensional structural comparison of (A) staurosporine bound to cAMP dependent protein kinase (PDB code 1STC reference #183) and (B) staurosporine bound to cyclin dependent kinase (PDB code 1AQI reference #183).

The two related isoflavones quercetin and genistein are members of a series of naturally occurring compounds which previously have been shown to have inhibitory activity against tyrosine kinases and Ser/Thr kinases. Genistein is a potent inhibitor of tyrosine kinases pp60v-src, EGFR kinase and insulin receptor kinase (4, 66). Similarly quercetin has been shown to have activity against EGFR and the Ser/Thr protein kinase PKC (2). Quercetin and not genistein has been shown as an effective inhibitor of the lipid kinase, phosphatidyl inositol (PtdIns) 3-kinase (194).

These isoflavone compounds show a remarkable selective structure-activity relationship when the replacement of hydroxyl groups with methyl groups leads to a substantial drop in their inhibitory activity (4, 66, 194). Hydroxylation of the 5' position of quercetin affects this compounds inhibitory activity versus MLC-kinase, casein kinase I and II while conversely modification of this position appears to play no role in its activity towards both cAMP dependent protein kinase and PKC. In general it has been demonstrated for the isoflavones that tyrosine kinases appear to be more sensitive to the level of hydroxylation than do Ser/Thr kinases (4).

These two compounds, quercetin and genistein, while structurally similar demonstrate substantially different inhibitory effects against APH(3')-IIIa. Quercetin was found to be a competitive inhibitor of APH(3')-IIIa activity (with respect to ATP binding) with a moderate K_{is} of $126 \pm 22 \mu\text{M}$. Genistein however displayed no inhibition of APH(3')-IIIa even when present at levels of $250 \mu\text{M}$. As discussed previously similar behavior had been noted for several kinases including PI3K which was strongly inhibited by quercetin, with a K_{is} of $3.8 \mu\text{M}$ while remaining unaffected by genistein (194).

A series of eight closely related compounds, the tyrphostins, were screened as potential inhibitors of APH(3')-IIIa. The structures all share a phenyl ring substituted at the para position with various functional groups. Many of these compounds show inhibition of tyrosine kinases. Tyrphostins A48, A51, B44 and B50 show specific inhibition of EGFR kinase with K_{i_s} values ranging from 100 nM to 2.5 μ M while species A1 and A63 are often used as negative controls of EGFR tyrphostin inhibition as their K_{i_s} are greater than 1 mM (64, 65, 97, 210). Of this family of compounds only tyrphostin A25 showed inhibition of APH(3')-IIIa. This species only demonstrated a moderate level of inhibition of APH(3')-IIIa activity when present up to a concentration of 350 μ M (~40% inhibition). For this reason no K_{i_s} was determined for this tyrphostin and this family of inhibitors was not further investigated. Although very little is known about the mechanism of tyrphostin inhibition it is clear that APH(3')-IIIa lacks determinants necessary for inhibitor activity. This would suggest that the active site of APH(3')-IIIa is structurally distinct from that of tyrosine protein kinases.

The most thoroughly studied group of protein kinase inhibitors are the isoquinoline sulfonamide derived compounds (87). Two families of isoquinoline have been described which differ in the position of the ring nitrogen (position 2 to 3). The placement of the nitrogen within the ring and variation of the side chain determine remarkable specificity of these inhibitors. Many studies have indicated that the closely related species H-7, H-8, H-9 and H-89 are effective inhibitors of protein kinases. All these compounds show competitive inhibition with respect to MgATP (87) suggesting an interaction at the ATP binding pocket. It is believed that the isoquinoline sulfonamide

ring mimics many of the interactions between the enzyme and its natural substrate MgATP. Several crystal structures now exist for EPKs with bound MgATP, AMP-PNP or isoquinoline sulfonamide inhibitors (19, 49, 51, 91, 200, 208, 214). These structures have permitted a detailed understanding of the interactions necessary for substrate/inhibitor binding.

The isoquinoline sulfonamide inhibitors H-7, H-9, HA-1004, CKI-7 and CKI-8 were assayed as potential inhibitors of APH(3')-IIIa activity. Surprisingly all compounds exhibited some inhibition of phosphotransferase function. The inhibitor HA-1004 which is substituted at the sulfonyl group with a guanidinoethyl group was found to be the most effective inhibitor of APH(3')-IIIa activity with a K_{is} of $48.9 \pm 12.3 \mu\text{M}$. The inhibition was found to be competitive towards ATP binding consistent with the proposal that the isoquinoline sulfonamide ring bound in the purine site of the protein kinase ATP binding pocket (51, 209). Subsequent studies demonstrated that all species were competitive inhibitors of ATP binding with K_{is} values ranging from 48.9 to 730 μM . Similar to the results obtained previously for the ATP analogue AMP-PNP it was found that the inhibitor H-9 was a non-competitive inhibitor of the second substrate kanamycin A with a K_{is} of $155 \pm 26 \mu\text{M}$ and a K_{ii} of $260 \pm 19 \mu\text{M}$ characteristic of an ordered substrate addition as previously described for APH(3')-IIIa.

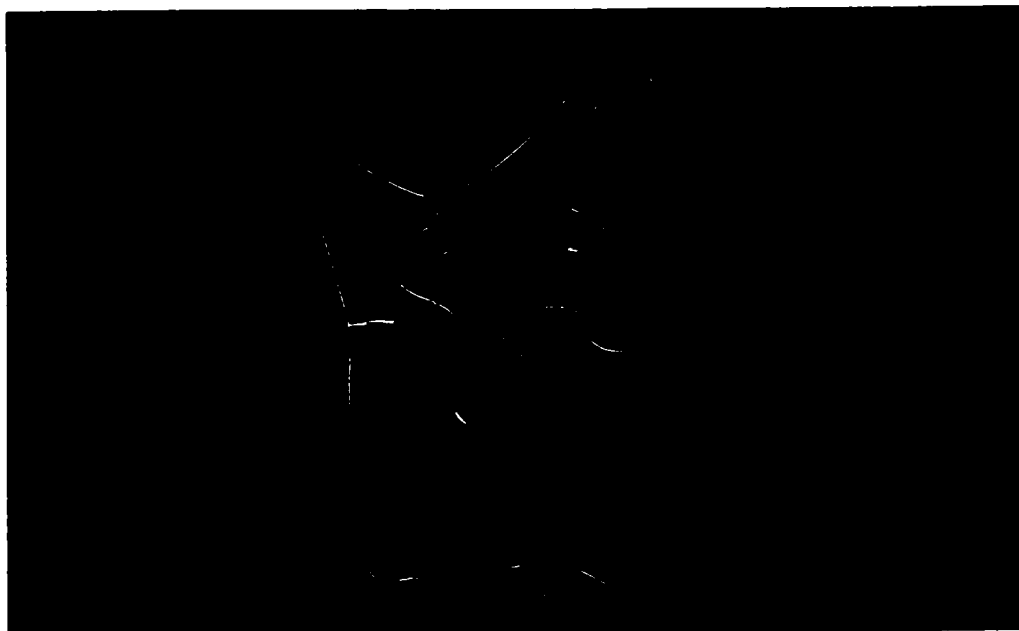
Upon examination of the inhibitors the compounds substituted with the aminoethyl group (H-9 and CKI-7) demonstrate intermediate inhibition with K_{is} values of 66.1 ± 7.5 and $138 \pm 40 \mu\text{M}$ versus ATP. The piperazine substituted compounds (methylpiperazine on H-7 and piperazine on CKI-8) are the least effective inhibitors

demonstrating K_{is} values of 730 ± 130 and 290 ± 89 μM for H-7 and CKI-8 respectively.

The guanidinoethyl substituted compound, HA-1004, had no C-series equivalent but was found to be the most effective inhibitor of APH(3')-IIIa activity.

Similar results have previously been noted for various EPKs where there is selective inhibition by either the H-series or C-series of isoquinoline sulfonamide inhibitors. While CK1 is inhibited by CKI-7 with a K_{is} of 8.5 μM towards ATP, its sister compound H-9 shows significantly reduced inhibitory activity with a 10 fold higher K_{is} . These two inhibitors CKI-7 and H-9 demonstrate K_{is} values of 550 and 3.6 μM respectively when tested on cAMP dependent protein kinase demonstrating that reversal of the ring nitrogen from position 2 (C-series) to position 3 (H-series) has a dramatic effect upon the specificity of these inhibitors. The crystal structure of cAMP dependent protein kinase with bound H-7, H-8 and H-89 (51) and the structure of CK1 with bound CKI-7 has helped identify interactions involved in inhibitor binding (209). The species H-7 bound to cAMP dependent protein kinase indicates a total of 50 Van der Waals interactions with many active site amino acid residues. Two hydrogen bonds are also involved in the inhibitor binding. The piperazine ring of H-7 adopts a chair conformation with an axial N-H bond at position N17 forming an H-bond with the backbone carbonyl of residue E170 (51). This residue as discussed previously is replaced with an alanine residue in C-src kinase and is believed to be involved in partially determining sensitivity to staurosporine. A second hydrogen bond between the backbone amide of V123 forms with N3 of the isoquinoline ring. While many of the interactions exist between cAMP dependent protein kinase and the other inhibitors H-8 and H-89 only the hydrogen bond

A.



B.

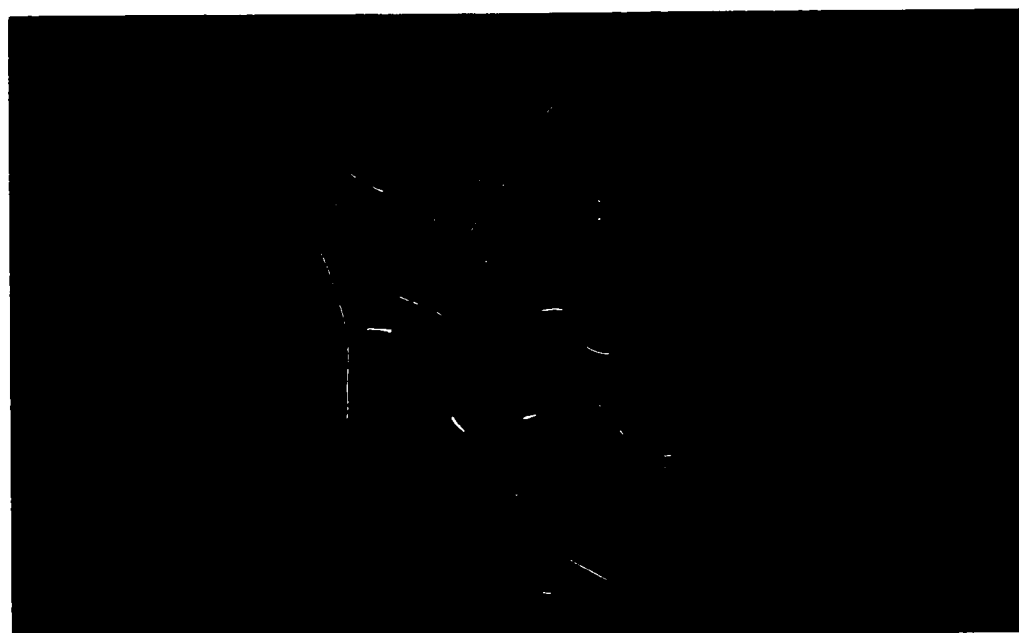


Figure 6.6. Three-dimensional structural comparison of (A) cyclic AMP dependent protein kinase with co-crystal ATP (1ATP reference #19) and (B) cyclic AMP dependent protein kinase with co-crystal H-7 isoquinoline inhibitor (1YDR reference #51).

between V123 and the nitrogen of the isoquinoline sulfonamide ring is observed for all three species (51). Similarly this interaction between the N2 position of CKI-7 and the backbone amide of L88 is involved in inhibitor binding (208, 209). Enzyme structures with bound ATP have also demonstrated the importance of the amide of V123 and L88 for a hydrogen bond with N1 of the purine base of ATP. Similarly, an identically positioned hydrogen bond is involved in binding of ATP to other protein kinases CDK2 (L83) (49) and ERK2 (M106) (213). Hidaka and colleagues have suggested that the presence of this nitrogen is crucial for the interaction of both the H and C series isoquinoline inhibitors with the ATP binding sites of EPKs (87). They have noticed that naphthalenesulfonamides which lack this nitrogen are relatively poor and non-selective inhibitors of EPKs (87, 183). Xu and coworkers have demonstrated that the structural basis for isoquinoline sulfonamide inhibitors centers around the hydrogen bond formed between the backbone amide of a residue (L88, V123, L83, etc) and the ring nitrogen of the inhibitor. APH(3')-IIIa forms a hydrogen bond between the backbone amide of A93 and N1 of ATP similar to that observed for many EPKs (89). It is proposed through our research that binding of the isoquinoline sulfonamide derived inhibitors will employ a similar binding strategy as observed for EPKs and thus this interaction will contribute to the specificity of inhibitor binding. This can be directly addressed through the crystallization of APH(3')-IIIa with bound inhibitor or alternatively through a more indirect means of computer assisted docking as was employed with CK1 and H-9 (209). It is apparent from the K_i values for both the H and C series isoquinolines that trends exist for structure/effectiveness of the inhibitors. The two piperazine derived structures,

H-7 and CKI-8, are the least effective inhibitors of their respective families. HA-1004, for which there is no C series equivalent, is the most effective inhibitor and is substituted with a guanidinoethyl group. The two remaining inhibitors, H-9 and CKI-7, demonstrate intermediate effectiveness. In each case the H series species is a more effective inhibitor than its C series counterpart suggesting that the active site pocket for APH(3')-IIIa is more similar to the ATP pocket of cAMP dependent protein kinase than to Ser/Thr kinases such as casein kinase-1. This is based upon studies demonstrating that H-series inhibitors are more effective and more specific for cAMP dependent protein kinase while C-series compounds are similarly more suited to inhibition of casein kinase-1 and closely related kinases (34, 51, 87, 209)

Similar studies completed by Denis Daigle demonstrated inhibition of AAC(6')-APH(2'') by many of the H-series and C-series inhibitors. Akin to results obtained for APH(3')-IIIa both species were competitive towards ATP and non-competitive towards the second substrate kanamycin A. While the isoquinoline inhibited AAC(6')-APH(2'') activity other protein kinase inhibitors assessed including genistein, quercetin and the indole carbazole staurosporine were not effective inhibitors of enzyme activity. All compounds assayed were found to inhibit APH(2'') activity while the AAC(6') function remained unaffected by the various compounds thus indicating that the inhibitors were specific for kinase activity consistent with results demonstrating binding at the ATP active site cleft. These studies suggest that although AAC(6')-APH(2'') and APH(3')-IIIa differ substantially at the primary sequence level and differ in their substrate profiles it is likely that the two enzymes share some active site homology similar to that observed

between the latter enzyme and EPKs structures. Studies to solve the crystal structure of AAC(6')-APH(2'') are presently underway.

While several of these isoquinoline sulfonamide inhibitors demonstrate rather substantial levels of APH(3')-IIIa inhibition this does not imply any therapeutic usefulness. Competitive inhibitors are frequently not the best choice for therapeutic agents owing both to the reversible nature of their interaction at the enzyme active site and that high substrate levels can overcome the inhibition due to a competitive inhibitors exclusive effect on K_m and not k_{cat} . Resistance of *E. coli* (harbouring APH(3')-IIIa) to kanamycin A was assessed in the absence or presence of either CKI-7 or HA-1004. It was found that the presence of these two isoquinoline derived inhibitors at 1 mM did not reverse antibiotic resistance in these cultures when grown in either liquid or solid media.

6.6 Protein kinase substrate studies

To further establish and characterize the potential functional similarity between APH(3')-IIIa and EPKs we investigated the ability of the former enzyme to phosphorylate many known EPK substrates. Given the structural similarity observed between APH(3')-IIIa and several EPKs and the inhibitory effect of both the H-series and C-series of protein kinase inhibitors it is conceivable that the aminoglycoside phosphotransferase might share a functional ability to phosphorylate protein kinase substrates. Myelin basic protein (MBP) is frequently used as a protein kinase substrate of broad specificity and is phosphorylated by various kinases including calmodulin-dependent protein kinase II, MAP kinases (p38, p42 and p44), PKC and PKA (146).

While MBP is a substrate for several kinases the site of phosphorylation differs for each of the listed EPKs making this an ideal broad range substrate (146). Initial assays suggested that MBP was a substrate for APH(3')-IIIa although the level of substrate phosphorylation appeared to be reduced when compared to phosphorylation of the aminoglycoside substrate kanamycin A. We attempted to determine the V_{max} and K_m for MBP but the quantities of substrate required for the assays were incompatible with the assay themselves. An estimate of k_{cat}/K_m was determined however by using a sub- K_m concentration of MBP (10 μ M). Under these limitations the Michaelis-Menten equation simplifies to:

$$v = [S][E_{tot}]k_{cat}/K_m$$

Both $[S]$ and $[E_{tot}]$ are known values and the rate of reaction (v) is obtained from the assay permitting a calculated value for k_{cat}/K_m . The value of k_{cat}/K_m for the substrate kanamycin A was found to be $1.43 \times 10^5 \text{ s}^{-1} \text{ M}^{-1}$ while this second order rate constant for MBP was calculated to be $4.5 \times 10^2 \text{ s}^{-1} \text{ M}^{-1}$. This indicates a 50 fold decrease in the catalytic efficiency using the substrate MBP when the assays were completed under identical conditions. Similar results were obtained by Denis Daigle for a second aminoglycoside modifying enzyme AAC(6')-APH(2'') where he found a 75 fold decrease in the catalytic efficiency for the substrate MBP (44).

The Ser/Thr protein kinase substrates MARCKS K and MARCKS R are two N-terminally acetylated peptides derived from the myristolated alanine-rich C-kinase substrate protein and are used as PKC substrates (146). These two peptide substrates

were phosphorylated by APH(3')-IIIa with rates of 58 and 53 fmol/min for the MARCKS K and MARCKS R respectively. This represents a 3.6 and a 3.9 fold decrease in rate of phosphorylation when compared to the natural substrate kanamycin A. The PKC substrate protamine is phosphorylated by APH(3')-IIIa at a rate 5 fold lower than that of kanamycin A. Denis Daigle has similarly demonstrated that the bifunctional enzyme AAC(6')-APH(2'') phosphorylates the substrates MARCKS K, MARCKS R and protamine as effectively as APH(3')-IIIa. Using purified casein kinase I and PKC, generously provided by Dr. R. Epand, I was unable to demonstrate phosphorylation of either kanamycin A or neomycin B with either enzyme. In an attempt to further characterize the site of phosphorylation of MARCKS K, MBP and protamine, phosphoamino acid analysis was completed by Denis Daigle on peptides phosphorylated by both APH(3')-IIIa and AAC(6')-APH(2'') (44). Phosphoamino acid analysis, performed by Denis Daigle, unambiguously identifies the site of phosphorylation on all substrates by both enzymes to be serine residues. Although the MARCKS peptides lack threonine residues, MBP has been demonstrated to be phosphorylated on threonine 97 by MAP kinase (52) and threonine 94 by calmodulin-dependent protein kinase II (172) suggesting such sites are available for modification. Other Ser/Thr protein kinase substrates assayed included casein, phosphorylated and dephosphorylated, histone H1 and Kemptide (Table 5.3). Unlike the substrates discussed previously neither APH(3')-IIIa nor AAC(6')-APH(2'') were capable of phosphorylating these kinase substrates. Two tyrosine kinase substrates; poly (Glu:Tyr) (4:1), a synthetic peptide substrate for tyrosine kinases, and p60^{c-src} substrate II, a known substrate for c-src kinase, were also

investigated as potential substrates for APH(3')-IIIa kinase activity. Neither of these two substrates were phosphorylated by APH(3')-IIIa.

The peptide and protein substrates phosphorylated including MARCKS peptides, MBP and protamine were all positively charged under the assay conditions employed while those substrates which were overall negatively charged such as poly (Glu:Tyr) were not substrates for APH(3')-IIIa. The relationship between substrate charge and phosphorylation by APH(3')-IIIa, however, is not exclusively charge related given that neither Kemptide nor histone H1 are substrates for the enzyme. The implication is that while overall charge is a minimal requirement for phosphorylation there are other factors, which govern their ability to function as substrates. It is possible that like many protein kinases there are preferred consensus sequence phosphorylation sites. Many features including neighboring amino acids surrounding the site of phosphorylation govern the consensus sequences. Ser/Thr protein kinases including cAMP dependent protein kinase, cGMP dependent protein kinase and PKC show strong preference for target sequences which contain basic residues (K or R) surrounding the site of modification (31, 98). Without identifying and further characterizing the site of phosphorylation of both MBP and protamine it is impossible to clearly identify a preferred consensus sequence for APH(3')-IIIa. Given that MARCKS K and MARCKS R and not Kemptide are substrates for APH(3')-IIIa kinase activity one might cautiously speculate that the enzyme requires charged residues both on the N-terminal and C-terminal side of the target serine. Similar preferences are observed for PKC substrates and cAMP dependent protein kinase substrates. Phosphorylase kinase shows that replacement of an arginine residue with an

alanine two amino acids to the carboxyl side of the serine leads to a 3 fold increase in K_m and a 16 fold decrease in V_{max} while the effect on cAMP dependent protein kinase is a 100 fold decrease in K_m and a 5 fold increase in V_{max} . Conversely replacement of an arginine residue 4 positions to the N-terminal side of the serine shows that phosphorylase kinase remains unaffected while cAMP dependent protein kinase shows a 100 fold decrease in V_{max} (98). These studies clearly serve to illustrate that these enzymes require quite stringent recognition sequence sites, which have been empirically identified.

Although one might expect APH(3')-IIIa to prefer positively charged substrates given that its natural substrates are highly charged amino sugars it is nonetheless remarkable that the enzyme is able to accommodate protein kinase substrates and in particular substrates MBP and protamine which are comparatively large next to aminoglycosides. Inspection of the crystal structure of APH(3')-IIIa demonstrates a significant difference between the second substrate binding pocket when compared to that of EPKs. While the EPKs have an open accessible active site, presumably designed to accommodate peptide substrates, the APH(3')-IIIa active site is more thoroughly blocked by domain III of the structure. Domain III consists of two antiparallel α -helices (αA and αB) connected by a 19 amino acid loose coil. Hon and coworkers have proposed that this 60 amino acid domain might provide a means for APH(3')-IIIa substrate selectivity (89). Thus the ability of APH(3')-IIIa to phosphorylate a number of peptide and protein substrates suggest a great deal of flexibility at the active site in order to accommodate these relatively large substrates.

One of the most highly conserved motifs identified in EPKs, H/YXDX3-4N, has similarly been identified in APH(3')-IIIa. The aspartate residue is tentatively identified as the active site catalytic base while the asparagine residue is involved in coordination of one of the magnesium ions (103, 121, 214). Although the second residue in this consensus sequence is listed as variable, until relatively recently it was believed to be a highly conserved arginine residue found in protein kinases. All members of the APH(3') family including the type IIIa phosphotransferase have a glycine at this position (glycine 189 APH(3')-IIIa numbering). This residue was mutated to an arginine residue to identify the impact if any upon APH(3')-IIIa protein kinase activity. Studies with the G189R mutant APH(3')-IIIa demonstrated that this change had a significant impact on aminoglycoside phosphorylation. While substrates such as kanamycin A, kanamycin B, neomycin B and ribostamycin were phosphorylated by the enzyme the specificity constant (k_{cat}/K_m) for each was significantly reduced as compared to the wild type enzyme. Changes in the specificity constant ranged from 0.036 fold for kanamycin B to 0.005 fold for ribostamycin. The effect was seen in both the k_{cat} and K_m values for all substrates. Aminoglycosides from both the 4,5-disubstituted and 4,6-disubstituted aminoglycosides appeared to be affected similarly by the mutation suggesting that a feature common to both classes of aminoglycosides was adversely affected. One feature shared by both the 4,5 and 4,6-disubstituted deoxystreptamine aminoglycosides is the central aminocyclitol ring. Those aminoglycosides that are substituted at the 1 position of the aminocyclitol ring with either an aminohydroxybutyryl group or an aminohydroxypropionyl group were no longer phosphorylated at detectable levels. It is

conceivable that the arginine side chain was unfavorably interacting with these groups thus preventing their ability to productively bind to the G189R mutant enzyme. Alternatively the amikacin, butirosin and isepamicin might adopt a unique conformation due to substitution at the 2 position and thus their binding would be reduced in the G189R mutant. Blazquez has previously isolated a G189D hydroxylamine derived mutant of APH(3')-IIa and has demonstrated using MICs that enzyme activity is 0.2% that of wild type (18). The MICs investigated were limited to kanamycin A and this agrees well with our data for APH(3')-IIIa [G189R] which demonstrated that the mutant had a 1500 fold decrease in k_{cat}/K_m for this aminoglycoside. From their results they cautiously speculate that this residue may be a critical determinant in the conformation of this region (18). Thus while APH(3')-IIIa and EPKs share substantial 3D-homology there still remains significant differences between the two enzymes which permit their different substrate specificities.

It was hoped that removal of the "Thumb Region" (Domain III) of APH(3')-IIIa would permit entry of larger substrates and thus improve the ability of the enzyme to phosphorylate protein kinase substrates. The mutant protein generated, APH(3')-IIIa [Δ 123-189], was found to be unstable under all circumstances and thus no mechanistic data was obtained from these studies.

The ability of APH(3')-IIIa to phosphorylate several Ser/Thr protein kinase substrates indicates a need to be aware of such activity when designing signal transduction experiments where frequently used selectable markers include a neomycin phosphotransferase (APH(3')-IIa) and a hygromycin phosphotransferase (APH(4)-I).

While the Ser/Thr kinase activities exhibited by APH(3')-IIIa are certainly not robust it is important to be aware of such activity when considering suitable selectable markers for signal transduction experiments. Such a concern has previously been noted by Maio and Brown (122). Their results have demonstrated that upon introduction of APH(3')-IIa as a neomycin selection marker in a U937 cell line there was significant perturbation of cellular pathways including PKC which led to gene expression. This activation, however, was found to be cell type specific (122). This helps to illustrate the importance of careful selection of resistance determinants in mammalian signal transduction experiments.

6.7 *Similarity of APH(3')-IIIa to Eukaryotic Protein Kinases*

It has long been speculated that APH(3') enzymes showed sequence homology to eukaryotic protein kinases suggesting a possible common evolutionary ancestor between the two enzyme families (21, 126). This is now supported by our biochemical studies which demonstrate that functionally APH(3')-IIIa is inhibited by EPK specific inhibitors and also the enzyme demonstrates a protein kinase like activity. Furthermore the structural similarity indicates that the enzymes employ similar catalytic and chemical mechanisms. In recent years it has been demonstrated that a number of aminoglycoside producing organisms also code for eukaryotic like protein kinases. Thus it seems possible that aminoglycoside phosphotransferases may have evolved from an ancestor that performed a different cellular function such as a protein kinase. A similar type of evolutionary descent may also have occurred for acetyltransferases where it has been

demonstrated that gentamicin 2' acetyltransferase affects peptidoglycan structure and thus impacts on cell morphology (148, 149). More recently the crystal structure of two acetyltransferases have been solved and both enzymes show similar GCN5-related N-acetyltransferase superfamily folds (201, 205). AAC(6')-II has been demonstrated to possess protein acetylation activity indicating that this enzyme is a functional and structural homologue of GCN5 histone acetyltransferases (205). This would suggest that acetyltransferases and by extension phosphotransferases may have evolved from their respective ancestral enzyme which may have been involved in a cellular pathway other than aminoglycoside detoxification.

Conclusion and Future Work

With the development of antibiotic resistance over the past half century it has become apparent that a detailed understanding of the molecular mechanisms by which bacteria circumvent therapeutic agents is required if the usefulness of these compounds is to be restored.

Aminoglycoside antibiotics have long been used as therapeutic agents for the treatment of tuberculosis and other clinically relevant infections. Their continued usefulness, however, is in jeopardy due to the increased high level resistance observed in both Gram positive and Gram negative organisms. A detailed understanding of aminoglycoside resistance is required if these antibiotics are to find continued use as chemotherapeutics.

Studies detailed within this thesis have helped broaden the understanding of APH(3')-IIIa. The ground work including substrate profile and a thorough detailing of the enzyme kinetic mechanism are essential to aid in the identification of substrate groups necessary for enzyme/substrate interactions. Additionally through the use of the ATP analogue FSBA we have identified K44 as a residue involved in ATP binding. This was subsequently confirmed by mutagenesis studies and X-ray crystallography studies. The three dimensional structure of APH(3')-IIIa has shed insight into the enzyme residues required for nucleotide binding and has demonstrated that APH(3')-IIIa shows structural similarity to many eukaryotic protein kinases. Thus although APH(3')-IIIa and EPKs show low overall primary sequence identity they do show gross structural similarity and

amazingly functional similarity. APH(3')-IIIa appears to belong to a superfamily of kinases based on their susceptibility to protein kinase inhibitors and ability to phosphorylate such substrates as myelin basic protein, protamine and MARCKS peptides. This similarity to EPKs suggest a possible descent from a common evolutionary ancestor. Such an evolutionary link would suggest that the family of APH(3') enzymes evolved from a enzyme that had a function distinct from its current role in aminoglycoside detoxification.

These studies while laying the ground work for understanding aminoglycoside detoxification need to be continued to achieve a better understanding of the enzyme chemistry required for its function. While ATP/enzyme interactions have been identified, the equally important aminoglycoside/enzyme substrate binding pocket remains to be clearly mapped. Studies are currently focusing on addressing this question. While much is known about the enzyme chemistry further studies are required to identify all residues involved in the detoxification of the aminoglycoside substrates.

References

1. **Adams, J. A., and S. S. Taylor.** 1992. Energetic limits of phosphotransfer in the catalytic subunit of cAMP- dependent protein kinase as measured by viscosity experiments. *Biochemistry*. **31**:8516-22.
2. **Agullo, G., L. Gamet-Payrastre, S. Manenti, C. Viala, C. Remesy, H. Chap, and B. Payrastre.** 1997. Relationship between flavonoid structure and inhibition of phosphatidylinositol 3-kinase: a comparison with tyrosine kinase and protein kinase C inhibition. *Biochem. Pharmacol.* **53**:1649-57.
3. **Ainsa, J. A., E. Perez, V. Pelicic, F. X. Berthet, B. Gicquel, and C. Martin.** 1997. Aminoglycoside 2'-N-acetyltransferase genes are universally present in mycobacteria: characterization of the *aac(2')-Ic* gene from *Mycobacterium tuberculosis* and the *aac(2')-Id* gene from *Mycobacterium smegmatis*. *Mol. Microbiol.* **24**:431-41.
4. **Akiyama, T., J. Ishida, S. Nakagawa, H. Ogawara, S. Watanabe, N. Itoh, M. Shibuya, and Y. Fukami.** 1987. Genistein, a specific inhibitor of tyrosine-specific protein kinases. *J. Biol. Chem.* **262**:5592-5.
5. **Akiyama, T., and N. Tanaka.** 1981. Ribosomal proteins S9 and L6 participate in the binding of [³H]dibekacin to *E. coli* ribosomes. *J. Antibiot* (Tokyo). **34**:763-9.
6. **Alberty, R. A.** 1958. On the determination of rate constants for coenzyme mechanisms. *J. Am. Chem. Soc.* **80**:1777-1782.

7. **Anand, M., B. D. Davis, and A. K. Armitage.** 1960. Uptake of streptomycin by *Escherichia coli*. *Nature*. 185:23-24.
8. **Anand, N. B., and B. D. Davis.** 1960. Damage by streptomycin to the cell membrane of *Escherichia coli*. *Nature*. 185:22-23.
9. **Azucena, E., I. Grapsas, and S. Mobashery.** 1997. Properties of a bifunctional bacteria antibiotic resistance enzyme that catalyzes ATP-dependent 2"-phosphorylation and acetyl-CoA-dependent 6'-acetylation of aminoglycosides. *J. Am. Chem. Soc.* 119:2317-2318.
10. **Backlow, S. C., R. T. Raines, W. A. Lim, P. D. Zamore, and J. R. Knowles.** 1988. Triosephosphate isomerase catalysis is diffusion controlled. Appendix: Analysis of triose phosphate equilibria in aqueous solution by ^{31}P NMR. *Biochemistry*. 27:1158-67.
11. **Barber, M.** 1963. Antibiotic and chemotherapy, 1st ed. pp 1-43, Livingstone, Edinburgh.
12. **Barycki, J. J., and R. F. Colman.** 1993. Affinity labeling of glutathione S-transferase, isozyme 4-4, by 4-(fluorosulfonyl)benzoic acid reveals Tyr115 to be an important determinant of xenobiotic substrate specificity. *Biochemistry*. 32:13002-11.
13. **Bazelyansky, M., E. Robey, and J. F. Kirsch.** 1986. Fractional diffusion-limited component of reactions catalyzed by acetylcholinesterase. *Biochemistry*. 25:125-30.
14. **Beauclerk, A. A., and E. Cundliffe.** 1987. Sites of action of two ribosomal RNA methylases responsible for resistance to aminoglycosides. *J. Mol. Biol.* 193:661-71.

15. **Bennett, W. S., Jr., and T. A. Steitz.** 1980. Structure of a complex between yeast hexokinase A and glucose. I. Structure determination and refinement at 3.5 Å resolution. *J. Mol. Biol.* **140**:183-209.
16. **Birge, E. A., and C. G. Kurland.** 1969. Altered ribosomal protein in streptomycin-dependent *Escherichia coli*. *Science*. **166**:1282-4.
17. **Bjare, U., and L. Gorini.** 1971. Drug dependence reversed by a ribosomal ambiguity mutation, *ram*, in *Escherichia coli*. *J. Mol. Biol.* **57**:423-35.
18. **Blazquez, J., J. Davies, and F. Moreno.** 1991. Mutations in the *aphA-2* gene of transposon Tn5 mapping within the regions highly conserved in aminoglycoside-phosphotransferases strongly reduce aminoglycoside resistance. *Mol. Microbiol.* **5**:1511-1518.
19. **Bossemeyer, D., R. A. Engh, V. Kinzel, H. Ponstingl, and R. Huber.** 1993. Phosphotransferase and substrate binding mechanism of the cAMP- dependent protein kinase catalytic subunit from porcine heart as deduced from the 2.0 Å structure of the complex with Mn²⁺ adenylyl imidodiphosphate and inhibitor peptide PKI(5-24). *EMBO J.* **12**:849-59.
20. **Bramley, H. F., and H. L. Kornberg.** 1987. Sequence homologies between proteins of bacterial phosphoenolpyruvate-dependent sugar phosphotransferase systems: identification of possible phosphate-carrying histidine residues. *Proc. Natl. Acad. Sci. USA.* **84**:4777-80.
21. **Brenner, S.** 1987. Phosphotransferase sequence homology. *Nature.* **329**:21.

22. Brouwer, A. C., and J. F. Kirsch. 1982. Investigation of diffusion-limited rates of chymotrypsin reactions by viscosity variation. *Biochemistry*. 21:1302-7.
23. Bryan, L. E., and S. Kwan. 1983. Roles of ribosomal binding, membrane potential, and electron transport in bacterial uptake of streptomycin and gentamicin. *Antimicrob. Agents Chemother.* 23:835-45.
24. Bryan, L. E., T. Nicas, B. W. Holloway, and C. Crowther. 1980. Aminoglycoside-resistant mutation of *Pseudomonas aeruginosa* defective in cytochrome c552 and nitrate reductase. *Antimicrob. Agents Chemother.* 17:71-9.
25. Bryan, L. E., and H. M. Van Den Elzen. 1977. Effects of membrane-energy mutations and cations on streptomycin and gentamicin accumulation by bacteria: a model for entry of streptomycin and gentamicin in susceptible and resistant bacteria. *Antimicrob. Agents Chemother.* 12:163-77.
26. Bryan, L. E., and H. M. Van Den Elzen. 1975. Gentamicin accumulation by sensitive strains of *Escherichia coli* and *Pseudomonas aeruginosa*. *J. Antibiot (Tokyo)*. 28:696-703.
27. Bryan, L. E., and H. M. Van den Elzen. 1976. Streptomycin accumulation in susceptible and resistant strains of *Escherichia coli* and *Pseudomonas aeruginosa*. *Antimicrob. Agents Chemother.* 9:928-38.
28. Buckel, P., A. Buchberger, A. Bock, and H. G. Wittmann. 1977. Alteration of ribosomal protein L6 in mutants of *Escherichia coli* resistant to gentamicin. *Mol. Gen. Genet.* 158:47-54.

29. **Caldwell, S. R., J. R. Newcomb, K. A. Schlecht, and F. M. Raushel.** 1991. Limits of diffusion in the hydrolysis of substrates by the phosphotriesterase from *Pseudomonas diminuta*. *Biochemistry*. **30**:7438-44.
30. **Carmel, G., B. Leichus, X. Cheng, S. D. Patterson, U. Mirza, B. T. Chait, and J. Kuret.** 1994. Expression, purification, crystallization, and preliminary x-ray analysis of casein kinase-1 from *Schizosaccharomyces pombe*. *J. Biol. Chem.* **269**:7304-9.
31. **Casnellie, J. E.** 1991. Assay of protein kinases using peptides with basic residues for phosphocellulose binding. *Methods Enzymol.* **200**:115-20.
32. **Chait, B. T., and S. B. Kent.** 1992. Weighing naked proteins: practical, high-accuracy mass measurement of peptides and proteins. *Science*. **257**:1885-94.
33. **Chang, F. N., and J. G. Flaks.** 1972. Binding of dihydrostreptomycin to *Escherichia coli* ribosomes: characteristics and equilibrium of the reaction. *Antimicrob. Agents Chemother.* **2**:294-307.
34. **Chijiwa, T., M. Hagiwara, and H. Hidaka.** 1989. A newly synthesized selective casein kinase I inhibitor, N-(2-Aminoethyl)-5-chloroisoquinoline-8-sulfonamide, and affinity purification of casein kinase I from bovine testis. *J. Biol. Chem.* **264**:4924-4927.
35. **Chow, J. W., M. J. Zervos, S. A. Lerner, L. A. Thal, S. M. Donabedian, D. D. Jaworski, S. Tsai, K. J. Shaw, and D. B. Clewell.** 1997. A novel gentamicin resistance gene in *Enterococcus*. *Antimicrob. Agents Chemother.* **41**:511-4.
36. **Cleland, W. W.** 1979. Substrate inhibition. *Methods Enzymol.* **63**:500-514.

37. **Cohen, P. T., and P. Cohen.** 1989. Discovery of a protein phosphatase activity encoded in the genome of bacteriophage lambda. Probable identity with open reading frame 221. *Biochem. J.* **260**:931-4.
38. **Cohen, P. T., J. F. Collins, A. F. Coulson, N. Berndt, and O. B. da Cruz e Silva.** 1988. Segments of bacteriophage lambda (orf 221) and phi 80 are homologous to genes coding for mammalian protein phosphatases. *Gene.* **69**:131-4.
39. **Cole, P. A., P. Burn, B. Takacs, and C. T. Walsh.** 1994. Evaluation of the catalytic mechanism of recombinant human Csk (C- terminal Src kinase) using nucleotide analogs and viscosity effects. *J. Biol. Chem.* **269**:30880-7.
40. **Collatz, E., C. Carlier, and P. Courvalin.** 1983. The chromosomal 3'5"-aminoglycoside phosphotransferase in *Streptococcus pneumoniae* is closely related to its plasmid-coded homologs in *Streptococcus faecalis* and *Staphylococcus aureus*. *J. Bacteriol.* **156**:1373-1377.
41. **Coombe, R. G., and A. M. George.** 1981. Mass spectral and ¹³C NMR analysis of aminoglycoside aminocyclitols modified by enzyme-catalyzed reaction. *Aust. J. Chem.* **34**:547-554.
42. **Costa, Y., M. Galimand, R. Leclercq, J. Duval, and P. Courvalin.** 1993. Characterization of the chromosomal *aac(6')-Ii* gene specific for *Enterococcus faecium*. *Antimicrob. Agents Chemother.* **37**:1896-903.
43. **Cundliffe, E.** 1989. How antibiotic-producing organisms avoid suicide. *Annu. Rev. Microbiol.* **43**:207-33.

44. **Daigle, D. M., G. A. McKay, P. R. Thompson, and G. D. Wright.** 1999. Aminoglycoside antibiotic phosphotransferases are also serine protein kinases. *Chem. Biol.* 6:11-18.
45. **Daigle, D. M., and G. D. Wright.** 1999. Prodigious substrate specificity of AAC(6')-APH(2''), an aminoglycoside antibiotic resistance determinant in enterococci and staphylococci. *Chem. Biol.* 6:99-110.
46. **Davies, C., D. E. Bussiere, B. L. Golden, S. J. Porter, V. Ramakrishnan, and S. W. White.** 1998. Ribosomal proteins S5 and L6: high-resolution crystal structures and roles in protein synthesis and antibiotic resistance. *J. Mol. Biol.* 279:873-88.
47. **Davis, B. D.** 1987. Mechanism of bactericidal action of aminoglycosides [published erratum appears in *Microbiol. Rev.* 1988 Mar;52(1):153]. *Microbiol. Rev.* 51:341-50.
48. **Davis, B. D., L. L. Chen, and P. C. Tai.** 1986. Misread protein creates membrane channels: an essential step in the bactericidal action of aminoglycosides. *Proc. Natl. Acad. Sci. USA.* 83:6164-8.
49. **De Bondt, H. L., J. Rosenblatt, J. Jancarik, H. D. Jones, D. O. Morgan, and S. H. Kim.** 1993. Crystal structure of cyclin-dependent kinase 2. *Nature.* 363:595-602.
50. **Edson, R. S., and C. L. Terrell.** 1991. The Aminoglycosides. *Mayo. Clin. Proc.* 66:1158-1164.
51. **Engh, R. A., A. Girod, V. Kinzel, R. Huber, and D. Bossemeyer.** 1996. Crystal structures of catalytic subunit of cAMP-dependent protein kinase in complex with

isoquinolinesulfonyl protein kinase inhibitors H7, H8, and H89. Structural implications for selectivity. *J. Biol. Chem.* 271:26157-64.

52. Erickson, A. K., D. M. Payne, P. A. Martino, A. J. Rossomando, J. Shabanowitz, M. J. Weber, D. F. Hunt, and T. W. Sturgill. 1990. Identification by mass spectrometry of threonine 97 in bovine myelin basic protein as a specific phosphorylation site for mitogen-activated protein kinase. *J. Biol. Chem.* 265:19728-35.
53. Ferretti, J. J., K. S. Gilmore, and P. Courvalin. 1986. Nucleotide sequence analysis of the gene specifying the bifunctional 6'-aminoglycoside acetyltransferase 2"-aminoglycoside phosphotransferase enzyme in *Streptococcus faecalis* and identification and cloning of gene regions specifying the two activities. *J. Bacteriol.* 167:631-8.
54. Fleming, A. 1929. *Brit J Exp Path* 10:226.
55. Fourmy, D., M. I. Recht, S. C. Blanchard, and J. D. Puglisi. 1996. Structure of the A site of *Escherichia coli* 16S ribosomal RNA complexed with an aminoglycoside antibiotic. *Science.* 274:1367-71.
56. Fourmy, D., M.I. Recht and J.D. Puglisi. 1998. Binding of neomycin-class aminoglycoside antibiotics to the A-site of 16S rRNA. *J. Mol. Biol.* 277:347-362.
57. Franklin, T. J., and G. A. Snow. 1975. in *The Development of Antimicrobial Agents* (Franklin, T.J., and Snow, G.A., Eds.) pp 7-10. Chapman and Hall, Ltd., London.
58. Fromm, H. J. 1979. Use of competitive inhibitors to study substrate binding order. *Methods Enzymol.* 63:467-485.
59. Fromm, H. J., and V. Zewe. 1962. Kinetic studies of yeast hexokinase. *J. Biol. Chem.* 237:3027-3032.

60. **Fry, D. C., S. A. Kuby, and A. S. Mildvan.** 1986. ATP-binding site of adenylate kinase: Mechanistic implications of its homology with *ras*-encoded p21 F1-ATPase, and other nucleotide-binding proteins. *Proc. Natl. Acad. Sci. USA.* **83**:907-911.
61. **Gates, C. A., and D. B. Northrop.** 1988. Alternative substrate and inhibition kinetics of aminoglycoside nucleotidyltransferase 2"-I in support of a Theorell-Chance kinetic mechanism [published erratum appears in *Biochemistry* 1989 Feb 21;28(4):1930]. *Biochemistry.* **27**:3826-33.
62. **Gates, C. A., and D. B. Northrop.** 1988. Determination of the rate-limiting segment of aminoglycoside nucleotidyltransferase 2"-I by pH and viscosity-dependent kinetics [published erratum appears in *Biochemistry* 1989 Feb 21;28(4):1930]. *Biochemistry.* **27**:3834-42.
63. **Gates, C. A., and D. B. Northrop.** 1988. Substrate specificities and structure-activity relationships for the nucleotidylation of antibiotics catalyzed by aminoglycoside nucleotidyltransferase 2"-I. *Biochemistry.* **27**:3820-5.
64. **Gazit, A., N. Osherov, I. Posner, P. Yaish, E. Poradosu, C. Gilon, and A. Levitzki.** 1991. Tyrphostins. 2. Heterocyclic and alpha-substituted benzylidenemalononitrile tyrphostins as potent inhibitors of EGF receptor and ErbB2/neu tyrosine kinases. *J. Med. Chem.* **34**:1896-907.
65. **Gazit, A., P. Yaish, C. Gilon, and A. Levitzki.** 1989. Tyrphostins I: synthesis and biological activity of protein tyrosine kinase inhibitors. *J. Med. Chem.* **32**:2344-52.

66. **Geahlen, R. L., N. M. Koonchanok, J. L. McLaughlin, and D. E. Pratt.** 1989. Inhibition of protein-tyrosine kinase activity by flavanoids and related compounds. *J. Nat. Prod.* **52**:982-6.
67. **Gibbs, C. S., and M. J. Zoller.** 1991. Rational scanning mutagenesis of a protein kinase identifies functional regions involved in catalysis and substrate interactions. *J. Biol. Chem.* **266**:8923-31.
68. **Gibbs, J. S., H. C. Chiou, J. D. Hall, D. W. Mount, M. J. Retondo, S. K. Weller, and D. M. Coen.** 1985. Sequence and mapping analyses of the herpes simplex virus DNA polymerase gene predict a C-terminal substrate binding domain. *Proc. Natl. Acad. Sci. USA.* **82**:7969-73.
69. **Gold, H. S., and R. C. Moellering, Jr.** 1996. Antimicrobial-drug resistance. *N. Engl. J. Med.* **335**:1445-53.
70. **Gorini, L.** 1974. Streptomycin and misreading of the genetic code, *In* Ribosomes (Nomura, M., Tissieres, A., and Lengyel P., Eds.). pp 791-803. Cold Spring Harbor Laboratory, Cold Spring Harbor.
71. **Gorini, L., and E. Kataja.** 1964. Phenotypic repair by streptomycin of defective genotypes in *E.coli*. *Proc. Natl. Acad. Sci. USA.* **51**:487-493.
72. **Grace, M. R., C. T. Walsh, and P. A. Cole.** 1997. Divalent ion effects and insights into the catalytic mechanism of protein tyrosine kinase Csk. *Biochemistry.* **36**:1874-81.
73. **Gratecos, D., and E. H. Fischer.** 1974. Adenosine 5'-O(3-thiotriphosphate) in the control of phosphorylase activity. *Biochem. Biophys. Res. Commun.* **58**:960-7.

74. Gray, G. S., and W. M. Fitch. 1983. Evolution of antibiotic resistance genes: the DNA sequence of a kanamycin resistance gene from *Staphylococcus aureus*. *Mol. Biol. Evol.* 1:57-66.
75. Gritz, L., and J. Davies. 1983. Plasmid-encoded hygromycin B resistance: the sequence of hygromycin B phosphotransferase gene and its expression in *Escherichia coli* and *Saccharomyces cerevisiae*. *Gene*. 25:179-88.
76. Guan, K. L., and J. E. Dixon. 1991. Evidence for protein-tyrosine-phosphatase catalysis proceeding via a cysteine-phosphate intermediate. *J. Biol. Chem.* 266:17026-30.
77. Hancock, R. 1964. Early effects of streptomycin on *Bacillus megaterium*. *J. Bacteriol.* 88:633-639.
78. Hancock, R. 1962. Uptake of ^{14}C streptomycin by some microorganisms and its relation to their streptomycin sensitivity. *J. Gen. Micro.* 28:493-501.
79. Hancock, R. E. 1981. Aminoglycoside uptake and mode of action--with special reference to streptomycin and gentamicin. I. Antagonists and mutants. *J. Antimicrob. Chemother.* 8:249-76.
80. Hanks, S. K., and A. M. Quinn. 1991. Protein kinase catalytic domain sequence database: identification of conserved features of primary structure and classification of family members. *Methods Enzymol.* 200:38-62.
81. Hanks, S. K., A. M. Quinn, and T. Hunter. 1988. The protein kinase family: conserved features and deduced phylogeny of the catalytic domains. *Science*. 241:42-52.

82. Hashimoto, E., K. Takio, and E. G. Krebs. 1982. Amino acid sequence at the ATP-binding site of cGMP-dependent protein kinase. *J. Biol. Chem.* 257:727-33.
83. Heil, A., G. Muller, L. Noda, T. Pinder, H. Schirmer, I. Schirmer, and I. v. Zabern. 1974. The amino-acid sequence of sarcine adenylate kinase from skeletal muscle. *Eur. J. Biochem.* 43:131-44.
84. Heinzl, P., O. Werbitzky, J. Distler, and W. Piepersberg. 1988. A second streptomycin resistance gene from *Streptomyces griseus* codes for streptomycin-3"-phosphotransferase. Relationships between antibiotic and protein kinases. *Arch. Microbiol.* 150:184-92.
85. Herbert, C. J., M. Sarwar, S. S. Ner, I. G. Giles, and M. Akhtar. 1986. Sequence and interspecies transfer of an aminoglycoside phosphotransferase gene (APH) of *Bacillus circulans*. Self-defence mechanism in antibiotic-producing organisms. *Biochem. J.* 233:383-93.
86. Herbert, J. M., E. Seban, and J. P. Maffrand. 1990. Characterization of specific binding sites for [³H]-staurosporine on various protein kinases. *Biochem. Biophys. Res. Commun.* 171:189-95.
87. Hidaka, H., M. Inagaki, S. Kawamoto, and Y. Sasaki. 1984. Isoquinolinesulfonamides, novel and potent inhibitors of cyclic nucleotide dependent protein kinase and protein kinase C. *Biochemistry.* 23:5036-5041.
88. Holmes, D. J., and E. Cundliffe. 1991. Analysis of a ribosomal RNA methylase gene from *Streptomyces tenebrarius* which confers resistance to gentamicin. *Mol. Gen. Genet.* 229:229-37.

89. **Hon, W. C., G. A. McKay, P. R. Thompson, R. M. Sweet, D. S. Yang, G. D. Wright, and A. M. Berghuis.** 1997. Structure of an enzyme required for aminoglycoside antibiotic resistance reveals homology to eukaryotic protein kinases. *Cell*. **89**:887-95.
90. **Hotta, K., C. B. Zhu, T. Ogata, A. Sunada, J. Ishikawa, S. Mizuno, Y. Ikeda, and S. Kondo.** 1996. Enzymatic 2'-N-acetylation of arbekacin and antibiotic activity of its product. *J. Antibiot.* (Tokyo). **49**:458-64.
91. **Hubbard, S. R., L. Wei, L. Ellis, and W. A. Hendrickson.** 1994. Crystal structure of the tyrosine kinase domain of the human insulin receptor. *Nature*. **372**:7416-754.
92. **Hurwitz, C., C. B. Braun, and C. L. Rosano.** 1981. Role of ribosome recycling in uptake of dihydrostreptomycin by sensitive and resistant *Escherichia coli*. *Biochim. Biophys. Acta*. **652**:168-76.
93. **Hurwitz, C., and C. L. Rosano.** 1962. Accumulation of label from ^{14}C -streptomycin by *Escherichia coli*. *J. Bacteriol.* **83**:1193-1201.
94. **Itoh, T.** 1976. Amino acid replacement in the protein S5 from a spectinomycin resistant mutant of *Bacillus subtilis*. *Mol. Gen. Genet.* **144**:39-42.
95. **Jacob, A. E., and S. J. Hobbs.** 1974. Conjugal transfer of plasmid-borne multiple antibiotic resistance in *Streptococcus faecalis* var. zymogenes. *J. Bacteriol.* **117**:360-72.
96. **Kamps, M. P., and B. M. Sefton.** 1986. Neither arginine nor histidine can carry out the function of lysine-295 in the ATP-binding site of p60src. *Mol. Cell. Biol.* **6**:751-7.

97. Keely, S. J., J. M. Uribe, and K. E. Barrett. 1998. Carbachol stimulates transactivation of epidermal growth factor receptor and mitogen-activated protein kinase in T84 cells. Implications for carbachol-stimulated chloride secretion. *J. Biol. Chem.* 273:27111-7.
98. Kemp, B. E., and R. B. Pearson. 1991. Design and use of peptide substrates for protein kinases. *Methods Enzymol.* 200:121-34.
99. Kennelly, P. J., and M. Potts. 1996. Fancy meeting you here! A fresh look at "prokaryotic" protein phosphorylation. *J. Bacteriol.* 178:4759-64.
100. Kettner, M., T. Macickova, and V. J. Kremery. 1991. in *Antimicrobial Chemotherapy in Immunocompromised Host, International Congress of Chemotherapy*, pp 273-275, Berlin.
101. Kim, H., L. Lee, and D. R. Evans. 1991. Identification of the ATP binding sites of the carbamyl phosphate synthetase domain of the syrian hamster multifunctional protein CAD by affinity labeling with 5'-[p-(Fluorosulfonyl)benzoyl]adenosine. *Biochemistry.* 30:10322-10329.
102. King, M. M., D. J. Shell, and A. P. Kwiatkowski. 1988. Affinity labeling of the ATP-binding site of type II calmodulin- dependent protein kinase by 5'-p-fluorosulfonylbenzoyl adenosine. *Arch. Biochem. Biophys.* 267:467-73.
103. Knighton, D. R., J. H. Zheng, L. F. Ten Eyck, N. H. Xuong, S. S. Taylor, and J. M. Sowadski. 1991. Structure of a peptide inhibitor bound to the catalytic subunit of cyclic adenosine monophosphate-dependent protein kinase. *Science.* 253:414-20.

104. Knowles, J. R. 1980. Enzyme-catalyzed phosphoryl transfer reactions. *Annu. Rev. Biochem.* 49:877-919.
105. Kocabivik, S., and M. H. Perlin. 1994. Amino acid substitutions within the analogous nucleotide binding loop (P-loop) of aminoglycoside 3'-phosphotransferase-II. *Int. J. Biochem.* 26:61-6.
106. Kocabiyik, S., and M. H. Perlin. 1992. Altered substrate specificity by substitutions at Tyr218 in bacterial aminoglycoside 3'-phosphotransferase-II. *FEMS Microbiol. Lett.* 72:199-202.
107. Kocabiyik, S., and M. H. Perlin. 1992. Site-specific mutations of conserved C-terminal residues in aminoglycoside 3'-phosphotransferase II: phenotypic and structural analysis of mutant enzymes. *Biochem. Biophys. Res. Commun.* 185:925-31.
108. Komatsu, H., and M. Ikebe. 1993. Affinity labelling of smooth-muscle myosin light-chain kinase with 5'- [p-(fluorosulphonyl)benzoyl]adenosine. *Biochem. J.* 296:53-8.
109. Kondo, S., A. Tamura, S. Gomi, Y. Ikeda, T. Takeuchi, and S. Mitsuhashi. 1993. Structures of enzymatically modified products of arbekacin by methicillin-resistant. *Staphylococcus aureus*. *J. Antibiot (Tokyo)*. 46:310-5.
110. Kramers, H. A. 1940. Brownian motion in a field force and the diffusion model of chemical reactions. *Physica (Utrecht)*. 7:284-304.
111. Kuhberger, R., W. Piepersberg, A. Petzet, P. Buckel, and A. Bock. 1979. Alteration of ribosomal protein L6 in gentamicin-resistant strains of *Escherichia coli*. Effects on fidelity of protein synthesis. *Biochemistry*. 18:187-93.

112. **Kuret, J., and H. Schulman.** 1984. Purification and characterization of a Ca^{2+} /calmodulin-dependent protein kinase from rat brain. *Biochemistry*. **23**:5495-504.
113. **Kyte, J.** 1995. Mechanism in Protein Chemistry. Garland Publishing Inc., pp. 284-289, New York.
114. **Lawrence, P. G., H. P. Lambert, and F. O'Grady.** 1981. Antibiotic and chemotherapy, 5th ed. pp 1-65. Churchill Livingstone, Edinburgh.
115. **Leatherbarrow, R. J.** 1992. Grafit, vol. 3.0. Erithacus Software Ltd., Staines, United Kingdom.
116. **Leclercq, R., and P. Courvalin.** 1991. Bacterial resistance to macrolide, lincosamide, and streptogramin antibiotics by target modification [published erratum appears in *Antimicrob. Agents. Chemother.* 1991 Oct;35(10):2165]. *Antimicrob. Agents Chemother.* **35**:1267-72.
117. **Le Goffic, F., M.L. Capman, F. Tangy, and M. Baillarge.** 1979. Mechanism of action of aminoglycoside antibiotics. Binding studies of tobramycin and its 6'-N-acetyl derivative to the bacterial ribosome and its subunits. *Eur. J. Biochem.* **102**:73-81.
118. **Livermore, D. M.** 1995. Beta-Lactamases in laboratory and clinical resistance. *Clin. Microbiol. Rev.* **8**:557-84.
119. **Longenecker, K. L., P. J. Roach, and T. D. Hurley.** 1996. Three-dimensional structure of mammalian casein kinase I: molecular basis for phosphate recognition. *J. Mol. Biol.* **257**:618-31.

120. **Lowe, E. D., M. E. Noble, V. T. Skamnaki, N. G. Oikonomakos, D. J. Owen, and L. N. Johnson.** 1997. The crystal structure of a phosphorylase kinase peptide substrate complex: kinase substrate recognition. *EMBO J.* 16:6646-58.
121. **Madhusudan, E. A. Trafny, N. H. Xuong, J. A. Adams, L. F. Ten Eyck, S. S. Taylor, and J. M. Sowadski.** 1994. cAMP-dependent protein kinase: crystallographic insights into substrate recognition and phosphotransfer. *Protein Sci.* 3:176-87.
122. **Maio, J.J., and F.L. Brown.** 1991. Gene activation mediated by protein kinase C in human macrophage and teratocarcinoma cells expressing aminoglycoside phosphotransferase activity. *J. Cell. Physiol.* 149: 548-59.
123. **Mann, M., and M. Wilm.** 1995. Electrospray mass spectrometry for protein characterization. *Trends Biochem. Sci.* 20:219-24.
124. **Martel, A., M. Masson, N. Moreau, and F. Le Goffic.** 1983. Kinetic studies of aminoglycoside acetyltransferase and phosphotransferase from *Staphylococcus aureus* RPAL. Relationship between the two activities. *Eur. J. Biochem.* 133:515-21.
125. **Martin, C. M., N. S. Ikari, J. Zimmerman, and J. A. Waitz.** 1971. A virulent nosocomial *Klebsiella* with a transferable R factor for gentamicin: emergence and suppression. *J. Infect. Dis.* 124:24-9.
126. **Martin, P., E. Jullien, and P. Courvalin.** 1988. Nucleotide sequence of *Acinetobacter baumannii* *aphA-6* gene: evolutionary and functional implications of sequence homologies with nucleotide-binding proteins, kinases and other aminoglycoside-modifying enzymes. *Mol. Microbiol.* 2:615-25.

127. **Matsumura, M., Y. Katakura, T. Imanaka, and S. Aiba.** 1984. Enzymatic and nucleotide sequence studies of a kanamycin-inactivating enzyme encoded by a plasmid from thermophilic bacilli in comparison with that encoded by plasmid pUB110. *J. Bacteriol.* **160**:413-20.
128. **Meggio, F., A. Donella Deana, M. Ruzzene, A. M. Brunati, L. Cesaro, B. Guerra, T. Meyer, H. Mett, D. Fabbro, P. Furet, and et al.** 1995. Different susceptibility of protein kinases to staurosporine inhibition. Kinetic studies and molecular bases for the resistance of protein kinase CK2. *Eur. J. Biochem.* **234**:317-22.
129. **Microbiology, A. S. F.** 1995. *Report of the ASM Task Force on the Antibiotic Resistance, American Society for Microbiology.* , Washington, D.C.
130. **Miller, M. H., S. C. Edberg, L. J. Mandel, C. F. Behar, and N. H. Steigbigel.** 1980. Gentamicin uptake in wild-type and aminoglycoside-resistant small- colony mutants of *Staphylococcus aureus*. *Antimicrob. Agents Chemother.* **18**:722-9.
131. **Moazed, D., and H. F. Noller.** 1990. Binding of tRNA to the ribosomal A and P sites protects two distinct sets of nucleotides in 16 S rRNA. *J. Mol. Biol.* **211**:135-45.
132. **Moazed, D., and H. R. Noller.** 1987. Interaction of antibiotics with functional sites in 16S ribosomal RNA. *Nature.* **327**:389-394.
133. **Montandon, P. E., R. Wagner, and E. Stutz.** 1986. *E. coli* ribosomes with a C912 to U base change in the 16S rRNA are streptomycin resistant. *EMBO J.* **5**:3705-8.
134. **Morris, V. J., and B. R. Jennings.** 1975. The effect of neomycin and streptomycin on the electrical polarisability of aqueous suspensions of *Escherichia coli*. *Biochim. Biophys. Acta.* **392**:328-34.

135. Muir, M. E., R. S. van Heeswyck, and B. J. Wallace. 1984. Effect of growth rate on streptomycin accumulation by *Escherichia coli* and *Bacillus megaterium*. *J. Gen. Microbiol.* 130:2015-22.
136. Munoz-Dorado, J., S. Inouye, and M. Inouye. 1991. A gene encoding a protein serine/threonine kinase is required for normal development of *M. xanthus*, a gram-negative bacterium. *Cell.* 67:995-1006.
137. Musser, J. M. 1995. Antimicrobial agent resistance in *Mycobacteria*: molecular genetic insights. *Clin. Microbiol. Rev.* 8:496-514.
138. Naganawa, H., M. Yagisawa, S. Kondo, T. Takeuchi, and H. Umezawa. 1971. The structure determination of an enzymatic inactivation product of 3',4'-dideoxykanamycin B. *J. Antibiot (Tokyo).* 24:913-4.
139. Nair, S. A., M. H. Kim, S. D. Warren, S. Choi, S. Zhou, L. C. Cantley, and D. G. Hangauer. 1995. Identification of efficient pentapeptide substrates for the tyrosine kinase pp60c-src. *J. Med. Chem.* 38:4276-83.
140. Neu, H. C. 1992. The crisis in antibiotic resistance. *Science.* 257:1064-73.
141. Nobuta, K., M. E. Tolmasky, L. M. Crosa, and J. H. Crosa. 1988. Sequence and expression of the 6'-N-acetyltransferase gene of transposon TN1331 from *Klebsiella pneumoniae*. *J. Bacteriol.* 170:3769-3773.
142. Omura, S., Y. Iwai, A. Hirano, A. Nakagawa, J. Awaya, H. Tsuchiya, Y. Takahashi, and R. Masuma. 1977. A new alkaloid AM-2282 Of Streptomyces origin. Taxonomy, fermentation, isolation and preliminary characterization. *J. Antibiot. (Tokyo).* 30:275-82.

143. Owen, D. J., M. E. Noble, E. F. Garman, A. C. Papageorgiou, and L. N. Johnson. 1995. Two structures of the catalytic domain of phosphorylase kinase: an active protein kinase complexed with substrate analogue and product. *Structure*. 3:467-82.
144. Ozaki, M., S. Mizushima, and M. Nomura. 1969. Identification and functional characterization of the protein controlled by the streptomycin-resistant locus in *E. coli*. *Nature*. 222:333-9.
145. Pal, P. K., W. J. Wechter, and R. F. Colman. 1975. Affinity labeling of the inhibitory DPNH site of bovine liver glutamate dehydrogenase by 5'-Fluorosulfonylbenzoyl adenosine. *J. Biol. Chem.* 250:8140-8147.
146. Pearson, R. B., and B. E. Kemp. 1991. Protein kinase phosphorylation site sequences and consensus specificity motifs: tabulations. *Methods Enzymol.* 200:62-81.
147. Pedersen, L. C., M. M. Benning, and H. M. Holden. 1995. Structural investigation of the antibiotic and ATP-binding sites in kanamycin nucleotidyltransferase. *Biochemistry*. 34:13305-11.
148. Payie, K.G., P.N. Rather, and A.J. Clarke. 1995. Contribution of gentamicin 2'-N-acetyltransferase to the O acetylation of peptidoglycan in *Providencia stuartii*. *J. Bacteriol.* 177:4303-4310.
149. Payie, K.G. and A.J. Clarke. 1997. Characterization of gentamicin 2'-N-acetyltransferase from *Providencia stuartii*: Its use of peptidoglycan metabolites for acetylation of both aminoglycosides and peptidoglycan. *J. Bacteriol.* 179:4106-4114.
150. Penefsky, H. S. 1977. Reversible binding of Pi by beef heart mitochondrial adenosine triphosphatase. *J. Biol. Chem.* 252:2891-9.

151. **Perez-Gonzalez, J. A., M. Lopez-Cabrera, J. M. Pardo, and A. Jimenez.** 1989. Biochemical characterization of two cloned resistance determinants encoding a paromomycin acetyltransferase and a paromomycin phosphotransferase from *Streptomyces rimosus* forma *paromomycinus*. *J. Bacteriol.* **171**:329-34.
152. **Plotz, P. H., and B. D. Davis.** 1962. Absence of a chloramphenicol-insensitive phase of streptomycin by *Escherichia coli*. *Nature.* **191**:1324-1325.
153. **Prade, L., R. A. Engh, A. Girod, V. Kinzel, R. Huber, and D. Bossemeyer.** 1997. Staurosporine-induced conformational changes of cAMP-dependent protein kinase catalytic subunit explain inhibitory potential. *Structure.* **5**:1627-37.
154. **Radika, K., and D. B. Northrop.** 1984. The kinetic mechanism of kanamycin acetyltransferase derived from the use of alternative antibiotics and coenzymes. *J. Biol. Chem.* **259**:12543-12546.
155. **Radika, K., and D. B. Northrop.** 1984. A new kinetic diagnostic for enzymatic mechanisms using alternative substrates. *Anal. Biochem.* **141**:413-417.
156. **Radika, K., and D. B. Northrop.** 1984. Substrate specificities and structure-activity relationships for acylation of antibiotics catalyzed by kanamycin acetyltransferase. *Biochemistry.* **23**:5118-22.
157. **Rather, P. N., H. Munayyer, P. A. Mann, R. S. Hare, G. H. Miller, and K. J. Shaw.** 1992. Genetic analysis of bacterial acetyltransferases: identification of amino acids determining the specificities of the aminoglycoside 6'-N-acetyltransferase Ib and IIa proteins. *J. Bacteriol.* **174**:3196-203.

158. **Rather, P. N., E. Orosz, K. J. Shaw, R. Hare, and G. Miller.** 1993. Characterization and transcriptional regulation of the 2'-N-acetyltransferase gene from *Providencia stuartii*. *J. Bacteriol.* 175:6492-8.
159. **Reinstein, J., M. Brune, and A. Wittinghofer.** 1988. Mutations in the nucleotide binding loop of adenylate kinase of *Escherichia coli*. *Biochemistry.* 27:4712-20.
160. **Robinson, M. J., P. C. Harkins, J. Zhang, R. Baer, J. W. Haycock, M. H. Cobb, and E. J. Goldsmith.** 1996. Mutation of position 52 in ERK2 creates a nonproductive binding mode for adenosine 5'-triphosphate. *Biochemistry.* 35:5641-6.
161. **Roestamadj, J., I. Grapsas, and S. Mobashery.** 1995. Loss of individual electrostatic interactions between aminoglycoside antibiotics and resistance enzymes as an effective means of overcoming bacterial drug resistance. *J. Am. Chem. Soc.* 117:(11060-11069).
162. **Rouch, D. A., M. E. Byrne, Y. C. Kong, and R. A. Skurray.** 1987. The *aacA-aphD* gentamicin and kanamycin resistance determinant of Tn4001 from *Staphylococcus aureus*: expression and nucleotide sequence analysis. *J. Gen. Microbiol.* 133:3039-52.
163. **Rudolph, F. B.** 1979. Product inhibition and abortive complex formation. *Methods Enzymol.* 63:411-436.
164. **Russo, M. W., T. J. Lukas, S. Cohen, and J. V. Staros.** 1985. Identification of residues in the nucleotide binding site of the epidermal growth factor receptor/kinase. *J. Biol. Chem.* 260:5205-8.

165. Sakon, J., H. H. Liao, A. M. Kanikula, M. M. Benning, I. Rayment, and H. M. Holden. 1993. Molecular structure of kanamycin nucleotidyltransferase determined to 3.0-Å resolution. *Biochemistry*. 32:11977-84.
166. Salauze, D., and J. Davies. 1991. Isolation and characterisation of an aminoglycoside phosphotransferase from neomycin-producing *Micromonospora chalybeata*; comparison with that of *Streptomyces fradiae* and other producers of 4,6-disubstituted 2-deoxystreptamine antibiotics. *J. Antibiot (Tokyo)*. 44:1432-43.
167. Sampson, N. S., and J. R. Knowles. 1992. Segmental motion in catalysis: investigation of a hydrogen bond critical for loop closure in the reaction of triosephosphate isomerase. *Biochemistry*. 31:8488-94.
168. Schatz, A., E. Bugie, and S. A. Waksman. 1944. Streptomycin, a substance exhibiting antibiotic activity against Gram-positive and Gram-negative bacteria. *Proc. Soc. Exp. Biol. Med.* 55:66-69.
169. Segel, I. 1975. *Enzyme Kinetics*. John Wiley & Sons, New York.
170. Shaw, K. J., P. N. Rather, R. S. Hare, and G. H. Miller. 1993. Molecular genetics of aminoglycoside resistance genes and familial relationships of the aminoglycoside-modifying enzymes. *Microbiol. Rev.* 57:138-163.
171. Shaw, K. J., P. N. Rather, F. J. Sabatelli, P. Mann, H. Munayyer, R. Mierzwa, G. L. Tetrikos, R. S. Hare, G. H. Miller, P. Bennett, and P. Downey. 1992. Characterization of the chromosomal *aac(6')-Ic* gene from *Serratia marcescens*. *Antimicrob. Agents Chemother.* 36:1447-1455.

172. **Shoji, S., J. Ohnishi, T. Funakoshi, K. Fukunaga, E. Miyamoto, H. Ueki, and Y. Kubota.** 1987. Phosphorylation sites of bovine brain myelin basic protein phosphorylated with Ca^{2+} -calmodulin-dependent protein kinase from rat brain. *J. Biochem. (Tokyo)*. 102:1113-20.
173. **Sigal, I. S., J. B. Gibbs, J. S. D'Alonzo, G. L. Temeles, B. S. Wolanski, S. H. Socher, and E. M. Scolnick.** 1986. Mutant ras-encoded proteins with altered nucleotide binding exert dominant biological effects. *Proc. Natl. Acad. Sci. USA*. 83:952-6.
174. **Sigmund, C. D., M. Ettayebi, and E. A. Morgan.** 1984. Antibiotic resistance mutations in 16S and 23S ribosomal RNA genes of *Escherichia coli*. *Nucleic Acids Res.* 12:4653-63.
175. **Simopoulos, T. T., and W. P. Jencks.** 1994. Alkaline phosphatase is an almost perfect enzyme. *Biochemistry*. 33:10375-80.
176. **Siregar, J. J., K. Miroshnikov, and S. Mobashery.** 1995. Purification, characterization, and investigation of the mechanism of aminoglycoside 3'-phosphotransferase type Ia. *Biochemistry*. 34:12681-8.
177. **Siuzdak, G.** 1994. The emergence of mass spectrometry in biochemical research [published erratum appears in *Proc. Natl. Acad. Sci. USA* 1995 Jan 17;92(2):646]. *Proc. Natl. Acad. Sci. USA*. 91:11290-7.
178. **Sondhi, D., W. Xu, Z. Songyang, M. J. Eck, and P. A. Cole.** 1998. Peptide and protein phosphorylation by protein tyrosine kinase Csk: insights into specificity and mechanism. *Biochemistry*. 37:165-72.

179. **Spotts, C. R., and R. Y. Stanier.** 1961. Mechanism of streptomycin action on bacteria: a unitary hypothesis. *Nature*. 192:633-637.
180. **Tai, P. C., B. J. Wallace, and B. D. Davis.** 1978. Streptomycin causes misreading of natural messenger by interacting with ribosomes after initiation. *Proc. Natl. Acad. Sci. USA*. 75:275-9.
181. **Tai, P. C., B. J. Wallace, E. L. Herzog, and B. D. Davis.** 1973. Properties of initiation-free polysomes of *Escherichia coli*. *Biochemistry*. 12:609-15.
182. **Tamaoki, T., H. Nomoto, I. Takahashi, Y. Kato, M. Morimoto, and F. Tomita.** 1986. Staurosporine, a potent inhibitor of phospholipid/ Ca^{++} dependent protein kinase. *Biochem. Biophys. Res. Commun.* 135:397-402.
183. **Tanaka, T., T. Ohmura, T. Yamakado, and H. Hidaka.** 1982. Two type of calcium-dependent protein phosphorylations modulated by calmodulin antagonists. Napthalenesulfonamide derivatives. *Mol. Pharmacol.* 22:408-412.
184. **Taylor, D. E., W. Yan, L. K. Ng, E. K. Manavathu, and P. Courvalin.** 1988. Genetic characerization of kanamycin resistance in *Campylobacter coli*. *Ann. Inst. Pasteur Microbiol.* 139:665-676.
185. **Thompson, C. J., R. H. Skinner, J. Thompson, J. M. Ward, D. A. Hopwood, and E. Cundliffe.** 1982. Biochemical characterization of resistance determinants cloned from antibiotic-producing *Streptomyces*. *J. Bacteriol.* 151:678-85.
186. **Thompson, J.D., D.G. Higgins, and T.J. Gibson.** 1994. CLUSTAL W: improving the sensitivity of progressive multiple sequence alignment through sequence

weighting, position-specific gap penalties and weight matrix choice. *Nucleic Acids Res.* 22:4673-80.

187. Thompson, P. R., D. W. Hughes, and G. D. Wright. 1996. Mechanism of aminoglycoside 3'-phosphotransferase type IIIa: His188 is not a phosphate-accepting residue. *Chem. Biol.* 3:747-55.

188. Toledo, L. M., and N. B. Lydon. 1997. Structures of staurosporine bound to CDK2 and cAPK--new tools for structure-based design of protein kinase inhibitors. *Structure.* 5:1551-6.

189. Tran Van Nhieu, G., and E. Collatz. 1987. Primary structure of an aminoglycoside 6'-N-acetyltransferase AAC(6')-4, fused *in vivo* with the signal peptide of the Tn3-encoded β -lactamase. *J. Bacteriol.* 169:5708-5714.

190. Trieu-Cuot, P., and P. Courvalin. 1983. Nucleotide sequence of the *Streptococcus faecalis* plasmid gene encoding the 3'5"-aminoglycoside phosphotransferase type III. *Gene.* 23:331-41.

191. Tsai, S. F., M. J. Zervos, D. B. Clewell, S. M. Donabedian, D. F. Sahm, and J. W. Chow. 1998. A new high-level gentamicin resistance gene, *aph(2'')-Id*, in *Enterococcus spp.* *Antimicrob. Agents Chemother.* 42:1229-32.

192. Umezawa, S., K. Tatsuta, T. Tsuchiya, and E. Kitazawa. 1967. Synthesis of neamine. *J. Antibiot (Tokyo).* 20:53-4.

193. Vetter, I. R., J. Reinstein, and P. Rosch. 1990. Complexes of *Escherichia coli* adenylate kinase and nucleotides: ^1H NMR studies of the nucleotide sites in solution. *Biochemistry.* 29:7459-67.

194. Vlahos, C. J., W. F. Matter, K. Y. Hui, and R. F. Brown. 1994. A specific inhibitor of phosphatidylinositol 3-kinase, 2-(4- morpholinyl)-8-phenyl-4H-1-benzopyran-4-one (LY294002). *J. Biol. Chem.* 269:5241-8.
195. Wain-Hobson, S., P. Sonigo, O. Danos, S. Cole, and M. Alizon. 1985. Nucleotide sequence of the AIDS virus, LAV. *Cell.* 40:9-17.
196. Waksman, S. A., and H. A. Lechevalier. 1949. Neomycin, a new antibiotic active against streptomycin-resistant bacteria, including tuberculosis organisms. *Science.* 109:305-307.
197. Wallace, B. J., P. C. Tai, E. L. Herzog, and B. D. Davis. 1973. Partial inhibition of polysomal ribosomes of *Escherichia coli* by streptomycin. *Proc. Natl. Acad. Sci. USA.* 70:1234-7.
198. Wells, J. A., D. B. Powers, R. R. Bott, T. P. Graycar, and D. A. Estell. 1987. Designing substrate specificity by protein engineering of electrostatic interactions. *Proc. Natl. Acad. Sci. USA.* 84:1219-23.
199. Williams, J. W., and D. B. Northrop. 1978. Kinetic mechanisms of gentamicin acetyltransferase I. *J. Biol. Chem.* 253:5902-5907.
200. Wilson, K. P., M. J. Fitzgibbon, P. R. Caron, J. P. Griffith, W. Chen, P. G. McCaffrey, S. P. Chambers, and M. S. Su. 1996. Crystal structure of p38 mitogen-activated protein kinase. *J. Biol. Chem.* 271:27696-700.
201. Wolf, E., A. Vassilev, Y. Makino, A. Sali, Y. Nakatani, and S. K. Burley. 1998. Crystal structure of a GCN5-related N-acetyltransferase: *Serratia marcescens* aminoglycoside 3-N-acetyltransferase. *Cell.* 94:439-49.

202. Woodcock, J., D. Moazed, M. Cannon, J. Davies, and H. F. Noller. 1991. Interaction of antibiotics with A- and P-site-specific bases in 16S ribosomal RNA. *EMBO J.* 10:3099-103.
203. Wright, G. D., A. M. Berghuis, and S. Mobashery. *in press*. Aminoglycoside antibiotics: structure, functions and resistance. .
204. Wright, G. D., and P. Ladak. 1997. Overexpression and characterization of the chromosomal aminoglycoside 6'-N-acetyltransferase from *Enterococcus faecium*. *Antimicrob. Agents Chemother.* 41:956-60.
205. Wybenga-Groot, L.E., Ka. Draker, G.D. Wright, and A.M. Berghuis. 1999. Crystal structure of an aminoglycoside 6'-N-acetyltransferase: defining the GCN5-related N-acetyltransferase superfamily fold. *Structure.* 7:497-507.
206. Wyatt, J. L., and R. F. Colman. 1977. Affinity labeling of rabbit muscle pyruvate kinase by 5'-p-Fluorosulfonylbenzoyladenine. *Biochemistry.* 16:1333-1342.
207. Wymann, M. P., G. Bulgarelli-Leva, M. J. Zvelebil, L. Pirola, B. Vanhaesebroeck, M. D. Waterfield, and G. Panayotou. 1996. Wortmanin inactivates phosphoinositide 3-kinase by covalent modification of Lys-802, a residue involved in the phosphate transfer reaction. *Mol. Cell. Biol.* 16:1722-33.
208. Xu, R. M., G. Carmel, R. M. Sweet, J. Kuret, and X. Cheng. 1995. Crystal structure of casein kinase-1, a phosphate-directed protein kinase. *EMBO J.* 14:1015-23.
209. Xu, R.-M., G. Carmel, J. Kuret, and X. Cheng. 1996. Structural basis for selectivity of the isoquinoline sulfonamide family of protein kinase inhibitors. *Proc. Natl. Acad. Sci. USA.* 93:6308-6313.

210. **Yaish, P., A. Gazit, C. Gilon, and A. Levitzki.** 1988. Blocking of EGF-dependent cell proliferation by EGF receptor kinase inhibitors. *Science*. **242**:933-5.
211. **Yoon, M. Y., and P. F. Cook.** 1987. Chemical mechanism of the adenosine cyclic 3',5'-monophosphate dependent protein kinase from pH studies. *Biochemistry*. **26**:4118-25.
212. **Zalacain, M., A. Gonzalez, M. C. Guerrero, R. J. Mattaliano, F. Malpartida, and A. Jimenez.** 1986. Nucleotide sequence of the hygromycin B phosphotransferase gene from *Streptomyces hygroscopicus*. *Nucleic Acids Res.* **14**:1565-81.
213. **Zhang, F., A. Strand, D. Robbins, M. H. Cobb, and E. J. Goldsmith.** 1994. Atomic structure of the MAP kinase ERK2 at 2.3 Å resolution. *Nature*. **367**:704-711.
214. **Zheng, J., D. R. Knighton, L. F. ten Eyck, R. Karlsson, N. Xuong, S. S. Taylor, and J. M. Sowadski.** 1993. Crystal structure of the catalytic subunit of cAMP-dependent protein kinase complexed with MgATP and peptide inhibitor. *Biochemistry*. **32**:2154-61.
215. **Zoller, M. J., N. C. Nelson, and S. S. Taylor.** 1981. Affinity labeling of cAMP-dependent protein kinase with p-fluorosulfonylbenzoyl adenosine. Covalent modification of lysine 71. *J. Biol. Chem.* **256**:10837-42.